Palaeogeographic Mapping and Depositional Trends of the Patchawarra Formation within the Tenappera Region.

Sam J. Kobelt, BSc. Hons. (University of Adelaide)

This thesis is submitted in partial fulfilment of the requirements for the
Honours Degree of Bachelor of Science (Petroleum Geology and Geophysics)
Australian School of Petroleum
The University of Adelaide
October, 2014

Acknowledgements

I would like to warmly thank my ASP supervisors, Khalid Amrouch and Peter McCabe for their continual support and assistance and helpful insights on numerous topics and concepts throughout the whole course of my project. I would like to thank Geoff Wood at Santos for his time spent rescuing me whenever I had gotten myself lost correlating the Patchawarra Formation. I would like to thank my Team Leader; Adam Hill for his ongoing support and making me feel welcome and a part of his team at Santos.

I would like to extend a sincere thank you and express my gratitude to my industry supervisor Brenton Schoemaker. For his relentless support and remarkable patience throughout the entirety of my project; from day to day problems such as software issues to in-depth geological discussions and guiding me through each step of my project and thesis preparations.

Abstract

The Patchawarra Formation is a coal dominated fluvio-lacustrine environment. These environments have complex geometries and facies distribution is difficult to predict spatially. This study defined palaeogeographic reconstructions using log-signature responses from equivalent chronostratigraphic intervals, modern fluvial analogues and regional TWT isochrons. This resulted in the definition of spatial distribution of fluvio-lacustrine facies throughout the Tenappera region, Cooper Basin, South Australia.

379 wells were correlated into 21 chronostratigraphic intervals wireline log responses. 6 electrofacies were identified from the gamma ray and sonic velocity log motifs. These were combined with modern fluvial analogues to yield 4 facies assemblages. Multiple modern analogues were considered suitable for the Patchawarra Formation in the Tenappera Region. The Ob River, Siberia is considered more suitable for depositional facies whereas the McKenzie River, Northwest Territories demonstrated the influence of a compressional stress regime on fluvial avulsion patterns and styles.

In order to map channel belt width within a chronostratigraphic interval empirical relationships from previous studies were applied. By measuring bankfull depth from well data an estimate of channel belt width is obtained. 532 bankfull measurements were taken giving a maximum bankfull depth of 8.2m, a minimum of 1.4m and a mean value of 5.1m. Channel belt width ranges were then estimated by applying bankfull population statistics to applicable linear regression curves. Channel belt width calculations gave a range of variability from 76m to 3625m, with an average channel belt width range from 1639-1908m. For the interpreted Patchawarra Formation intervals there were eight populations with similar channel belt ranges.

High resolution palaeogeographic reconstruction of the Patchawarra Formation within the Tenappera Region allows for better prediction of facies distribution. There are two distinguishable periods of fluvial deposition in the upper and lower Patchawarra Formation. Ultimately, the paleogeographic maps aid assessment of field prospects by defining depositional channel fairways which control reservoir distribution. These techniques could be applied to other fluvial dominated petroleum systems.

Table of Contents

Chapter 1: Introduction

The Permian-Triassic Cooper Basin is an intracratonic basin covering approximately 130,000 square kilometres in northeast South Australia and southwest Queensland (Figure 1.1). The Tenappera Trough Region within the Cooper Basin, (Figure 1.2) is comprised of the major fields; Della, Dullingari, Epsilon, Stokes and Toolachee as well as a number of smaller fields (Figures 1.2 & 1.3). The Early-Mid Permian Patchawarra, Toolachee and Tirrawarra Formations are major gas producing intervals of the Tenappera Trough Region, within the Cooper Basin (Apak, 1994; Lang, 2001; Strong, 2002). The Patchawarra Formation is characterised by a meandering fluvial-lacustrine succession, dominated by coal intervals (Thornton, 1979; Apak, 1994; Lang *et al*, 2001; Strong *et al*., 2002). The Ob River, Western Siberia has been accepted as the best modern day analogue for the Patchawarra Formation (Lang *et al.*, 2001). In this study, a number of other analogues have been recognised as also being suitable for analogue studies.

Reservoir facies of the Patchawarra Formation are from channel fill and point bar sands. Mapping and reservoir characterisation of the fluvio-lacustrine Patchawarra Formation has historically been difficult due to the tortuous geometry of main channel pathways and complexity of splay deposits (Lang *et a.l*, 2001). Picking and tracking of sub-formational reservoir facies within the Patchawarra Formation has proven to be difficult due to high reflectivity of the abundant coals on the seismic signature; resulting in poor seismic resolution of sub-formational intervals of the Patchawarra Formation (Strong *et al.,* 2002).

Structural influence is a primary control on accommodation space creation and has a large control on fluvial distributions and stacking pattern geometries (Lang *et al.,* 2001). Discreet compressional events intermittently reactivated pre-Permian basement structures throughout the development of the Cooper Basin (O'Driscoll, 1980; Kuang 1985, Roberts *et al.,* 1990; Apak 1995). Reactivation of existing structures resulted in uplift, changing the palaeo-slope and accommodation space/sediment supply ratio (Strong *et al.,* 2002). Changes in structure in turn affected sedimentation patterns, such as; channel belt switching, channel belt migration, depositional hiatuses and erosion.

Strong *et al.,* (2002) have successfully applied sequence stratigraphic concepts to the Patchawarra Formation in the Cooper Basin and produced high resolution palaeogeographic maps defining reservoir facies geometries and distributions within the Moomba and Big Lake Field Area. A similar workflow and framework shall be adopted for the Tenappera Trough Region in this study.

This study attempts to predict channel distribution patterns away from well control through palaeogeographic mapping of signature log intervals of the Patchawarra Formation in the Tenappera Trough Region. All 376 within the study area contain Patchawarra intersections and were correlated using the pre-established chronostratigraphic framework for the Cooper Basin defined by Santos. Fluvial facies of the Patchawarra Formation were then interpreted from log data comprising; crevasse splay, overbank, levee, peat mire and channel fill/point bar deposits. Image log data, where available, was analysed to give paleoflow directions for given intervals from tilt-corrected sedimentary structures. Palaeographic reconstruction maps were made for each chronostratigraphic interval, using the interpreted log signatures. Analogues were also used as a guiding control when reconstructint palaeogeographic maps.The Ob River was acknowledged as the best modern day analogue for the depositional systems in the Patchawarra Formation, while The Kuparuk River, North Slope, Alaska and Mackenzie Rivers Northwest Territory, Canada were recognised as bearing similarities in structural controls on depositional patterns to the Patchawarra Formation.

A better understanding of reservoir facies distribution has particular significance in refining play concepts and aiding in future exploration and development strategies in the Tenappera Trough Region.

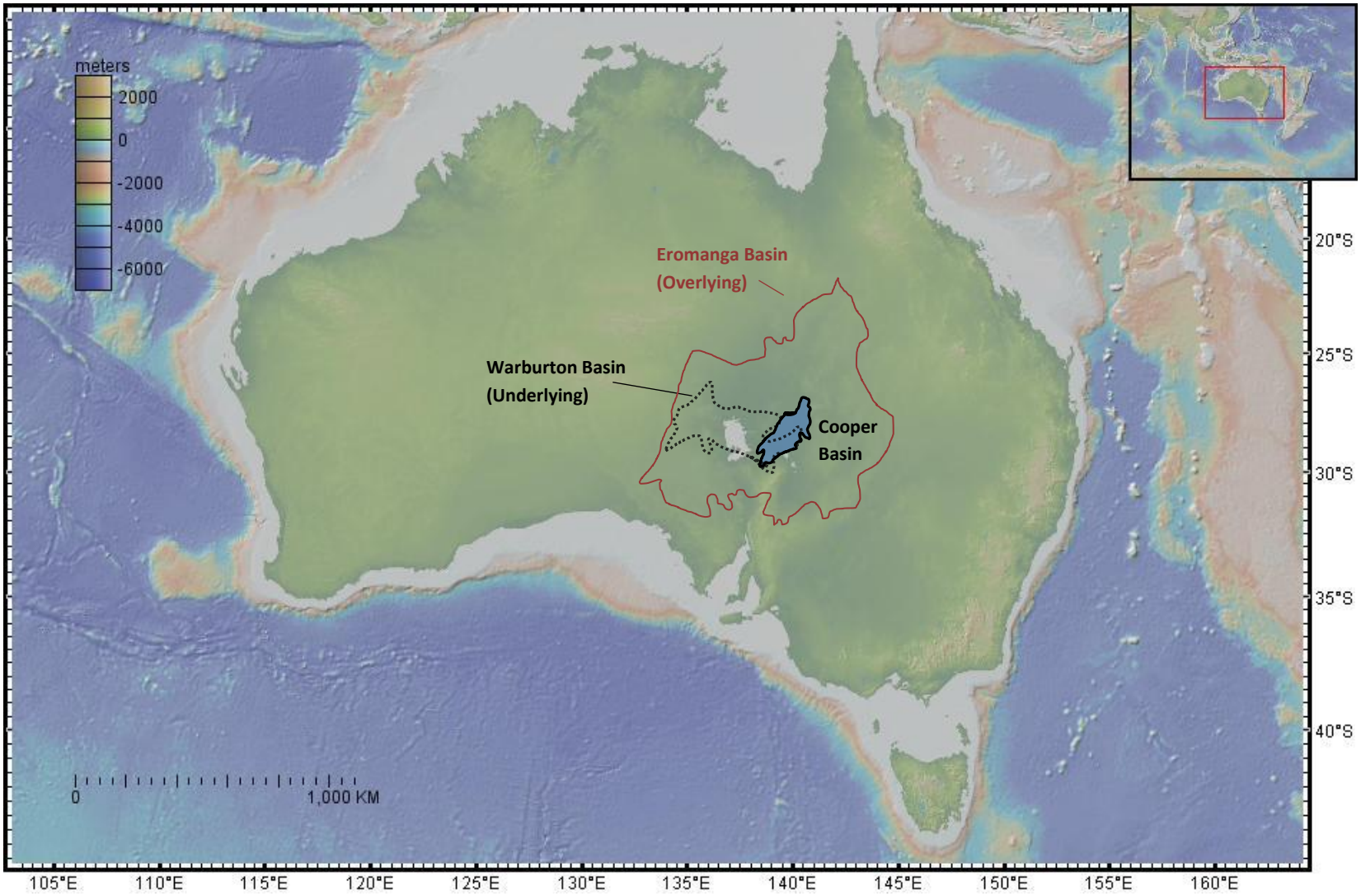

Figure 1.1: Locality map of the Cooper Basin, Australia. The underlying Warburton Basin is depicted by the dashed black line, and the overlying Eromanga Basin is depicted by the maroon solid line. (Modified from GeoMapapp Database, 2014).

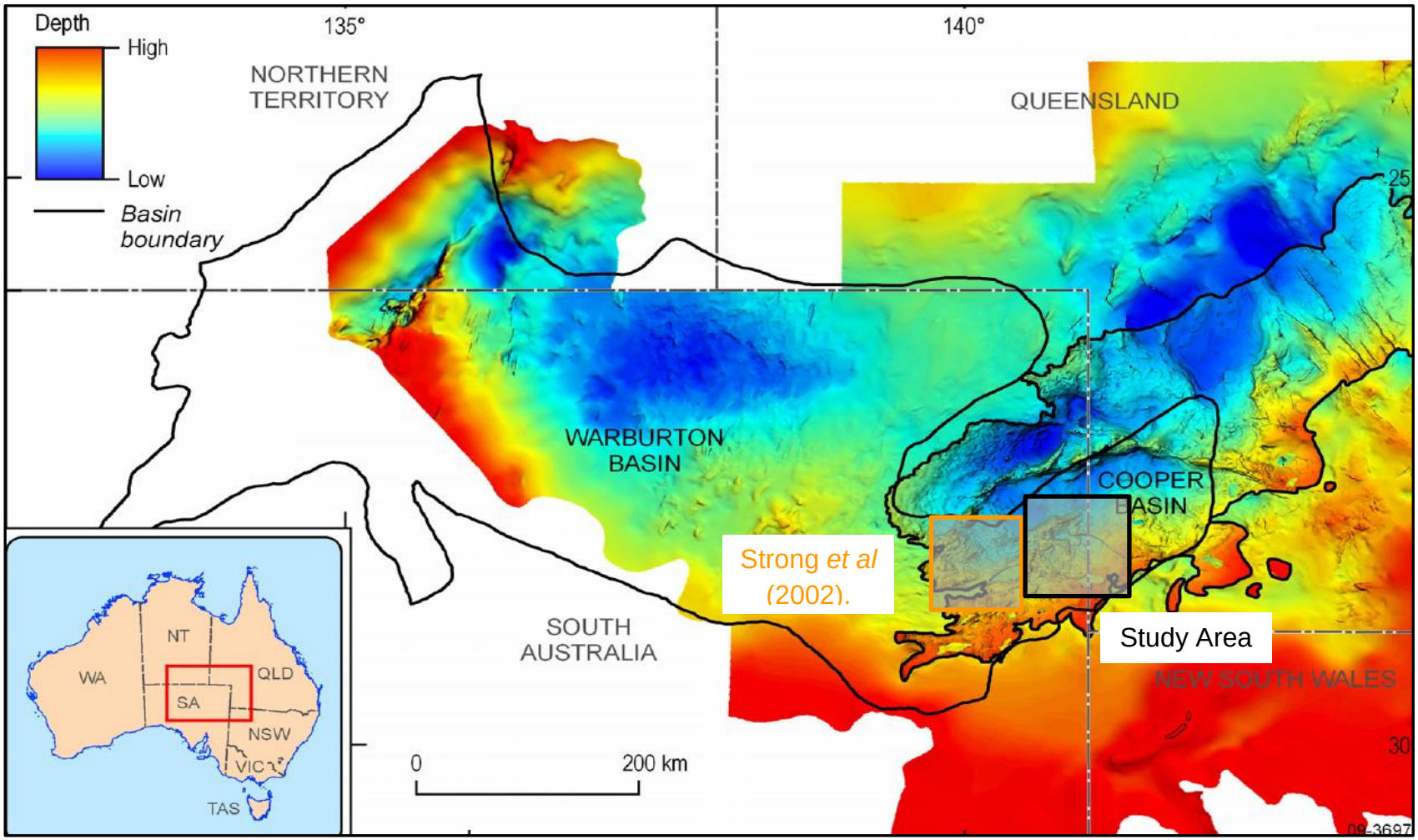

Figure 1.2: Study area location within the Cooper Basin shaded grey and outlined black, and underlying Warburton Basin. The Strong *et al*. (2002) study area referred to in this paper is denoted by the grey box, outlined orange. Colour scheme shows depth (relative) to seismic 'ZU00' basement horizon. (From Radke, 2009, modified from PIRSA, 2007)

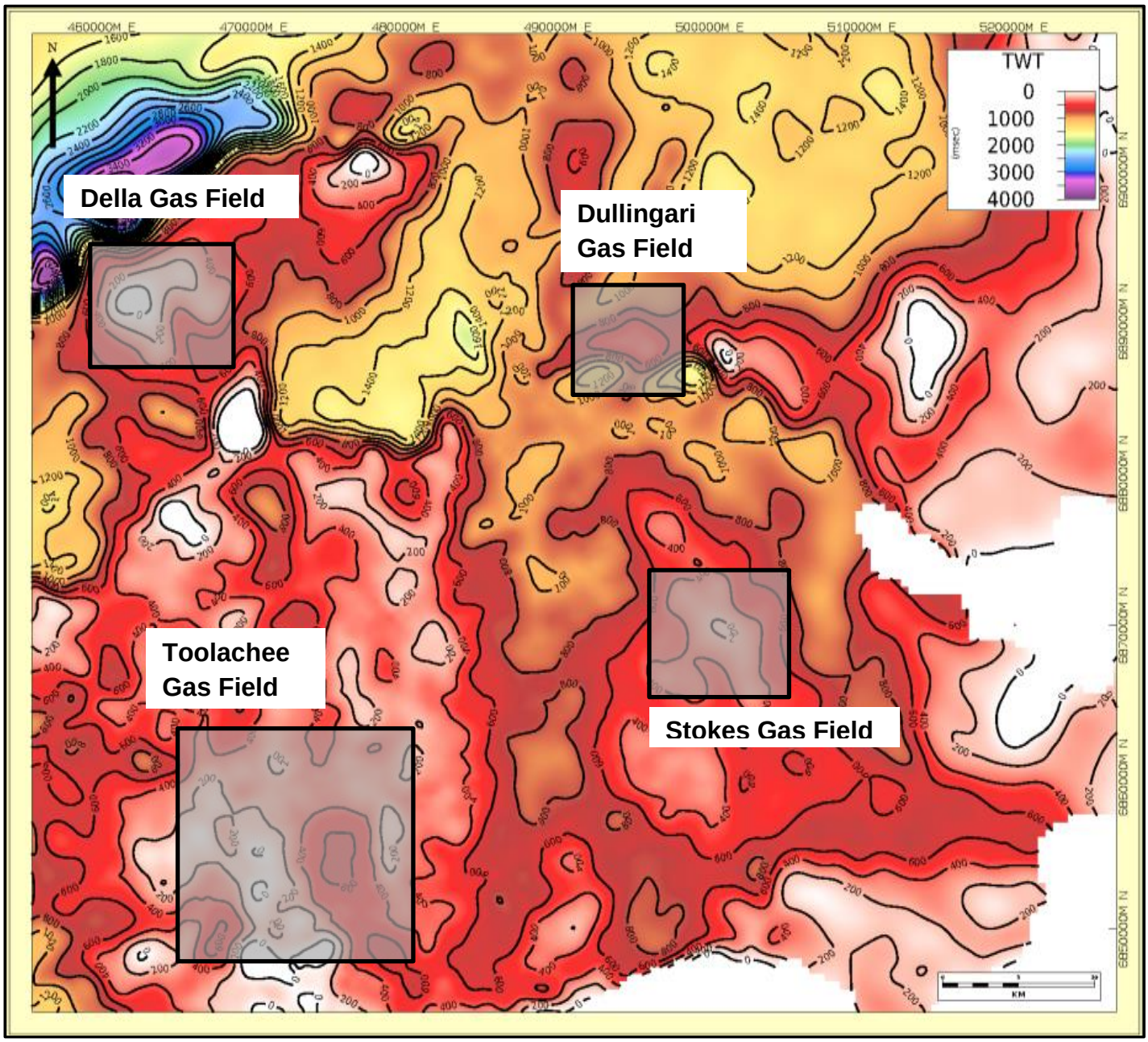

Figure 1.3: Tenaperra Trough Region study area. Major gas producing fields within the study area are highlighted. Colour scale shows isochron thickness of the Patchawarra Formation.

Chapter 2: Geological Setting

2.1 Basin setting

The Permian-Triassic Cooper Basin is an intracratonic basin covering approximately 130,000 square kilometres in northeast South Australia and southwest Queensland (Figure 1.1). The Cooper Basin unconformably overlies the Cambrian-Devonian Warburton Basin in the southwest and Carboniferous granitic intrusives/associated metasediments in the northeast (Battersby, 1976; Gatehouse, 1986, Apak 1995). The more extensive Mesozoic Eromanga Basin overlies the Cooper Basin (Gravestock and Jensen-Schmidt 1998). Strata within the Cooper Basin were deposited in nonmarine; glacial, fluvial and lacustrine environments (Sprigg 1958, 1961;Kapel, 1966; Martin, 1967a; Thornton, 1979; Apak 1995). Intermittent reactivation of pre-Permian basement structures strongly influenced the development of the Cooper Basin (O'Driscoll, 1980; Kuang 1985, Roberts *et al*., 1990; Apak 1995). The reactivation of pre-existing structures is evidenced by crestel unconformities, tilted blocks, inversion and the vertical and lateral variation of chronostratigraphic intervals of the Cooper Basin (Apak, 1995; Lang *et al.,* 2001; Strong *et al.,* 2002).

The Cooper Basin has both northeast and northwest trending major structural grains (Figures 2.1 and 2.2) and to a lesser extent; a north trending fabric also (Sprigg, 1961; Stuart, 1976; Thornton, 1979; Apak *et al.,* 1997). A wide variety of structural models have been put forward to account for this complex structure and evolution of the Cooper Basin. The most recent works have identified an anisotropic stress field over time, with the Cooper Basin developing under a compressive regime (Apak *et al*., 1997; Gravestock and Jensen-Schmidt 1998; Jensen-Schmidt 2006). Compression intermittently reactivated pre-existing structures with northeast and northwest structural trends during the evolution of the Cooper Basin (Apak *et al.,* 1997; Gravestock and Jensen-Schmidt 1998; Jensen-Schmidt, 2006).

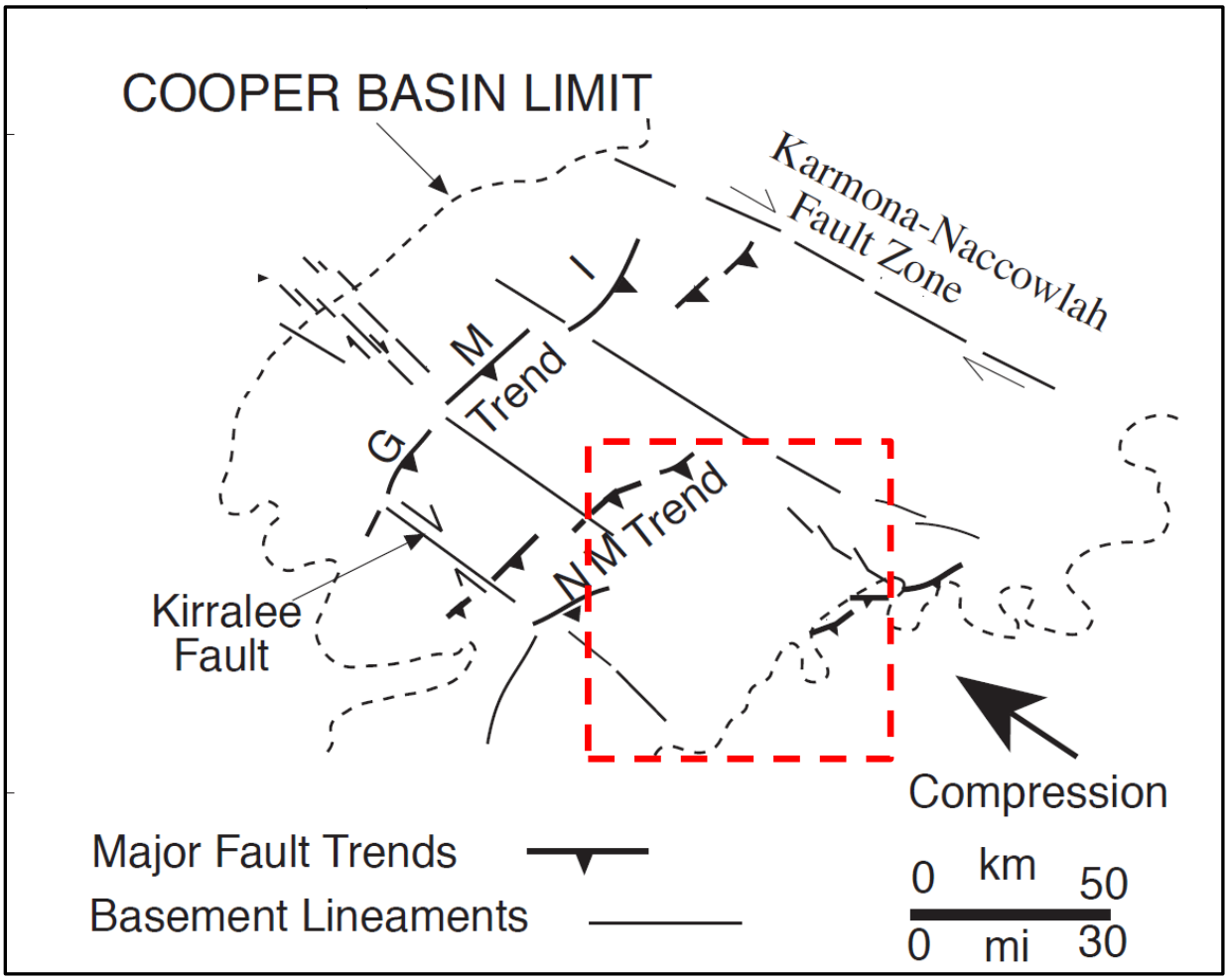

Figure 2.1: Major structural elements of the underlying basement of the Cooper Basin. The basin has major northeast striking structural grains from the Adelaidean extension event (annotated as Major Fault Trends). These faults were initiated as normal and relay faults. Later Ordovician to Mid-Carboniferous compression oriented in a NW-SE direction resulted in the Karmona-Naccowlah trend as well as the GMI and NM faults being reactivated as thrust trends striking to the NE and wrench faulting creating a sub-ordinate NW striking grain (From Apak *et al*., 1997). The red dashed line approximately outlines the Tenappera Region study area.

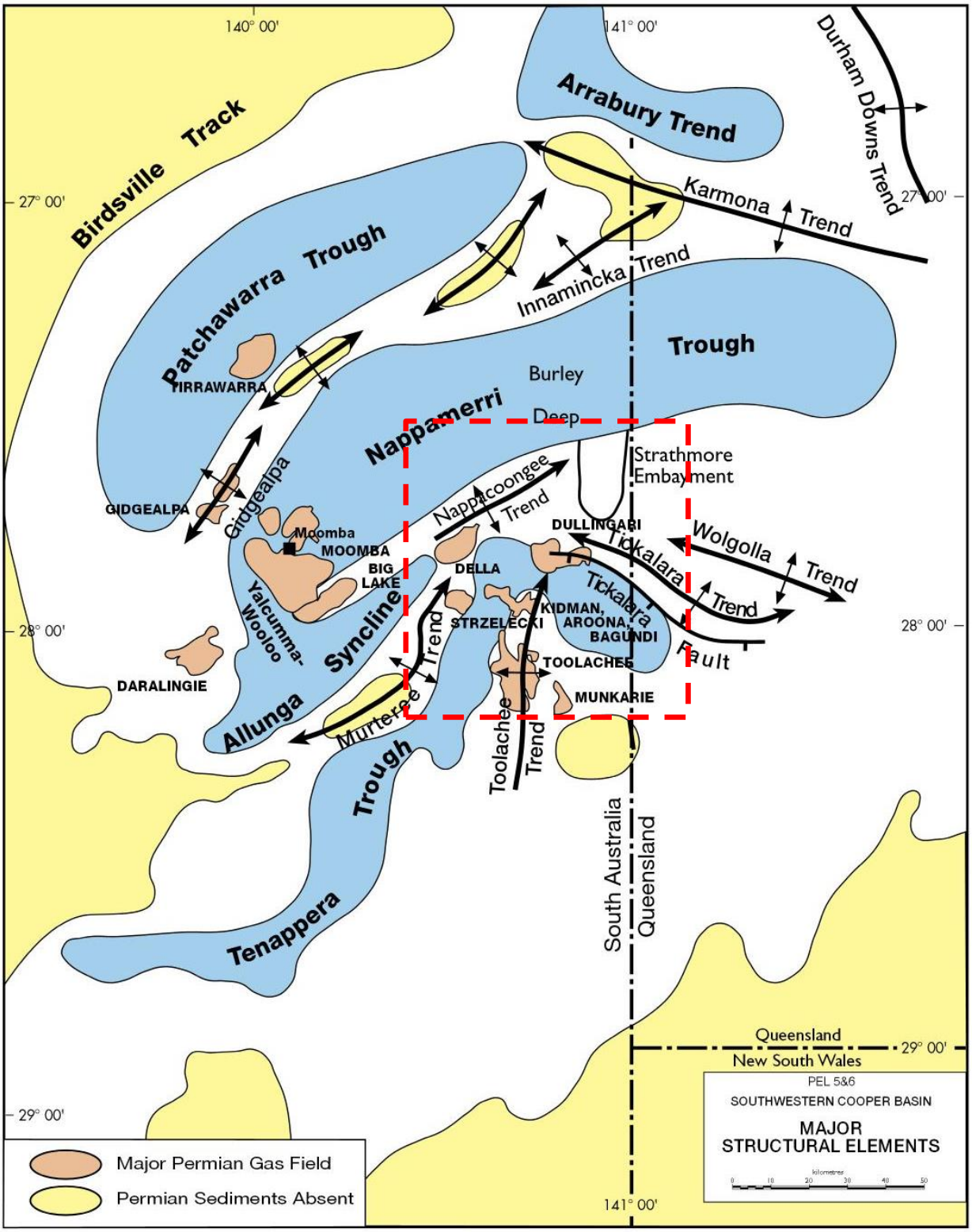

Figure 2.2: Major structural elements of the Cooper Basin with major depocentres shaded in blue. It can be seen from inspection with Figure 2.1 that the underlying basement structures have a strong influence on the Cooper Basin structural and depositional architecture. The red dashed line outlines the Tenappera Region study area.

2.2 Structural evolution

The structural evolution of the Cooper Basin can be separated into three stages: 1) Development of Pre-Permian existing basement structure, 2) Syn-depositional structural growth events during the Permian-Triassic and 3) Post depositional structuring events. Reactivation of pre-existing basement architecture had a major structural influence on the Cooper Basin, while basin floor morphology controlled early depositional patterns of the basin (Apak 1995, Gatehouse *et al*.,1995, Gravestock and Jensen-Schmidt 1998).

Basement structure and morphology (Pre-Permian)

The earliest recognised structural features in the region record extension in the underlying Precambrian Craton during the late Adelaidean (650-575 Ma) (Veevers and Powell, 1984). Extension was orientated in an NE-SW direction, in what was the eastern extent and a passive margin of the Australian Craton (Evans, 1988; Apak *et al.,* 1997). The Adelaidean NE-SE extension event resulted in the deep seated NE-SW striking relay and normal faults that define the large scale structural grain of the region, shown in Figure 2.1 (Wopfner, 1960; Sprigg 1958, 1961; Apak *et al.,*1997). The Delamerian Orogeny in the Ordovician marks the transition from the passive margin extensional regime to a compressive regime, driven by the initiation of the subduction of the Pacific plate under the Australian Plate (Foden, 2002; Glen, 2005). Many orogenic events took place during this period of compression, lasting from the Ordovician till the mid-Carboniferous (Apak *et al.*, 1997). The two most significant compressional events during this time were the Alice Springs (450-325Ma) and Kanimblan/Thomson Orogenies (340-320Ma) (Apak *et al*., 1997; Gravestock and Jensen-Schmidt 1998). The Alice Springs Orogeny was a N-S compressional event mainly effecting the crystalline cratonic basement to the west, while the Kanimblan/Thomson Orogeny was a E-W compressional event deforming the recently accreted sediments to the east, forming the Lachlan Fold Belt into a neocraton, shown in Figure 2.3 (Foster and Gray, 2008; Veevers, 1984; Kuang, 1985; Apak 1995; Klootwitjk, 2000; Glen, 2013).

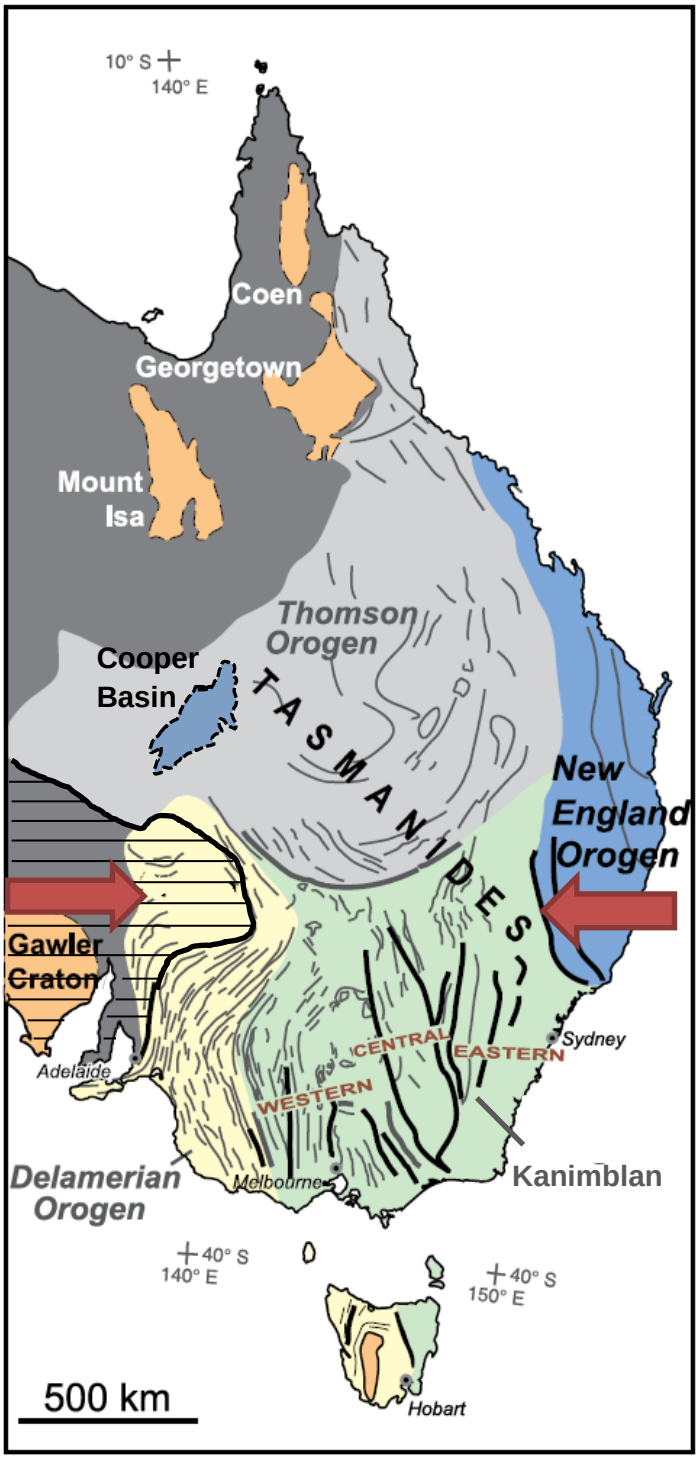

Figure 2.3: Tectonic architecture of the Eastern Australian margin during the compressive period before the Cooper Basin formation showing the Delamerian and Kanimblan orogens. The Delamerian Orogeny (520-500Ma) deformed Neoprotorozoic to Cambrian sediments of the Eastern Australian Margin, adding the recently accreted sediments to the Australian Craton. The extent of the Delamerian Orogen is depicted by the crème shaded area. The Kanimblan/Thomson Orogen (340-320Ma) was similar in style: deforming the recently accreted sediments in a compressive regime, further adding to the Australian Craton. The extent of the Kanimblan/Thomson Orogens are depicted by the green and grey shaded areas. These accretionary orogenic events result in the intracratonic setting of the Cooper Basin, unlike the underlying Warburton Basin which was a marginal marine basin. (Modified from Foster and Gray, 2009)

The Ordovician to the mid-Carboniferous compressional period resulted in the formation of the Karmona-Naccowlah trend, separating the Cooper Basin into a southern and a northern sub-basin, shown in Figures 2.1 and 2.2 (Apak *et al.,*1997). The northern sub-basin has a thinner Permian section and a thicker Triassic section suggesting Post-Permian tilting (Apak, 1995; Radke, 2009). The southern sub-basin has pronounced NW and NE structural grains. In the southern sub-basin the compressional period reactivated large scale Adelaidean extensional NE fault systems; creating the major Gidgealpa-Merrimelia-Innamincka (GMI) and Nappacoongee-Murteree (NM) trends (Figures 2.1and 2.2). The GMI and NM trends divide the Cooper Basin into three main depocentres in the southern part of the basin (Figure 2.2). These NE trends were then displaced vertically and horizontally by wrench faulting, creating a sub-ordinate NW structural grain (Kuang 1985; Roberts *et al*., 1990; Apak 1995, Gravestock and Jensen-Shmidt. 1998). The lack of Preserved Devonian strata, exposure of granites with deep emplacement depths on the Cooper Basin floor and highly weathered basement profiles intersected in drillholes indicate rapid uplift during the Late Carboniferous (Apak 1995, Gravestock and Jensen-Schmidt 1998).

Syn Depositional Structuring (Permian-Triassic)

The Cooper Basin was initiated and characterised by compressional reactivation and inversion of pre-Permian structures (Wopfner, 1960; Sprigg,1961; Kuang, 1985; Roberts *et al*., 1990; Apak *et al.,* 1997). Thermal sag resulting from the extensive granite emplacement during the Carboniferous has also been attributed to the overall subsidence and down warping of the basin (Gallagher, 1988; Gravestock and Jensen-Schmidt 1998). The compression was caused by the formation of the Pangea super-continent that resulted in worldwide orogenesis and glaciation (Stampflia, 2013). Stress directions of compressions during the Cooper Basin formation are poorly constrained, however, NE trending folds and faults suggest a NW-SE or E-W compressional stress regime (Apak *et al.,*1997).

The Cooper Basin floor was an erosional land surface shaped by rapid uplift and glacial scouring (Veevers, 1994; Gravestock and Jensen-Schmidt, 1998). Early Cooper Basin depositional patterns reflect infill of these basement land surface features and were deposited during the waning stages of glaciation (Wopfner, 1981; Veevers, 1984; Kuang 1985; Gravestock and Jensen-Schmidt, 1998).

Pronounced compressional events successively rejuvenated structural features resulting in uplift, while slight downwarping and tectonic quiescence was experienced in-between these discreet uplift events (Apak 1995, Gravestock and Jensen-Shmidt, 1998). Uplift events are marked by erosional unconformities and depositional hiatuses on the uplifted highs and continual deposition in the low areas. Quiescent periods are recorded by widespread and continual deposition across the basin (Apak, 1995; Gravestock and Jensen-Schmidt, 1998). Three significant uplift events are recognised during Cooper Basin deposition. Two uplift events during the Sakmarian are marked by the lower and mid Patchawarra unconformities; VU45 and VU75. The third uplift event marked by the Mid to Late Permian Daralingie Unconformity, which was more long lived and significant than the two Sakmarian uplifts (Apak, 1995; Lang *et al*., 2001; Strong *et al*., 2002). The Daralingie Unconformity represents a large time gap and erodes into large sections of Earlier Permian Formations and sometimes onto basement (e.g. The Della and Strzelecki Highs).

Post Depositional Structuring (Jurassic-Cenozoic)

Cooper Basin deposition terminated in the Late Triassic due to a widespread compressional event resulting in basin wide uplift and the Nappamerri erosional unconformity (Thornton, 1979; Alexander and Sansome, 1996; Mavromatidis, 2007)). Eromanga Basin deposition initiated in the Early Jurassic during subsequent downwarping after the Cooper Basin termination event (Thornton, 1979; Alexander and Sansome, 1996). Eromanga deposition was widespread and continuous from the Early Jurassic to Late Cretaceous, controlled by thermal decay subsidence and tectonic activity on the Australian plate margins (Gallagher and Lambeck, 1989; Gravestock and Jensen-Schmidt, 1998). The cessation of Eromanga deposits is marked by the Late Cretaceous-Tertiary unconformity, attributed to a widespread compressional uplift driven by accelerated spreading and increased rotation of the Australia-Antactica plate boundary (Moore and Pitt, 1984; Kuang, 1985; Finlayson *et al*., 1990).

The Eromanga Basin deposition was the last major depositional period in the region. The Cenozoic is characterised by continued compressional uplift and exhumation with very minor periods of sedimentation (Moore and Pitt, 1984; Shaw, 1991;

Mavromatidis, 2007). The compressional uplift continued rejuvenation of existing faults and further enhanced structures in the Cooper Basin (Apak *et al.,* 1993).

2.3 Cooper Basin Stratigraphy

The Cooper Basin depositional pattern strongly responded to structural reactivation and quiescent down warping periods through regressive and transgressive cycles respectively (Kuang, 1985; Veevers and Powell, 1987; Apak, 1994). The Cooper Basin experienced a transition from a cool temperate climate in the Permian to a more humid climate by the Triassic which is also reflected in the Cooper Basin stratigraphy (Veevers and Powell, 1987; Alexander, 1998). Figure 2.4 outlines the Cooper Basin stratigraphy.

The Compression that is responsible for the initiation of the Cooper Basin in the Mid-Carboniferous is also thought to have triggered the formation of a widespread continental ice sheet at this time (Veevers and Powell, 1987; Alexander, 1998). The Glaciation reached a peak during the Westphalian to Stephanian and had retreated by the Sakmarian (Veevers and Powell, 1987; Alexander, 1998).The basal units of the Cooper Basin; the Merrimelia and Tirrawarra Formations are terminoglacial and glaciofluvial deposits. These units were deposited unconformably onto the glacially scoured and eroded basement paleo-land surface (Thornton, 1979; Veevers, 1984; Alexander, 1998). The Merremelia and Tirrawarra Formations in-filled topographic lows and were not uniformly distributed across the basin.

The Merrimelia Formation is a heterolithic proglacial unit with numerous lithotypes (Alexander, 1998). The Tirrawarra Formation is interpretted as a terminoglacial braided stream deposit (Kapel, 1972; Battersby, 1976). It has been proposed that rather than being two separate chronostratigraphic formations; the Merrimelia and Tirrawarra formations are interfingered and coeval facies of the same glacial origin (Williams and Wild, 1984; Chaney *et al*., 1997). The interfingering relationship records the successive advancement and retreat stages of the continental glaciers. The early predominance of the Merrimelia Formation and the later predominance of the Tirrawarra also support this interpretation, as terminoglacial facies would be expected to dominate during the waning stages of glaciation.

Cooper Basin Stratigraphy

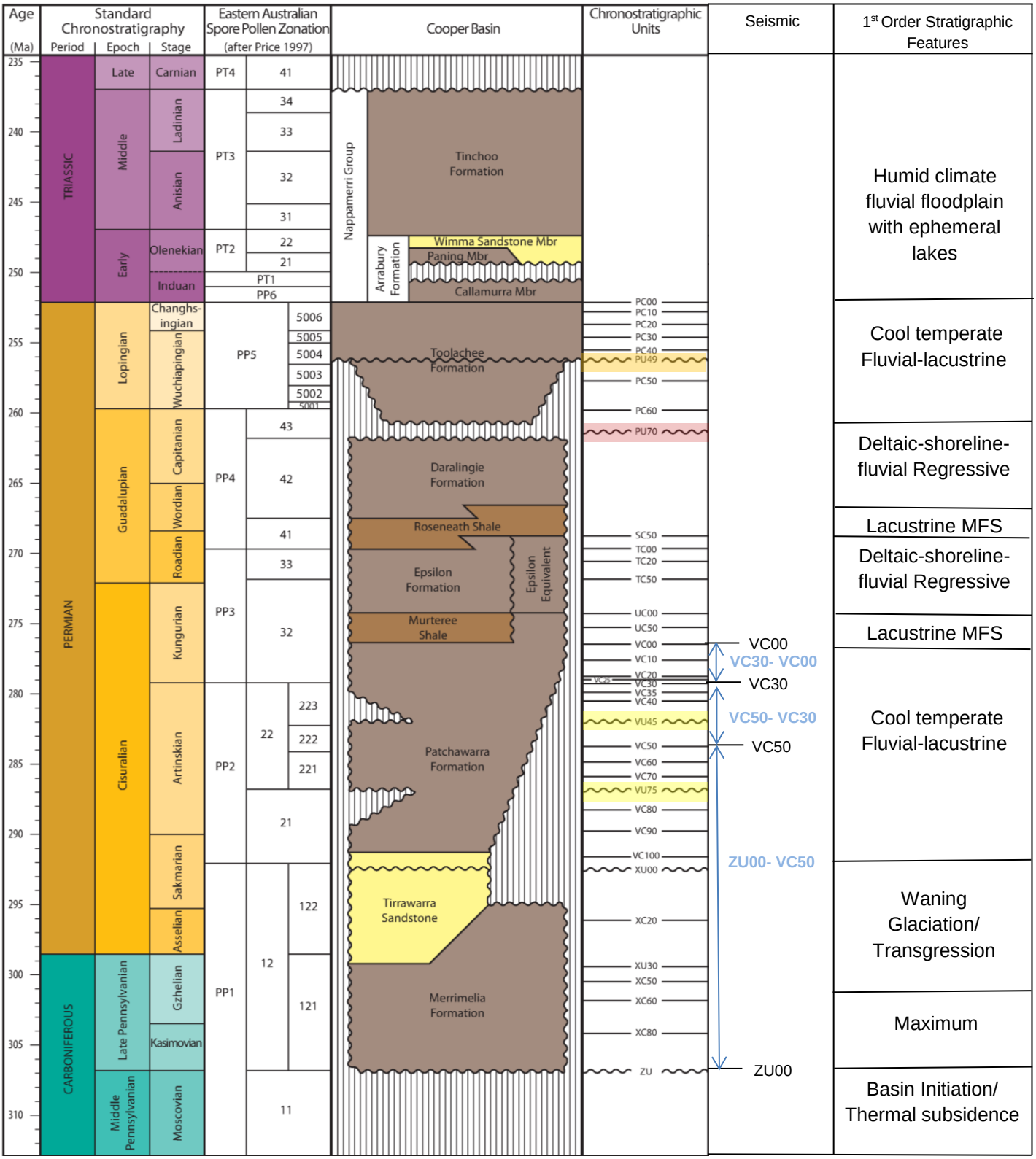

Figure 2.4: Cooper Basin Stratigraphic Column. The seismic horizons and intervals (In blue) significant to this study are shown. There are two notable erosional events caused by minor compressional uplift within the Permian Patchawarra Formation, indicated by the VU45 and VU75 horizons (highlighted in yellow). The Daralingie Unconformity indicated by the PU70 horizon (highlighted in red) horizon indicates a much longer lived and extensive erosional event. The mid Toolachee unconformity, indicated by the PU49 horizon (highlighted in orange), was also an extensive erosional event but not as significant as the Daralingie Unconfomity. MFS = maximum flooding surface. (Modified from Santos, 2013)

The Patchawarra Formation is the first Formation that was extensively deposited across the entire Cooper Basin, which in some areas has been eroded off of intra-basin highs by the Mid-Late Permian erosional event marked by the Daralingie Unconformity (Alexander, 1998). The Patchawarra directly overlies basement and where present; the Tirrawarra/Merrimelia glacial formations. The Patchawarra Formation is characterised by a meandering fluvial-lacustrine succession, dominated by coal intervals (Thornton, 1979; Apak, 1994; Lang *et al*, 2001; Strong *et al*., 2002). Overall the Patchawarra Formation is transgressive and can be roughly divided into three units (Apak, 1994). The Basal Patchawarra is a post-glacial sand dominated unit with minor silts and coals. The coals have been attributed to raised peat mires; forming on highs as they were being slowly submerged (Seggie, 1997; G. Wood; Pers Comms, 2014). The middle Patchawarra unit is a meandering fluvial system, containing; channel belt, floodplain/lacustrine, peat mire and crevasse splay facies assemblages. The upper Patchawarra unit is similar to the middle unit, however it has increased floodplain/lacustrine and peat mire dominance due to transgression into the deep-water lacustrine environment (Murturee Shale) (Stuart, 1976; Gravestock and Jensen-Schmidt, 1998).

The Murturee Shale marks the end of the first fluvial cycle and the beginning of two lacustrine transgressive/regressive cycles of the Murturee-Eplison and Roseneath-Daralingie Formations(Stuart, 1976, Apak, 1995). Both the Murturee and Roseneath Shales are widespread lacustrine units representing transgressive and high stand cycles. Continual and widespread depositions are suggested from both the uniform thickness and lithology for both formations (Battersby, 1976; Thornton, 1979; Apak, 1995). The Murturee and Roseneath Shales are absent on the GMI and NM trends mainly due to non-deposition (Stuart, 1976; Thornton, 1979; Apak, 1995). The Epsilon and Daralingie Formations are characterised by deltaic, shoreline and floodplain deposits representing regressive lacustrine cycles (Battersby 1976, Thornton, 1979; Alexander, 1998).

A major uplift during the Late Permian resulted in a long lived and widespread erosional event, marked by the Daralingie Unconformity (Wopfner 1966; Thornton, 1979; Gray and Roberts, 1984).

The Toolachee Formation disconformably overlies the earlier Permian Formations and unconformably overlies older basement rocks along intra-basin highs; where erosion from the Daralingie Unconformity was most extensive (Gravestock and Morton 1984; Alexander, 1998). The Toolachee Formation is interpreted as being deposited in a fluvio-lacustrine environment (Stuart, 1976; Thornton, 1979, Apak, 1995).

The Late Permian-Triassic Nappamerri Group conformably overlies the Toolachee Formation and is unconformably overlain by the Eromanga Basin (Papalia 1969; Alexander, 1998). The palaeo-latitude of the Cooper Basin Region was high (as in the Permian). The Nappamerri Group was deposited at a similar palaeo-latitude as the Gidgealpa Group, however the climate had changed to humid (Retallack *et al*., 1996). The Nappameri Group can be summarised by a floodplain environment with associated ephemeral lakes in low lands, pedogenic profiles in exposed areas; cut by low-sinuosity rivers (Alexander, 1998).

Chapter 3: Fluvial Style and Stacking Patterns of the Patchawarra Formation.

3.1 Introduction

In order to successfully correlate into genetic coeval units and to then reconstruct and map palaeogeographic intervals of the Patchawarra Formation it is necessary to first define and understand the fluvial style and stacking patterns. It has been established and accepted by a number of authors that the Patchawarra Formation was deposited by high sinuosity meandering river systems working through floodplain, peat mire and lacustrine upland environments (Stuart, 1976; Battersby, 1976; Thornton, 1979; Stanmore and Johnstone, 1988; Alexander, 1998; Strong *et al*., 2002).

3.2 Meandering river definition

Many authors have recognised the limitations in current river system classification schemes and acknowledged that a river system cannot be classified by one single parameter because river systems often exhibit a combination of each defined fluvial style (Rust, 1978; Miall, 1996; Leeder, 1999; Bridge, 2003, Gibling, 2006;). For this reason a working definition of a meandering river system must be established for this study.

For the purpose of this study a meandering river system is defined as: A river with a single channel which deposits predominantly through point bar deposition on the inner bank and erosion on the outer bank of the channel, resulting in lateral migration of the channel (Miall, 1978; Cant, 1982; Nichols, 2009) as in; Figures 3.1 and 3.2). Meandering systems dominate where banks are unstable, promoting lateral migration and erosion into the substrate (Smith, 1983). Lateral migration of a channel results in the deposition of a channel belt over time (Figure 3.2).

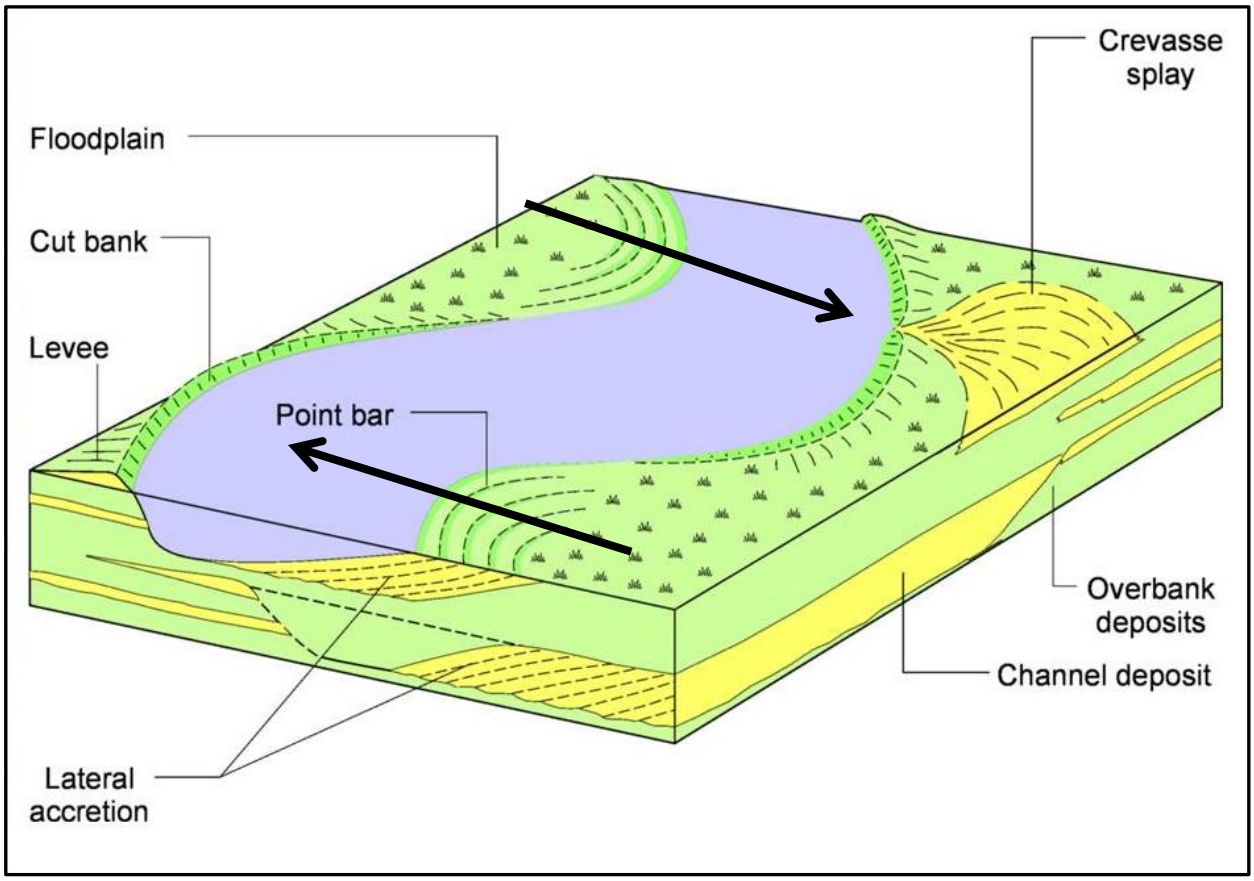

Figure 3.1: Schematic diagram of the morphological features of a meandering river system, detailing the geometry of floodplain, point bar and crevasse splay deposits. The lateral accretion of point bars on the inner bend and erosion of the cutbanks on the outer bend of the river result in lateral migration of the system in the direction of the black arrows, therefore becoming more sinuous (Modified from Nichols, 2009).

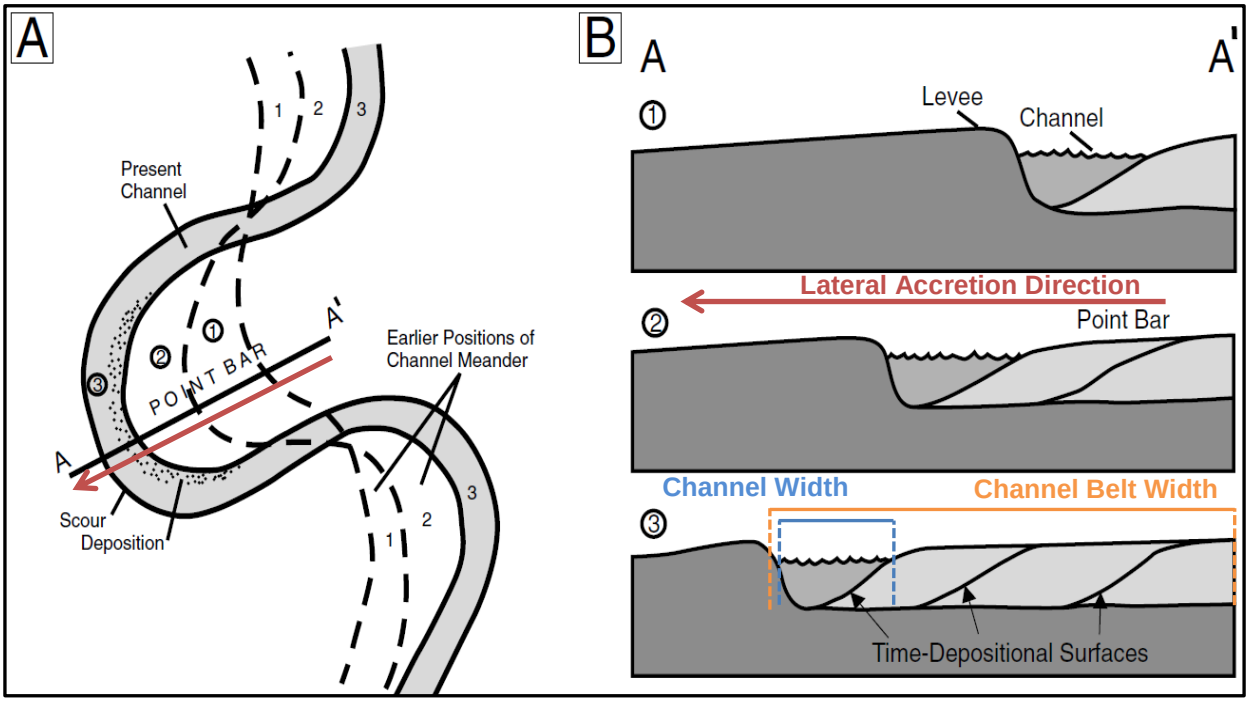

Figure 3.2: A plan form (A) and cross sectional (B) schematic view of a laterally accreting point bar deposit of a meandering river. A –Plan form view depicting the lateral migration of the channel with time; the dashed lines marked 1 and 2 represent previous channel positions relative to the present channel positon. B – Cross sectional view of the point bar deposition, showing the lateral migration of the channel, and the preservation of point bars, inclined in the direction of channel migration denoted by the direction of the red arrow. Channel width and channel belt width are annotated, and the difference between the two is highlighted. (Modified from Slatt, 2006).

3.3 Meandering river deposit terminology

The lateral accretion of point bars is the primary mechanism of channel belt formation (Figure 3.2). Point bar deposits are generally a fining upward sandy succession; this is due to the helical flow within a meandering river system, which is also responsible for the erosion of the cutbank due to high shear stress and point bar deposition on the inner bend wirh weaker shear stress (Figure 3.2). Point bar deposits characteristically show large scale cross-bedding at the base and smaller sets of laminations towards the top of the deposit (Boggs Jr., 2006, Figure 3.3). As the channel migrates laterally, the top of the point bar becomes the overbank and floodplain fines cap the point bar deposits (Leeder, 1999; Nichols, 2009). The lateral accretion of a meandering river channel creates a channel belt, consisting of a number of point bar deposits from individual channels being laterally accreted over time (Figure 3.2). Channel belt deposits rather than individual channels of meandering systems are what are preserved in plan form geometry. The palaeogeographic reconstructions of this study focus on the mapping of these channel belts and associated crevasse splay deposits (discussed below) that form the reservoir facies in the Patchawarra Formation.

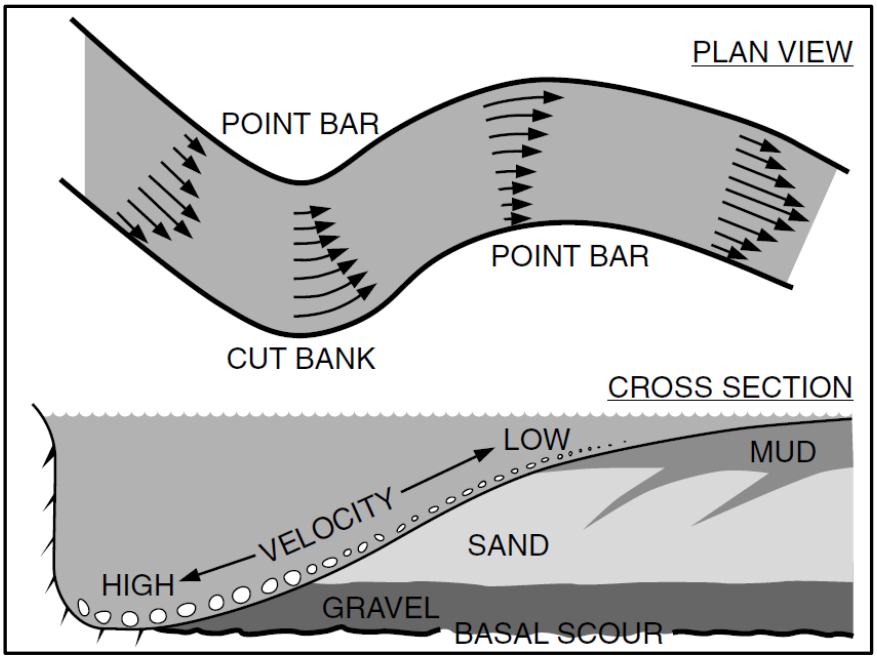

Figure 3.2: A schematic diagram outlining how a fining upward point bar deposit is formed due to the difference in water flow velocity within a channel body. Arrows in the plan view depict how water velocity changes through bends in a channel resulting in erosion on outer bends and deposition of point bar deposits on inner bends, with an increasing velocity towards the thalweg (Modified from Slatt, 2006).

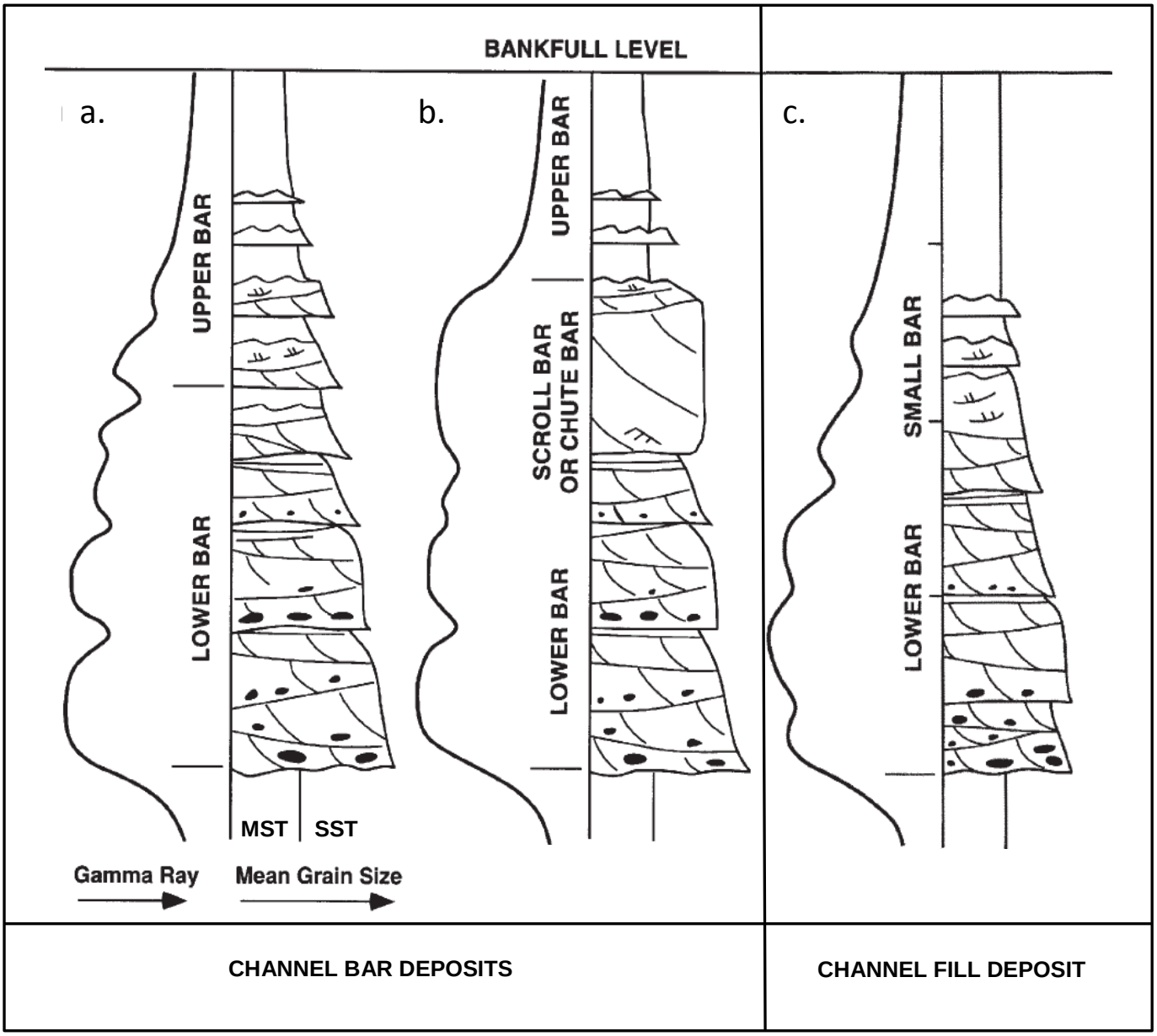

Figure 3.3: Type sections of channel bar and channel fill deposits. a.) Shows a typical channel bar deposit. b.) Shows a typical channel bar deposit with a chute or scroll bar crosscutting the main point bar deposit, which in turn is overlain by an upper bar deposit. c.) Shows a typical channel fill deposit, note that the lower bar deposit is similar to the lower bars of the channel bar deposits but the absence of an upper bar deposit and a mud plug at the top of the deposit characterises the channel fill deposit. MST= mudstone, SST = sandstone. (Modified from Bridge and Tye, 2000).

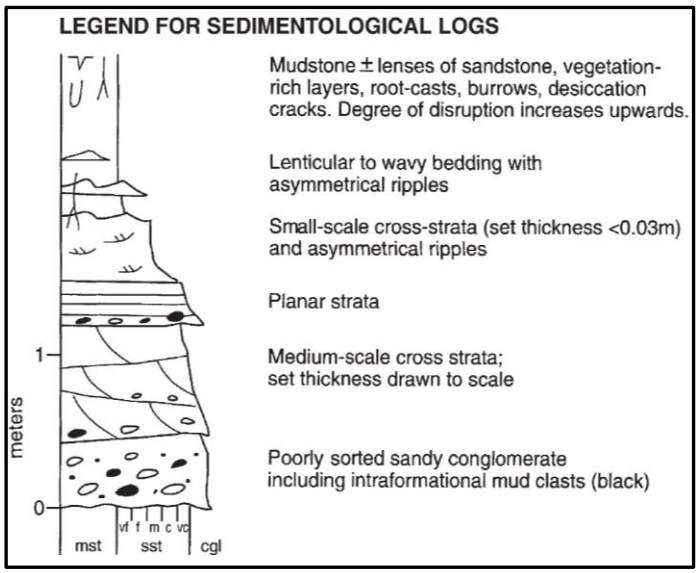

Chanel fill deposits also form within the channel system. Channel fill deposits form due to a progressively weaker channel flow (generally due to channel avulsion), resulting in finer grained deposition over time and a fining upwards succession being preserved (Boggs Jr., 2006; Nichols, 2009, Figure 3.3). Fine grained channel abandonment deposits generally overlie channel fill deposits.

Floodplains form laterally adjacent to channels and form the substrate which channels erode into and migrate (Smith, 1983, Figure 3.1). Floodplain deposits accumulate during seasonal flooding, resulting in fine grained deposition. Floodplain deposits form when the discharge rate exceeds the capacity of the channel (Nichols, 2009). As the water leaves the confines of the channel, it spreads out over the floodplain surface and loses velocity quickly. This velocity reduction results in proximal deposition of sands and silts leaving only a suspended clay load being transported and deposited away from the channel onto the more distal floodplain (Nichols, 2009).

Crevasse splays also form due to a breach of the channel. The breach initiates with a discreet breach of the levee that then widens and increases in size, volume and flow velocity (Slatt, 2006; Nichols, 2009). The increase in flow velocity results in a coarsening upwards silt-sand succession being preserved.

The Patchawarra Formation has been accepted as a meandering fluvial system deposited in a cool temperate climate from the following lines of evidence:

- Upward fining sand successions with coarse grained pebble lags, interpreted as point bar deposits from a meandering system (Apak, 1994; Alexander, 1998)
- Very fine grained mudstones and shales interpreted as flood basin and back swamp deposits overlying fining upwards point bar deposits (Williams, 1982).
- Palynological data containing entirely non-marine palyno-flora (Strong *et al*., 2002)
- Thick regionally extensive coal intervals with low ash and low sulphur content, suggesting formation from cool temperate peat blankets (Taylor *et al.,* 1988; Strong *et al.,* 2002).

- Recent spectral decomposition of 3d seismic data, showing preservation of meandering river plan-form geometries such as ox bow lakes and channel fill deposits (Nakanashi and Lang, 2001).

3.4 Three dimensional Architecture of channel bodies

Gibling (2006) introduced a model that divides channel bodies into single-story versus multistorey and mobile versus fixed channel geometries (Figure 3.4). This classification acknowledges the large influence of bank migration (lateral accretion), avulsion and vertical aggradation on channel bodies. Figure 3.4 shows how both multistorey and single storey channel bodies can be either mobile or fixed and that whether a channel body is single or multi storey is a function of both channel aggradation and reoccupation frequency. Reoccupation frequency is a factor controlled by geomorphic controls and fluvial stacking patterns (discussed below in 3.5 and 3.6). Meandering river systems create mobile channel bodies that can be either multi or single story, dependent on the stacking pattern nature.

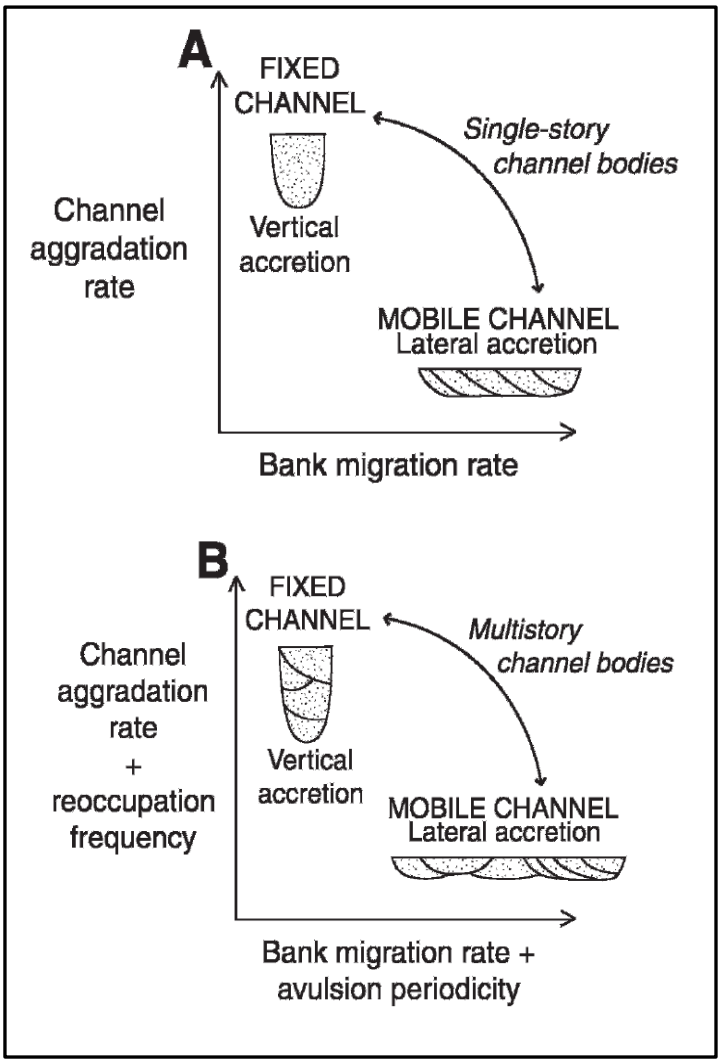

Figure3.4: Conceptual Diagram outlining the balance between the governing factors that influence the geometries of both single (A) and multi-story channel bodies (B). A high bank migration rate promotes lateral accretion and results in mobile channel body geometry. Conversely a low bank migration rate favours vertical accretion and fixed channel body geometry. (From Gibling, 2006).

3.5 Fluvial stacking patterns

Sequence stratigraphic concepts have been successfully converted and applied to the nonmarine realm to better understand the 3D architecture of channel bodies in fluvial-lacustrine environments (Galloway, 1989; Etheridge *et al*., 1998; Shanley and McCabe, 1994; Aitken and Flint, 1995; Posamentier and Allen, 1999, Lang *et al*., 2001, cited by Lang *et al.*, 2002).

The concept of sea level that governs sequence stratigraphic frameworks in marine environments cannot be applied to continental settings (Shanley and McCabe, 1994; Posamentier and Allen, 1999). Instead, accommodation space creation (A) relative to sediment supply (SS) (sometimes referred to as 'the fluvial equilibrium profile') for non-marine strata is comparable to sea level for marine strata (Shanley and McCabe, 1994; Posamentier and Allen, 1999; Lang *et al*., 2001.). It is useful to describe the amount of accommodation space creation versus sediment supply as a ratio: SS/A. The main factors that control SS/A are tectonic tilting, subsidence rate, fluvial discharge and sediment supply changes. Climate in turn controls both sediment supply and fluvial discharge to a high degree (Catuneanu, 2003). A sequence stratigraphic model relating SS/A relationships to fluvial systems tracts is adopted for this study (Shanley and McCabe, 1991; Wright and Marriott, 1993). Figure 3.5 outlines the fluvial systems tracts in relation to the SS/A ratio and the fluvial stacking pattern geometries that result. Fluvial systems tracts for this model are outlined below:

Fluvial low stand systems tract (LST)

During times of little to no accommodation creation and therefore a high SS/A ratio; lateral accretion dominates and reworking of sediments results in increased channel mobility and ultimately the amalgamation of channels to form laterally extensive sheet sand deposits (Figure 3.5a).

Fluvial transgressive systems tract (TST)

When the accommodation creation rate increases, the SS/A starts to decrease; channel mobility decreases and channels are able to vertical aggrade due to increased accommodation, resulting in increased channel isolation (Figures 3.5b, 3.5c). Peat mire and small lake formation is favourable when SS/A is decreasing.

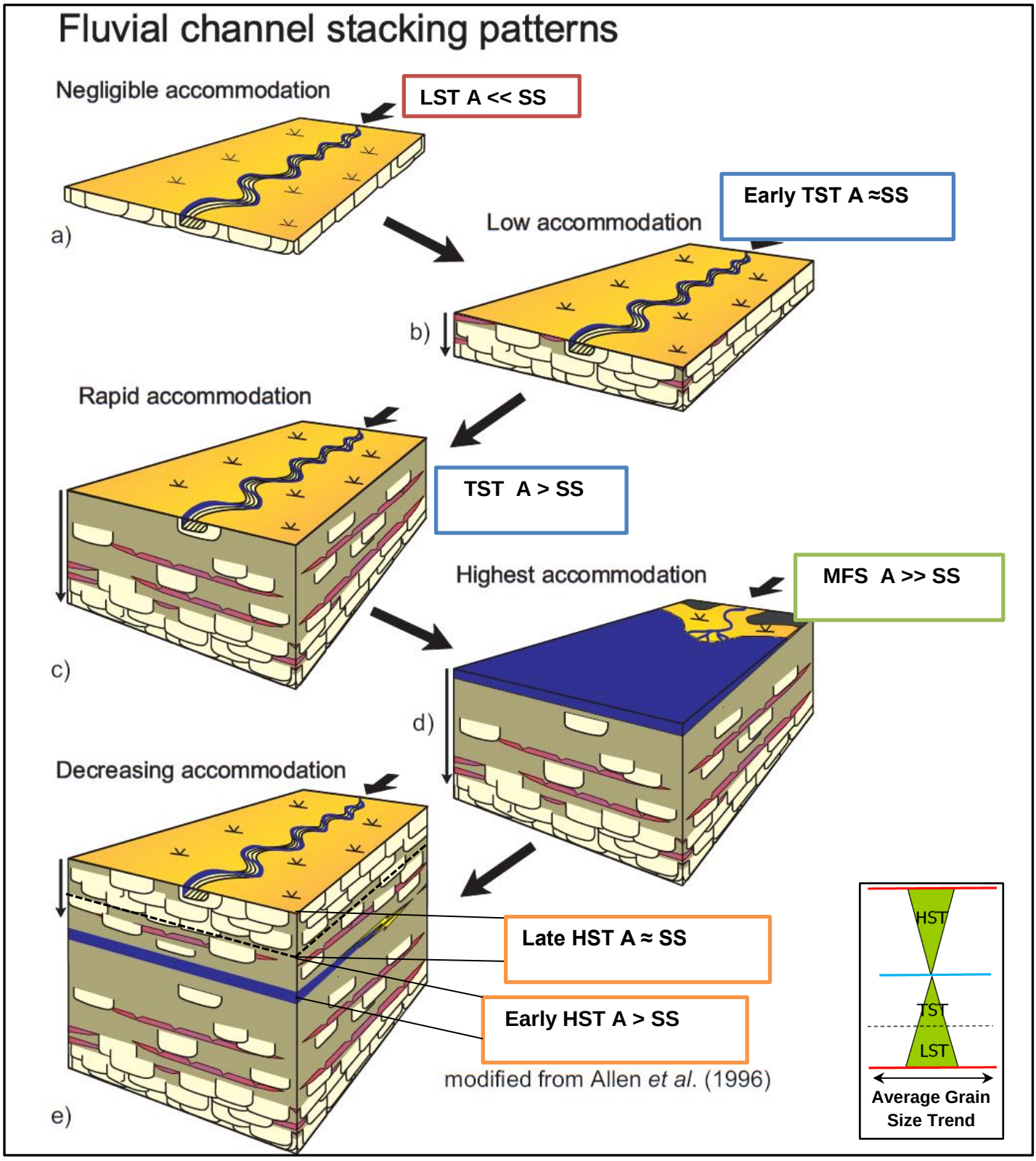

Figure 3.5: Fluvial channel stacking patterns as a result of SS/A and fluvial systems tracts. a.) Shows a low SS/A ratio, resulting in amalgamated channel sands of an LST. B.) Shows the initiation of a TST and a decrease in the SS/A ratio, channels are able to vertically aggrade and start to become more isolated. c.) Shows the continuation of a TST and the resultant isolation of channel bodies. d.) Shows the lowset SS/A ratio, sediment supply cannot keep up with accommodation creation and a widespread flooding event results. e.) Initiation of a decrease in accommodation, SS/A starts to increase and channels begin to become more connected with decreasing accommodation into the late HST where channel connectivity becomes high. A = accommodation space creation, SS = sediment supply (from Lang *et al*., 2001, modified from Allen *et al.* 1996). Bottom right- Average grain size trend depicts broad trend of the fluvial systems tracts.

Fluvial maximum flooding surface (MFS)

At the highest rates of accommodation creation, SS/A is at its lowest. Sedimentation is unable to keep up with accommodation creation and widespread flooding results (Figure 5d). Peat mires are drowned out and large lakes develop.

Fluvial high stand systems track (HST)

Directly after a fluvial MFS, sediment supply starts to catch up to accommodation space and SS/A increases. Channels are initially able to vertically aggrade during the early HST, but with increasing sediment supply become more mobile and vertical aggradation becomes more dominant with increasing SS/A towards the late HST (Figure 5e).

3.6 Superimposed channels

Channels accrete and migrate laterally through the floodplain. Over time channels can reoccupy the same space, migrating over and eroding into a previous channel deposit (Bridge and Mackey, 1993; Bridge and Tye, 2000; Gibling, 2006). Reoccupation results in superimposed, channel sequences stacked on top of one another (Figure 3.6). This superposition of channel systems results in the interconnectivity of channel bodies. However; within a channel system, smaller scale erosive events result in super position of bed forms within the same channel system such as chute bars or erosional bedding planes due to a higher energy influx (Bridge and Tye, 2000). The similarity of both the superimposed channel belts and superimposed intra-channel bed forms make it difficult to distinguish between the two using only vertical data (Bridge, 2003; Bridge and Tye 2000; Gibling 2006). Figure 3.6 outlines the various superposition geometries that can result due to reoccupation of a channel belt over the same space. 7a. shows the green channel overlying the purple channel; however over bank deposits separate the two channel deposits and the green channel has not eroded into the purple channel deposits. Both deposits can be distinguished and channel body depths measured from wireline log data. 7b. shows the superposition of three stacked channels. The red channel has entirely eroded the orange channel while the green channel has partially eroded into the red channel. If the basal erosional surface of the green channel onto the red channel can be identified; then the green channel depth can be measured from log data. The original depth of the red channel cannot be identified. 7c. shows the superposition of two channels, similar to the situation in 7b.

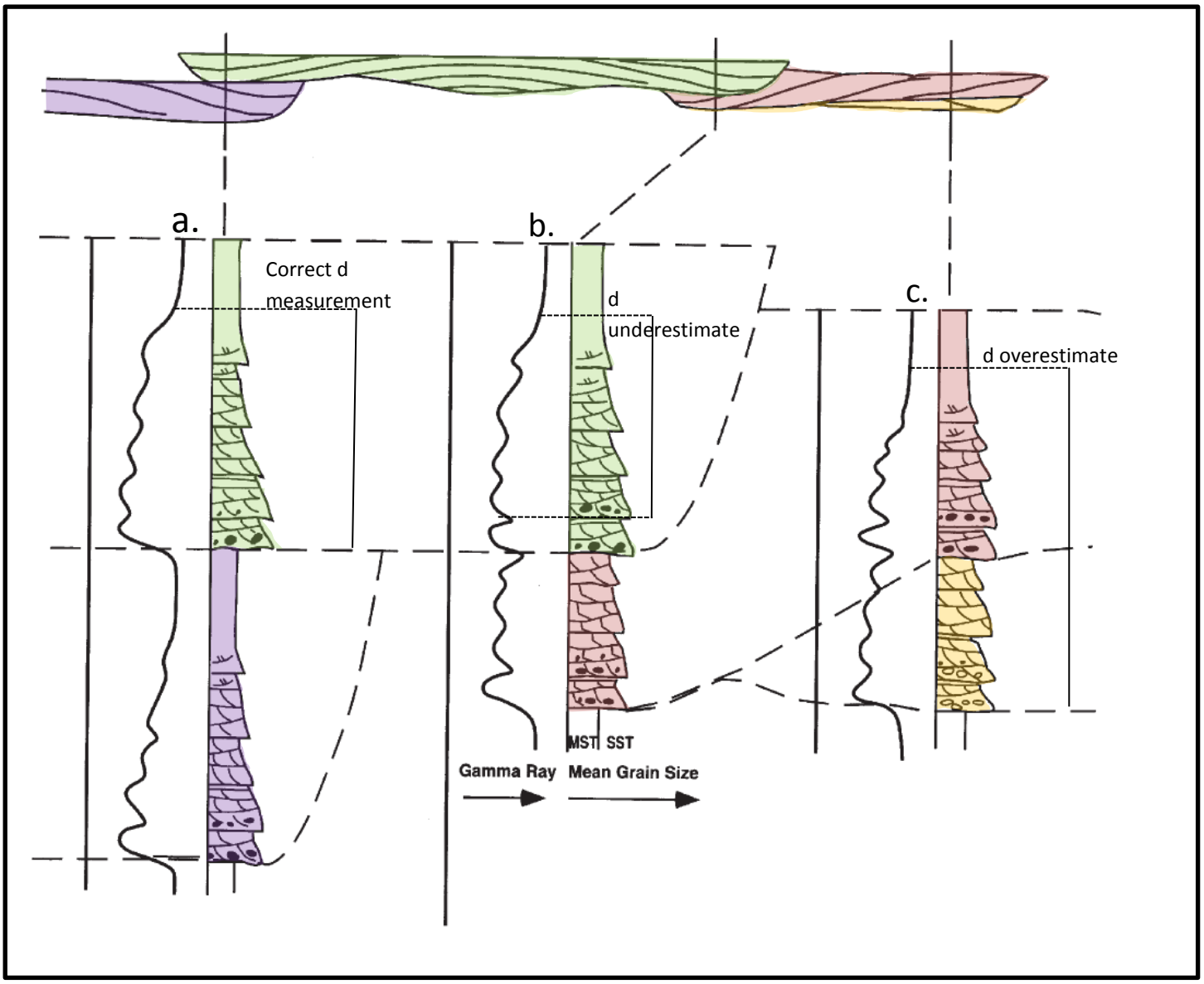

Figure 3.6: Superposition of channel belts. Individual channel belts have been shaded for clarity. Log on the left hand side is an idealised gamma-ray log while right hand side shows idealised sedimentary log including likely bedforms. MST = mudstone, SST = sandstone. a.) Shows two channels that are isolated from each other and not superimposed. The two channels are separated by overbank deposits and both channels are easily distinguishable. b.) Superposition of one channel (Green) into two others (Red and Orange). The orange channel has been entirely eroded by the red channel and the red channel has been partially eroded by the green channel. C.) Superposition of one channel onto another. The red channel has partially eroded into the orange channel. Examples of a correct, under, and over measurement of bankfull depth are also shown, highlighting the difficulty of bankfull determination from wireline log data.

3.7 Determining channel depth from one dimensional data.

The depth of a single story channel is measured by the bankfull depth (Bridge and Mackey, 1993). The definition of the bankfull depth of a channel is illustrated in Figure 3.7. Bankfull depths can be approximated to the thickness of a full channel bar or channel fill deposit (Bridge and Mackey, 1993; Bridge and Tye, 2000; Gibling, 2006).

In wireline log data, bankfull depth is defined as the last fining upward succession of a sand body, including the overlying over bank deposits, sometimes capped by a coal (Strong *et al*., 2002, Figure 3.6). As discussed above in 3.6; a single storey channel deposit can be difficult to differentiate from a superimposed multistorey channel deposit using only 1D data (Bridge and Tye, 2000; Miall, 2014). Using Figure 3.6 as an example; bankfull deposits could be measured for:

- Both the green and purple channel deposits in case a, because they are not superimposed.
- Only the green channel deposit in case b.
- Only the red channel deposit in case c.

There is a danger that the combined thickness of the multistorey stacked channel deposits in cases b and c could be misinterpreted as a single storey channel and bankfull depth overestimated (case 7c). Similarly if an erosive bedding surface within a single channel deposit (as discussed in 3.6) is interpreted as the base of a new channel storey eroding into an older channel deposit, the bankfull depth will be underestimated (case 7b).

3.8 Estimating channel belt width from one dimensional data

A channel belt deposit is preserved over time in plan form geometry; this study therefore focusses on mapping channel belt bodies in palaeogeographic intervals, rather than individual channels. A number of authors have explored different relationships and techniques between bankfull thickness and channel belt width in ancient and modern day meandering systems. The various authors used both large compiled datasets and data from specific study areas to derive empirical regression equations relating bankfull thickness to channel belt width. For a comprehensive summary of these works see Tables 1-A and 1-B in Shanley (2004) and Gibling (2006) pp:741-747.

Relationships derived by Robinson and McCabe (1997) will not be used in this study because their study focused on a braided river system. Gibling (2006) compiles a dataset

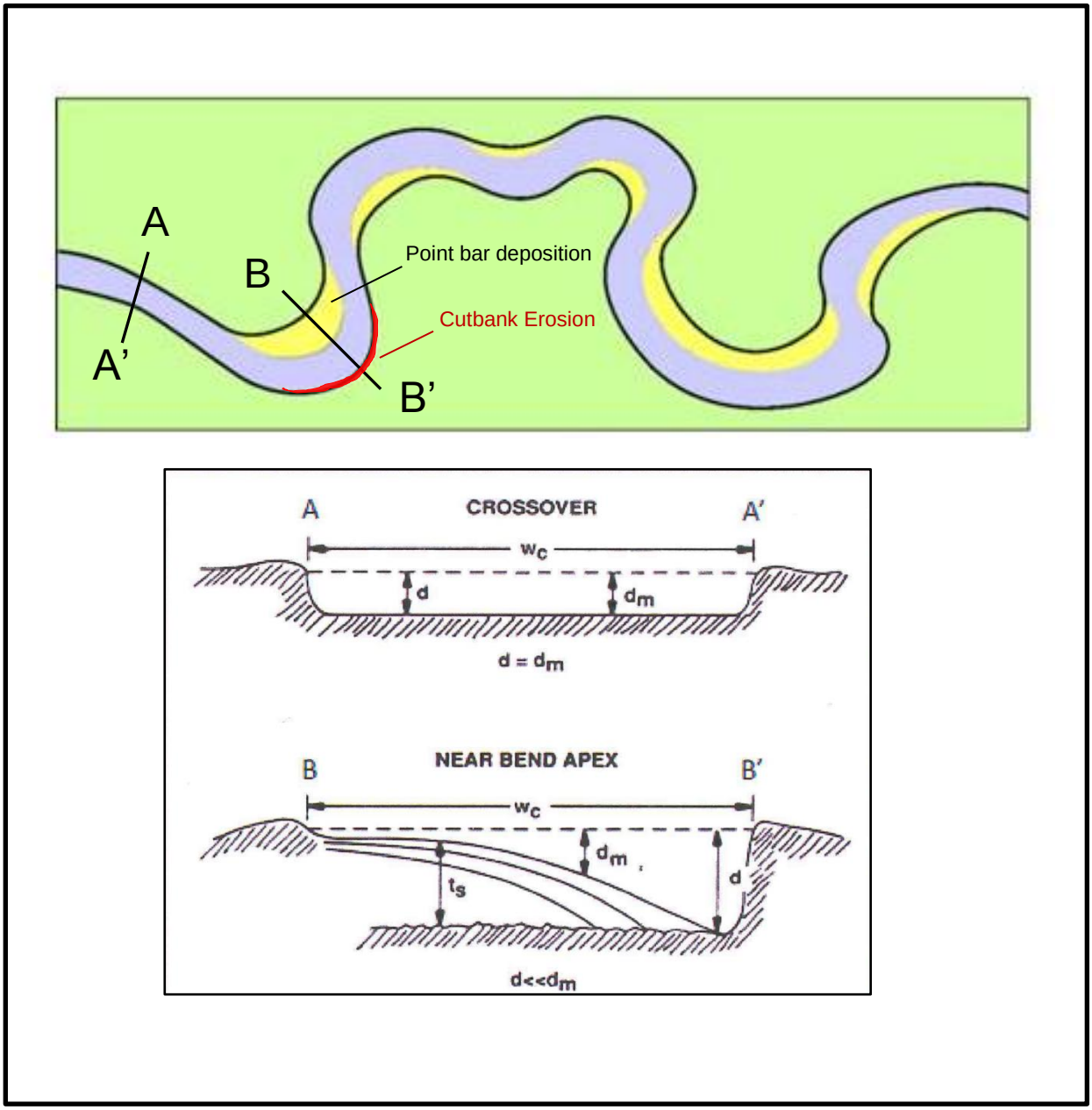

Figure 3.7: Schematic diagram showing the bankfull depth at different points in a meandering channel. The cross sections show the relationship between maximum bankfull depth, d_m, bankfull depth, d, and storey thickness t_s. Cross section A-A' shows the channel at the crossover, where flow velocity and channel depth is uniform across the channel. d is equal to d_m across the entire channel, and no storey deposition takes place. B-B' shows the channel at the near bend apex, where velocity is highest at B' and lowest at B. d is only equal to d_m at the thalweg (B'), where no stories are deposited. Where stories are deposited, d_m is equal to the sum of the t_s and d. (Modified from Bridge and Mackey and from Nichols, 2009).

of both ancient and modern day river systems; however, Gibling (2006) provides only a large envelope of possible channel belt width to bankfull thickness ratios (W/T) from the entire data set and does not derive empirical regression equations. For this reason the Gibling (2006) dataset will not be used in this study for channel belt width estimation, Although; Gibling (2006) outlines well the wide range of W/T for meandering deposits, even within a single system.

Strong *et al*. (2002) identified 8 empirical regression equations from previous authors that were suitable for channel belt width estimates for palaeogeographic reconstruction of the Patchawarra Formation. These equations are summarised below:

All of the equations used follow an empirical regression relationship; that relates any two variables by a power law, in this case; Channel belt width to bankfull depth (Collinson, 1978; Williams, 1986; Fielding and Crane, 1987; Bridge and Mackey 1993). The equations follow the general form:

$W_c = x\ h^{y}$ (equation 1).

Where,

W_c = Channel belt Width

h = bankfull height

x = constant

y = constant number (exponent).

Collinson (1978)

Collinson (1978) combined equations from previous works of both Leeder (1973) and Carlston (1965) and related them to observed ancient deposits and modern rivers. Carlston's equation related channel belt width to discharge rate while Leeder's equation related bankfull depth to channel belt width:

$$W_c = 65.6\ h^{1.57}$$

It was noted by Bridge and Mackey (1993) that Collinson did not make the distinction between maximum bankfull depth and channel depth, and suggested that they were

equal. Furthermore Bridge and Mackey (1993) highlighted that Collinson combined the two equations that were themselves based on different measurement units. However, despite these highlighted caveats; Collinson's equation was still accepted by Bridge and Mackey (1993) and is still accepted in present literature (Strong *et al*, 2002; Gibling, 2006).

Williams (1986)

Williams used published literature measurements of meandering systems to test the Langbein and Leopold theory (1966), relating sinuosity to channel belt width. Williams derived 31 empirical equations relating channel belt geometries and sizes. The equation derived relating bankfull height to channel width was:

$W_c = 148.00h^{1.52}$

This was proven by Williams (1986) by statistical means to be a robust empirical equation.

Fielding and Crane (1987)

Fielding and Crane evaluated all river systems including: braided, anastomosing, straight, meandering and incised valley fills. Fielding and Crane derived empirical equations for the entire fluvial spectrum:

$W_c = 0.01h^{2.9}$ (End member case: Incised, straight, confined channels)

$W_c = 0.95h^{2.07}$ (Some lateral migration, excludes highly incised and confined channels)

$W_c = 12.1h^{1.85}$ (Best fit line of all data)

$W_c = 64.6h^{1.54}$ (Modern meandering systems)

$W_c = 513h^{1.35}$ (End member case: completely unrestricted lateral flows, attributed to gravelly braided streams)

For this study the modern meandering system equation shall be used.

Bridge and Mackey (1993)

Bridge and Mackey (1993) conducted a robust study of sandstone body dimensions, using processed based theoretical modelling. Bridge and Mackey (1993) ran a number of simulations investigating the width and thickness relationship of fluvial sandstone bodies in response to the following varying inputs:

- Channel belt aggradation rate

- Avulsion period
- Overbank sedimentation rate
- Avulsion periodicity
- Bankfull depth
- Tectonic tilting of the floodplain
- Depth of burial (compaction factor effecting channel deposit thickness)

Bridge and Mackey (1993) also integrated and combined empirical regression equations from previous authors as well as observed data from modern rivers and ancient deposits. Bridge and Mackey formulated the following equations:

$W_c = 59.86h^{1.8}$ (Process based regression determined)

$W_c = 45.76h^{1.52}$ (Combined with Leeder, 1973,)

$W_c = 192.01h^{1.37}$ (Best fit line of all data compiled in the study and calculated results)

$W_c = 107.53h^{1.52}$ (Combined with Leeder, 1973,)

$W_c = 86.10h^{1.57}$ (Combined with Crane, 1982)

All of the above equations by Bridge and Mackey (1993) are well accepted within the literature (Gibling 2006; Strong *et al*., 2002; Shanley, 2004) and will be used in this study. The Equations selected in this study follow Strong *et al.* (2002). These Equations were identified by Strong *et al*. (2002) as being the most applicable to the Patchawarra Formation from the various lines of evidence discussed above. The study area of the Strong *et al.* (2002) study is very proximal to the Tenappera region study area (Figure 1.2) and so the fluvial style is expected to be very similar for these two studies.

It must be noted that while these empirical equations are the best form of estimating channel belt width from bankfull measurements; these empirical equations relate one variable (bankfull depth) to another (channel belt width). However, channel belts form and are preserved in response to a number of variables as both proven and outlined by Bridge and Mackey (1993). Therefore it is impossible and statistically illogical to try and model exactly; an output that is dependent on a number of variable inputs, using only one of those inputs (Williams, 1986). In this sense broad generalities and ranges of variability are reflected in the empirical equations, not calculated relationships.

Chapter 4: Data and Methods

4.1 Introduction

The Tenappera Trough Region covers an area covered approximately 6400 km^2 (figure 1.2). The study utilised all 379 wells in the area containing Patchawarra intersections. The pre-existing chronostratigaphic framework currently used by Santos for Cooper Basin stratigraphy was adopted to correlate all intervals into high resolution genetic units. Correlation of the Patchawarra was carried out using gamma ray (GR) and sonic (DT) wireline logs. A cross plot was generated for GR vs. DT to determine likely lithologies with a typical colour scheme to aide in the correlation process. Within the study area the Patchawarra Formation was divided into 20 correlatable genetic intervals bounded by 19 key surfaces and 2 major unconformities. An electro facies log scheme was established for the correlated wells. Log signature maps were then generated for each interval. Palaeocurrent direction was interpreted from 2 wells with available image log data. Analogue studies identified geometric relationships and structural controls on channel belts deposited from a cool-temperate, peat dominated meandering river system. Channel belt width estimation was carried out using pre-established empirical thickness to width plots and measured sand thicknesses for each interval. 2D seismic sections were utilised over present day structural highs to determine relative timing of uplift where Patchawara sections were absent.

Palaeogeographic reconstructions were then carried out for each interval, using analogues, palaeocurrent interpretations, available Seismic horizon thickness maps and channel belt width calculations as guiding controls.

The workflow for this study is outlined in Figure 4.1.

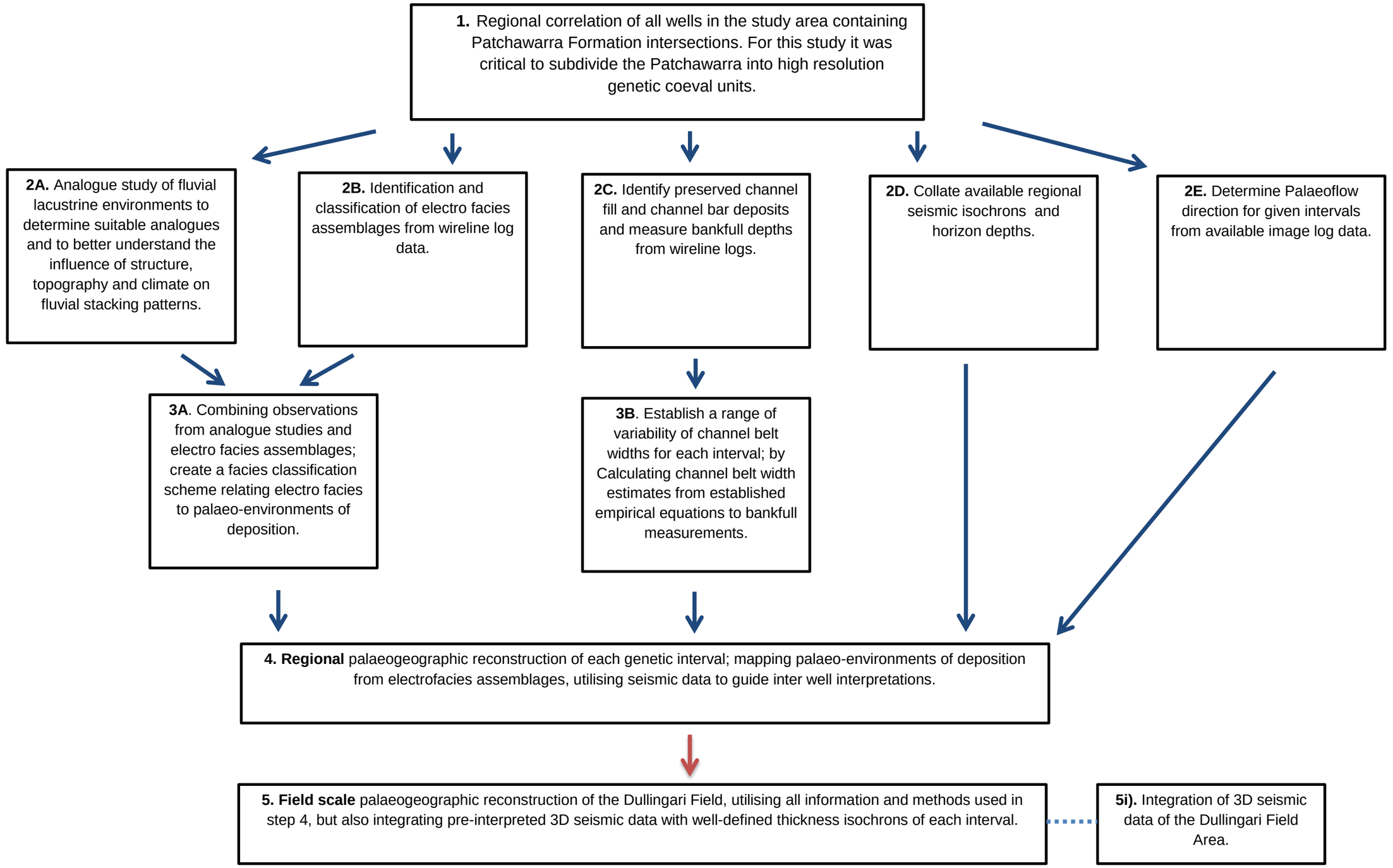

Figure 4.1: Workflow diagram for this study, outlining key steps undertaken to achieve the aims outlined. Step 5 was not achieved due to time restraints but is recommended for further work.

4.2 Wireline Well-Log Data

379 wells in the study area intersect the Patchawarra Formation, all of which were utilised in this study (Figure 4.2). The majority of these wells penetrate basement and therefore represent the full Cooper Basin section present at a given well location.

Gamma ray and sonic wireline logs were the primary data used for correlating wells as well as determining facies associations. 22 wells have partial wireline data, but the lower parts of the well were not logged, this is particularly evident in the Northern Dullingari Field beyond the VC50 horizon.

Wireline log tracks were accessed through Paradigm Geolog software.

4.3 Image Log Data

Image log data for the Patchawarra Formation has been acquired in two wells within the study area: Crowsnest 2 and Dullingari North 18. The image log was acquired with a 6 padded Simultaneous Acoustic and Resistivity Tool (STAR), however only the resistivity mandrel was operated and no acoustic data was recorded. The data was acquired for the identification of natural fracture sets and *in situ* stresses. The focus of this data acquisition and processing was therefore structural and not sedimentological. Cross bedding imaging is poor and no sedimentological data has been previously measured and recorded from it. The image log data has been corrected for borehole deviation.

4.4 Seismic Data

3.4.1 Regional Scale Seismic Data

Three regional scale combined interval isochron maps were used in the study; VC00-VC00 (Figure 4.2), VC30-VC50 (Figure 4.3) and VC50-ZU00 (Basement) (Figure 4.4) isochron maps. Regional mapping of each individual interval using 2D seismic data alone is not possible for the Patchawarra Formation due to the abundance and irregularity of coal layers in the formation (Strong *et al*., 2002).

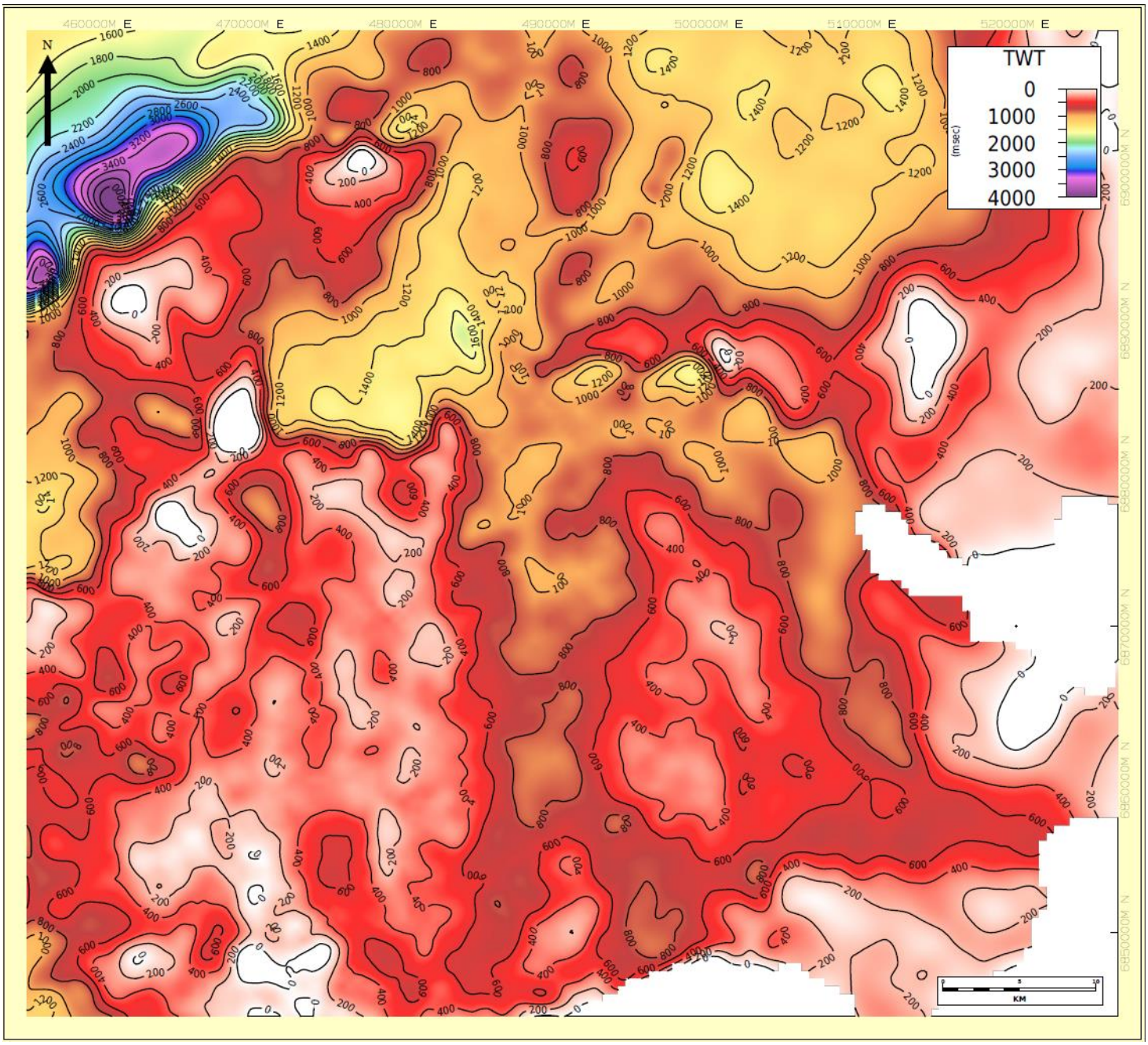

Figure 4.2: VC00-ZU00 isochron thickness map. Isochron Thickness colour scale is in TWT. All wells used in the study are shown. 2D seismic lines are annotated A-A' over the Burke Field and B-B' over the Nappacoongee Trend. Note the different TWT scale/colour scheme for each isochron.

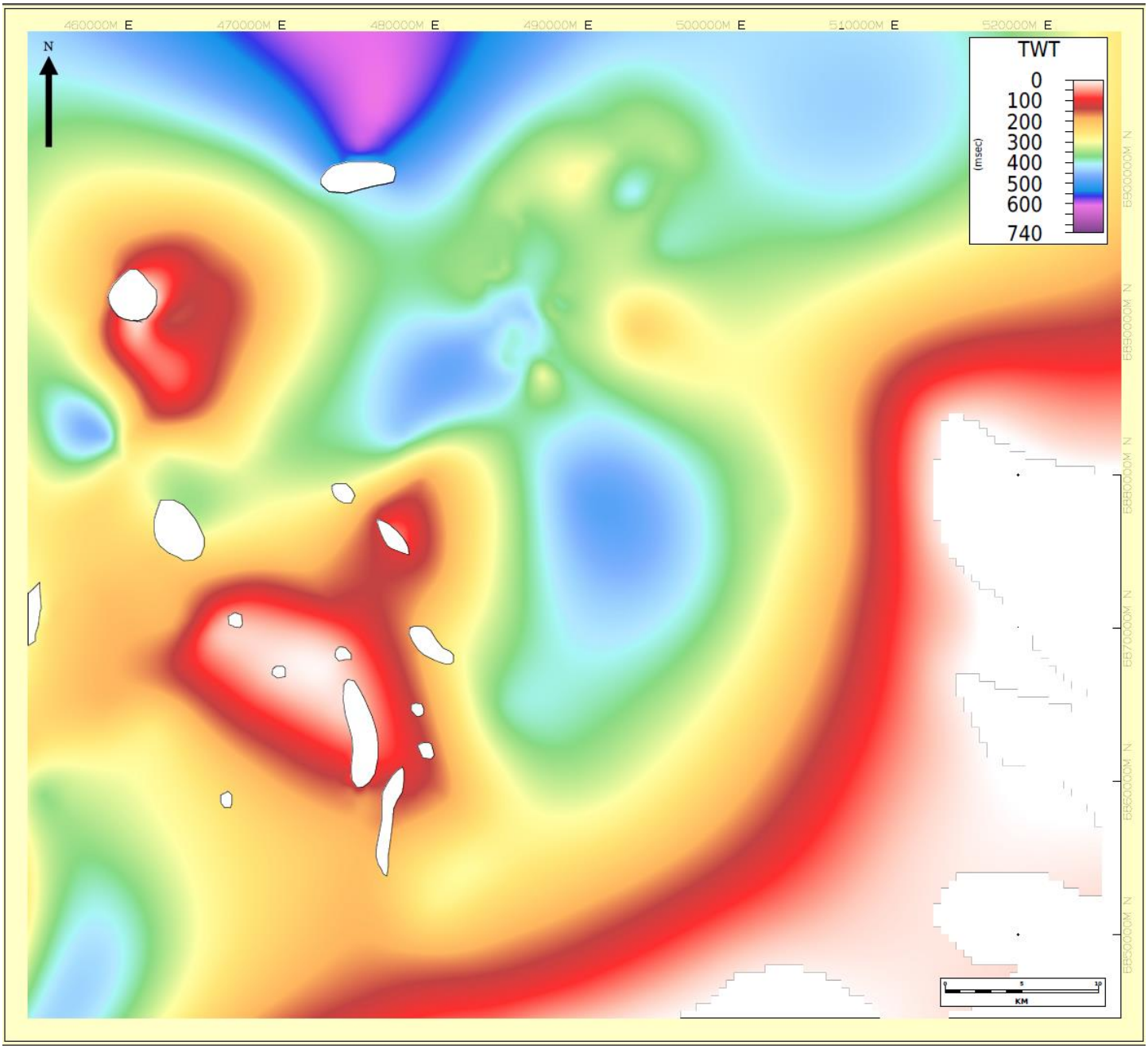

Figure 4.3: VC30- VC50 isochron thickness map. Thickness colour scale is in TWT. All wells used in the study are shown. Note the different TWT scale/colour scheme for each isochron.

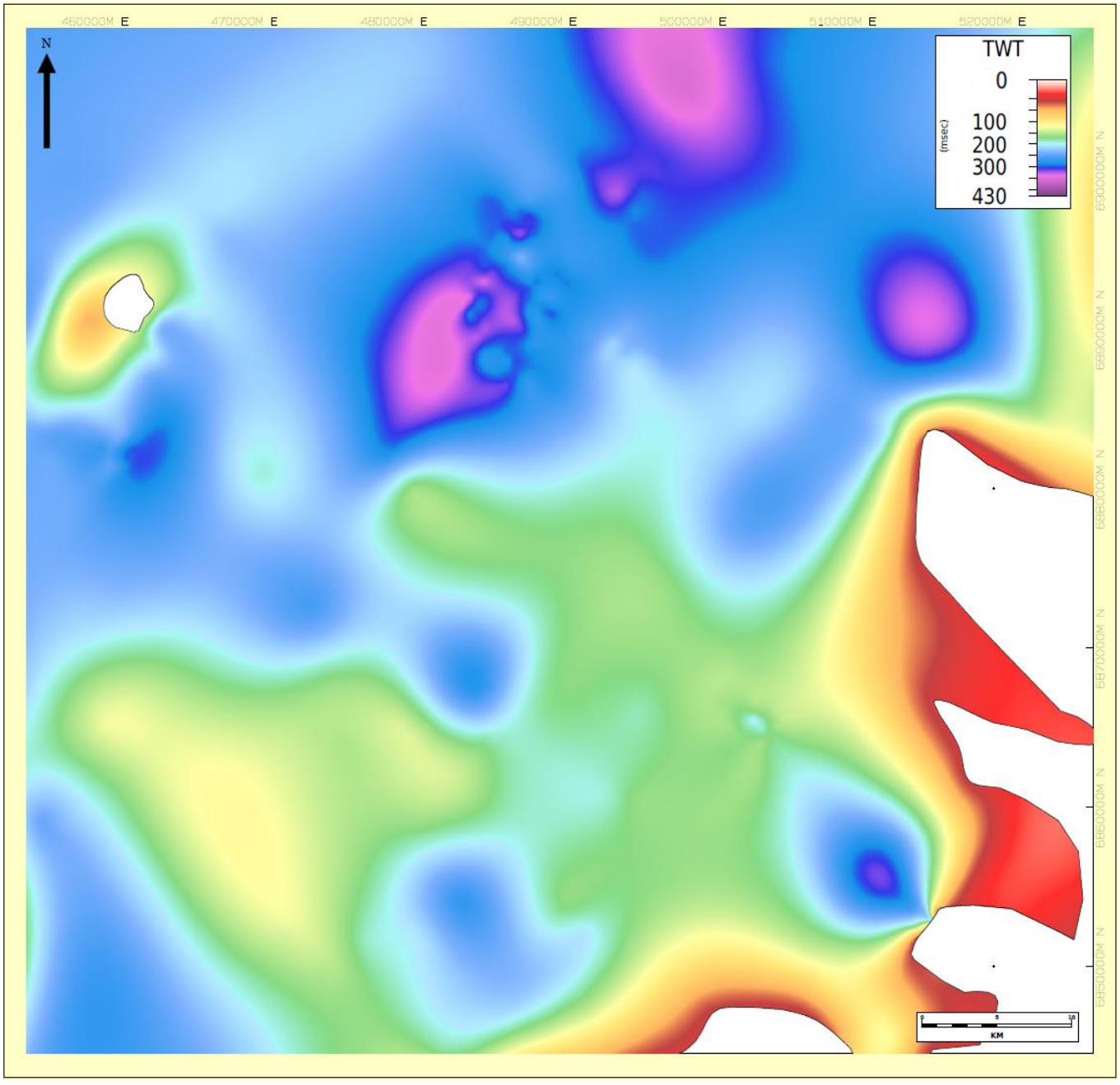

Figure 4.4: VC00- VC30 isochron thickness map. Thickness colour scale is in TWT. All wells used in the study are shown. Note the different TWT scale/colour scheme for each isochron.

The Z horizon depth structure map is a culmination of many 2D seismic data sets of numerous vintages and has been processed and mapped with well log control for the entire Cooper Basin. The Z horizon marks the Top Basement Horizon and includes the Merrimelia/Tirrawarra Formations informally as basement.

Two 2D seismic lines over the: Burke/Dullingari field and the Nappacoongee Trend, were utilised to determine relative timing of uplift and distinguish non-depositional surfaces from post-depositional erosional surfaces (Figure 4.2).

4.5 Correlation of the Patchawarra Formation into Genetic Coeval Units.

4.5.1 Rationale

Before palaeogeographic reconstructions could be carried out; The Patchawarra Formation in all wells in the study area had to be chronostratigraphically correlated into coeval, genetic intervals. Coeval intervals form the basis of the log signature maps from which palaeogeographic reconstruction could be interpreted.
A robust chronostratigraphic framework dividing the Patchawarra Formation into high resolution genetic intervals, well constrained with palynology has been developed and is currently used by Santos (Figure 4.5) (Apak 1994; Apak *et al*. 1997; *Lang et al.,* 2001; Lang *et al*., 2002; Strong *et al.,* 2002; Wood, G., 2004). However, this framework had only been confidently applied to 33 of the 379 wells correlated in detail.

It is important to note that a well-defined and comprehensive palynological framework has been developed for the Patchawarra Formation for the entire Cooper Basin. However; local high temperatures within the Tenappera Trough Region (Figure 4.6) due to radioactive decay in underlying granitoids have resulted in palynomophs being thermally altered and carbonised (Wood, G., Pers Comms, 2014). Therefore palynological data is very scarce and where present; assemblages are poorly preserved and limited. For this reason biostratigraphic correlation cannot be implemented in the study area.

In some fields, such as the Dullingari and Stokes fields, correlation had been made on field wide scales. These correlations were of differing vintages and in some cases identified different key surfaces and intervals. Therefore it was necessary and vital to

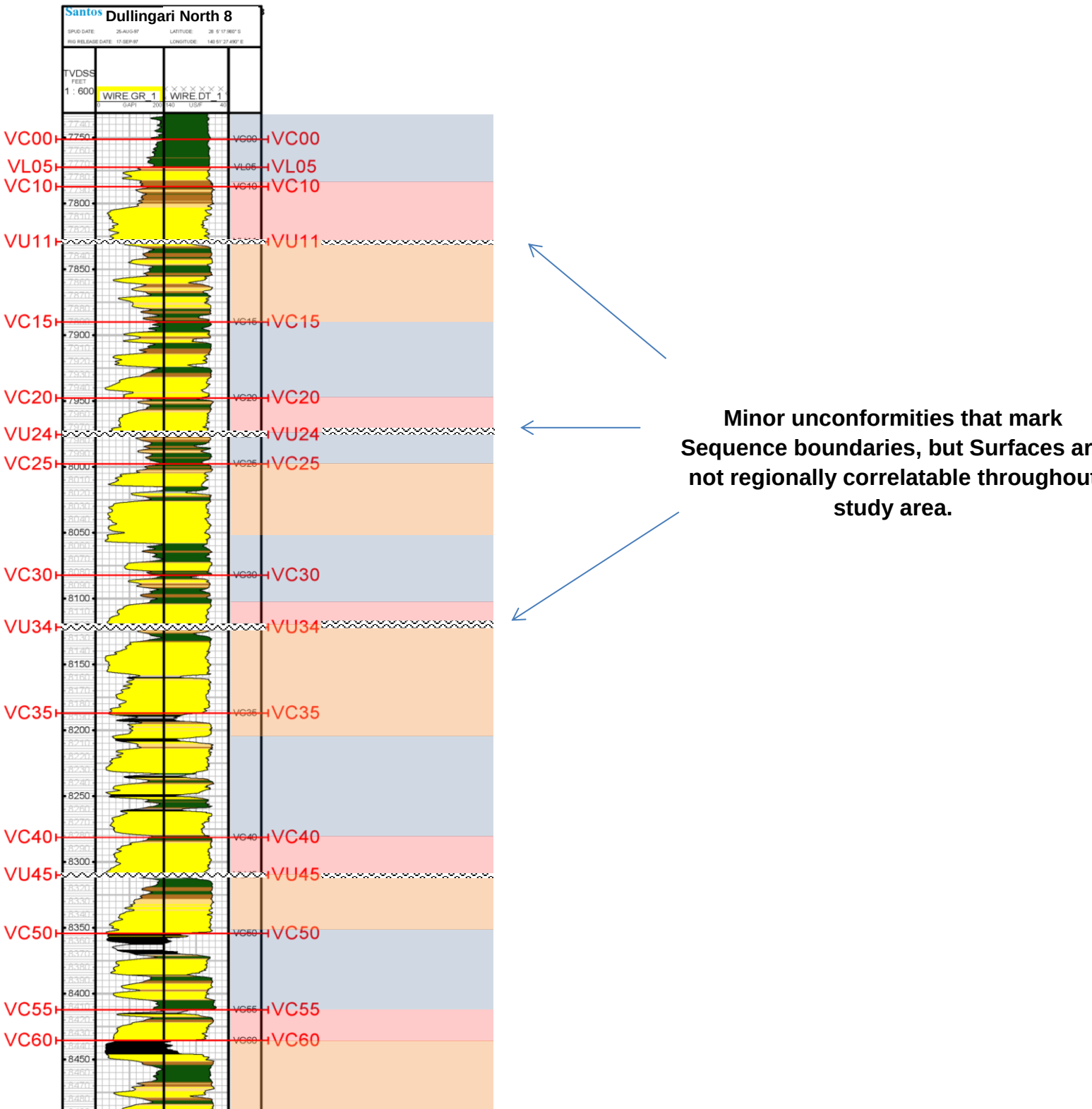

Figure 4.5: Chronostratigraphic Framework adopted and applied to a well within the study area. (Cross plot colour scheme applied) MFS surfaces and regional coals are the best surfaces to track using wireline data, and correspond to a High GR response but generally an indifferent DT response from other siliclastics, sometimes a slight inflection to a slower sonic velocity. Systems tracts have also been adopted, and it can be seen that the systems tracts do not always correspond to characteristic fluvial sections, indicating a high degree of autocyclic control within the meandering fluvial system.

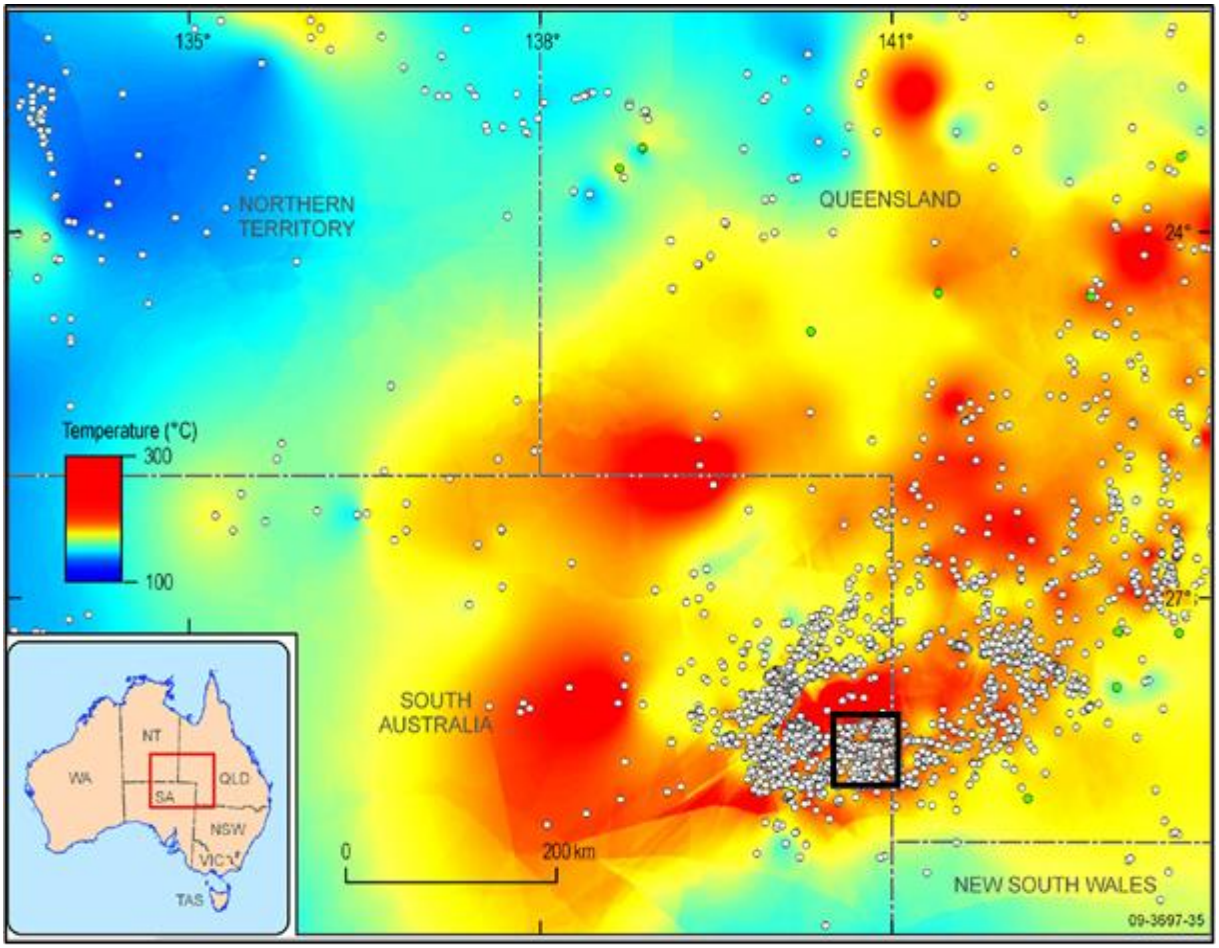

Figure 4.6: Regional subsurface temperature map of the Cooper-Eromanga Basin. Extrapolated from bottom hole temperature data to 5km depth. Map shows local high temperatures in the Tenaperra Trough Region. The study area is outlined by the black area. (From Radke, 2009, modified from Chopra and Holgate, 2005).

first correlate all wells in the study area consistently, using the established chronostratigraphic framework.

The correlation of the wells in the study area was achieved using the following steps:

- Constructing a cross plot for GR vs. Dt to visualise likely lithologies with a typical colour scheme.
- Identifying the chronostratigraphic framework, recognising key surfaces and genetic intervals.

- Constructing a skeleton grid of wells composed of two N-S and two E-W cross sectional lines, containing 10-15 wells each.
- Correlating skeleton grid wells with reference wells
- Loop correlating wells from skeleton grid lines with other skeleton grid lines and reference wells, to ensure consistency.

Correlating remaining wells to skeleton wells, ensuring consistency on both field wide and regional scales.

4.5.2 Gamma ray vs. sonic velocity log as a visualisation of likely lithology

A cross plot of GR vs DT was constructed using Geolog software, to visualise likely lithologies. Six polygons were defined from the cross plot, based on typical log responses for the given lithologies (Figure 4.6). Typical log responses for basic lithologies are set out in Serra (1975), Serra *et al*., (1980) and Rider (1990). These authors conclude that gamma ray logs are an acceptable proxy for grain size in most siliclastic systems, with the exception of coal, that shares a very low gamma response with sand. The use of the DT log is primarily for the differentiation of coal from sand. It is important to caution that Rider (1990) outlines the many caveats of using gamma-ray logs for litho-typing and notes that there are many exceptions. However, the typical log responses hold true within the Patchawarra Formation, with no notable perturbations (Apak, 1994, Alexander, 1998, Strong *et al.*, 2002).

The cross-plot used has been constructed using typical log responses for lithology that has then been adapted to better represent lithologies within the Patchawarra Formation (Santos Internal Document, 2014). The cross-plot created was then applied to the tracks on all wells during correlation (Figure 4.7)

4.5.3 Identifying and adopting the chronostratigraphic framework of the Patchawarra Formation.

The Chronostratigrahic Framework of the Patchawarra Formation has been developed through the work of numerous authors (Kuang, 1985; Veevers and Powell, 1987; Apak 1994; Apak *et al.* 1997; Lang *et al.*, 2001; Lang *et al.,* 2002; Strong *et al*., 2002; Wood, G., 2004). The emphasis of these works has been the identification and correlation of key surfaces that separate time equivalent intervals. Lang *et al.,* (2002) identify key surfaces in the fluvial-lacustrine as maximum flooding surfaces (MFS) and Sequence Boundaries (SB).

Maximum flooding surfaces mark the maximum value of SS/A and mark the change from a non-filling to a filling nature (Posamentier and Allen, 1999). Maximum flooding surfaces are marked by a high gamma log response and the inflection point between a fining upwards succession and a coarsening upwards succession (Figure 4.8a). Maximum flooding surfaces can also be marked by coals if the conditions suitable for peat development (Figure 4.8b).

Sequence boundaries are marked by an unconformity and result from the creation of negative accommodation space (Lang *et al.,* 2002). Within the setting of the Patchawarra Formation this equates to the intermittent uplift events discussed in Chapter 2. Sequence boundaries are much more difficult to identify on the log response than MFS. Sequence boundaries are generally marked by an erosional sand scour surface, represented on the log signature by a low gamma sand body with a sharp boundary (Figure 4.8c).

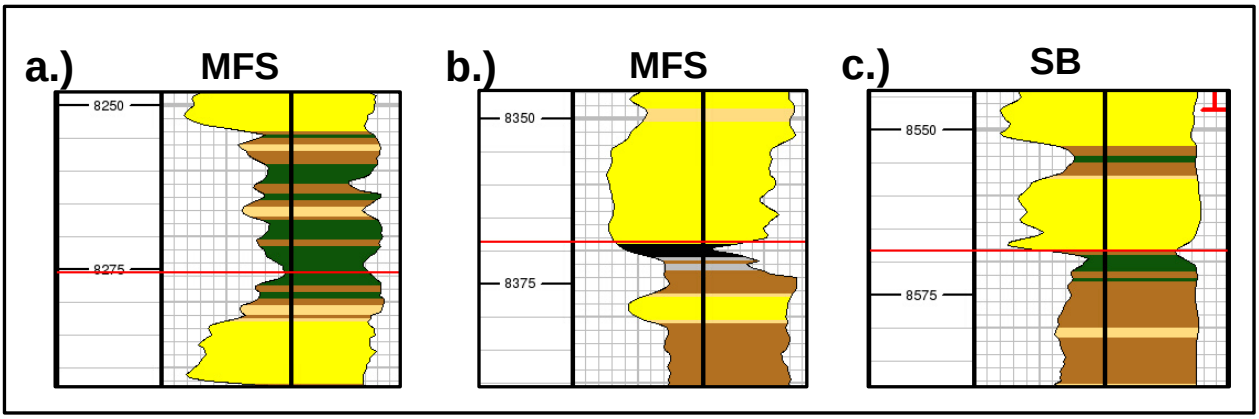

Figure 4.8: Key surfaces (marked by red line) used within the chronostratigraphic framework. a.) Shows the MFS defined as the high GR inflection between a fining upward and a coarsening upward succession. b.) Shows the MFS where peat development was favourable, marked by a coal. c.) Shows a sequence boundary defined by an erosional sand scour surface, marked by a sharp low GR response.

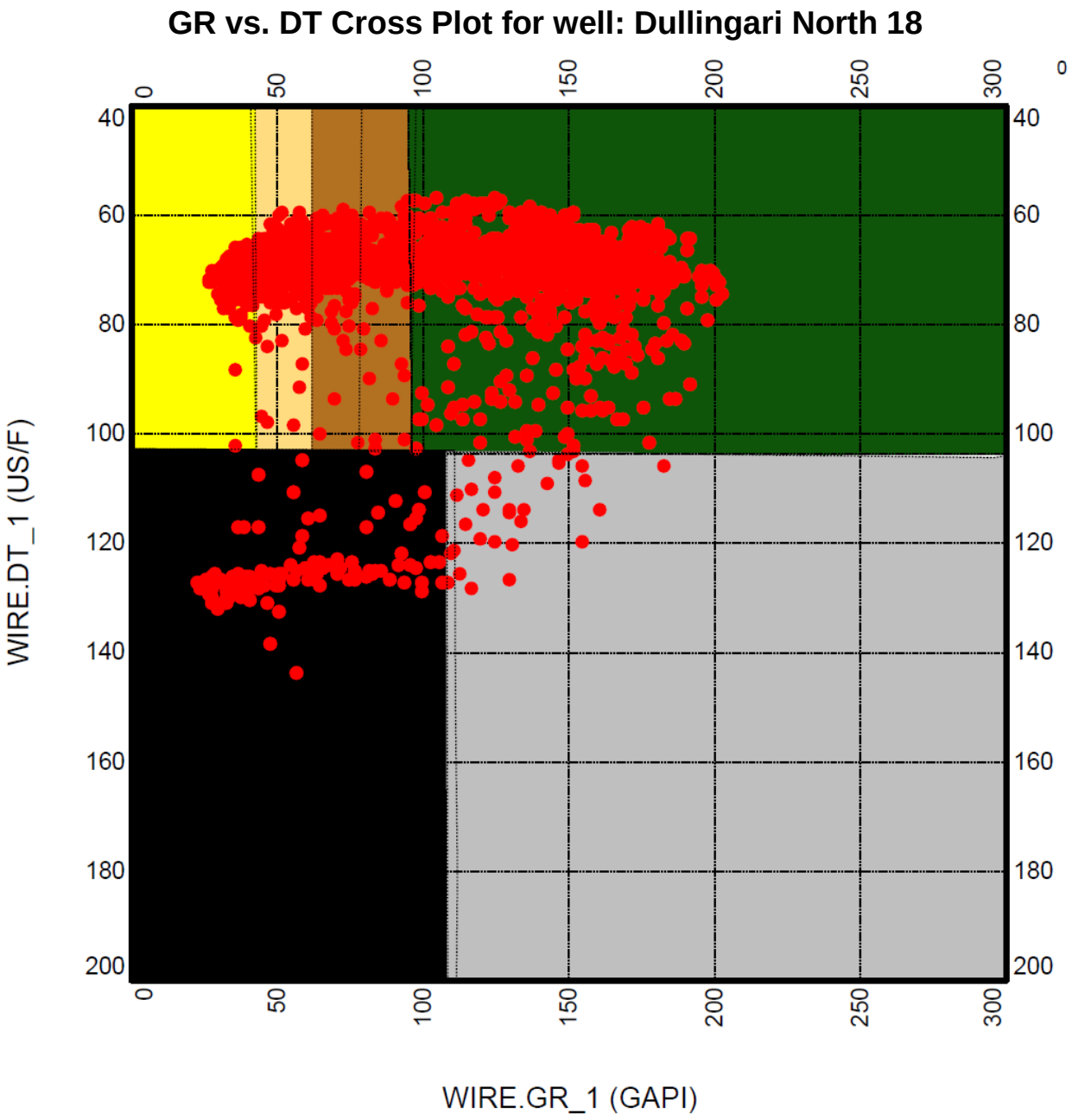

Lithology	DT (µs/ft)	GR (GAPI)
Sand	32-110	0-42
Silty Sand	40-110	42-61
Sandy Silt	40-110	61-93
Shale	40-110	93+
Coal	110+	0-109
Carbonaceous Shale	110+	109+

Figure 4.6: GR vs DT cross plot. GR is plotted on the X-axis and is measured in industry standard (GAPI) units. DT is measured on the Y-axis and is measured in industry standard Inverse of Sonic velocity or 'slowness' units (micro-seconds per foot).The cross plot contains 6 polygons that divide the log tracks into lithofacies. The red dots show the distribution of data points of a single well (Dullingari North 18). The lithology at each point corresponds to the polygon that the point is in within the cross plot. The legend table shows values for each polygon and colours representing each lithology

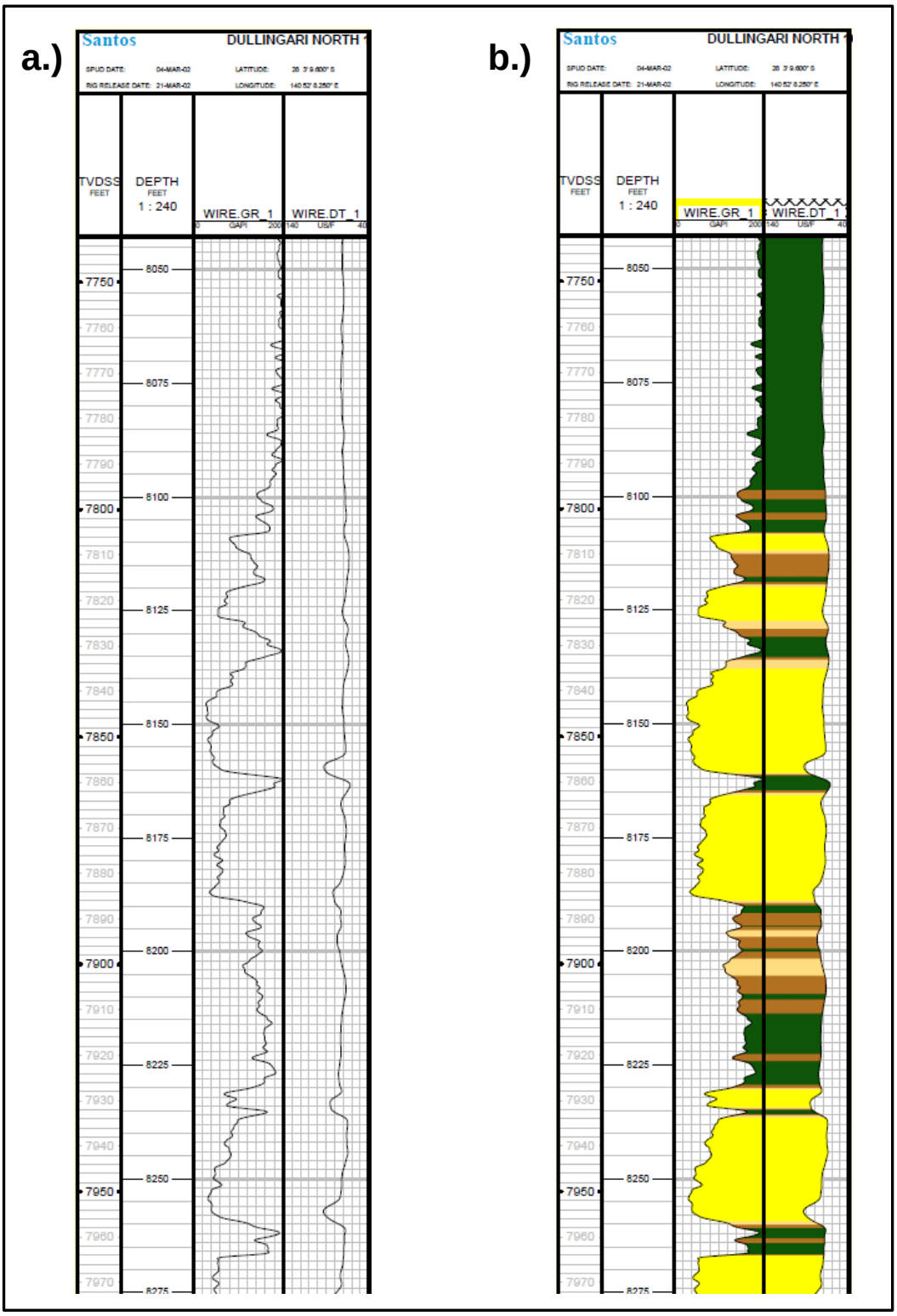

Figure 4.7: Example of GR and DT log tracks of the upper Patchawarra Formation from a well within the study area (Dullingari North 16). a.) Shows the original log tracks before the cross plot was generated and applied. b.) Shows the log tracks with the cross plot lithology colour scheme. The colour scheme aides in likely lithology visualisation and assists in correlation.

4.6 Palaeocurrent from Image log Data.

Simultaneous Acoustic and Resistivity (STAR) micro-resistivity image log data was analysed for both Crowsnest 2 and Dullingari North 18 wells, to attempt to identify bedding and cross bedding features in sandstones beds of the Patchawarra Formation. If cross bedding foresets can be distinguished from the image logs, then a palaeocurrent direction can be determined.

Because the wellbore is cylindrical, any planar dipping structure intersecting the wellbore is expressed in a sinusoidal form on the wellbore surface(Figure 4.9). This sinusoidal wave can be resolved to give the dip of the plane relative to the wellbore. Once corrected for the deviation of the wellbore from vertical, then the true dip of the plane is determined. Structural dip is then corrected for using shale bedding; using the assumption that shale bedding was initially deposited horizontally and any tilting is due to post-depositional structuring (Figure 4.10). This then gives the original dip and dip direction of the intersected plane.

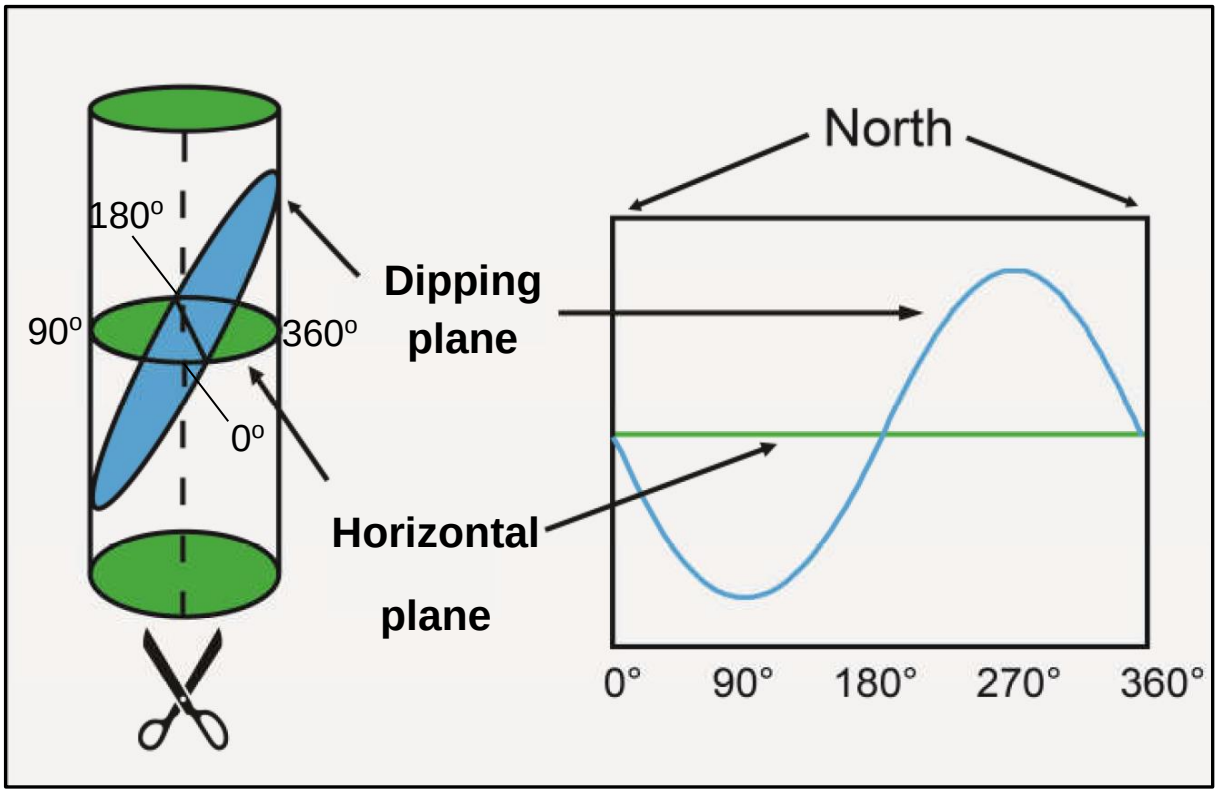

Figure 4.9: A 3D representation of how a horizontal and a dipping plane intersect a wellbore. When the wellbore surface is 'unravelled' as a 2D surface; the horizontal plane is still horizontal and the dipping plane is expressed as a sinusoidal curve. The waveform increases in amplitude with increasing dip of the plane. Image log data measures the well bore surface (a 2D surface) and so image log data is measured in the form of a sinusoidal waveform. (Modified from JRS, 2012).

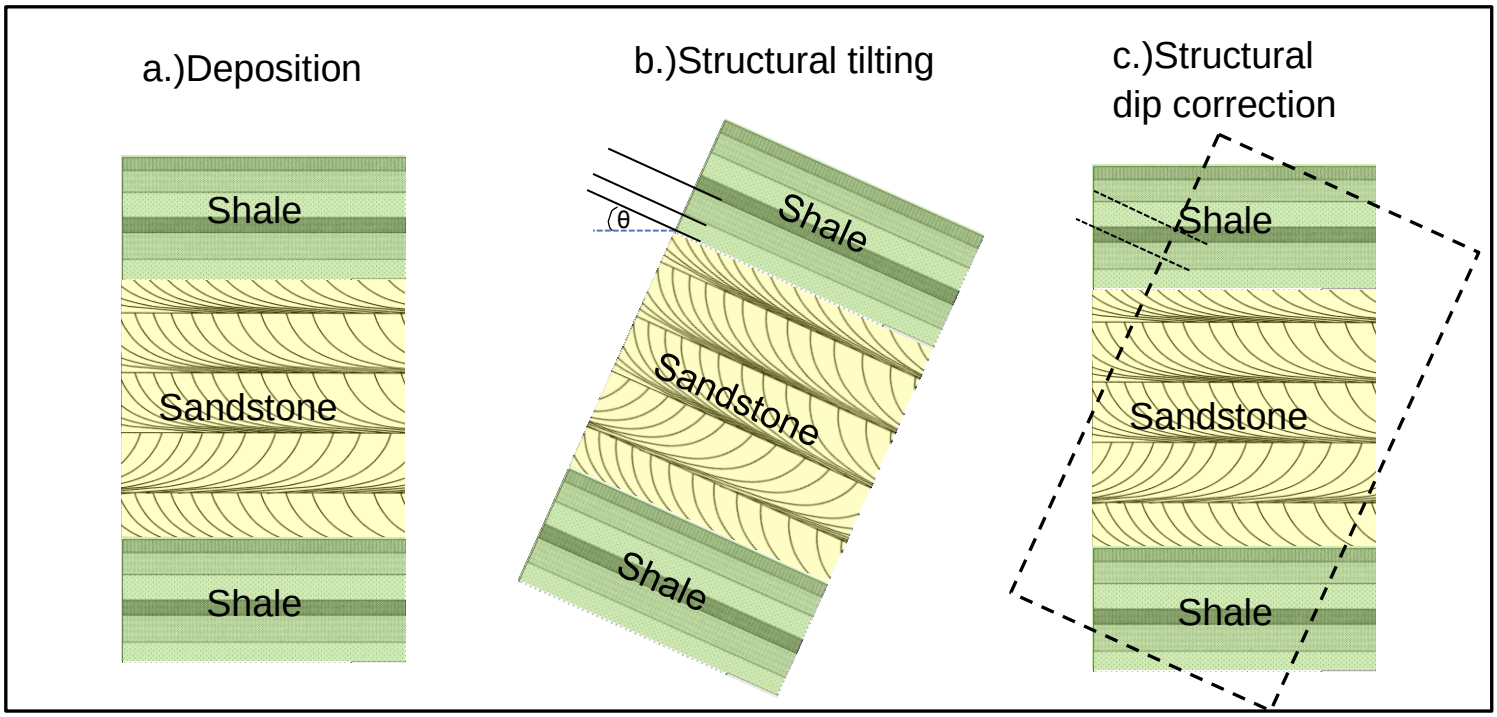

Figure 4.10: A schematic diagram of structural tilt correction based on shale bedding. a.) Shows the original depositional geometry of a column of strata intersected by the wellbore. Deposition of sandstone cross bed foresets are inclined in the direction of flow while shale beds are horizontal. b.) Shows the effect structural tilting has on the strata. C.) Outlines the correction calculation necessary to back rotate the column back to the original geometry, by aligning shale bedding back to horizontal; so that now the sandstone cross beds are in their original geometry also. θ = dip of shales beds, which is equal to structural tilt dip because shales were deposited horizontal.

The STAR micro-resistivity image log measures both sonic and micro-resistivity of the wellbore. Therefore for cross beds to be imaged, a lithological contrast must be present and preserved within the foresets of the cross-beds.

The image log data was already corrected for wellbore deviation from vertical. The image log data was loaded in to Paradigm Geolog Software. Cross bed foresets were interpreted as sinusoidal waveforms within sand bodies. Sinusoidal waveforms were picked by picking the trough and peak of the waveform. Dip calculations were then automatically carried out by Paradigm Geolog software, giving the dip of the interpreted cross bed foreset planes. Structural tilt correction was calculated by back-rotating shale bedding dip back to horizontal, giving original dip and azimuth of interpreted cross bed structures.

4.7 Channel Belt Width Estimate Calculation.

An accurate estimate of fluvial channel belt widths is required to be able to accurately reconstruct palaegeographic intervals of the Patchawarra Formation. Fluvial facies of the Patchawarra Formation are from a meandering river system; comprising crevasse splay, overbank, levee and channel fill/point bar deposits (Strong *et al*, 2002). Reservoir facies are from channel fill and point bar sands.

The key outcome of this study is to map and determine geometries of reservoir facies of the Patchawarra Formation away from well control on a regional scale. This further drives the importance of an accurate channel belt width estimate.

As outlined in Chapter 3; various authors have both proposed methods of determining channel belt width estimates from 1D well data, as well as highlighted the inherent errors and caveats associated with such techniques (Fielding and Crane 1987; Bridge and Mackey 1993b; Bridge and Tye 2000, Tye, 2011, Gibling, 2006.). In summary, the large variability in both alluvial morphology and preservation potential of facies, results in a complex and highly variable alluvial stratigraphy of m eandering river systems (Tye, 2001). It is debatable if channel belt can be estimated from 1D well data alone (Tye, 2001; Miall, 2014)). However, an attempt is made in this study using the best available practices to estimate the variability of channel belts within the Patchawarra Formation. This variability is captured in a maximum, minimum and a mean channel belt width range estimate being calculated using a number of published equations plotted as a set of lines for visualisation and ease of use (Figure 4.11)

4.8 Analogue study

A study was carried out on various modern day analogues using open source satellite imagery (Google Earth), to analyse channel belt morphological features, in particular:

- Channel belt width and sinuosity
- Structural controls on channel belt avulsions and switching over time.
- The effect of floodplain, peat mire and basement substrates on channel belt lateral migration patterns.

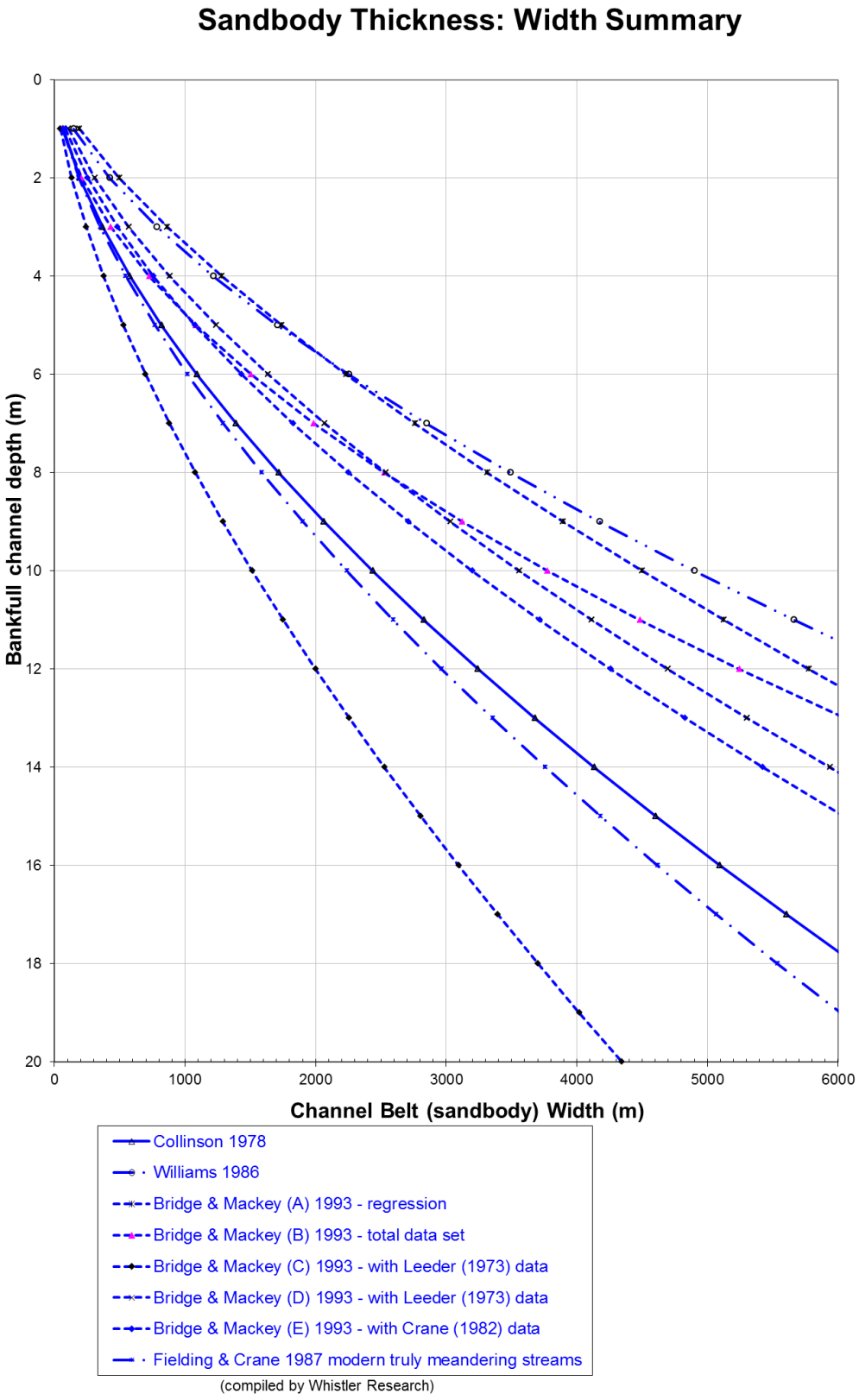

Figure 4.11: A plot of all selected literature regression equations, plotting bankfull depth vs. channel belt width. The plot is a good way to visualise the data set. Bankfull measurements of the Patchawarra Formation made in this study can be applied to this plot.

- Vertical stacking patterns and 3D facies geometries such as; floodplain, interfluve, peat mires and channel belts.

The following rivers were studied:

- Kuparuk/Sag Rivers, Northern Alaska
- Mackenzie River Northwest Territory,
- Ob River, Siberia

4.9 Electrofacies

The results and interpretations from both the analogue study and electrofacies observed during correlation were both combined to produce electrofacies assemblages that reflect composite fluvial-lacustrine environments of deposition. The large time period (10^5-10^6 years) of the chronostratigraphic intervals mapped generally results in multiple facies being juxtaposed within an interval. And so a characterisation to best reflect the composite interval as a whole was the approach taken.

4.10 Palaeogeographic Reconstruction Mapping

It is important to note that the scope of this study differs to Strong *et al*. (2002). For this study the entire Patchawarra Formation was reconstructed from VC00-ZU00, mapping chronostratigraphic intervals between regional chronostratigraphic horizons; VC horizons and the major regional unconformities; VU45 and VU75 (Table 1). The Sequence Boundaries VU11, VU24 and VU 34 were not used as interval horizons because it was not possible to correlate these horizons regionally. While Strong *et al*., (2002) mapped local smaller chronostratigraphic intervals. The intervals VC80-VC100 were not mapped individually because correlation of individual intervals past the VU75 unconformity cannot be made with confidence, and therefore chrono stratigraphic intervals cannot be identified accurately.

Log tracks and interval tops were loaded into Petra Software, where log signature maps for each interval (Table 4.1) were generated. GR Log tracks were displayed on the log signature maps scaled at varying vertical scales for optimal visualisation vertical scale at a set width of 1000 map units. A cross plot colour scheme as

outlined in Section 4.5 was applied to the tracks for visualisation. Figure 4.12 is an example of the log signature map produced for the VC25-VC30 interval.

Palaeogeographic interpretation was made using all preceding results and interpretations as guiding controls:

-Log signatures to determine electrofacies assemblages

-Seismic to guide trends away from well control

-Channel belt width estimates to guide channel belt system interpretation

-2D seismic analysis to determine the relationship between non-depostion and post erosional deposition on present day structural highs.

Palaeogeogrpahic reconstructions of all 17 intervals can be found in Appendix A.

Chronostratigraphic Intervals Mapped	
Strong et al., (2002)	This Study
VC00-VL05	VC00-VL05
VL05-VC10	VC05-VC10
VC10-VU11	VC10-VC15
VC20-VL22	VC15-VC20
VL22-VC25	VC20-VC25
VL43-VL44	VC25-VC30
VL44-VU45	VC30-VC35
VL48-VC50	VC35-VC40
VC55-VC60	VC40-VU45
VC60-VC65	VU45-VC50
	VC50-VC55
	VC55-VC60
	VC60-VC65
	VC65-VC70
	VC70-VU75
	VU75-VC80
	VC80-ZU00

Table 4.1: Comparison between the chronostratigaphic intervals mapped between this study and those mapped by Strong *et al.*, (2002) in the Moomba/big Lake Region(Figure 1.2) . Green shading shows where the same intervals were mapped for each study.

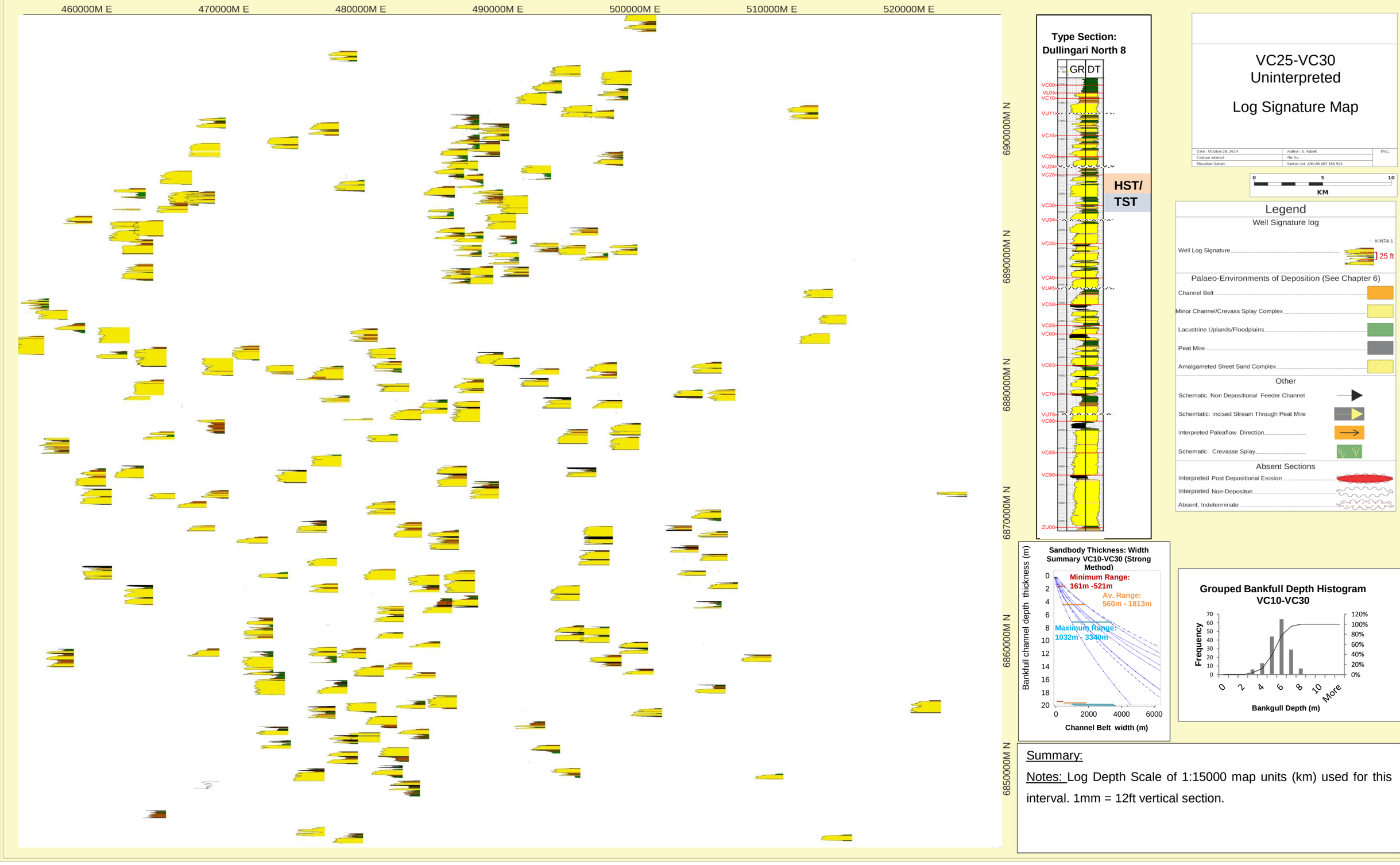

Figure 4.12: Example of a generated log signature map used for palaeogeographic interpretation for the VC25-VC30 interval.

Chapter 5: Analogue Study

5.1 Introduction

Analogues can be used to better predict and model both areal geometry and vertical stacking patterns of a subsurface formation. Present day analogues are used to describe the sediment dispersal patterns of a river system and the spatial arrangement of depositional environments. While ancient analogue outcrops provide information on how fluvial systems are preserved in 3D geometry. In this study, modern fluvial analogues are used to predict palaeo-environments outside of well control. A suitable analogue for the Patchawarra Formation needs to satisfy the following criteria (Lang *et al*., 2001, Strong *et al.*, 2002):

- Formed within an intracratonic basin.
- Slow sedimentation rate.
- Extensive fluvial system, dominated by meandering rivers but with some braided and anastomosing rivers.
- Cool temperate climate, similar to the Early-Mid Permian temperature of the then high latitude Cooper Basin.
- Abundance of raised peat mires, (generally requiring a high water table to sustain growth and preservation) and over bank deposits.
- Compressional structural features such as thrust and wrench faulting; influencing depositional trends over time.

There are no known modern day or ancient analogues that satisfy all of the above criteria. Therefore this chapter aims to assess different analogues and evaluate the extent that the above criteria control depositional patterns in each case.

5.2 Review of Commonly Used Analogues

5.2.1 The Ob River

The Ob River, Siberia is a commonly applied analogue for the Patchawarra Fm for the following reasons (Lang *et al*., 2001, Strong *et al.,* 2002):

- Large, dominant peat mires, supported by an elevated water table.
- Cool temperate climate and high latitude

- Meltwaters in spring/summer causing extensive overbank sedimentation
- Orientation of the fluvial axis to basement lineaments

The Ob River is not a perfect analogue for the Patchawarra Fm and bares the following disparities to the Patchawarra Fm:

- The Ob River system freezes over annually. While it is suspected that the Patchawarra experienced freezing events it is not interpreted that the Patchawarra experienced widespread freezing annually.
- The Ob River watershed is an order of magnitude larger (10^6 vs 10^5 km^2) than the Cooper Basin.
- The Ob River is not an intracratonic Basin, and drains into the Arctic Ocean. However; Because of the large expanse of the Ob River system, it can be argued that the majority of the upstream Ob River is largely beyond the influence of the marine realm.

5.2.2 Rangal Coal Measures, Bowen Basin, Queensland.

The Rangal Coal measures are considered a suitable ancient analogue for the Patchawarra Fm for the following reasons:

- Coal seams of the Rangal Coal Measures are of a similar thickness and type (low ash, low suphur) to coals in the Patchawarra Formation (Lang *et al*., 2001).
- Similar facies assemblages from a ‘waterlogged alluvial plain’ (Beeston and Draper, 1991).

The Rangal Coal Measures of the Bowen Basin differ to the Patchawarra Fm in that they were deposited in a foreland basin with a rapid subsidence rate driven by back thrust loading (Fielding *et al*., 1993). Fielding *et al*., (1993) report a repeatedly changing fluvial style of The Rangal Coal Measures in response to rapid fluctuations in sediment supply; due to periodic back thrusting events. It can therefore be argued that the suitability of The Rangal Coal Measures is questionable due to the large differences in sedimentation rates and structural style (Lang *et al*., 2001).

5.3 Satellite Imagery Analysis of Modern Day Systems

5.3.1 The Ob River, Siberia.

For this study the Ob River shall be used to illustrate depositional environments and use then as models for palaeo-environments of deposition. 5 depositional environments are distinguished and are outlined in Figure 5.1a and 5.1b.

5.3.2 MacKenzie River, Northwest Territories, Canada.

The Mackenzie River is an example of how pre-existing thrust fault structures and tectonic tilting can influence the course and style of a river system over time. The Mckenzie Ranges Region is currently under a compressive regime (Heidbach, *et al*., 2008) and is experiencing glacial isostatic rebound (Clague and James, 2002). Figure 5.2a shows a satellite image of the Mckenzie River.

Interpretation:

Figure 5.2b shows the same satellite image with structural geology overprinted and previous river positions annotated while Figure 5.2c shows an interpretted schematic cross section of the underlying structural geology. The Mackenzie River has avulsed from its original position due to tectonic tilting towards the southwest from isostatic rebound causing uplift in the north-eastern North American Plate (Figure 5.3) (Clague and James, 2002). The thrust faults would have been reactivated at discreet times, further confining the river to the north-eastern down thrown fault blocks; however the overall tectonic tilting has caused the river to switch periodically across the upthrown fault blocks, towards the southwest to the current position

5.3.3 The Colville/Sag Rivers, North Slope, Alaska.

The Colville River and Sag Rivers form a part of the North Slope fluvial system (Figure 5.4) draining into the Beafort Sea from the Brooks Ranges. Lacustrine environments become more prominent to the west in the coastal plain. The two rivers are similar in style upstream in the foothills; structurally confined sandy braided and meandering rivers (Figure 5.3, C and D). Downstream the Colville River becomes more sinuous where it is able to cut into lacustrine uplands and migrate to the west (Figure 5.3, A). Conversely, The Sag River is structurally confined downstream and remains braided, switching within the structural corridor (Figure 5.3, B). Upstream of C the Colville River is strongly perturbed and follows the strike of an

underlying thrust fault.This analogue highlights how the underlying substrate, structure and slope can locally change the fluvial style of a river, within an area comparable to the area of the Tenappera Region.

5.4 Discussion:

Previous authors have outlined the strong influence of compressive reactivation and tilting on depositional patterns in the Cooper basin during the Permian (Apak *et al*., 1997; Gravestock and Jensen-Schmidt 1998; Jensen-Schmidt, 2006). The Ob River, does not exhibit such a strong communication with structural controls and the system is too large and expansive, but reflects the depositional environments of the Patchawarra Formation well (Lang *et al.,* 2001). Conversely the McKenzie River shows an excellent example of structural controls on fluvial deposition, but does not reflect the depositional environments of the Patchawarra well. It is important to note the elevation of the McKenzie (9,000 ft) and Franklin Ranges (4,500 ft) are notably higher than the paleo-highs during deposition of the Patchawarra Formation (100-200ft), and so this represents an extreme case of structural influence.

There appears to be no perfect modern day or ancient analogue for the Patchawarra Fm. This study has not identified an analogue that exhibits all of the depositional and structural elements that are observed in the Patchawarra Fm. Therefore, a number of analogues have been analysed to better understand these elements to assist in palaeogeographic reconstructions.

Figure 5.1a: The Ob River, Siberia. The image shows a slightly larger area than the Tenaperra Trough Area. This image is taken upstream (east) where a major tributary enters the river. To the west the Ob River joins the Irtysch River (increasing in width) and then ultimately drains north into the Arctic Ocean. The major channel receives input from multiple tributary systems from the north and south (Image from Google Earth, 2014).

Figure 5.1b: The same image as in figure 5.1a. with interpreted depositional environments: Green: Floodplain & Lacustrine uplands dominated by lakes, with minor peat development and tributaries draining into major channel belt. Orange:. Major channel belt, consists of the present day channel position, point bars, oxbow lakes and smaller channels in interfluve areas. Black: Raised peat mire, peat dominated with minor lakes, confines channel belt and forces it to migrate to the north. Yellow: Crevasse splay/overbank deposit: consists of overbank deposits, overlain by episodes of crevasse splay deposition with some minor channel also includes channel belt abandonment; as the channel migrates in one direction small lakes develop where the channel was (Image from Google Earth, 2014).

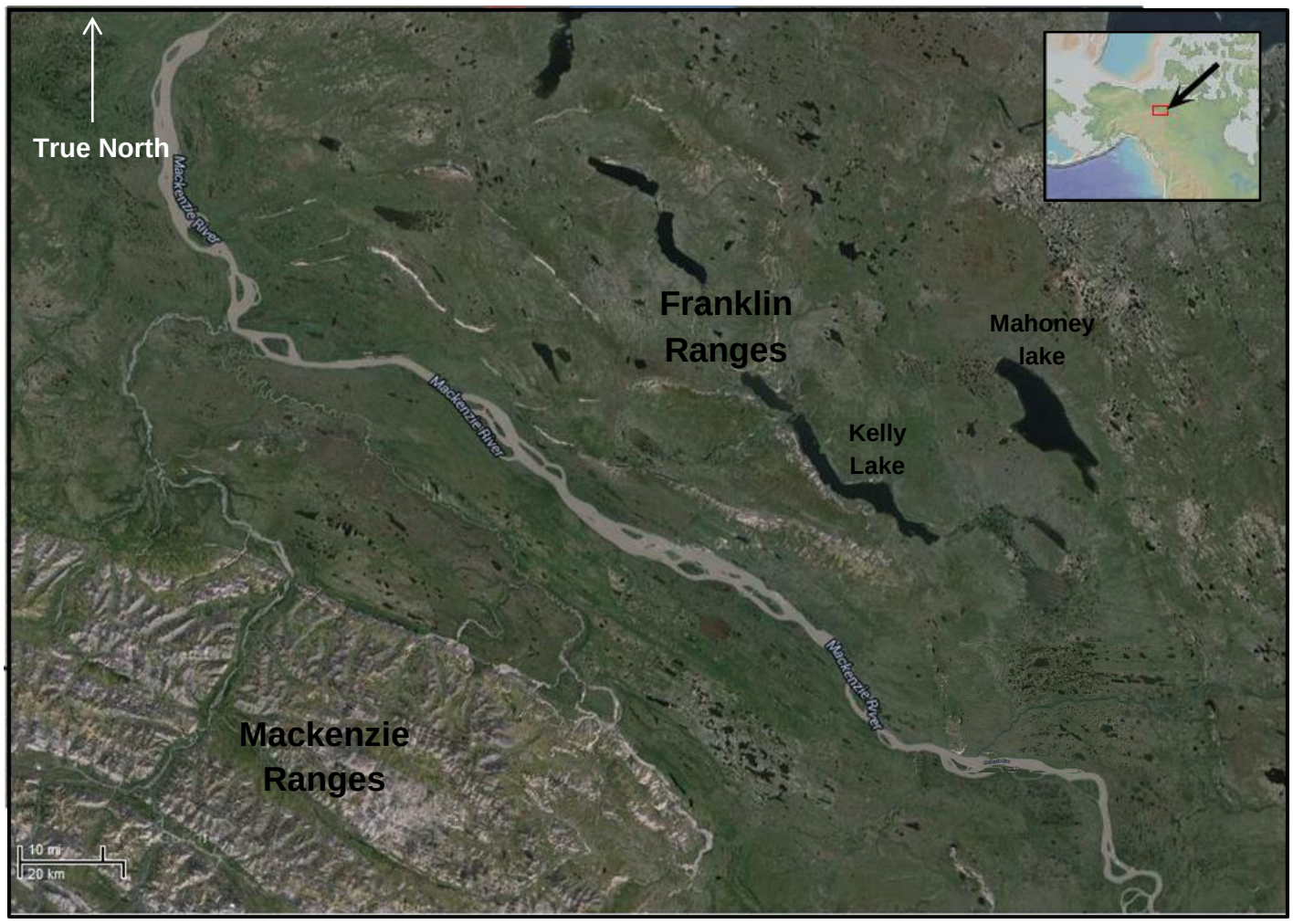

Figure 5.2a: Satelitte image of Upstream Mckenzie River, North West Territories, Canada. The Current fluvial style is braided, with lacustrine environments dominating to the north-east. Tributary drainage patterns off of the Mckenzie Ranges are narrow and structurally controlled. Once off of the ranges, the tributaries become more sinuous, but still adhere to the strong northwest striking structural grain (Image from Google Earth, 2014).

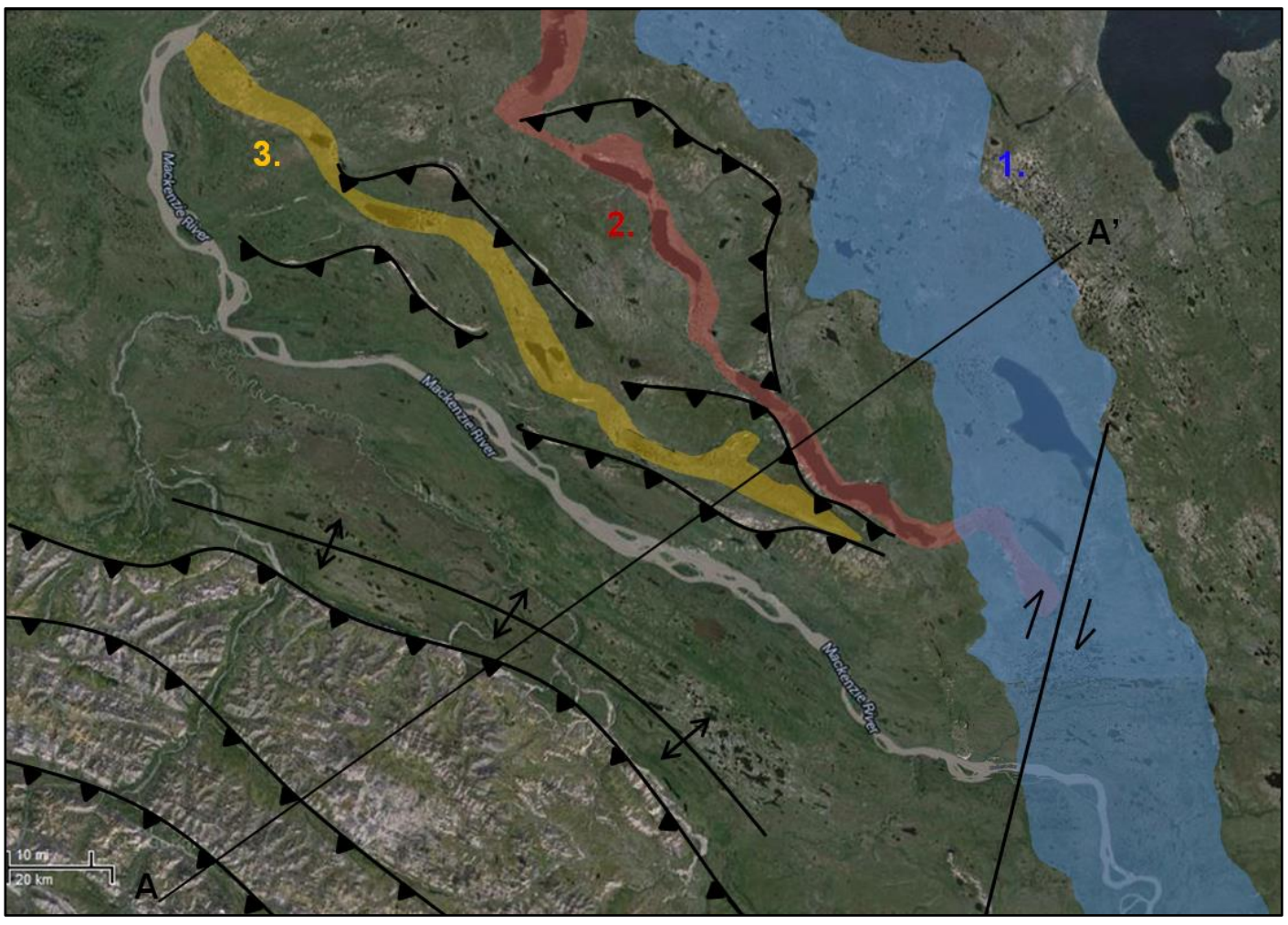

Figure 5.2b: The Mackenzie River with interpreted structure sourced from the Geological Survey of Canada (Geological Survey of Canada, 1998, Geology of Canada Series no. 7). Previous river positions are annotated 1(blue),2 (pink) and 3 (orange). River position one suggests a wider meandering system that is now overlain by a lacustrine abandonment environment. River positions 2 and 3 suggest that the river was much more defined and is now occupied by deeper lacustrine environments. The present river position is heavily structurally confined. Vertical accretion is expected to occur rather than lateral migration (Image from Google Earth, 2014).

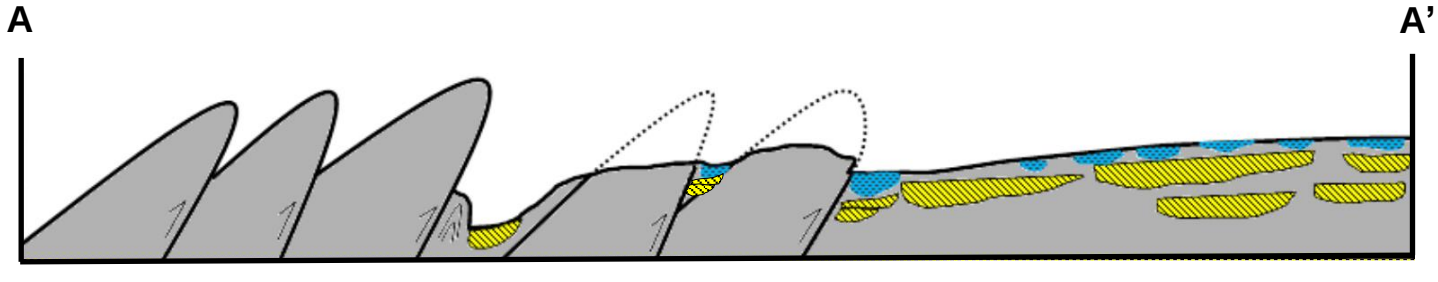

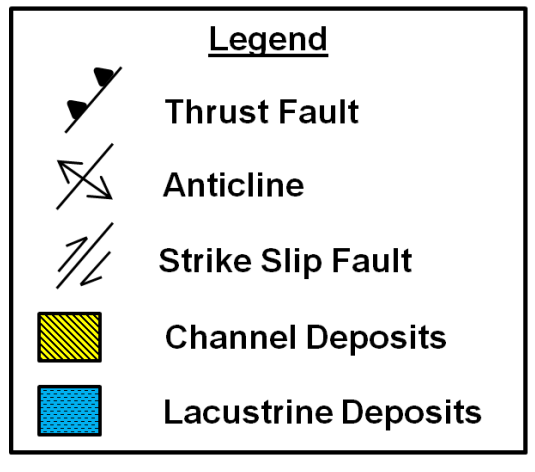

Figure 5.2c: Schematic cross section of the line A-A'. The cross section shows the interpreted deposits that would be expected to be encountered in the subsurface as a result of the avulsion pattern over the structure and subsequent lacustrine abandonment deposits forming above previous channel deposits.

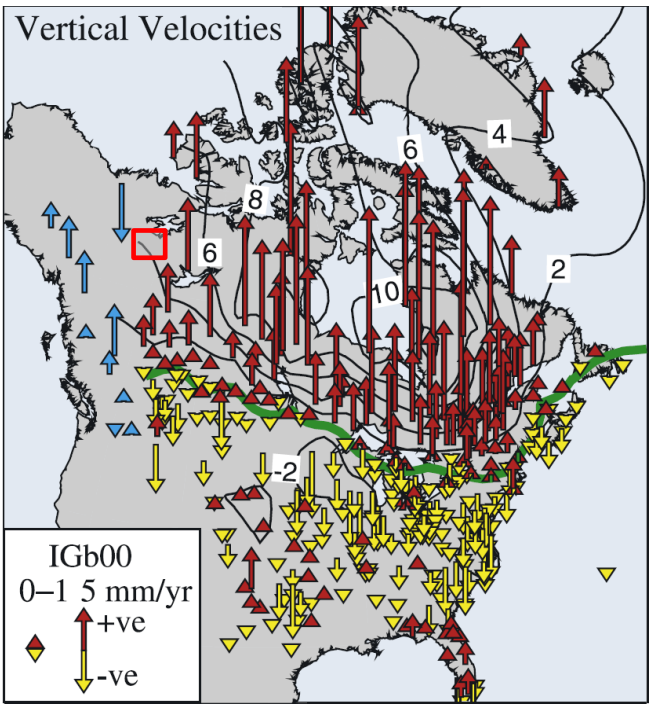

Figure 5.3: Isostatic rebound of the North Eastern American Plate, vertical velocities are denoted by arrows and velocity contours are annotated with values. The green line represents ‘The Hinge Line’ of zero vertical velocity, separating subsidence from uplift. The study area of the Mckenzie River is shown in red (From Sella *et al*., 2007.)

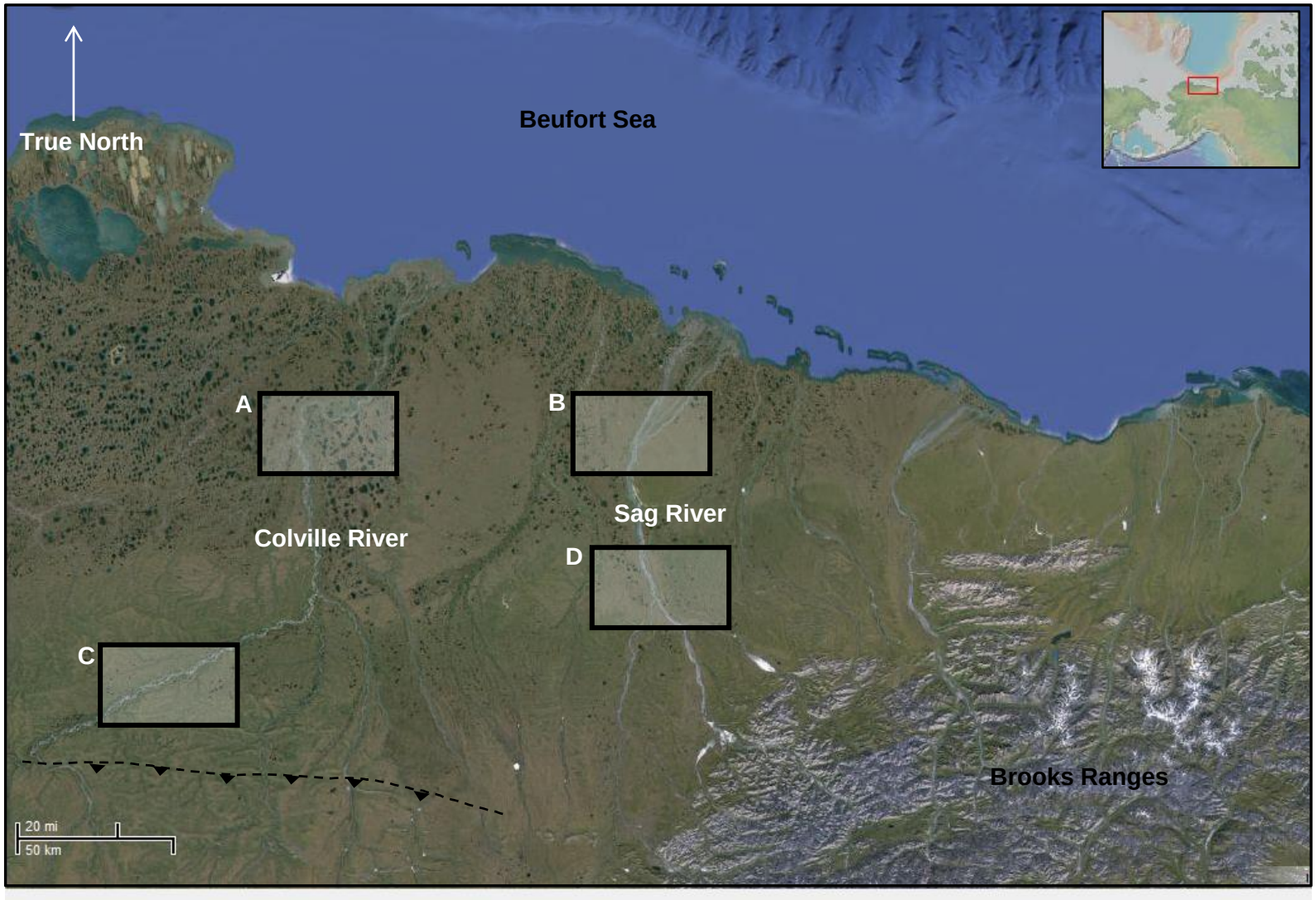

Figure 5.4a: The Colville and Sag Rivers, North Slope Alaska. Both rivers drain from the Brooks Ranges through the foothills and coastal plains into the Beufort Sea. The coastal plain becomes more lacustrine dominated towards the west. This figure highlights the difference in fluvial styles of two different rivers within the same drainage system. The black dotted line denotes an underlying thrust fault controlling the Colville river's path upstream (Department of Natural Resources, State of Alaska, 2008)(Image from Google Earth, 2014).

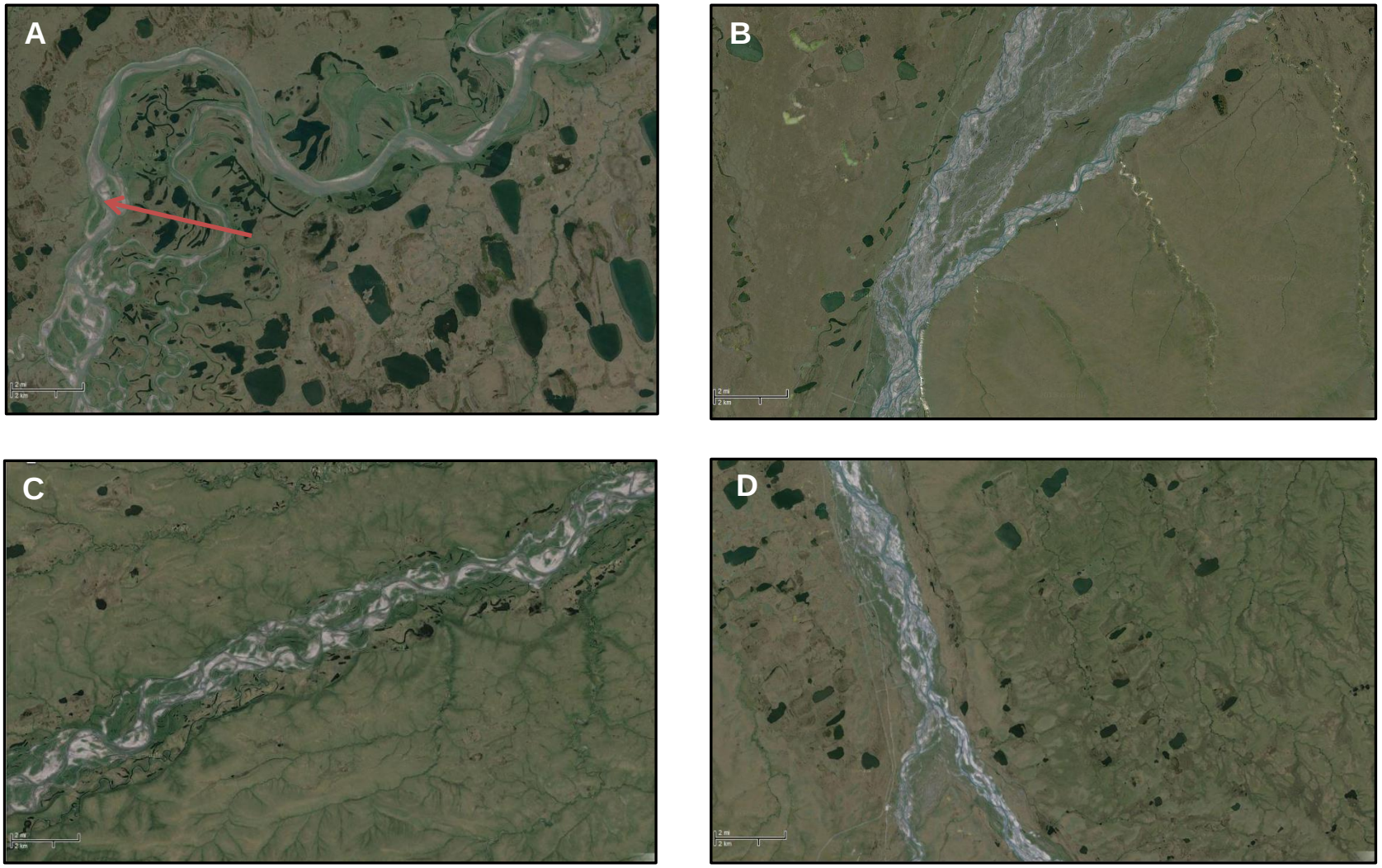

Figure 5.4b: The Colville River is a structurally confined sandy meandering river upstream (C) that becomes more sinuous and less confined downstream (A). The Sag River is a braided river system. It is also structurally confined upstream (D) however structural confinement and possibly a steeper slope locally, result in a gravelly braided stream persisting through the coastal plain (B). Red arrow in A denotes channel migration direction into the lacustrine dominated uplands to the west.

Chapter 6: Electrofacies Assemblages and Palaeo-Environments of Deposition

6.1 Introduction

A rock lithofacies or facies has been defined by a number of authors as a rock unit with a specified set of characteristics that can be generally attributed to a certain process or depositional environment (Reading and Levell, 1996; Posamentier and Walker 2006). Serra and Abbot (1980) extended and applied the concept of lithofacies to geophysical log signatures defining an electrofacies as: a set of log responses that differentiates one lithotype from another lithotype. By this definition; an electrofacies has already been partially established in this study by the construction of the GR vs. DT cross plot discussed in 4.5.2, differentiating the log responses into likely lithologies. Wherever a lithology is described herein; this is interpreted from cross plot colour scheme values.

Electrofacies assemblages were defined and interpreted based on the GR and DT log response shapes and vertical stacking patterns of likely lithologies; referred to as log motifs. For a detailed definition of log motifs of fluvio-lacustrine environments see Serra's Sedimentary Environments from Wireline Logs (1985).

Six electrofacies assemblages were recognised within the study area based on their log motifs. These electrofacies assemblages were then related to depositional environments defined from the Ob River to determine four palaeo-environments of deposition that constitute the mapping units of the palaeogeographical maps.

6.2 Electrofacies Assemblages Identified

Facies 1

Description:

Log signature: Spiky, irregular GR and DT motif, 5-25ft in thickness. In general: High GR (150-200 GAPI) and fast sonic velocity (50-60 US/F), with interruptions of low GR and slightly slower DT responses. Coals are identified by a very low GR response (>20GAPI) and a high DT (>120 µs/ft), and are generally thin (1-3ft). Rare carbonaceous shales.

Interpretation:

Overall high GR response due to clays falling out of suspension, suggests a distal overbank or lacustrine environment. Organic matter from minor soil development and vegetation would also contribute to a high GR response, further suggesting an overbank environment. Sand and siltstone beds produce low GR and slightly faster sonic responses, therefore these spikey low GR responses are caused by small interbeds of sand and silt onto the overbank or a discreet pulse of sand silt deposition into a lake.

Facies 2

Description:

Boxcar or blocky low GR motif, 5-35ft in thickness. In general: Low GR (10-50 GAPI) and a low DT(50-60US/F). Although blocky in nature, shows a slightly convex shape, curving towards lower GR of shales (>150), fining upwards rapidly. Individual beds can be distinguished within the boxcar shape by slightly differing GR and DT responses, with upward fining GR trends within a single bed sometimes distinguishable.

Interpretation:

Low GR blocky motif suggests sand deposition within a fluvial environment. Rapid fining upwards nature at the top of the sand suggests that it is a channel fill deposit. Blocky low GR motif also can be due to a multistorey channel deposit and is difficult to determine from wireline data alone (Chapter 3).

Facies 3

Description:

Characteristic bell shaped motif, 5-20ft in thickness. Low GR (10-50 GAPI) response at base trending to high GR (180GAPI) at the top, with a relatively steady DT (50-60US/F). Gently fining upwards. Coarse grained sands fining upwards to silts, then to shales.

Interpretation:

Basal unit with low GR fining upwards nature suggests a fluvial nature. The smooth fining upwards succession that also fines through the silts and clays suggests a very uniform and constant decrease in flow velocity and therefore a point bar deposit is

interpreted. The concave shape at the base of the deposit is not due to sand grain size alone. The base of the unit is expected to be a coarse grained scour surface (High GR response), the low GR perturbation is due to mud clast rip up and deposition causing a decrease in the GR response (P. McCabe 2014, pers. comm.).

Facies 4

Description:

Thick coal layers, 10-30ft in thickness, Low GR, high DT (>110). Coals generally overly a finer grained shale deposit.

Interpretation:

Large thickness of coal indicates a raised peat mire environment; based on the interpretation that all large peat accumulation and preservation in the Patchawarra Formation was from raised peat mires (Taylor *et al*., 1988).

Facies 5

Description:

Funnel shaped motif, coarsening upwards 10-15ft in thickness. Silts with GR response from 85 (GAPI) coarsen upwards to sands with GR responses up to 110 (GAPI). At the upwards boundary of the funnel motif, an abrubt deflection back to a GR (shale) is observed.

Interpretation:

Coarsening upward profile, silt to sand grain size trend with an abrubt deflection back to shale all suggest a crevasse splay deposit.

Facies 6

Description:

Very low GR motif, with no spikes, only small variation in GR and DT. In general very low GR response (185-190 GAPI) and high DT response (60-70 US/F)

Interpretation:

Large deep water or isolated lake deposit, with no high energy influxes. Clay settling out of suspension was the only form of deposition.

6.3 Palaeo-Environments of Deposition

The large time period (10^5-10^6 years) of the chronostratigraphic intervals mapped generally results in multiple facies being juxtaposed within an interval. And so a characterisation to best reflect the composite interval as a whole is the best approach for mapping chronostratigraphic intervals. The large influence of fluvial systems tracts on depositional environments has also been observed (see Chapter 3) and so environments can be expressed as a function of each systems tract.

Channel Belt Environment.

Electrofacies environments:
Characterised by electrofacies 2 and 3. With subordinate intervals of electrofacies 1 separating cycles of electrofacies 2 and 3 to varying degrees.

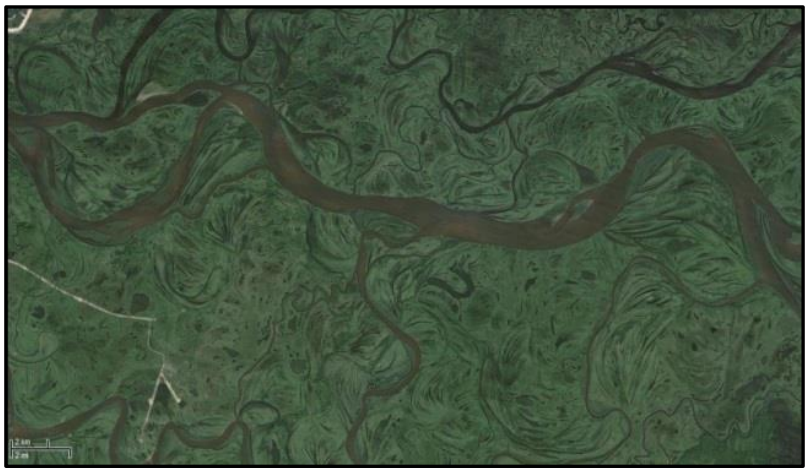

Interpreted electrofacies environments: Stacked channels including: point bar, channel fill and multi-storey channel deposits. Floodplain fines separate individual channel stories but channels can also be amalgamated and multistorey.

LST character:	**TST character:**	**HST character:**
Characteristic amalgamated, truncated, multistorey and reworked sheet sands.	Majority of sands are isolated bankfull deposits resulting from vertical aggradation caused by large accommodation space creation.	Early HST: Isolated bankfull deposits. Increase in stacked channel sands past early HST, as sediment supply increases
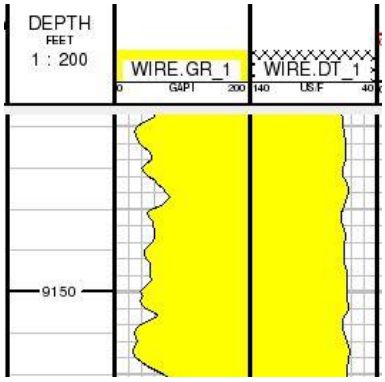	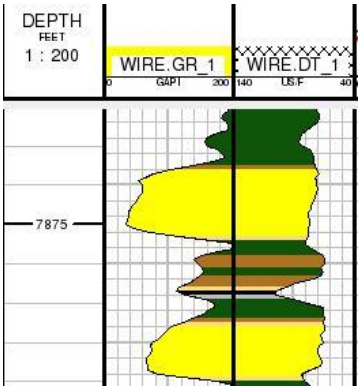	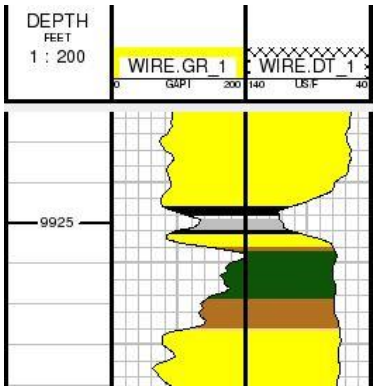

Lacustrine Upland/Floodplain Environment.

Electrofacies environments: Characterised by electrofacies 1 and 6. Minor amounts of electrofacies 2.

Interpreted electrofacies environments: Floodplain and lacustrine deposits generally form on raised uplands. Ephemeral sheetfloods and minor tributaries are responsible for discrete sand deposits.

LST character:	**TST character:**	**HST character:**
Increased silt and sand fraction due to increased sheet flooding events, sands regularly cut through floodplain but are isolated.	Finer grained over bank deposits/deep lacustrine with lesser or no sand/silt deposits due to reduced sheet flooding.	Shales more dominant, lesser sands and silts. Shales may show higher GR response due to increased settling. Peat formation favourable.
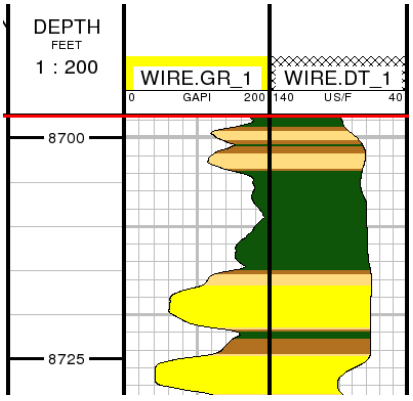	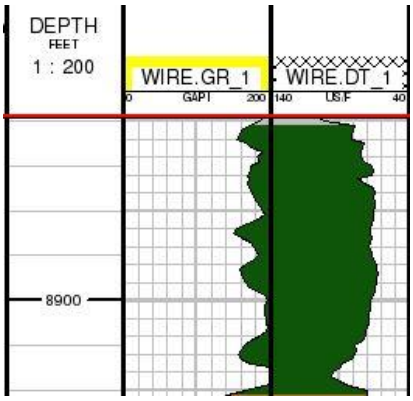	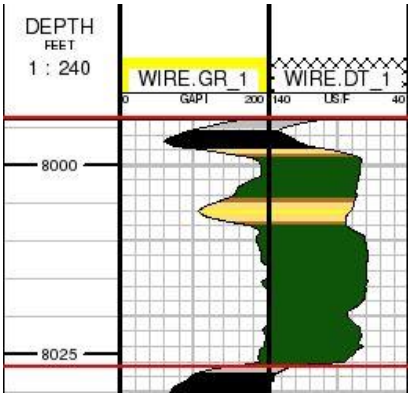

Raised Peat Mire Environment.

Electrofacies environments: Characterised by electrofacies 1 and 6. Minor amounts of electrofacies 2.

Interpreted electrofacies environments: Floodplain and lacustrine deposits generally form on raised uplands. Ephemeral sheetfloods and minor tributaries are responsible for discrete sand deposits.

LST character: Peat mires restricted to structural highs and ontop of lake fills	**TST character:** Thicker widespread peat mire development	**HST character:** Common for peat mire development during mid-late HST when sediment supply increases to reduce water table.
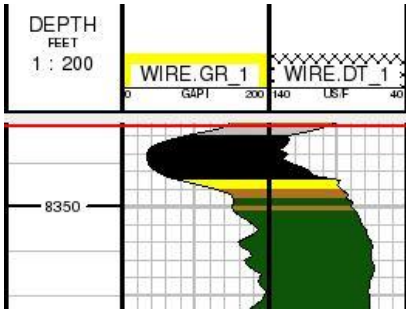	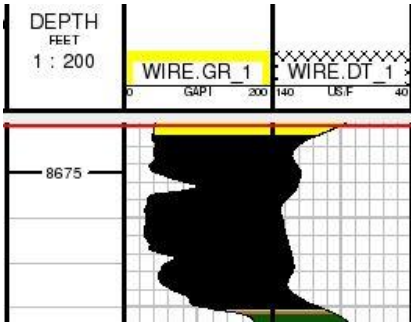	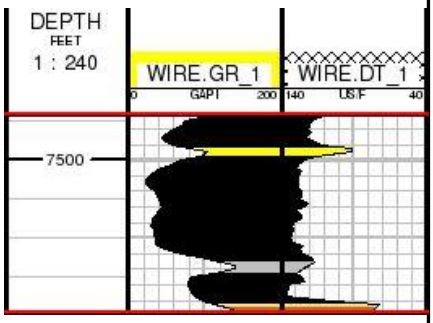

Crevasse Splay and Minor Channel/Channel Margin Environment.

Electrofacies environments:
Characterised by electrofacies 2, 3 and 5. With varying fractions of electrofacies 1.

Interpreted electrofacies environments: Crevasse splay and minor channel complex, interbedded with overbank fines.

LST character:	**TST character:**	**HST character:**
Frequent crevasse splay deposits often superimposed on previous crevasse splays. Less overbank clays and higher sand content.	Less frequent and finer grained crevasse splay deposits, larger overbank clay percentage.	Regular crevasse splay deposits within overbank clays
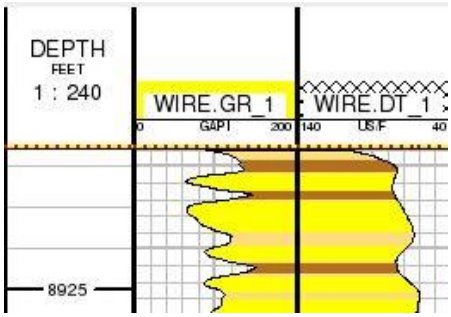	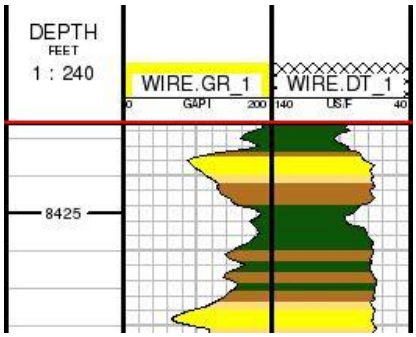	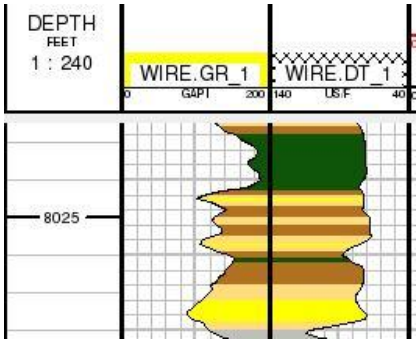

Chapter 7: Palaeo-flow from Image Log Data.

7.1 Introduction

Paleo-flow indicators were determined using available image log data from two wells in the study area (Figure 7.1). Original cross bedding dip and azimuth direction were calculated for each well, by identifying structural tilt zones from shale bedding (Figures 7.2 and 7.3), then performing back rotation calculations . By plotting a rose diagram of all original cross bedding dips, the fluvial style of the channel system could be assessed. Dip walk out plots were generated for each well, enabling palaeo-flow directions for each interval to be determined.

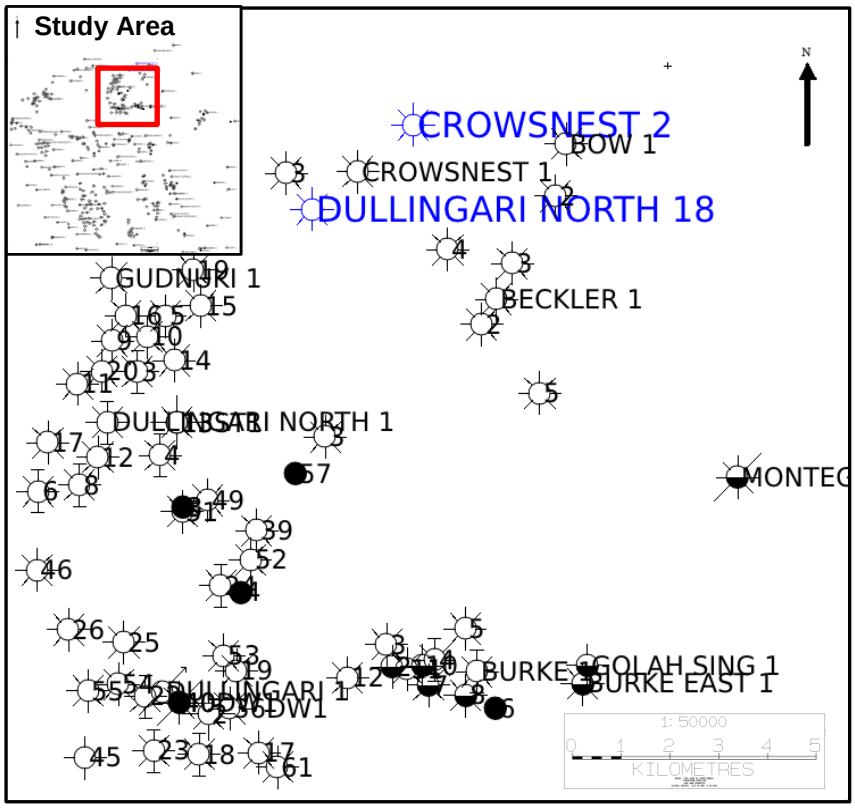

Figure 7.1: Location of the two wells in the study area with image log data available. The Distance between Crowsnest 2 and Dullingari North 18 top of hole is measured as 3.2km.

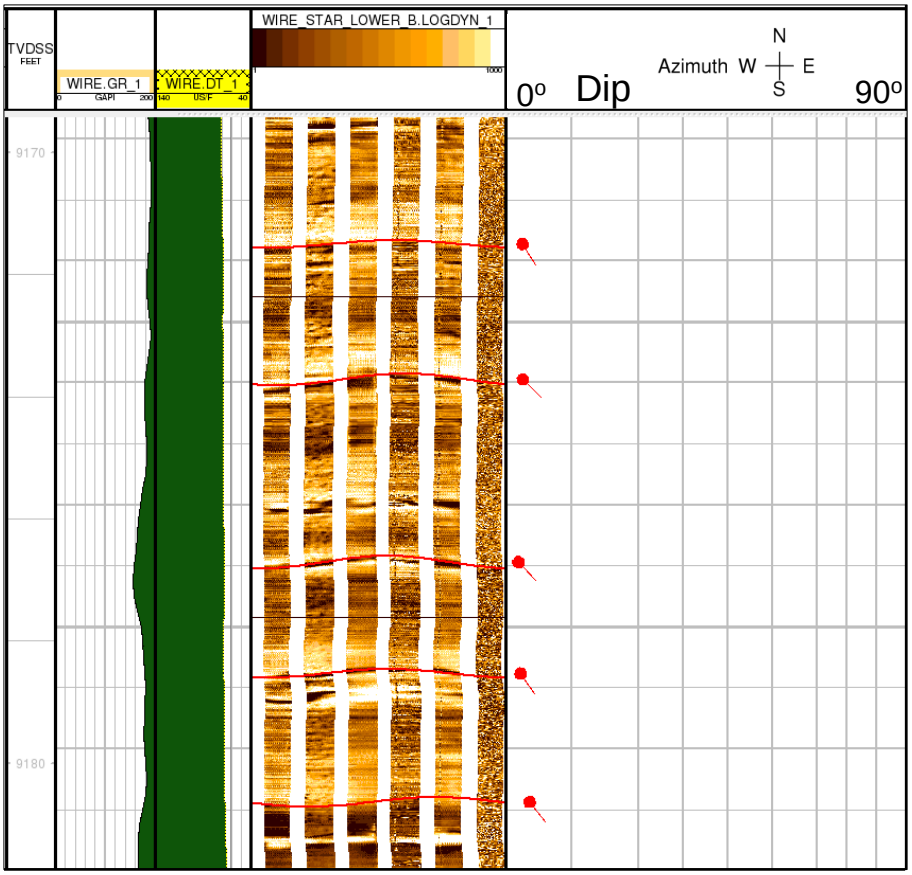

Figure 7.2: Example of sinusoids from dipping shale beds. The beds are dipping slightly (3-5º) towards 124º. This is equated to structural tilt of the interval, and is back rotated to horizontal for this section. Image pad 4 (far right) is noisy and is not able to be interpreted.

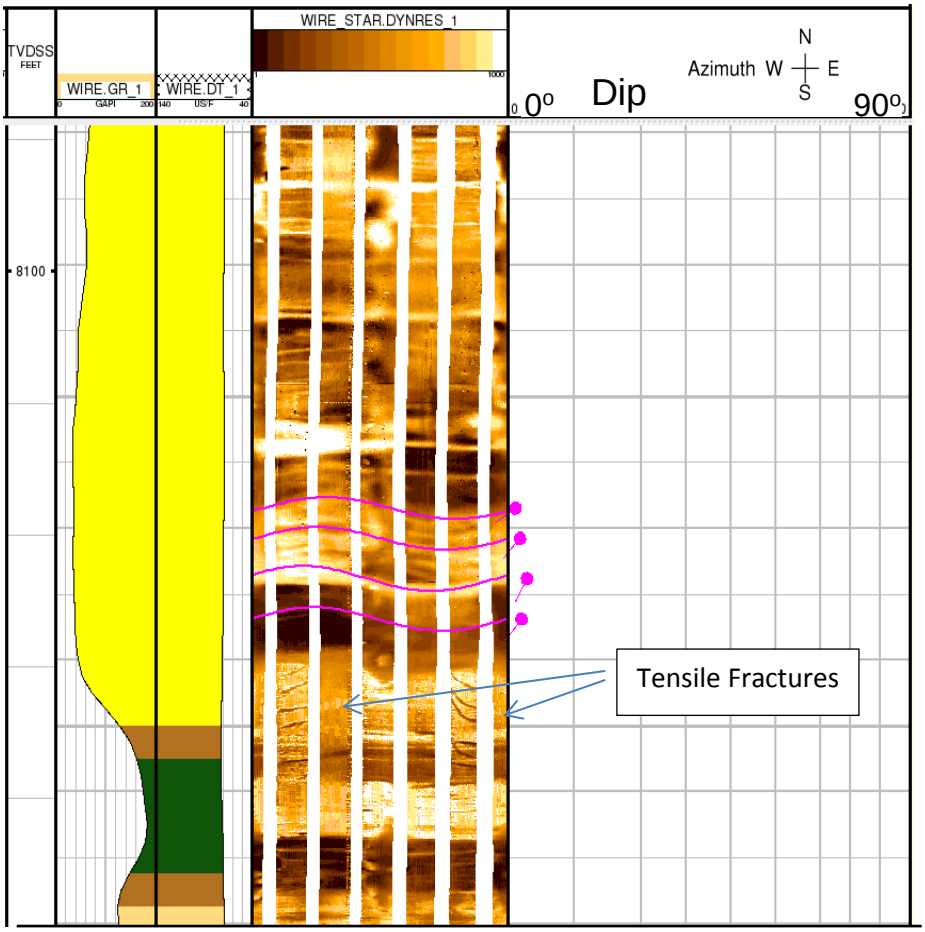

Figure 7.3: Example of sinusoids from cross bed foresets in a sandbody. The cross beds are dipping slightly (1-4º) towards 190º. Tensile fractures are also observed in the image and the difference between the two features in this case is easily identifiable.

7.2 Image Log Quality

It is important to appreciate the limitations of the image log data before interpretation is carried out, especially noting any orientation deviations or uncertainties, that will adversely affect any palaeo-flow inferences.

Dullingari North 18.

Overall image log data is good. The tool held a constant orientation with minimal rotation. Overpulls from coal washout zones resulted in some areas of data being of poor resolution. (Baker Atlas, STAR Image Log Report, 2002).

Crowsnest 2.

Overall the image log data is poor. The tool held a steady orientation with slight rotation. Poor resolution of image log data resulted from borehole rugosity throughout the survey, however it is still interpretable. Pad 4 was noisy and irreconcilable. (Baker Atlas, STAR Image Log Report, 2002).

7.3 Observations

Dullingari North 18.

31 cross bed surfaces were interpreted in sandstone bodies, from VC00-VU75. 5 structural tilt zones were identified from shale bedding (Table 7.1).

A dip vector walkout plot and rose diagram of the cross bedding data set is shown in Figure 7.4a and 7.4b. Cross bedding dips consistently dips towards the SSE, except within the VC30-VC35 interval where cross-bed dips are irregular (inset Figure 7.4a).

Table 7.1: Structural Tilt Zones: Dullingari North 18			
Zone	Depth (ftRT)	Thickness (ft)	Tectonic Tilt Dip/Azimuth
1	8400 - 8471	71	2.3 / 157
2	8471 - 8497	26	4.1 / 117
3	8497 - 8599	102	5.3 / 164
4	8599 - 8725	126	2.8 / 007
5	8725 - 8960	235	2.5 / 095

Table 7.1: Structural dip zones determined from shale bedding dips for the Dullingari North 18 well.

Dip Vector Walkout Plot for Original Cross Bedding: Dullingari North 18

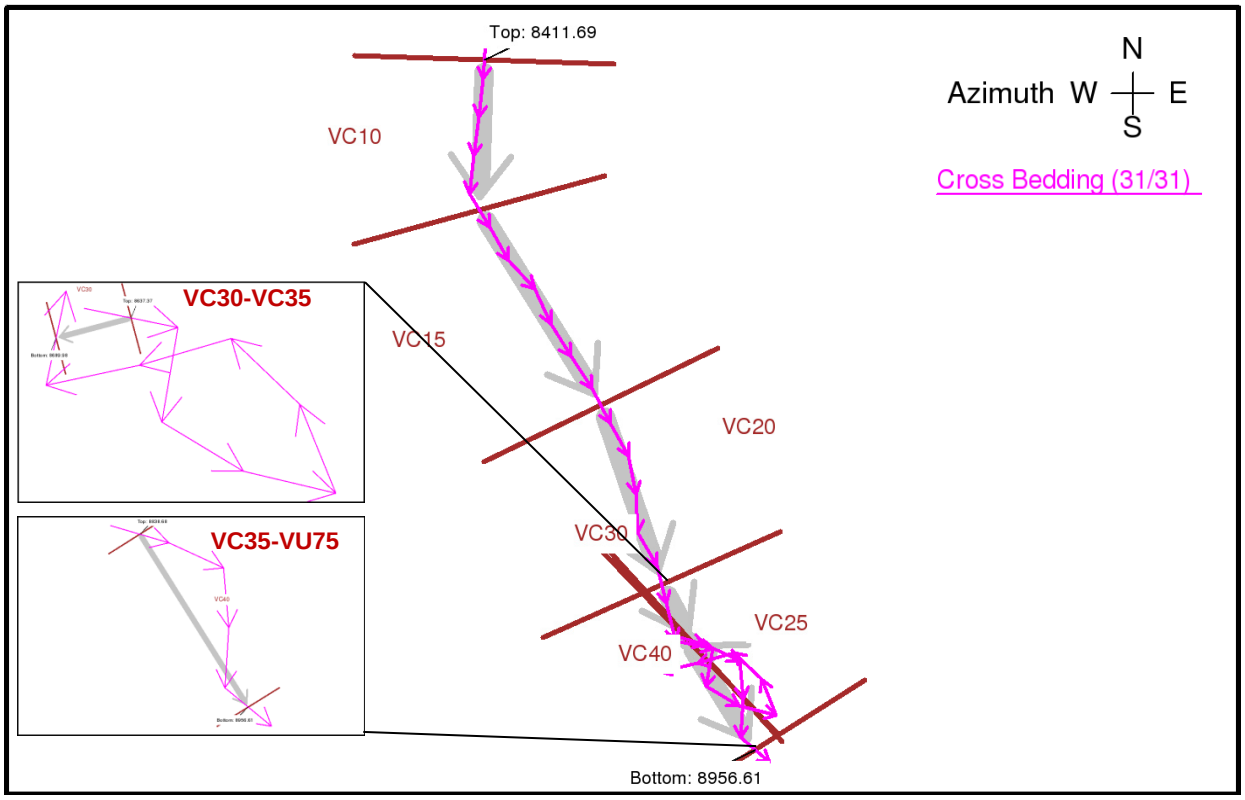

Figure 7.4a: Dip vector walk out plot showing all intervals measured from VC00-VU75, VC30-VC35 and VC35-Vu75 have been separated and shown inset to highlight the disconformance of the VC30-VC35 interval to the trend of the rest of the data set.

Rose Diagram of Cross Bedding: Dullingari North 18

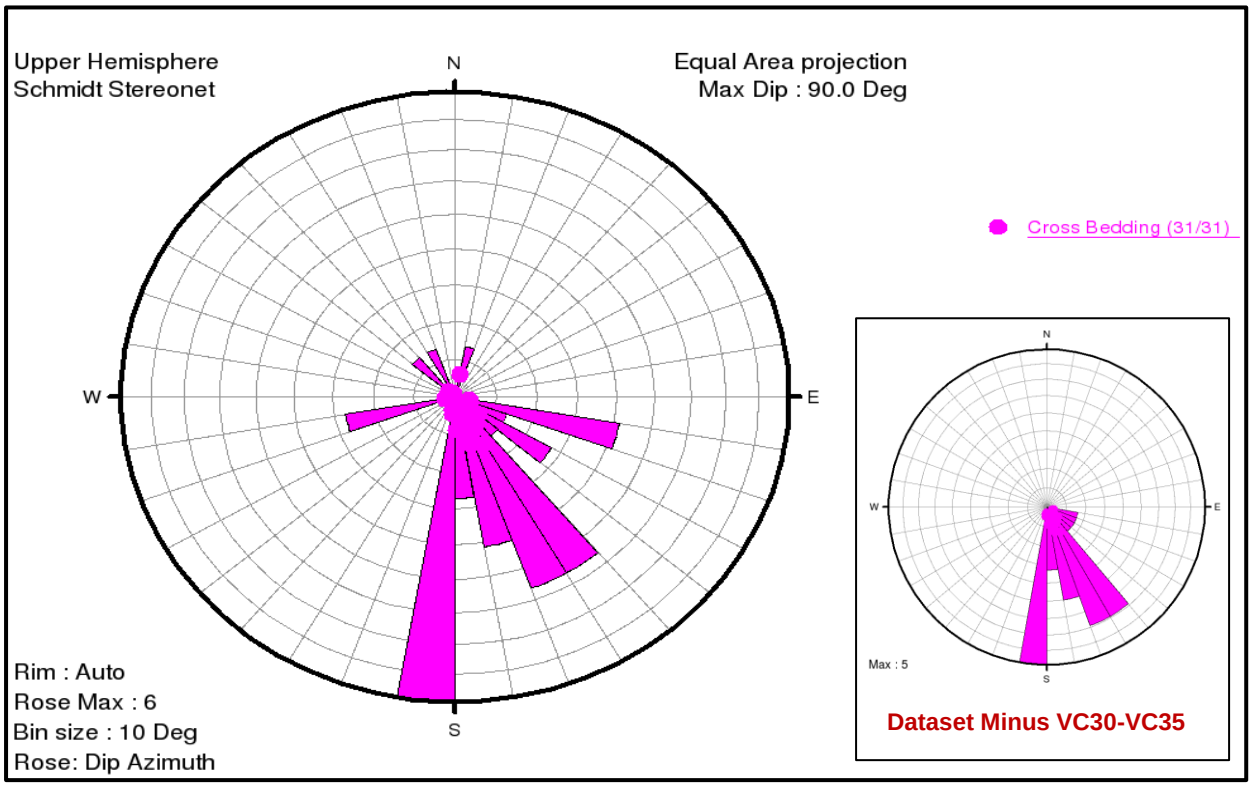

Figure 7.4b: Rose diagram showing cross bed dips from all intervals measured from VC00-VU75. The dataset with VC30-VC35 is shown inset to highlight the trend of the rest of the intervals.

Crowsnest 2.

26 cross bed surfaces were interpreted in sand bodies from VC00-VC85. 5 structural tilt zones were identified from shale bedding (Table 7.2). A dip vector walkout plot and rose diagram of the cross bedding data set is shown in Figure 7.5a and 7.5b. 3 cross-bed dip trends are present: VC00-VC35: north, VC35-VC55: southwest, VC55-VC80: east.

Table 7.2: Structural Tilt Zones: Crowsnest 2			
Zone	Depth (ftRT)	Thickness (ft)	Tectonic Tilt Dip/Azimuth
1	8760 - 8834	74	7.5 / 352
2	8834 – 9088	254	6.0 / 021
3	9088 – 9197	109	8.6 / 124
4	9197 – 9342	145	4.2 / 243
5	9342 - 9620	278	3.0 / 079

Table 7.2: Structural dip zones determined from shale bedding dips for the Crowsnest 2 well.

7.4 Interpretation

Dullingari north 18:

The interval VC30-VC35 in Dullingari North 18 is irregular and does not follow the trend within the rest of the well data nor does it show any relationship to the nearby Crowsnest 2 well during that interval. This can be interpreted as an interval with frequent variation in local flow direction, where channels are migrating frequently in different orientations and typical of a meandering system with little to no confinement. The remainder of the Dullingari North 18 well shows a consistent southeast dipping trend, suggesting a palaeo-flow direction to the southeast, and a possible structural alignment causing the consistent flow in a single direction.

Crowsnest 2:

The three dip trends show quite consistent flow patterns during each period, suggesting a strong structural alignment or control for each trend. This control could also come from confinement by a peat mire, however it is unlikely that confinement from a peat mire would change so discretely and repeatedly.

Dip Vector Walkout Plot for Original Cross Bedding: Crowsnest 2

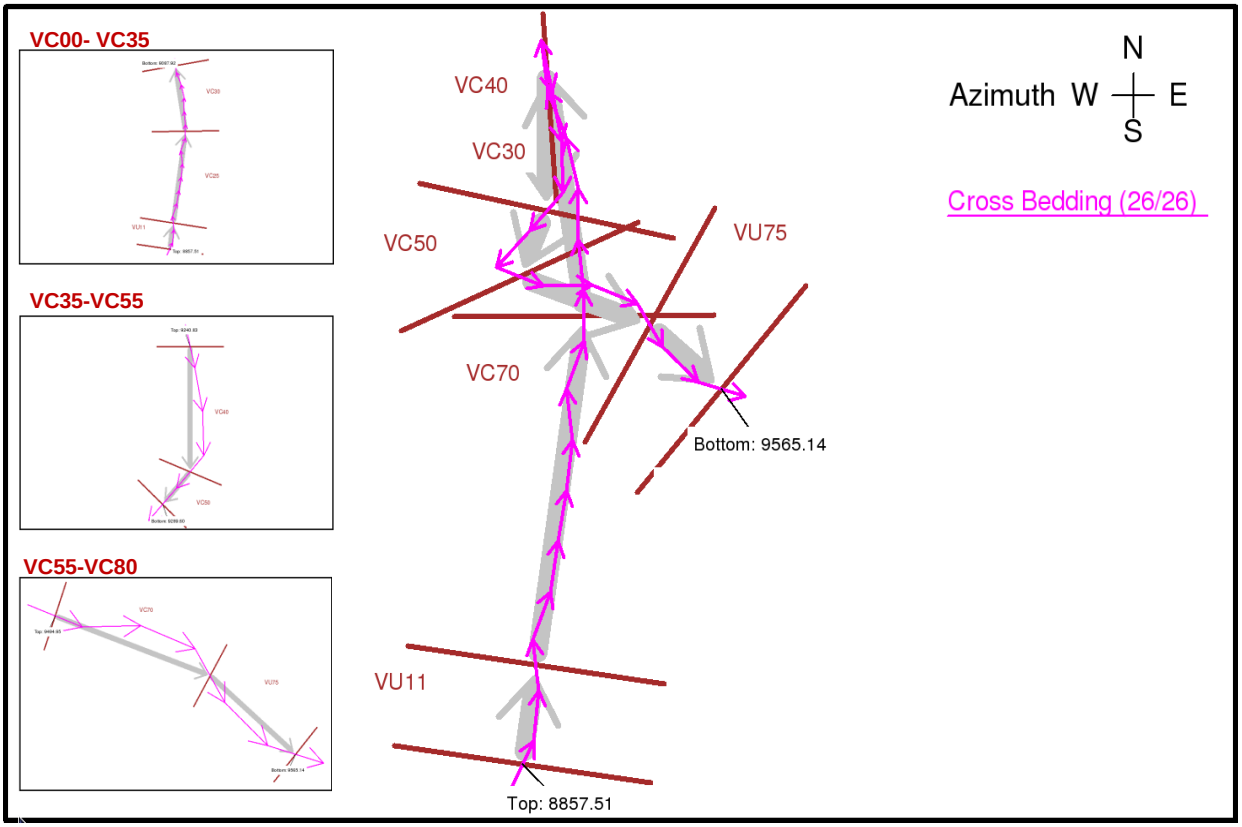

Figure 7.5a: Dip vector walk out plot showing all intervals measured from VC00-VC85, The three dip trends observed have been separated and are shown inset.

Rose Diagram of Cross Bedding: Crowsnest 2

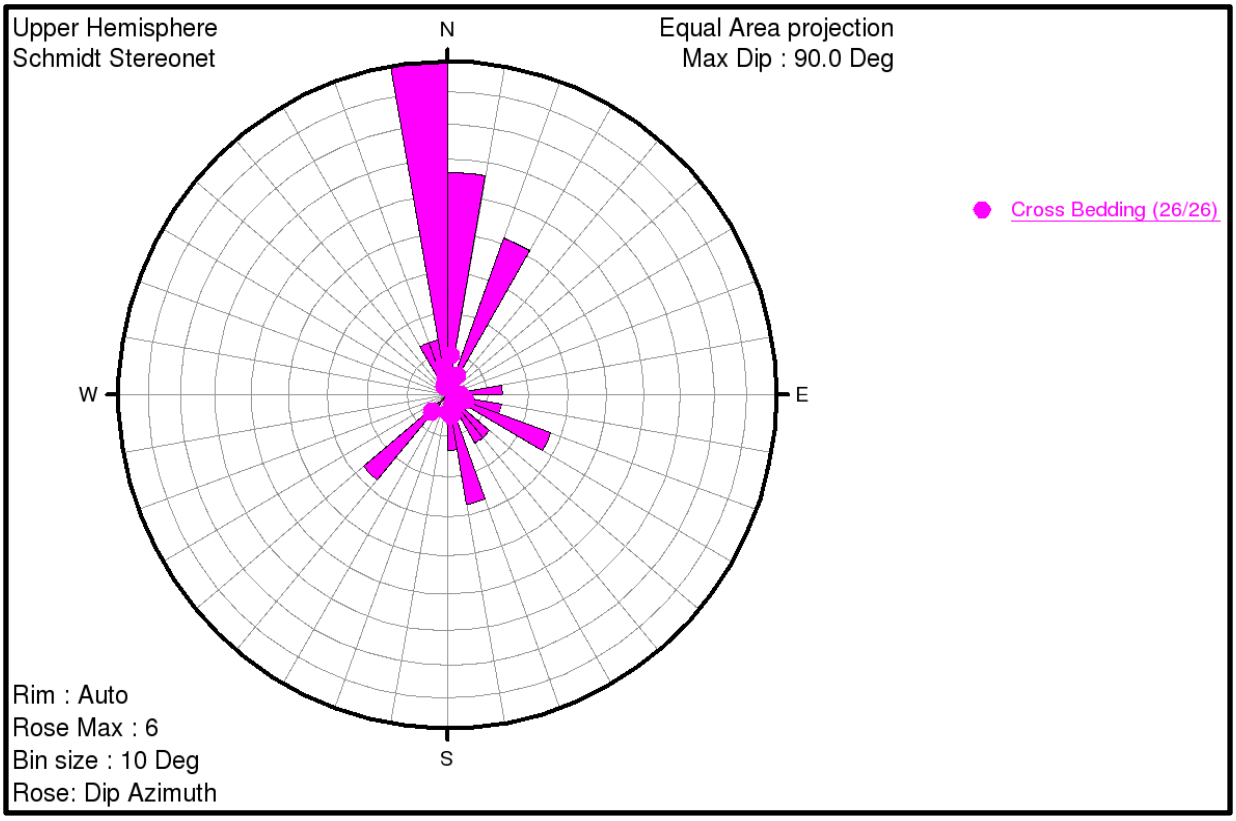

Figure 7.5b: Rose diagram showing cross bed dips from all intervals measured from VC00-VC85. No disconformable data is noticeable in this data set and so the data set is shown as a whole.

The three changes in palaeoflow trend suggest a broad scale structural control, with each change in dip trend corresponding to a change in structure. These three trends approximately coincide with the VU45 and VU75 tectonic events and could be attributed to structural reactivation and modification of the palaeo-slope from these regional events.

Both data sets show a high dispersion in the rose diagrams, confirming the fluvial style of a meandering river.

7.5 Discussion

It has been documented by previous authors that the regional flow direction is towards the north into the major depocentre of the Nappamerri Trough (Stuart 1976; Apak, 1994; Apak *et al*., 1997). The results of this image log study suggest a consistent south easterly flow direction from Dullingari North 18, while it suggests three well-defined palaeo-flow trends in the Crowsnest 2 Well. The regional depositional trend cannot be contradicted based on this data alone and so this data suggests a locally more complex drainage network; that ultimately drains into the Nappamerri Trough, working through finer palaeohighs and structural constraints. This is supported by the large discrepancy in the two wells studied that are themselves closely spaced (approximately 3 km), but show consistent trends within each well. The conclusion that it is difficult to determine with confidence; a regional depositional trend or axis from scarce image log data can also be made.

Chapter 8: Channel Belt Width Estimation

8.1 Introduction

A total of 532 bankfull measurements (as defined in Chapter 3.7) were measured from all wells within the study area. Only measurements where a high confidence that true bankfull depth was being measured were used in the statistical analysis (436 measurements). Intervals with similar bankfull depth populations were grouped together to form a larger more robust data set. The minimum, maximum and mean bankfull depths were then determined for each group. These three statistical values were then applied to the selected literature regression curves (outlined in Chapter 3.8) to determine a range for maximum, minimum and average channel belt widths for each group.

8.2 Bankfull Measurement

As discussed in Chapter 3.6-3.7, it is difficult to accurately determine a bankfull deposit from wireline data alone. For this reason measurements were given a confidence rating of 1-3, based on how confident that a true bankfull was being measured. Only measurements with a confidence rating of 1 or 2 (totalling 436 measurements) were used further in statistical analysis (Appendix D). Bankfull Measurements were corrected for compaction using the arbitrary 10% suggested by Bridge and Mackey (1993). It is possible to apply local compaction data from the Cooper Basin to the bankfull measurements, however seeming as the bankfull measurements were then applied to the linear regression curves to give a large range of variability, this was not deemed to be necessary for this application.

8.3 Statistical Analysis of Bankfull Measurement Data

For each genetic interval a population distribution histogram of bankfull depths was generated. Each histogram was then compared to overlying and underlying intervals and it was observed that groups of intervals were very similar and could be binned into larger groups (Figure 8.1 is used as an example, see Appendix B for individual and group histograms). From the statistical analysis 8 groups were defined (Table 8.1).

8.4 Applying Bankfull Data to Regression Curves

The maximum, minimum and mean bankfull depth values for each group were then applied to the literature regression graph to determine a range of channel belt widths

for each statistical value; the VC30-VU45 is used again as an example (Figure 8.2), for individual plots see Appendix C.

8.5 Discussion

The bankfull measurement populations could be expected to have a bimodal distribution: one population for larger channels and one for smaller tributary channels. However this is due to a sampling bias, smaller bankfulls were generally overlooked and not measured as major channel belts are the focus of the estimation. The minimum values of the channel belt width estimates are expected to be too small for the resolution of the palaeogeographic mapping; this population is encompassed in the minor channel facies assemblage rather than the major channel belt assemblages that this calculation focusses on. It was originally expected that the bankfull and channel belt widths would reflect the different systems tracts of the Patchawarra Formation. For example channel belt widths for a TST interval were expected to be wider than channel belt widths of LST and HST intervals. This was not observed to be the case, instead; consecutive intervals were apart of larger data sets (for example VC30-VU45 below). This indicates a longer period (spanning over several intervals) control over the channel belt widths. This longer period control on channel belt width could be attributed to tectonic tilting (see Chapter 3.8 for controls on channel belt width).

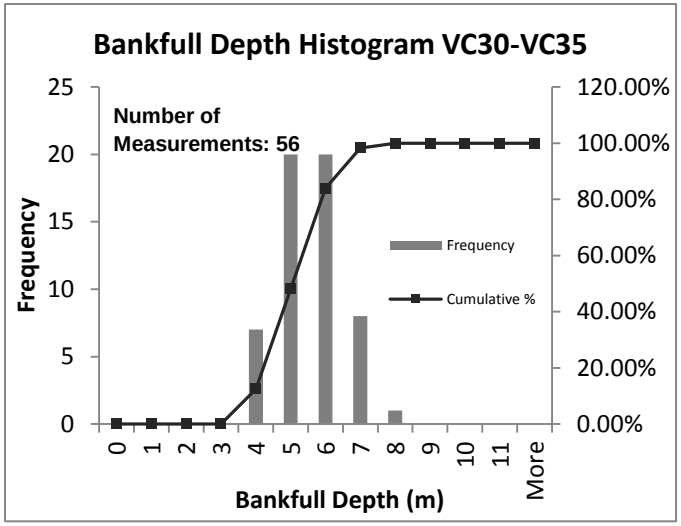

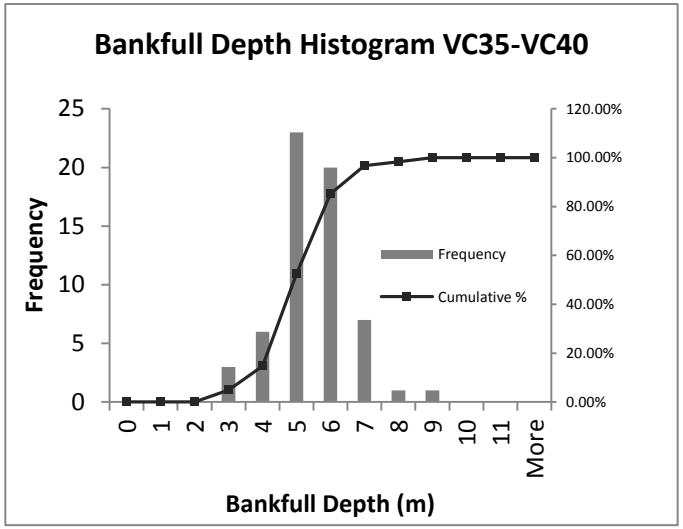

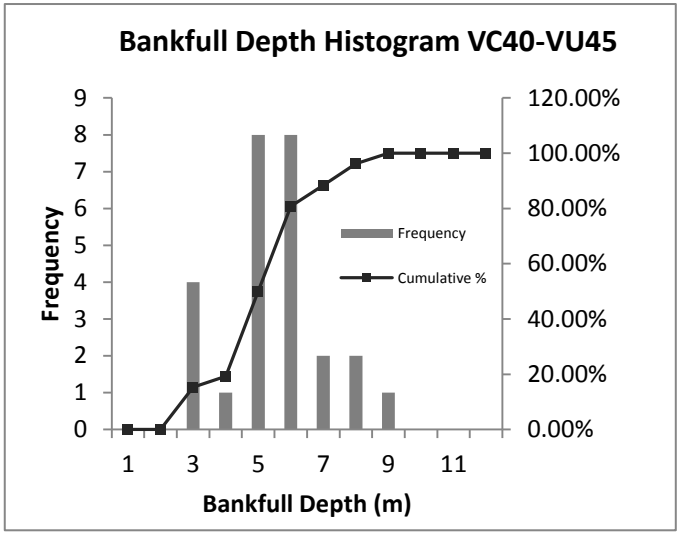

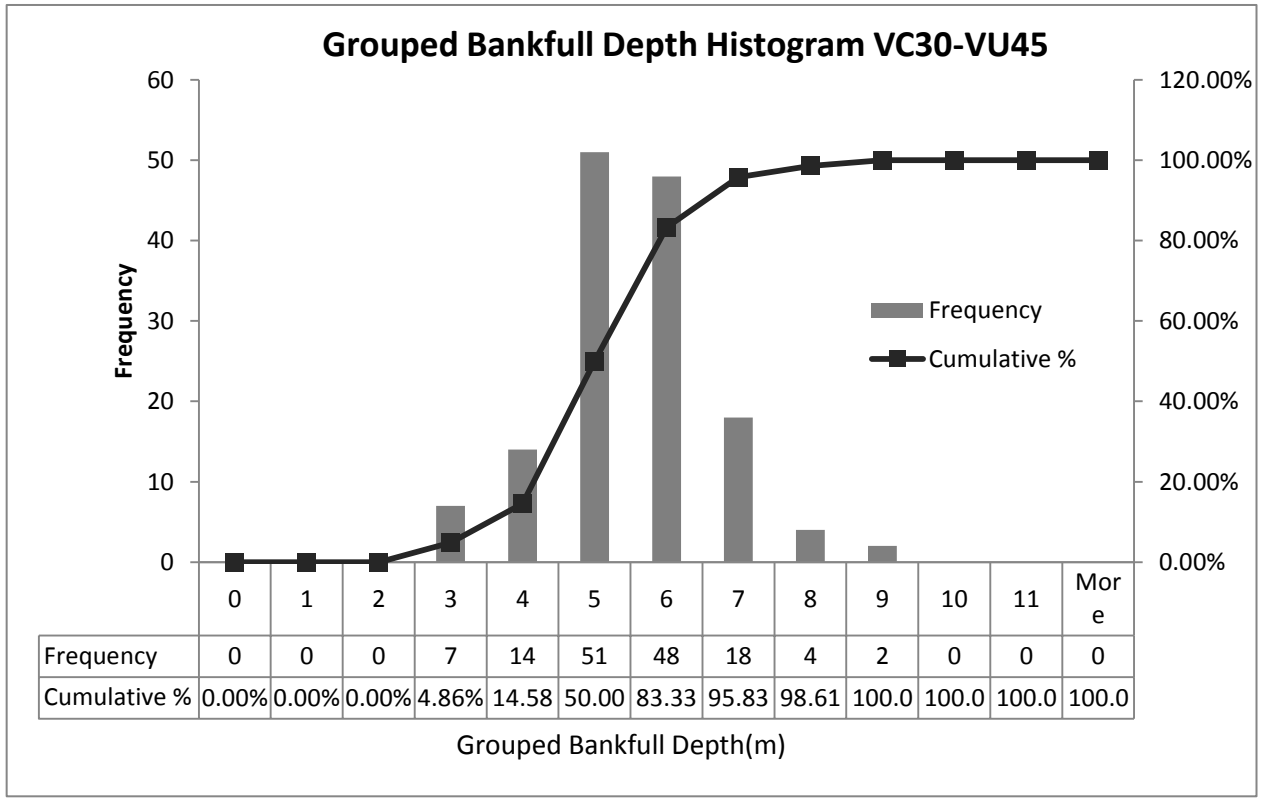

	0	1	2	3	4	5	6	7	8	9	10	11	More
Frequency	0	0	0	7	14	51	48	18	4	2	0	0	0
Cumulative %	0.00%	0.00%	0.00%	4.86%	14.58	50.00	83.33	95.83	98.61	100.0	100.0	100.0	100.0

Figure 8.1: Histograms of the three intervals VC30-VC35, VC35-VC40 and VC40-VU45, all of the intervals have a normal distribution with peaks at 5-6m, the combined group histogram has the same peaks but has a smoother distribution and a slightly larger range due to a more complete data set. For a full set of all histograms and grouped histograms, see Appendix B.

Table 8.1: Interval Group Bankfull Depths			
Group	Maximum (m)	Minimum (m)	Mean (m)
VC00-VL05	NA	NA	NA
VL05-VC10	4.6	1.4	2.6
VC10-VC30	7.8	2.3	5.2
VC30-VU45	8.2	2.3	5.0
VU45-VC55	7.8	2.7	5.4
VC55-VC60	7.8	1.8	5.6
VC60-VC65	7.3	2.7	5.2
VC65-VU75	7.3	3.7	5.3
VU75-VC100	6.4	2.7	4.9

Table 8.1: Data divided into Interval group with maximum, minimum and mean bankfull depth measurements. Measurements have been corrected for compaction by an arbitrary 10% as discussed in Section 8.2 above.

Group	Statistical Bankfull Value	Depth (m)	Minimum Channel Belt Width (m))	Maximum Channel Belt Width (m)
VL05-VC10	min	1.4	76	247
	avg.	2.6	196	632
	max	4.6	465	1505
VC10-VC30	min	2.3	161	521
	avg.	5.2	561	1814
	max	7.8	1033	3340
VC30-VU45	min	2.3	162	525
	avg.	5.0	528	1709
	max	8.2	1121	3625
VU45-VC55	min	2.7	207	670
	avg.	5.4	594	1921
	max	7.8	1039	3359
VC55-VC60	min	1.8	112	362
	avg.	5.6	628	2030
	max	7.8	1039	3359
VC60-VC65	min	2.7	207	670
	avg.	5.2	561	1814
	max	7.3	939	3037
VC65-VU75	min	3.7	334	1081
	avg.	5.3	577	1867
	max	7.3	939	3037
VU75-VC100	min	2.7	207	670
	avg.	4.9	512	1657
	max	6.4	769	2487

Table 8.2: Maximum and minimum calculated channel belt width ranges for each interval group.

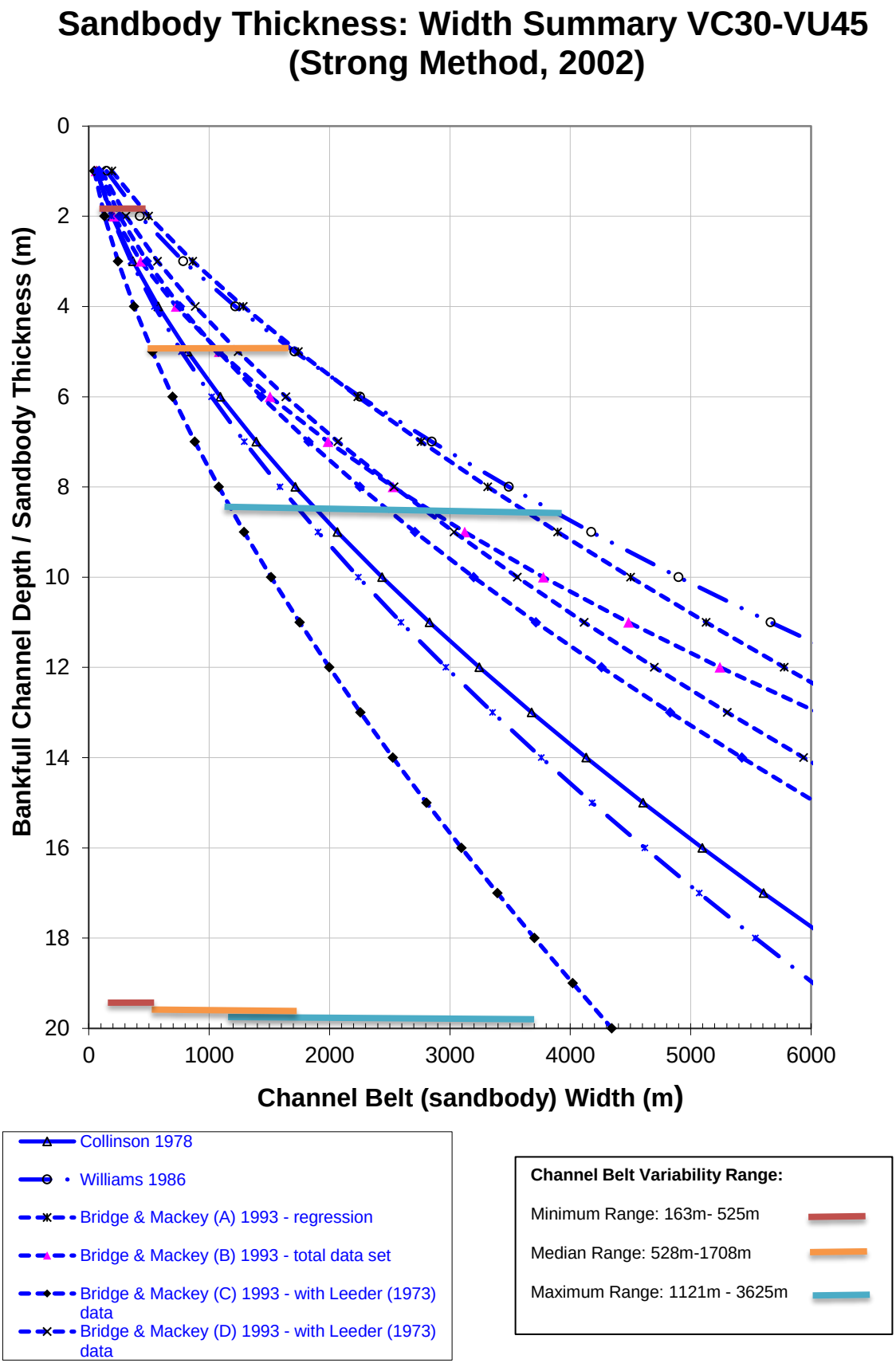

Figure 8.2: Interval group VC30-VU45 channel width estimate from literature regression curves. A larger range is always calculated for the mean and maximum values from the expanding nature of the curves, increasing exponentially.

Chapter 9: Palaeogeographic Mapping

9.1 Introduction

Palaeogeographic reconstructions were interpreted for all Patchawarra Intervals. Structural trends were observed within the study area that had a pronounced influence on depositional patterns (Apak, 1994) and are defined in Figure 9.1 and referenced herein. Non-deposition versus erosional contacts have been interpretted where stratigraphic intervals are absent. Depositional trends were interpreted with a high degree of confidence in the southern part of the study area where well data is dense while in the northern area depositional trends and drainage directions have more uncertainty. All palaeogeographic maps are listed in Appendix A.

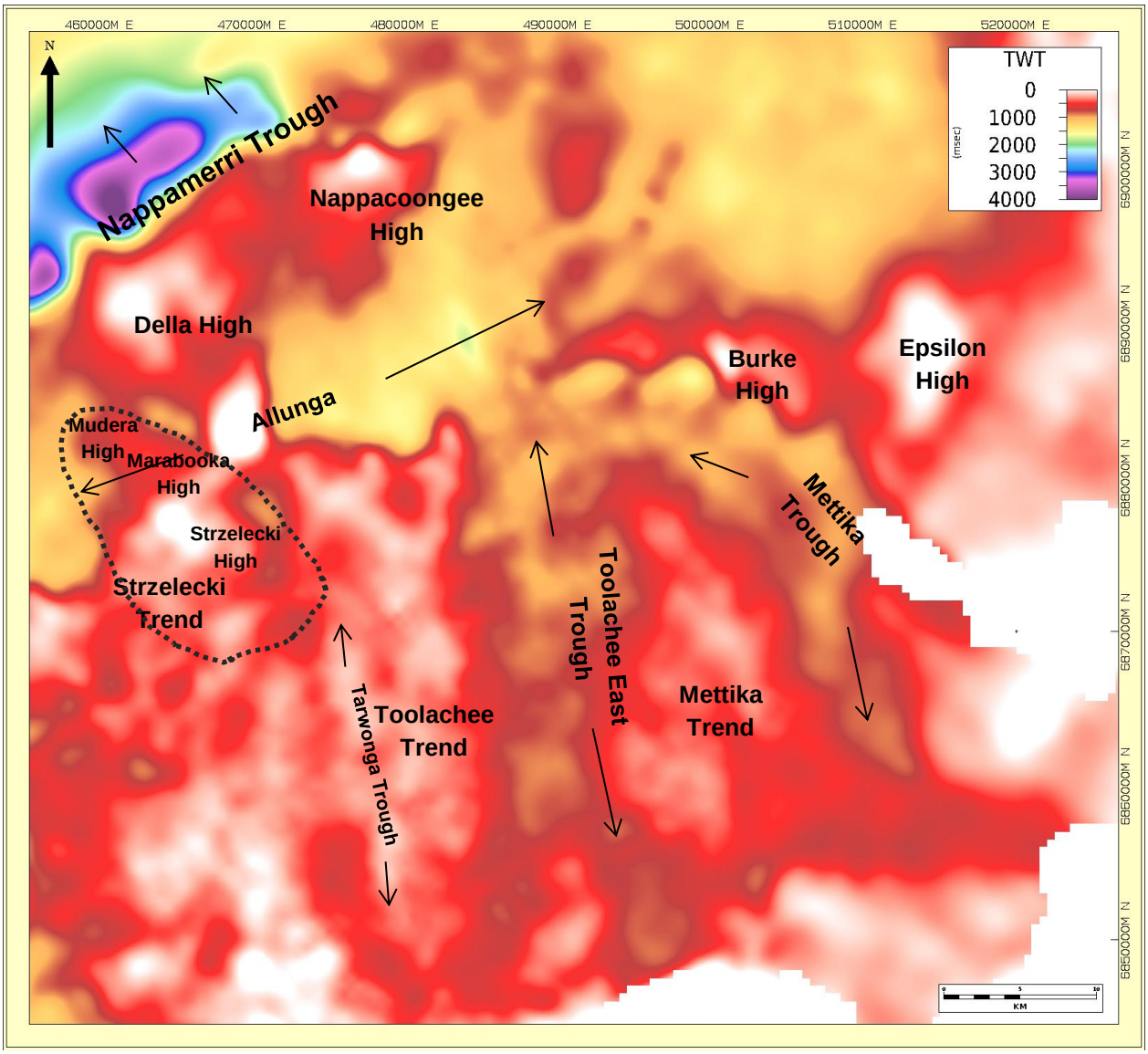

Figure 9.1: Full Patchawawarra isochron (TWT). Trends are defined as multiple structures, whereas highs are more discreet individual structures. Both the Toolachee and Mettika Trends have smaller troughs and peaks within the structural trend, that are not distinguishable from this isochron. The Strezelecki Trend is annotated by the dashed line and includes the Mudera and Marabooka highs.

9.2 Results: Palaeogeographic Mapping Elements

9.2.1 Non deposition versus Post Depositional Erosion on Structural Highs

A number of sections are absent on various structural highs within the study area. Although the sections are absent, the difference between non-deposition or post-depositional erosion has large implications for channel belt axes and depositional trends around the absent sections. The interpretations were made using depositional onlap contacts and observations on 2D seismic lines where available.

Insufficient sub formational picks of the Patchawarra Formation in seismic sections over the Strezelecki Trend restrict any seismic interpretation of erosion versus non-deposition. The Strzelecki Trend has been interpreted as a fault bounded pop up structure activated during the VU45 compressive event by previous authors (Apak, 1994; Menpes, 2002). This lead to the interpretation that the absent sections on the Strezelecki high are due to post depositional erosion from the VU45 event. A preserved VC60-VC65 section on the Mudera High lead to the the interpretation that the Mudera/Marabooka Highs are fault segments of the larger Strezelecki Trend and that these segments experienced less uplift and erosion than the Strezelecki High.

Structural regions interpreted with confidence as non-depositional palaeo-highs are represented by white polygons. These regions are interpreted as having some minor depositional phases, but with no preservation potential. Non-depositional/unpreserved feeder channels off of the basement high in the south and east were recognised as a significant sediment source and denoted schematically using black arrows.

Structures interpreted with post depositional erosion are represented by red polygons.

Areas where the differentiation between non-deposition and erosion could not be made are represented by the red/white cross hatched polygons. It should be noted that the degree of uncertainty on non-deposition versus erosional contacts is relatively high without detailed analysis of seismic data. Figure 9.2 schematically illustrates the difficulty of determining the nature of absent stratigraphic sections on structural highs from well intersections alone. Greater constraints could be determined with detailed 3D seismic interpretation on the areas in question.

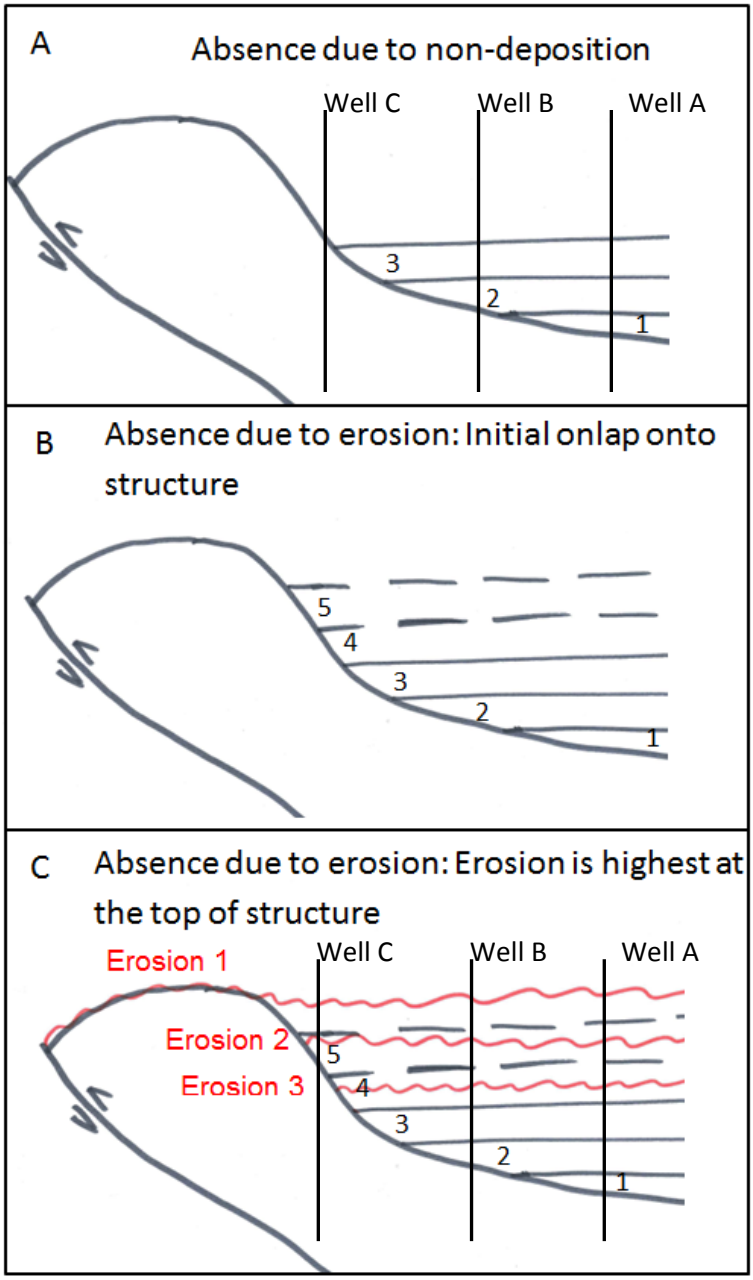

Figure 9.2: Outlines the preference of structural high points to be the last to be onlapped but also the first to be eroded. In this schematic example, units 1-3 are preserved on the flank of the structure. A shows the successive onlap of units 1-3, with no further deposition onto the high, units 4-5 are not present because they were not initially deposited. B shows the successive onlap of units 1-5 onto the structure through time. C shows the downward progression of the erosional profile due to a compressive uplift event through time (erosion 1-3). Unit 5 is the first to be eroded, then unit 4. Units 1- 3 are still preserved and units 4-5 are absent due to erosion. The vertical sections intersected in the wells A,B & C are the same for both absent sections. Therefore it is difficult to determine the difference between erosion and non-deposition from intersections around a structure alone .

9.3 Discussion

9.3.1 Uncertainties in Palaeogeographical Mapping from Wireline Data

The nature of meandering fluvial systems results in a complex areal arrangement of depositional environments. However it was observed that fluvial systems are fractal in nature as discussed in Chapters 5 & 6. For example within a channel belt there are subordinate facies such as interfluves, oxbow lakes, lacustrine abandonment and minor channel systems (Figure 9.3a).

Figure 9.3 shows how the well distribution in the area would represent the modern day environments if intersected in the subsurface.

-Figure 9.3a is entirely within a channel belt environment, intersecting mainly point bar deposits from numerous channel deposits.

-Figure 9.3b intersects mainly lacustrine environments in the uplands. Even within the channel belt system; a similar number of data points (5) intersect lake abandonment environments as data points intersecting sandy braid bar deposits (7), misrepresenting the channel facies as an environment; 50% sand rather than 90-100%.

-Figure 9.3c again intersects upland environments; the minor channel in the north is favourably intersected 7 times, while the major channel is intersected 8 times.

This highlights the insufficient sample spacing and spatial sampling bias of well data to deal with both the spatial variability of meandering fluvial environments as well as the complexity of facies assemblages within a single environment. Palaeogeographic interpretations were carried out with these limitations in mind, resulting in numerous facies assemblages being within a single interpreted environment.

9.3.2 Uncertainties in Channel Belt Mapping

Where well data is sparse (e.g. the north of the study area) palaeogeographic interpretation has a high degree of uncertainty with a greater reliance on modern analogues and the available TWT isochrons. Channel trends are extrapolated from the nearest point in these areas where no well data is present. This is always the case in the northern part of the study area where channels enter the Nappamerri Trough (Figure 9.4).

Interval isochrons constrain interpretations outside well control for example; basement lineaments and associated depressions are interpretted to control the channel axes. The VU75-VC80 and the VC80-ZU00 palaeomaps (Appendices A16 & A17) demonstrate this where NE striking lineaments constrain the channel axes. Figure 9.3 is an example of the uncertainty of the channel belt interpretation where no well data is present in the northern study area. In Figure 9.3 the dashed line shows two other probable channel positions that could be interpreted with the same level of uncertainty.

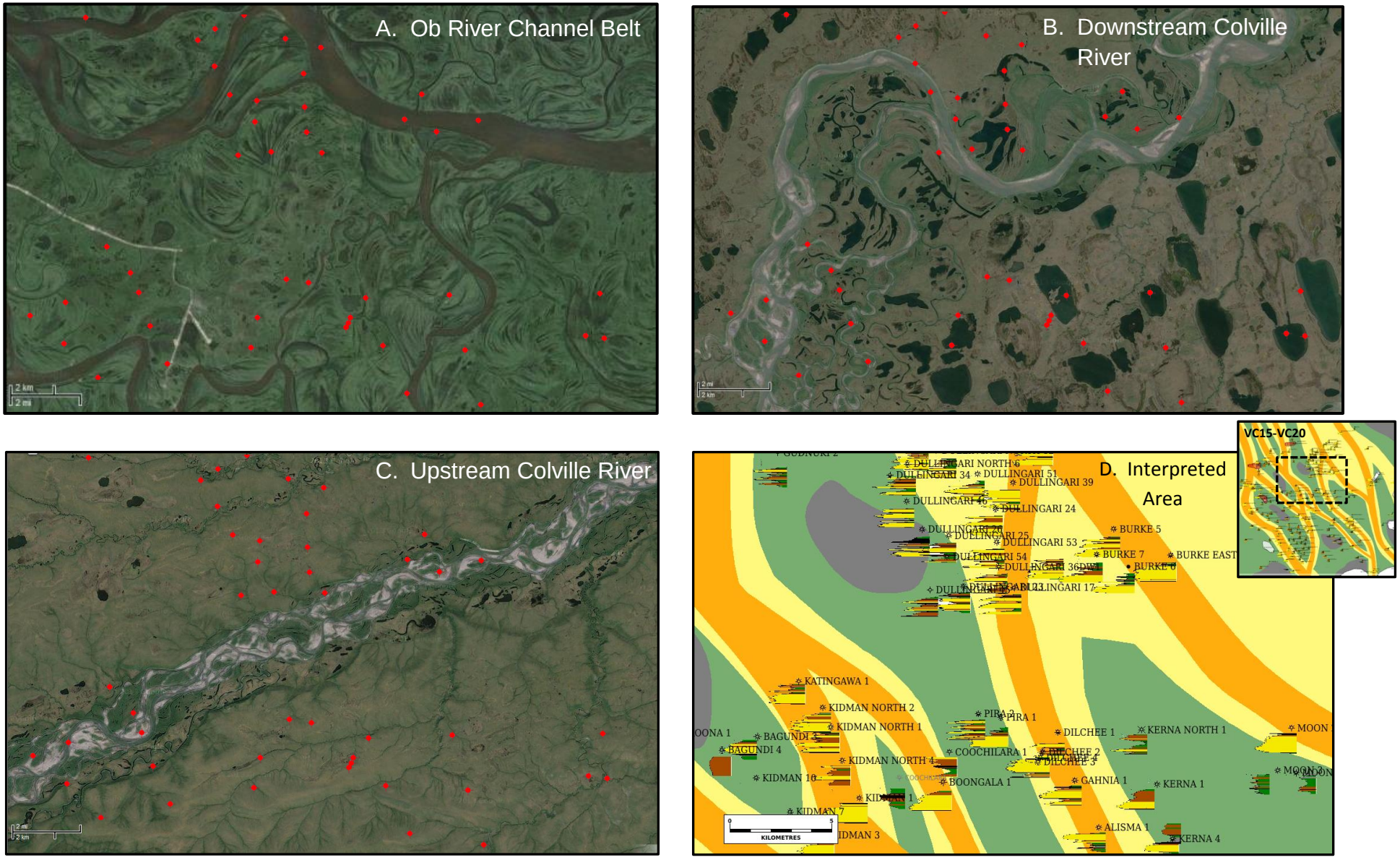

Figure 9.3: Analogue environments studied previously in chapters 5 and 6 compared with a palaeogeographic interpretation of the VC15-VC20 interval. The red points overlain onto the analogue images in A,B & C represent the same well distribution as in the mapping area in D. A- Within a single channel belt system in the Ob River, all of the data points would intersect sandy point bar deposits.

Figure 9.4 shows the VC25-VC30 interval where the channel north of Pooraka 1 is interpreted to deflect slightly towards the north, this interpretation was made based on both the regional trend of the other channel belt drainage directions and isochrons suggesting drainage directly into the Nappamerri Trough. A channel belt could have been interpreted draining directly north anywhere from the Della 14 well to the Pooraka well with a similar level of confidence (dashed oultines).

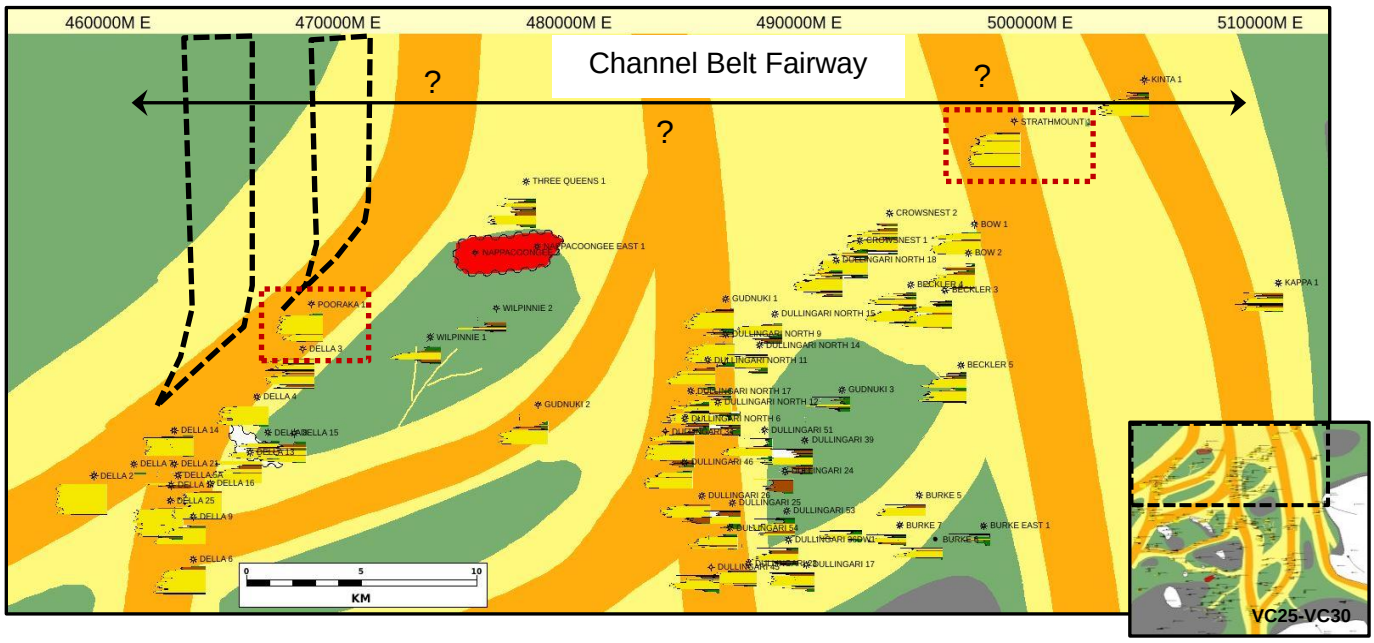

Figure 9.4: Shows the uncertainty of channel belt position in the north of the study area away from well control for the VC25-VC30 interval. It is possible that the channel intersected in the Della wells in the northwest could drain directly north into the Nappamerri Trough, rather than continuing northeast and deflecting north as it was interpreted. Similarly the exact channel belt locations north of the Dullingari wells could be interpreted anywhere within the channel belt fairway with a similar degree of confidence. Both of the channel belts in the east are each only intersected by one well, highlighting the ambiguity of the location of the channel belts both north and south of the well intersections.

Strathmount 1 (Figure 9.4) is the only well intersecting the interpreted channel while the Bow/Beckler wells suggest that they are within the fairway but do not intersect the main channel belt. In these areas individual channels are interpreted to be within a channel belt fairway draining into the Nappamerri Trough, but their exact location is inferred and interpreted to conform to the well data. This highlights the uncertainty in the interpretation of individual channel belt directions away from the well control in the northern study area.

Chapter 8 outlined how channel belt width calculations were calculated for intervals to better constrain maximum and minimum width variabilities for each interval. However, it is observed that meandering rivers increase in sinuosity downstream with an increase in flow capacity (Leopold *et al*., 1957). Therefore channel belt widths are expected to increase in size towards the north as they migrate from the flank of the basin and eventually drain into the Nappamerri Trough. Although Chapter 8 did not address the spatial variability of channel belt width a small investigation is made below. Figure 9.4 shows an example of a channel belt system interpreted from the VC65-VC70 interval widening downstream towards the Dullingari/Beckler Field. Table 9.1 shows a maximum channel width calculation for the VC65-VC70 interval divided spatially into upstream (south) and downstream (north) domains.

Table 9.1: Example of Channel Belt Width Calculation for Spatially Sorted Data.

	Number of Measurements	Average Bankfull Measurements (m)	Maximum Channel Belt Width (m)
SOUTHERN WELLS	4	5.2	1814
NORTHERN WELLS	8	5.8	2141

The calculated channel widths are larger for the downstream wells supporting the interpretation of an increasing channel belt width downstream as the channels coalesce. The interpreted channels in this interval are all wider than the maximum channel belt width calculated from this isolated example set but are still within the larger grouped interval VC65-VU75 maximum range (939-3038m). This reiterates the limitations of the use of the channel belt width estimation method being used too literally and specifically as discussed in Chapter 3.7 & 3.8, but confirms that it is very useful for qualitatively defining channel belt width relationships and applied broadly to a large data population.

9.4 Depositional Trends of the Patchawarra Formation in the Tenappera Region.

The depositional trend of the mid and lower Patchawarra Formation VU45-VC100 experienced a very different depositional style to the Upper Patchawarra due to

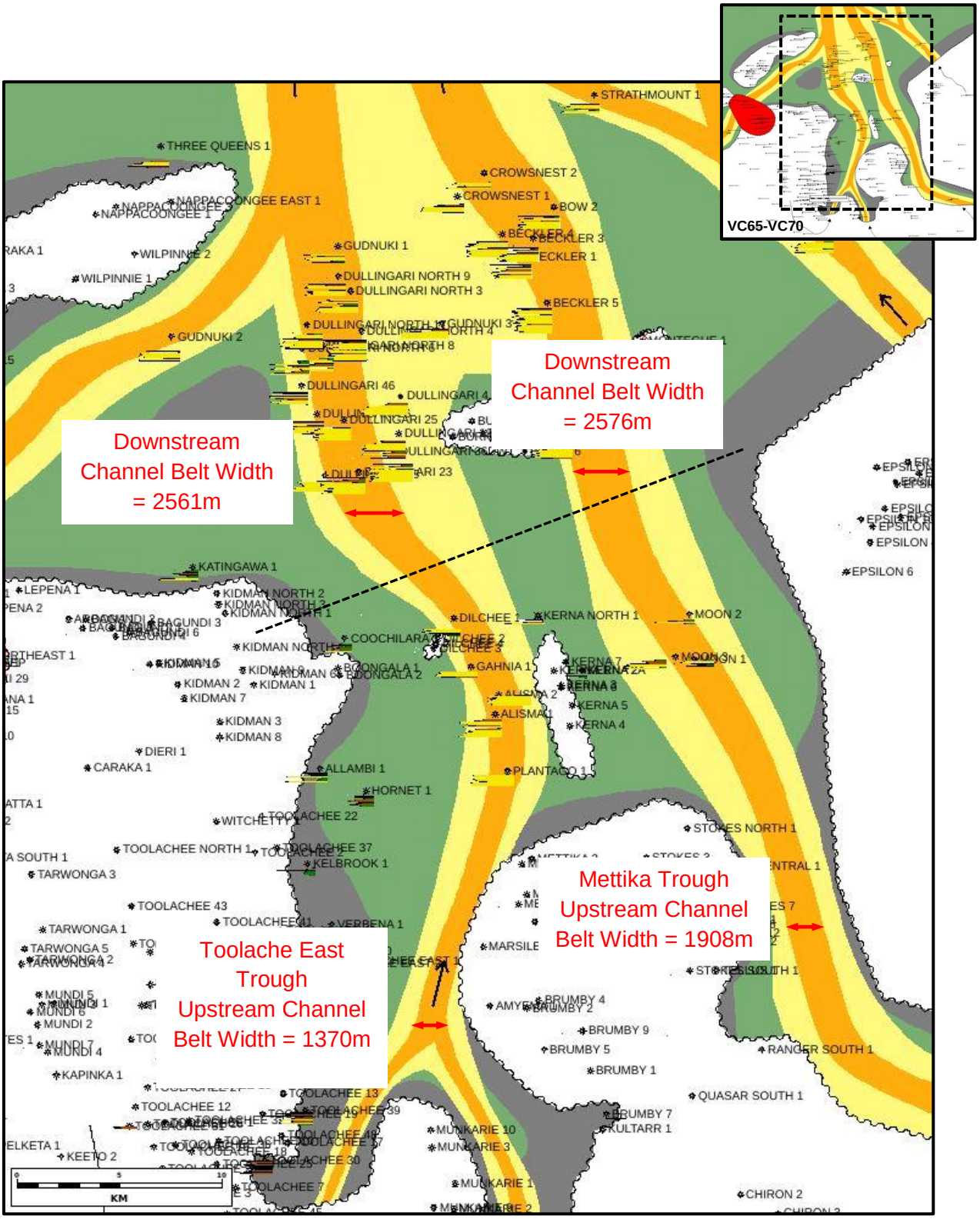

Figure 9.5. Example of increasing channel belt width of a channel belt system downstream towards the north. The dashed black line indicates the separation into upstream/downstream wells used for the example calculation. The channel belts are interpreted to be less structurally confined downstream in the Dullingari Area than in the Toolachee East and Mettika Troughs as well as having a shallower gradient, resulting in a larger channel belt width.

mainly allocyclic controls. The lower Patchawarra is characterised by a basin fill architecture, basement lows infilled with lacustrine/floodplain deposits, with course grained sediment being supplied through the three main troughs (Allunga, Toolachee East and Mettika Troughs) from the basement uplands along major depositional axes. The sporadic switching of the major troughs from high sediment supply back to lacustrine/floodplains, suggests a large control from the basement erosion profile to the south on coarse grained sedimentation. The sediment supply from this erosional profile governed the changing position of the major depositional axes over time. The basement erosional profile was in turn most likely governed by tectonic events, either tilting or faulting of major blocks, altering the sediment supply into the Tenappera Region. Likewise active faulting within the Tenappera Region during the mid-lower Patchawarra influenced depositional trends also. This is exemplified by the Burke Field. The Burke Field was activated during both the VU45 and VU75 events, both directly eroded sediments on the high, as well as diverted the depositional axis from the Mettika Trough towards the west and to a lesser extent; to the east also. This to some degree can be attributed to the frequent sand sections in the Dulllingari Field, concentrating deposition from the Mettika Trough with the Toolachee East Field. Even once the basin was in-filled in areas, depositional trends during the mid-lower Patchawarra still followed the same depositional trends governed by structural basement troughs. This suggests that compaction during this period played a large role in preserving the structural corridors even after initial in-filling.

The Upper Patchawarra VC00-VU45 was markedly different in style than the mid-lower Patchawarra. Channels were generally broader and did not follow structural corridors through intervals (except locally in the Toolachee Trend during initial infilling). Although depositional trends were not governed strongly by structure, local structures did influence flow, such as the Della High from the VC20-VU45. However these structural controls acted more as local diversions of flow around the discreet palaeo-highs rather than as major structural controls. Large sheet sands were deposited during the VC20-25 and VC30-VC40 intervals during approximate LSTs. These sheet sands were unconfined and highly reworked, leaving only small areas of floodplain preserved. This is much more typical of an unconfined meandering system during a LST. The Upper Patchawarra section seams to behave much more like an unconfined meandering system and is controlled more by autocyclic controls.

The VC00-VC15 intervals constitute a transgressive lacustrine period; these lacustrine deposits were not the focus of the study. Facies assemblages of these deposits were not considered in the framework, although they were included so that these intervals could be mapped. These intervals would be mapped best within the framework of the lacustrine Murturee Shale, using a deltaic lacustrine facies framework such as the framework outline by Kelts *et al.* (1991) rather than the fluvial framework established and used in this study.

Chapter 10: Applications and Recommendations

10.1 Analogue Application and Suitability

Analogues are widely referred to for a number of exploration and production applications for the Patchawarra Formation across the Cooper Basin. Therefore a better understanding of which elements of a particular analogue apply to certain features of the Patchawarra result in a better application when using such analogues.

The mid-lower Patchawarra was found to be highly structurally controlled, with depositional axes confined to basement lows and sediment supply highly controlled by basement source influxes. This depositional style does not fit the Ob River Analogue well. Instead, this period of deposition can be better related to the McKenzie River and Colville/Sag Rivers. Both of these analogues show a higher degree of similarity than the Ob River for the Patchawarra Formation in the Tenappera Region. The tectonic tilting in the McKenzie River has been attributed to isostatic rebound (Clague and James, 2002; Sella *et al.*, 2007). The lower Patchawarra formed in a period of post worldwide glaciation (Veevers and Powell, 1987; Alexander, 1998) and so it can be postulated that isostatic rebound similarly could have affected both structuring and regional tilting during the mid-lower Patchawarra period. This could explain the pronounced uplift events (VU45 & VU75) and ‘pop-up’ structures; forming as a result of load removal from the glacial rebound (Bolt, P, Pers Comms, 2014). The Colville/Sag Rivers are highly structurally confined by underlying basement geology. There is very little substrate for a fluvial system to be able to erode into and meander except in the northwest of the area where it starts to increase in sinuosity as a function of this (See Chapter 5.3.1). This style of geomorphology is interpreted in the lower Patchawarra sections. These analogues however, are not a perfect match for the lower Patchawarra either; the VC50 and VC60 horizons within the lower Patchawarra are both thick expansive coals that are regionally correlatable and covered the entire Tenappera study area. These analogues are not dominated by peats, this again highlights the lack of a perfect analogue for the Patchawarra Formation.

The Ob River was confirmed to be the most applicable analogue to the upper Patchawarra section. The upper Patchawarra was found to be structurally unconfined, with enough substrate previously deposited to be able to work through as a broad meandering system. The Ob River analogue represents these much closer than the lower-mid Patchawarra Sections.

10.2 Direct Applications and Recommendations for the Tenappera Region

10.2.1Applications

The immediate result of this study is that reservoir facies have been mapped for each regionally correlatable chronostratigraphic interval across the study area. Combined structural/stratigraphic and stratigraphic onlap plays are the major play types for the Patchawarra Formation. Within the Patchawarra Formation; large primary porosity loss in reservoir sands has been due to compaction related diagenesis, with no secondary porosity reported (Stuart, 1976). Reservoir porosity and permeability is strongly related to original depositional features such as sand grain size and sorting (Gravestock *et al.,* 1998*)*. Therefore reservoir quality, to a degree can be approximated to channel sand quality in a regional sense.

Ultimately the generated palaeogeographic interval maps can be combined with seismic data to assess prospectivity of stratigraphic/structural plays by both assessing likelihood of sand intersected at a certain interval and likely reservoir quality within an identified structural feature, such as a four way dip closure or structural flank.

10.2.2 Recommendations

The largest source of uncertainty during palaeogeographic mapping was channel belt position and drainage direction away from well control, particularly in the northern study area. This was due to poor seismic grids of intervals that were too large (VC00-VC30 for example) and that were poorly interpolated (Visible bullseyes generated by point sources from individual wells). These seismic grids were contoured in 2004, since then new 2D lines and 3D Volumes have been shot, and many more wells have been drilled. Therefore reinterpreting and interpolating the available seismic into smaller isochrones of chronostratigraphic intervals is the first recommendation that would have the most notable effect on this work.

Locally, 3D Volumes such as the Dullingari Field could be interpretted to produce high resolution isochrons of mapped intervals. This would allow a detailed examination of the facies distributions on a field scale.

10.3 Workflow Application

The workflow used in this study can be applied to similar fluvio-lacustrine petroleum systems to better constrain facies distributions using available wireline data. This study highlights the essential use of suitable analogues coupled with an appropriately formulated electro-facies assemblage to successfully map facies distributions away from well control.

The workflow is thought to be highly applicable to the Patchawarra Formation in other regions of the Cooper Basin. The workflow is not considered applicable to the Epsilon Formation however; it is a second order lacustrine regressive cycle and contains shoreface and deltaic facies as well as floodplain deposits (Battersby 1976, Thornton, 1979; Alexander, 1998). Therefore it is expected that the workflow would deal with these environments similarly as it did with the VC00-VL05 and VL05-VC10 intervals.

The Piceance Basin, Colorado has been considered analogous to the Cooper Basin. The Piceance Basin developed under a compressive regime within a meandering fluvial environment (Sanborn, 1971). Prominent plays within the Piceance Basin are stratigraphic pinch out and structural onlap plays targeting channel reservoir facies (Spencer, 1988). Therefore by using the workflow established in this study; reservoir facies could be better confined and potential plays could be identified in the Piceance Basin.

The importance of high resolution chronostratigraphic subdivision into genetic units is also emphasised for the most effective mapping of facies distributions. This is best exemplified by the mapped intervals VC20-VC25, VC30-VC35 and VC35-VC40 where individual cycles could not be defined and an amalgamated complex was interpretted for the majority of the mapping area.

The channel belt width calculation method used in this study proved to be an effective method for constraining fluvial channel belt widths on a regional scale. Further investigation into calculating individual channel belt widths for individual channel belts, once mapped (Discussed in 9.4.2) could further constrain channel belt locations within an interval.

The determination of palaeo-flow from image log data revealed that the sinuous nature and stacking patterns of a meandering fluvial system results in a potentially complex palaeo-flow direction within a single well intersection that may not be able to be resolved into a regional drainage direction. Therefore regional palaeo-flow directions may only be determinable within areas with numerous wells with image log data.

Chapter 11: Conclusions

The palaeogeographic reconstruction of chronostratigraphic intervals of the Patchawarra Formation has resulted in a better understanding of the different fluvial styles through time and depositional trends within the Tenappera Trough Region. Palaeogeographic reconstruction intervals can be used to better predict spatial distributions of reservoir facies. These, in turn can be used to assess prospectivity of a proposed well location, by constraining the probability of intersecting particular sands for a given interval. Key outcomes of the study are outlined below:

- No single present day analogue was identified as being perfectly analogous to the Patchawarra Formation in the Tenappera Region. However, the Ob River was acknowledged as the best analogue representing the depositional environments of the Patchawarra Formation. While the McKenzie and Colville/Sag Rivers were identified as being structurally confined and influenced by a compressive structural architecture. These controls affected the McKenzie and Colville/Sag Rivers by influencing the style of the river system and avulsion patterns over time.
- The Patchawarra Formation was determined to have two distinct fluvial styles. The mid-lower Patchawarra Formation was governed by a basin fill architecture and highly dependent on allogenic controls. During this time the Patchawarra Formation filled in basement lows with lacustrine/floodplain deposits. Course grained sedimentation sourced from the basement to the west feed into the Tenappera Region via troughs. Sporadic switching of coarse grained sediment supply between the major troughs suggests a changing basement erosional profile through time. This period of deposition can be better related to the McKenzie/Colville River Analogues. With the exception of large and dominant coals from the VC70-VC50 time, not seen in these analogue environments.
- Six electrofacies were observed within the Patchawarra Formation, these were applied to the present day analogue of the Ob River to establish 4 palae-environments of deposition that constitute the facies mapping units of the palaeogeographic reconstructions.

- Palaeoflow indicators were analysed from the available two wells with medium-poor quality image log data recorded from resistivity mandrel logs only. Palaeoflow was determined but was highly complex, confirming the complexity of a meandering fluvial system but rendering a regional palaeo-flow direction indeterminable.
- 532 bankfull measurements were made from 1D wireline data. The entire data set gave a maximum bankfull depth of 8.2m, a minimum of 1.4m and a mean value of 5.1m after allowing for compaction. These measurements were then applied to selected linear regression curves. Channel belt width calculations gave a range of variability from 76m to 3625m, with an average channel belt width range from 1639-1908m.

The workflow of this study is thought to be applicable to the Patchawarra Formation across the Cooper Basin, the Toolachee Formation and other petroleum systems that are dominated by a fluvial architecture in particular, the Piceance Basin, Colorado.

Chapter 12: References

Aitken, J.F. and Flint, S.S., 1995. The application of high resolution stratigraphy to fluvial systems: a case study from the upper Carboniferous Breathitt Group, Eastern Kentucky, USA. Sedimentology Vol. 42: 3-30.

Alexander, E.M. and Sansome, A., 1996. Lithostratigraphy and environments of deposition. In: Alexander, E.M. and Hibburt, J.E. (Eds), The petroleum geology of South Australia. Vol 2: Eromanga Basin. South Australia. Department of Mines and Energy. Report Book, 96/20.

Alexander, E.M., 1998, Lithostratigraphy and Environments of deposition. In: Gravestock, D.I. and Jensen-Schmidt, B, 1996. Structural setting. In: Gravestock, D.I., Hibburt, J.E. and Drexel, J.F. (Eds), 1998. The petroleum geology of South Australia, Volume 4: Cooper Basin. South Australia. Department of Primary Industries and Resources. Report Book 98/9.

Allen, G.P., Lang, S.C., Musakti, O. and Chirinos, A., 1996. Application of sequence stratigraphy to continental successions: implications for Mesozoic cratonic interioir basins of Eastern Australia. In: Mesozoic Geology of the Eastern Australia Plate Conference. GSA, Extended Abstracts Vol. 43:22-36.

Apak, S. 1994, Structural Development & Control on Stratigraphy and Sedimentation in the Cooper Basin, Australia. Ph.D. Thesis, Univeristy of Adelaide.

Apak, S. 1995. Compressional Control on Sediment and Facies Distribution SW Nappamerri Syncline and Adjacent Murteree High, Cooper Basin. APPEA Journal, pp 190-202.

Apak ,S.N., Stuart, W.J, Lemon, N.M., 1997, Structural Evolution of the Permian-Triassic Cooper Basin, Australia: Relation to Hydrocarbon Trap Styles. AAPG Bulletin, Vol.18: 533-555.

Battersby, D.G., 1976. Cooper Basin gas and oil fields. In: Leslie, R.B., Evans, H.J. and Knight, C.L. (Eds), Economic geology of Australia and Papua New Guinea, 3, Petroleum. Australasian Institute of Mining and Metallurgy. Monograph Series, Vol. 7:321-368.

Boggs Jr., S., 2006. Principles in Sedimentology and Stratigraphy, Pearson Prentice Hall.

Beeston, J.W. and Draper, J.J., 1991. Organic matter deposition in the Bandanna Formation, Bowen Basin. Queensland Geological Society Journal, Vol. 2: 35-51.

Bridge, J.S., and Mackey, S., 1993. A theoretical study of fluvial sandstone body dimensions: International Association of sedimentologists Special Pub. No. 15, p. 213-236.

Bridge, J. S., and Tye, R. S., 2000, Interpreting the dimensions of ancient fluvial channel bars, channels, and channel belts from wireline-logs and cores:AAPG Bulletin, v. 84, n. 8, p. 1205-1228.

Bridge, J.S., 2009, Rivers and Floodplains Forms, Processes, and Sedimentary Record, John Wiley & Sons, Ltd, Hoboken.

Catuneanu, O. & Geological Association of Canada. Mineral Deposits Division. 2003. Sequence stratigraphy of clastic systems, Geological Association of Canada, St. John's, NewFoundLand.

Cant, D.J., 1982, Fluvial facies models. In: Middleton, G.V. (Eds). Scholle, P.A. and Spearing, D, 1982. Sandstone depositional environments. AAPG memoir, 31: 115-138.

Chaney, A.J., Cubitt, C.J. and Williams, B.P.J., 1997. Reservoir potential of glacio-fluvial sandstones: Merrimelia Formation, Cooper Bas in, South Australia. APPEA Journal, Vol. 37(1):154-176.

Chopra, P. N., and Holgate, F., 2005, A GIS Analysis of temperature in the Australian Crust: Proceedings, World Geothermal Congress 2005, Antalya, Turkey, 24-29 April 2005.

Clague, J. J., and T. S. James 2002. History and isostatic effects of the last ice sheets in southern British Columbia, Quat. Sci. Rev., 21, 71– 87.

Collinson, J.D., 1978, Alluvial Sediments. In: Reading, H.G., Sedimentary Environments and Facies: Elsevier, N.Y: 15-59.

Etheridge, F.G., Wood, L.J and Schumm, S.A., 1998. Cyclic variable controlling fluvial sequence development: problems and perspectives. In: Relative Role of eustacy, climate and tectonism in continental rocks. Shanley, K.W. and McCabe. P.J., (eds). SEPM Special Publication, 59: 17-30.

Evans, P. R., 1988. The formation of petroleum and geological history of Australia. Petroleum in Australia: the first century. APEA Special Publication., 26-47.

Fielding, C. R., and Crane, R. C., 1987. An application of statistical modeling to the prediction of hydrocarbon recovery factors in fluvial reservoir sequences. In: Ethridge, F., G., Flores, R. M., and Harvey, M. D., (eds.), Recent developments in fluvial sedimentology, SEPM Special Publication no. 39, p. 321-327.

Fielding, C.R., Falkner, A.J. and Scott, S.G., 1993. Fluvial response to foreland basin overfilling: the Late Permian Rangal Coal Measures in the Bowen Basin, Queensland. Australia. In: C.R. Fielding (Editor), Current Research in Fluvial Sedimentology. Sediment. Geol., 85: 475-497.

Finlayson, D.M., Leven, J.H., Wake-Dyster, K.D. & Johnstone, D.W., 1990 . A crustal image under the basins of southern Queensland along the Eromanga-Brisbane Geoscience transect. In: Finlayson, D.M. The Eromanga-Brisbane Geoscience Transect: a guide to basin development across Phanerozoic Australia in southern Queensland. Bureau of Mineral Resources, Australia, Bulletin 232:153-176.

Foden, J. D., Elburg, M. A., Turner S. P., Sandiford, M. A, O'Callaghan, J. G., *et al.* 2002. *Granite production in the Delamerian Orogen, South Australia*. Geological Society MLA citation Journal of the Geological Society, 2002 Vol. 159(5):557-575.

Foster, D.A., and Gray, D.R., 2008. Paleozoic crustal growth, structure, strain rate, and metallogeny in the Lachlan orogen, eastern Australia, in Spencer, J.E., and Titley, S.R., eds., Ores and orogenesis: Circum-Pacific tectonics, geologic evolution, and ore deposits: Arizona.

Gallagher, K.L., 1988. The subsidence history and thermal state of the Eromanga and Cooper Basins. Australian National University (Canberra). Ph.D. thesis (unpublished).

Gallagher, K. and Lambeck, K., 1989. Subsidence, sedimentation and sea-level changes in the Eromanga Basin. Basin Research, Vol 2: 115-131.

Galloway, W.E., 1989. Genetic stratigraphic sequences in basin analysis: architecture and genesis of flooding surface bounded depositonal units. AAPG Bulletin Vol. 73: 125-42.

Gatehouse, C.G., 1986. The geology of the Warburton Basin in South Australia. Australian Journal of Earth Sciences, Vol. 33:161-180.

Gatehouse, C.G., Fanning, C.M. and Flint, R.B., 1995. Geochronology of the Big Lake Suite, Warburton Basin, northeastern South Australia. South Australia. Geological Survey. Quarterly Geological Notes. Vol. 128:8-16. Geological Society Digest Vol. 22: 213-225.

Gibling, M.R., 2006, Width and thickness of fluvial channel bodies and valley fills in the geological record: A literature compilation and classification: journal of sedimentary research, Vol. 6: 195-206.

Glen, R. A., 2013. Refining Accretionary Orogen Models for the Tasmanides of Eastern Australia. Australian Journal of Earth Sciences Vol: 60(3): 315-70.

Glen, R. A., 2013. The Tasmanides of Eastern Australia. In: Vaughan, A.P. M., Leat, P. T. & Pankhurst, R. J. Terrane Processes at the Margins of Gondwana, 23-96. Special Publication of the Geological Society, London 246.

Gravestock, D.I. and Jensen-Schmidt, B, 1996. Structural setting. In: Gravestock, D.I., Hibburt, J.E. and Drexel, J.F. (Eds), 1998. The petroleum geology of South Australia, Vol. 4: Cooper Basin. South Australia. Department of Primary Industries and Resources. Petroleum Geology of South Australia Series:47-67.

Gravestock, D.I., Alexander, E.M., Morton J.G.G., Sun, X. 1996. Reservoirs and Seals. In: Gravestock, D.I., Hibburt, J.E. and Drexel, J.F. (Eds), 1998. The petroleum geology of South Australia, Vol. 4: Cooper Basin. South Australia. Department of Primary Industries and Resources. Petroleum Geology of South Australia Series: 47-67.

Gray, R. J. and Roberts, D. C., 1984. A seismic model of faults in the Cooper Basin, APPEA Journal Vol. 24: 421-28.

Heidbach, O., Tingay, M., Barth, A., Reinecker, J., Kurfeß, D., and Müller, B., 2008. The World Stress Map database release doi:10.15.94/GFZ.WSM.Rel2008.

Kapel, A.J., 1966a. The Coopers Creek Basin. APEA Journal, Vol. 6:71-75.

Kapel, A.J., 1972. The geology of the Patchawarra area, Cooper Basin. APEA Journal, Vol. 12: 53-56.

Kelts, K. R, Anadon, P, Cabrera, 1991. AAPG and International Association of Sedimentologists *Lacustrine facies analysis*. IAS Special Publication No. 13.

Klootwijk, C.T., 2000. Australian palaeomagnetism, rockmagnetism, and environmental magnetism 2000 : abstracts. Australian Geological Survey Organisation. Workshop abstract.

Kuang, K.S.,1985. History and style of Cooper-Eromanga Basin structures. APPEA Journal. Vol 6:71-75.

Lang, S.C., Kassan, J., Benson, J.M., Grasso, C.A. and Avenell, L.C.2000. Applications of modern and ancient geological analogues in characterisation of fluvial and fluvial-lacustrine deltaic reservoirs in the Cooper Basin. APPEA Journal, p.393-416.

Lang, S. *et al*. 2001. The Application of Sequence Stratigraphy to Exploration and Reservoir Develop66ment in the Cooper-Eromanga-Bowen-Surat Basin System. APPEA Journal, pp.233-250.

Lang, S.C., Ceglar, N.F., Spencer, G. & Kassan, J. 2002. High resolution sequence stratigraphy, reservoir analogues, and 3D seismic interpretation - Application to exploration and reservoir development in the Baryulah complex, Cooper Basin, southwest Queensland. APPEA Journal Vol. 42:511-522

Leeder, M. R., 1999, Sedimentology and sedimentary basins : from turbulence to tectonics, 2nd ed, Wiley-Blackwell, Oxford.

Leopold, L.B., Wolman, M., Gordon,. 1957, River Channel Patterns: Braided, Meandering, and Straight. USGS Professional Paper: 282-B.

McCabe, P.J., 2014. Personal Communications, numerous conversations July-October 2014.

Martin, C.A., 1967a. Moomba a South Australian gas field. APEA Journal, Vol. 7(2):124-129.

Mavromatidis, A., 1997. Quantification of Exhumation in the Cooper-Eromanga basins and its implications for hydrocarbon exploration. Ph.D. thesis, The University of Adelaide, Australia, pp 1–330.

Miall, A.D., 1978. Lithofacies types and vertical profile models in braided river deposits: a summary. Canadian Society of Petroleum Geologists, Bulletin, Vol. 69: 710-721.

Miall, A.D., 1996. The Geology of Fluvial Deposits; sedimentary facies, basin analysis and petroleum geology. Springer, Berlin.

Miall, A.D., 2014. Fluvial depositional systems, Springer Geology, Chapter 2.

Moore, P.S., Pitt G.M., 1984. Cretaceous of the Eromanga Basin- implications for hydrocarbon exploration. APPEA Journal Vol. 24: 358–376.

Nakanishi, T. and Lang, S.C, 2001. The search for stratigraphic traps goes on-visualisation of fluvial-lacustrine successions in the Mooorari 3D survey, Cooper-Eromanga Basin, APPEA Journal Vol. 41: 115-37.

Nakanishi, T. *et al*. 2002. Constructing a portfolio of stratigraphic traps in fluvial-lacustrine successions, Cooper–Eromanga Basin. APEA Journal Vol. 42: 65-82.

Nichols, G., 2009, Sedimentology and stratigraphy (2nd ed). Hoboken, NJ Wiley and sons.

O'Driscoll, E.S.T., 1980. The double Helix in global tectonics. Tectonophysics Journal Vol. 63, pp397-417.

Papalia, N., 1969. The Nappamerri Formation. APEA Journal, Vol. 9: 108-110.

PIRSA, 2007.– Petroleum and Geothermal in South Australia. DVD

Posamentier, H.W. and Allen, G.P., 1999. Siliclastic sequence stratigraphy- concepts and applications. SEPM Concepts In Sedimentology and Palaeontology #7.

Posamentier, H. W. & Walker, R.G. & American Association of Petroleum Geologists 2006. SEPM Special Publication, Vol. 84: 1-17.

Radke, B. 2009. Hydrocarbon and Geothermal Prospectivity of Sedimentary Basins in Central Australia; Warburton, Cooper, Pedirka, Galilee, Simpson and Eromanga Basins. Geosecience Australia Record 2009/25.

Retallack, G.J., Veevers, J.J. and Morante, R., 1996. Global coal gap between Permian Triassic extinction and Middle Triassic recovery of peat-forming plants. Geological Society of America. Bulletin, Vol. 108(2):195-207.

Rider, M.H. 1990. Gamma-ray log shape used as a facies indicator: critical analysis of an oversimplified methodology. Geological society, London, special publications Vol. 48:27-37.

Roberts, D.C., Carroll, P.G. and Sayers, J., 1990. The Kalladeina Formation: a Warburton Basin Cambrian carbonate play. APEA Journal. Vol. 30:166-183.

Robinson, J.W. and P.J, McCabe 1997. Sandstone-body and shale-body dimensions in a braided fluvial system: Salt Wash Sandstone Member (Morrison Formation), Garfield County, Utah. Bulletin of the American Association of Petroleum Geologists. Vol. 81(8): 1267-1291.

Rust, B.R., 1978. A classification of alluvial channel systems. In: Miall, A.D. ŽEd.., Fluvial Sedimentology. Canadian Society of Petroleum Geologists Memoir 5:187–198.

Sanborn, A.F., 1971. Possible future petroleum of the Uinta and Piceance Basins and vicinity, northeast Utah and northwest Colorado, in Cram, I.H., ed., Future petroleum provinces of the United States-Their geology and potential: American Association of Petroleum Geologists Memoir 15, Vol. 1: 489-537.

Seggie, R.J, 1997. Reservoir characterisation of the Moorari/Woolkina field complex, Cooper Basin. APPEA Journal, Vol. 37(1):70-86.

Sella, G. F., Stein, S., Dixon, T. H., Craymer, M., James, T. S., Mazzotti, S., and Dokka, R. K., 2007. Observation of glacial isostatic adjustment in ‘‘stable’’ North America with GPS, Geophys. Res. Lett., 34.

Serra, O. 1975. Fundamentals of well-log interpretation. 1, The acquisition of logging data, Elsevier ; Pau : Elf Aquitaine, Amsterdam ; New York.

Serra, O. and H. T. Abbott, 1980. The contribution of logging data to sedimentology and stratigraphy, SPE 9270, 55th Annual Fall Technical Conference and Exhibition, Dallas, Texas, 19p.

Serra, O., Baldwin, J. and Qurein, J., 1980. Theory interpretation and practical application of natural gamma-ay spectroscopy. SPWLA, twenty-first Ann. Log. Symp. Trans., Paper Q.
.
Serra, Oberto & Schlumberger Limited 1985. Sedimentary environments from wireline logs, 2nd ed, Schlumberger, New York.

Shanley, K.W. and McCabe. P.J., (eds), 1998. Relative role of eustacy, climate and tectonism in continental rocks. SEPM Special Publication, 59.

Shaw R,D., 1991. Tertiary structuring in Southwest Queensland:implications for petroleum exploration. Explor Geophys Vol. 22: 339–344.

Smith, D.G., 1983, Anastomosed fluvial deposits: modern examples from Western Canada. In: Collinson, J., Lewin, J. ŽEds.., Modern and Ancient Fluvial Systems. Special Publication of the International Association of Sedimentologists 6, Blackwell,
Oxford, pp. 155–168.

Spencer, C.W., and Wilson, R.J., 1988, Petroleum geology and principal exploration plays in the Uinta-Piceance-Eagle Basins Province, Utah and Colorado: U.S. Geological Survey Open-File Report 88-450-G: 35.

Sprigg, R.C., 1958. Petroleum prospects of western parts of the Great Australian Artesian Basin. AAPG Bulletin, Vol. 42(10): 2465-2491.

Sprigg, R.C., 1961. On the structural evolution of the Great Artesian Basin. APEA Journal. Vol. 1: 37-56.

Stampflia, G.M., Hocharda, C., Vérarda, C., Wilhema, C., vonRaumerb, J., 2013. The formation of Pangea, Tectonophysics Vol. 8 Article No. 593.

Stanmore, P.J. and Johnstone, E.M., 1988. The search for stratigraphic traps in the southern Patchawarra Trough, South Australia. APEA Journal, Vol. 28: 156-166.

Strong, P.C., Wood, G.R., Lang S.C., Jollands, A., Karalaus, E., Kassan, J. 2002. High resolution palaeogeographic mapping of the fluvial-lacustrine Patchawarra formation in the Cooper Basin, South Australia, APPEA Journal. Vol.42:65-81.

Stuart, W.J., 1976. The genesis of Permian and lower Triassic reservoir sandstones during phases of southern Cooper Basin development. APEA Journal Vol. 16:37-47.

Taylor, G.H., Liu, S.Y. and Smyth, M., 1988. A new light on the origin of Cooper Basin oil. APEA Journal,, Vol. 28:303-309.

Thornton, R.C.N., 1979. Regional stratigraphic analysis of the Gidgealpa Group, southern Cooper Basin, Australia. South Australia. Geological Survey. Bulletin, 49.

Veevers, J.J. and Powell, C. McA., 1984. Uluru and Adelaidean regimes. In: Veevers, J.J. (ed.), Phanerozoic earth history of Australia: Oxford England, Clarendon Press: 329-39.

Veevers, J.J. and Powell, C.McA., 1987. Late Palaeozoic glacial episodes in Gondwanaland ref lected. In: Transgressive–regressive depositional sequences in Euramerica. Geological Society of American Bulletin, Vol. 98:475-487.

Williams, B.P.J. and Wild, E.K., 1984. The Tirrawarra Sandstone and Merrimelia Formation of the southern Cooper Basin, South Australia the sedimentation and evolution of a glaciofluvial system. APEA Journal, Vol. 24(1):377-392.

Williams, B.P.J., 1982. Facies analysis of Gidgealpa Group reservoir rocks, southern Cooper Basin, South Australia. Internal Report for Santos. (unpublished).

Wood, G. 2014. Personal communications, numerous conversations July-October 2014.

Wood, G. Santos Internal document. Unpublished.

Wopfner, H., 1960.On the Structural Development in the Central Part of the Great Artesian Basin. Trans. Roy. Soc. S. Austr. Vol. 81: 179-19.

Wopfner, H., 1966. A case history of the Gidgealpa gas field, South Australia. Australasian Oil and Gas Journal, 12(11):29-53.

Wopfner, H., 1981. Development of Permian intracratonic basins in Australia. In: Cresswell, M.M. and Vella, P. (Eds), Gondwana Five. 5th International Gondwana Symposium, Wellington, 1980. Proceedings: 185-190.

Appendix A: Palaeogeographic Maps

460000M E 470000M E 480000M E 490000M E 500000M E 510000M E 520000M E

6900000M N
6890000M N
6880000M N
6870000M N
6860000M N
6850000M N

N W E S

Type Section: Dullingari North 8

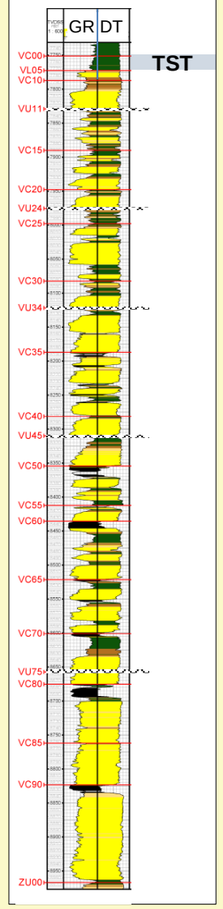

Appendix A1

VC00-VL05 Palaeogeographic Reconstruction

Date : November 6, 2014	Author : S. Kobelt	ENCL
Contour Interval :	File No. :	
Elevation Datum :	Santos Ltd ABN 80 007 550 923	

0 5 10
KM

Legend

Well Signature log

Well Log Signature — KINTA 1, 25 ft

Palaeo-Environments of Deposition (See Chapter 6)

- Channel Belt
- Minor Channel/Crevass Splay Complex
- Lacustrine Uplands/Floodplains
- Peat Mire
- Amalgameted Sheet Sand Complex
- Lacustrine Foreshore Sands (Not Part of Framework Facies)
- Lacustrine/ Lacustrine Delta Complex (Not Part of Framework Facies)

Other

- Schematic: Non Depositional Feeder Channel
- Schematic: Incised Stream Through Peat Mire
- Interpreted Paleaflow Direction
- Schematic: Crevasse Splay

Absent Sections

- Interpreted Post Depositional Erosion
- Interpreted Non-Depositon
- Absent, Indeterminate

<u>Summary:</u> This interval marks the advancement of the Murturee Lake. Frequent minor channel systems dominate the south western area of the map draining into the lake, while the north east is dominated still by floodplain facies.This interval was mapped to complete the full Patchawarra section, however would be better represented using a lacustrine deltaic framework.

<u>Notes:</u>

-Lacustrine shoreface interpreted by coarsening upwards sands. Lacustrine deltas and lacustrine environments were not defined because they are not the focus of mapping this interval.

-Log depth scale of 1:10000 map units (km) used for this interval. 1mm = 8ft vertical section.

460000M E 470000M E 480000M E 490000M E 500000M E 510000M E 520000M E

6900000M N 6890000M N 6880000M N 6870000M N 6860000M N 6850000M N

N W E S

KINTA 1 STRATHMOUNT 1 THREE QUEENS 1 NAPPACOONGEE 1 NAPPACOONGEE EAST 1 CROWSNEST 2 CROWSNEST 1 BOW 1 BOW 2 DULLINGARI NORTH 18 BECKLER 4 BECKLER 3 KAPPA 1 POORAKA 1 WILPINNIE 2 WILPINNIE 1 GUDNUKI 1 DULLINGARI NORTH 15 DULLINGARI NORTH 9 DULLINGARI NORTH 14 DULLINGARI NORTH 11 DULLINGARI NORTH 1 DULLINGARI NORTH 17 DULLINGARI NORTH 12 DULLINGARI NORTH 6 DULLINGARI 34 DULLINGARI 51 DULLINGARI 39 DULLINGARI 46 DULLINGARI 24 DULLINGARI 26 DULLINGARI 25 DULLINGARI 53 DULLINGARI 35 DULLINGARI 28 DULLINGARI 17 BECKLER 5 GUDNUKI 3 GUDNUKI 2 BURKE 5 BURKE 12 BURKE 7 BURKE EAST 1 BURKE 6 DELLA 3 DELLA 4 DELLA 14 DELLA 15 DELLA 10 DELLA 13 DELLA 7 DELLA 20 DELLA 2 DELLA 1A DELLA 17 DELLA 16 DELLA 25 DELLA 9 DELLA 6 EPSILON 9 EPSILON 1 EPSILON 3 EPSILON 7 EPSILON 8 EPSILON 11 EPSILON 4 EPSILON 6 ROSENEATH 2 MUDERA 2 MUDERA 4 MOONA 1 MUDERA 6 MARABOOKA 3 MARABOOKA 2 MARABOOKA EAST 1 LEPENA 1 LEPENA 2 KATINGAWA 1 KIDMAN NORTH 2 KIDMAN NORTH 1 KIDMAN NORTH 4 KIDMAN 1 KIDMAN 7 KIDMAN 3 KIDMAN 10 AROONA 1 BAGUNDI 3 BAGUNDI 4 STRZELECKI 1 STRZELECKI 17 STRZELECKI 24 STRZELECKI 29 STRZELECKI 5 STRZELECKI 15 STRZELECKI 25 MARANA 1 COOLCON SOUTH 1 NANIMA 1 WANARA 1 DIERI 1 CARAKA 1 PIRA 2 PIRA 1 DILCHEE 1 DILCHEE 2 DILCHEE 4 DILCHEE 3 KERNA NORTH 1 MOON 2 MOON 3 MOON 1 BOONGALA 1 GAHNIA 1 KERNA 1 ALISMA 1 KERNA 4 ALLAMBI 1 PLANTAGO 1 HORNET 1 BARATTA WEST 1 BARATTA 1 BARATTA 2 BARATTA SOUTH 1 WITCHETTY 1 TOOLACHEE NORTH 1 TOOLACHEE 2 KELBROOK 1 TARWONGA 3 METTIKA 3 METTIKA 1 STOKES NORTH 1 STOKES 3 STOKES CENTRAL 1 STOKES 8 STOKES 4 STOKES 1 STOKES 2 STOKES SOUTH 1 TEEGAL 1 MIRANDA 1 WILLS 1 CHILDIE 1 CHILCARRIE 1 TARWONGA 1 TARWONGA 5 TOOLACHEE 43 TOOLACHEE 41 TOOLACHEE 40 VERBENA 1 TOOLACHEE 5 TOOLACHEE 44 TOOLACHEE 52 TOOLACHEE EAST 1 TOOLACHEE 9 TOOLACHEE 4 TOOLACHEE 23 MUNDI 5 MARSILEA 1 AMYEMA 1 BRUMBY 2 BRUMBY 9 BRUMBY 5 BRUMBY 1 TOOLACHEE 24 TOOLACHEE 35 TOOLACHEE 34 TOOLACHEE 38 TOOLACHEE 42 TOOLACHEE 27 MURTEREE 1 GRYSTES 1 MUNDI 7 KAPINKA 1 RANGER SOUTH 1 QUASAR SOUTH 1 BARCOOLOO 1 TOOLACHEE 39 TOOLACHEE 19 TOOLACHEE 33 TOOLACHEE 10 TOOLACHEE 18 TOOLACHEE 30 PELKETA 1 KEETO 2 KEETO 1 TOOLACHEE 3 TOOLACHEE 7 TOOLACHEE 45 TOOLACHEE 20 MATARANKA 1 CANBERRA 1A TILPAREE A1 LANCER 1 PLOTOSUS 1 MUNKARIE 3 MUNKARIE 1 MUNKARIE 5 KULTARR 1 CHIRON 2 CHIRON 1 PYTHON 1 EGLINT 1 CURRUMBIN 1 GIDGEE 1 COOLCON SOUTH 1

Type Section: Dullingari North 8

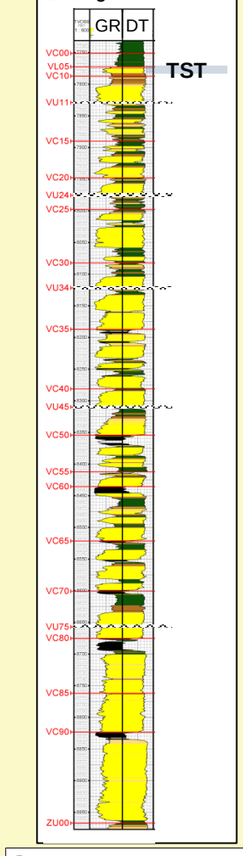

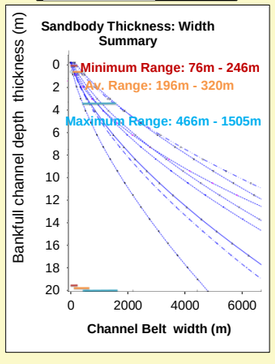

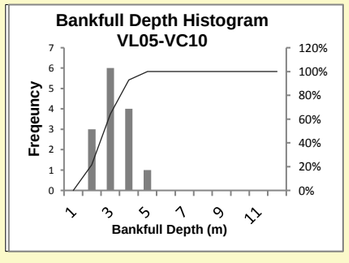

Appendix A2

VL05-VC10 Palaeogeographic Reconstruction

Date : October 28, 2014	Author : S. Kobelt	ENCL
Contour Interval :	File No. :	
Elevation Datum :	Santos Ltd ABN 80 007 550 923	

0 5 10 KM

Legend

Well Signature log

Well Log Signature — KINTA 1 — 25 ft

Palaeo-Environments of Deposition (See Chapter 6)

- Channel Belt
- Minor Channel/Crevass Splay Complex
- Lacustrine Uplands/Floodplains
- Peat Mire
- Amalgameted Sheet Sand Complex
- Lacustrine Foreshore Sands (Not Part of Framework Facies)
- Lacustrine/ Lacustrine Delta Complex (Not Part of Framework Facies)

Other

- Schematic: Non Depositional Feeder Channel
- Schematic: Incised Stream Through Peat Mire
- Interpreted Paleaflow Direction
- Schematic: Crevasse Splay

Absent Sections

- Interpreted Post Depositional Erosion
- Interpreted Non-Depositon
- Absent, Indeterminate

Summary: This interval marks the true onset of lacustrine transgression. Coarsening upwards sands are encountered in the northern limits of the area; these are interpreted as shoreface sands and mark the lake edge. The presence of shoreface sands also implies sufficient wave action from the lake. This interval is acknowledged as having lacustrine delta/coastal plain features but these are not the focus of this study

Notes: -Log Depth Scale of 1:10000 map units (km) used for this interval. 1mm = 8ft vertical section.

460000M E
470000M E
480000M E
490000M E
500000M E
510000M E
520000M E
6900000M N
6890000M N
6880000M N
6870000M N
6860000M N
6850000M N
N
W
E
S

Type Section: Dullingari North 8

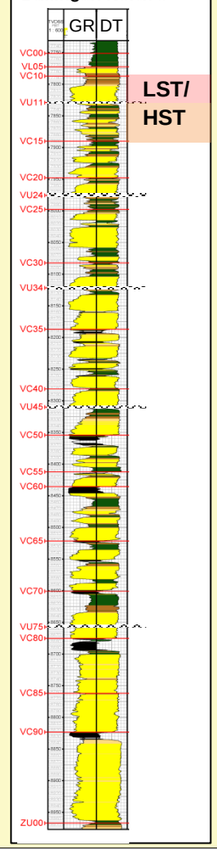

Appendix A3

VC10-VC15 Palaeogeographic Reconstruction

Date : October 28, 2014	Author : S. Kobelt	ENCL
Contour Interval :	File No. :	
Elevation Datum :	Santos Ltd ABN 80 007 550 923	

0 5 10
KM

Legend

Well Signature log

Well Log Signature — KINTA 1 — 25 ft

Palaeo-Environments of Deposition (See Chapter 6)

- Channel Belt
- Minor Channel/Crevass Splay Complex
- Lacustrine Uplands/Floodplains
- Peat Mire
- Amalgameted Sheet Sand Complex

Other

- Schematic: Non Depositional Feeder Channel
- Schematic: Incised Stream Through Peat Mire
- Interpreted Paleaflow Direction
- Schematic: Crevasse Splay

Absent Sections

- Interpreted Post Depositional Erosion
- Interpreted Non-Depositon
- Absent, Indeterminate

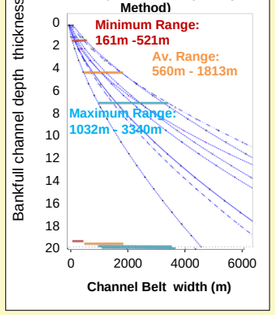

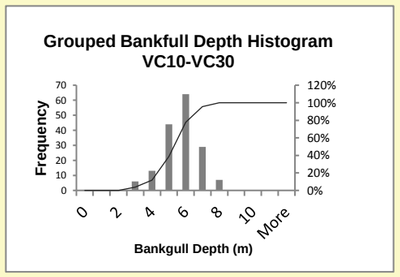

Summary: Second order transgressive interval. Sandy axis around the Bagundi/Kidman Fields suggesting Kidman Structure is active/influencing sedimentation.Channel belts are notably more complex and sinuous than other intervals.

Notes: Log Depth Scale of 1:10000 map units (km) used for this interval. 1mm = 8ft vertical section.

460000M E 470000M E 480000M E 490000M E 500000M E 510000M E 520000M E

6900000M N 6890000M N 6880000M N 6870000M N 6860000M N 6850000M N

N W E S

KINTA 1 STRATHMOUNT 1 THREE QUEENS 1 NAPPACOONGEE 3 NAPPACOONGEE EAST 1 POORAKA 1 WILPINNIE 2 WILPINNIE 1 DELLA 3 DELLA 4 GUDNUKI 2 DELLA 14 DELLA 15 DELLA 10 DELLA 13 DELLA 2 DELLA 7 DELLA 20 DELLA 5A DELLA 27 DELLA 16 DELLA 15 DELLA 9 DELLA 6 MUDERA 2 MUDERA 4 MOONA 1 MARABOOKA 3 MUDERA 6 MARABOOKA 2 MARABOOKA 4 MARABOOKA EAST 1 LEPENA 1 LEPENA 2 AROONA 1 BAGUNDI 3 BAGUNDI 4 KATINGAWA 1 KIDMAN NORTH 2 KIDMAN NORTH 1 KIDMAN NORTH 4 KIDMAN 10 KIDMAN 1 KIDMAN 7 KIDMAN 3 STRZELECKI 1 STRZELECKI 17 STRZELECKI 24 STRZELECKI 29 STRZELECKI 5 STRZELECKI 15 STRZELECKI 25 MARANA 1 COOLOON SOUTH 1 DIERI 1 CARAWA 1 WANARA 1 NANIMA 1 STRZELECKI 2 BARATTA WEST 1 BARATTA 1 BARATTA 2 BARATTA SOUTH 1 TARWONGA 3 TOOLACHEE NORTH 1 WITCHETTY 1 CHILDIE 1 CHILCARRIE 1 TARWONGA 1 TARWONGA 5 TOOLACHEE 43 TOOLACHEE 5 TOOLACHEE 44 TOOLACHEE 41 TOOLACHEE 40 VERBENA 1 TOOLACHEE 52 TOOLACHEE 4 TOOLACHEE 9 TOOLACHEE EAST 1 TOOLACHEE 23 MUNDI 5 MURTEREE 1 GRYSTES 1 MUNDI 7 KAPINKA 1 TOOLACHEE 24 TOOLACHEE 35 TOOLACHEE WEST 14 TOOLACHEE 38 TOOLACHEE 42 TOOLACHEE 27 TOOLACHEE 39 TOOLACHEE 32 TOOLACHEE 10 TOOLACHEE 30 TOOLACHEE 28 TOOLACHEE 3 TOOLACHEE 7 TOOLACHEE 45 TOOLACHEE 20 BARCOOLOO 1 PELKETA 1 KEETO 2 KEETO 1 MATARANKA 1 TILPAREE A1 LANCER 1 PLOTOSUS 1 CROWSNEST 2 CROWSNEST 1 DULLINGARI NORTH 18 BOW 1 BOW 2 BECKLER 4 BECKLER 3 BECKLER 5 GUDNUKI 1 DULLINGARI NORTH 15 DULLINGARI NORTH 9 DULLINGARI NORTH 14 DULLINGARI NORTH 11 DULLINGARI NORTH 17 DULLINGARI NORTH 12 DULLINGARI NORTH 6 DULLINGARI 34 DULLINGARI 51 DULLINGARI 39 DULLINGARI 46 DULLINGARI 24 DULLINGARI 26 DULLINGARI 25 DULLINGARI 53 DULLINGARI 54 DULLINGARI 36 DULLINGARI 23 DULLINGARI 17 GUDNUKI 3 BURKE 5 BURKE 7 BURKE 6 BURKE EAST 1 PIRA 2 PIRA 1 COOCHILARA 1 DILCHEE 1 DILCHEE 2 DILCHEE 3 BOONGALA 1 KERNA NORTH 1 GAHNIA 1 KERNA 1 ALISMA 1 KERNA 4 PLANTAGO 1 ALLAMBI 1 HORNET 1 KELBROOK 1 METTIKA 3 METTIKA 1 MARSILEA 1 AMYEMA 1 BRUMBY 2 BRUMBY 9 BRUMBY 5 BRUMBY 1 KULTARR 1 MUNKARIE 3 MUNKARIE 1 MUNKARIE 5 KAPPA 1 BECKLER 5 EPSILON 9 EPSILON 1 EPSILON 3 EPSILON 8 EPSILON 11 EPSILON 7 EPSILON 6 ROSENEATH 2 MOON 2 MOON 3 MOON 1 STOKES NORTH 1 STOKES 3 STOKES CENTRAL 1 STOKES 8 STOKES 4 STOKES 1 STOKES 2 STOKES SOUTH 1 RANGER SOUTH 1 QUASAR SOUTH 1 CHIRON 2 CHIRON 1 TEEGAL 1 MIRANDA 1 WILLS 1 PYTHON 1 EGLINT 1 GIDGEE 3 GIDGEE 1 DURRUMBUL 1

Type Section: Dullingari North 8

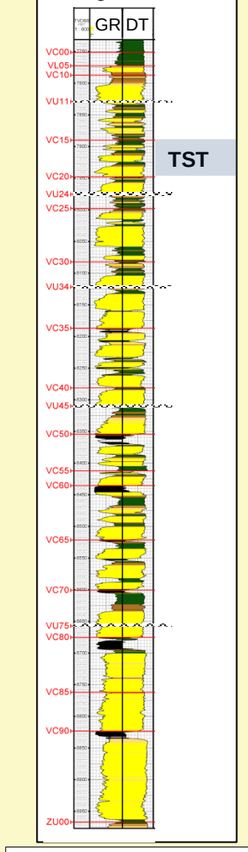

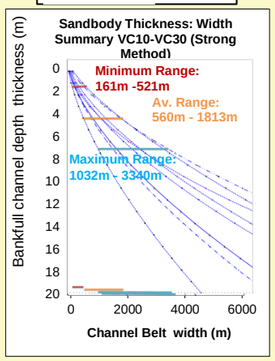

Appendix A4

VC15-VC20 Palaeogeographic Reconstruction

Date : October 29, 2014	Author : S. Kobelt	ENCL
Contour Interval :	File No. :	
Elevation Datum :	Santos Ltd ABN 80 007 550 923	

0 5 10 KM

Legend

Well Signature log

Well Log Signature — KINTA 1 — 25 ft

Palaeo-Environments of Deposition (See Chapter 6)

- Channel Belt
- Minor Channel/Crevass Splay Complex
- Lacustrine Uplands/Floodplains
- Peat Mire
- Amalgameted Sheet Sand Complex

Other

- Schematic: Non Depositional Feeder Channel
- Schematic: Incised Stream Through Peat Mire
- Interpreted Paleaflow Direction
- Schematic: Crevasse Splay

Absent Sections

- Interpreted Post Depositional Erosion
- Interpreted Non-Depositon
- Absent, Indeterminate

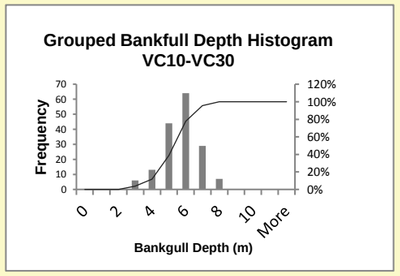

<u>Summary:</u> First order TST within a second order TST. Net flow towards the northwest.

<u>Notes:</u> Log Depth Scale of 1:20000 map units (km) used for this interval. 1mm = 16ft vertical section.

460000M E 470000M E 480000M E 490000M E 500000M E 510000M E 520000M E

6900000M N 6890000M N 6880000M N 6870000M N 6860000M N 6850000M N

N W E S

Regular coals between sands indicate a peat mire environment interupted by clastic coarse grained sand depostion

Type Section: Dullingari North 8

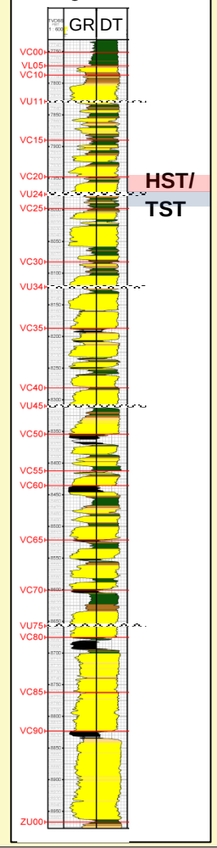

Sandbody Thickness: Width Summary VC10-VC30 (Strong Method)

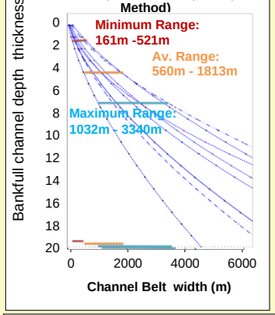

Appendix A5

VC20-VC25 Palaeogeographic Reconstruction

Date : October 29, 2014	Author : S. Kobelt	ENCL
Contour Interval :	File No. :	
Elevation Datum :	Santos Ltd ABN 80 007 550 923	

0 5 10
KM

Legend

Well Signature log

Well Log Signature — KINTA 1 — 25 ft

Palaeo-Environments of Deposition (See Chapter 6)

- Channel Belt
- Minor Channel/Crevass Splay Complex
- Lacustrine Uplands/Floodplains
- Peat Mire
- Amalgameted Sheet Sand Complex

Other

- Schematic: Non Depositional Feeder Channel
- Schematic: Incised Stream Through Peat Mire
- Interpreted Paleaflow Direction
- Schematic: Crevasse Splay

Absent Sections

- Interpreted: Post Depositional Erosion
- Interpreted: Non-Depositon
- Absent, Indeterminate

Grouped Bankfull Depth Histogram VC10-VC30

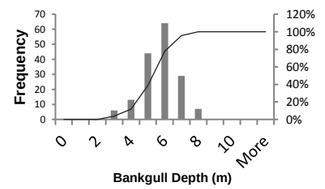

Summary: Sheet sands dominate similarly to the VC30-VC40 interval, due to the VU24 sequence boundary and subsequent TST. Generally two sands are distinguishable throughout the interval. This interval could be further divided into the VU24-VC25 and VC20-VU25 intervals for higher resolution reconstructions

Notes: Log Depth Scale of 1:15000 map units (km) used for this interval. 1mm = 12ft vertical section.

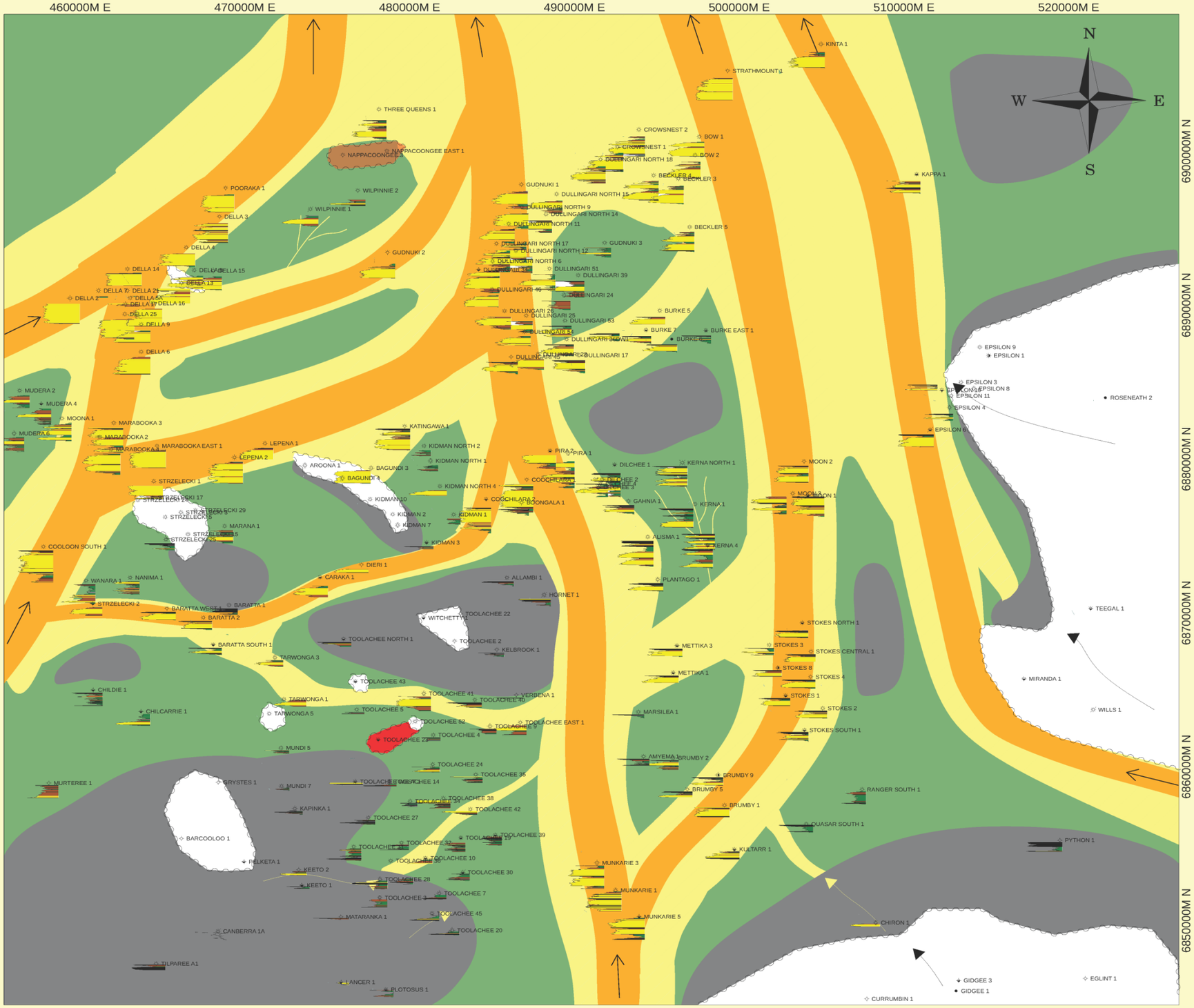

Type Section: Dullingari North 8

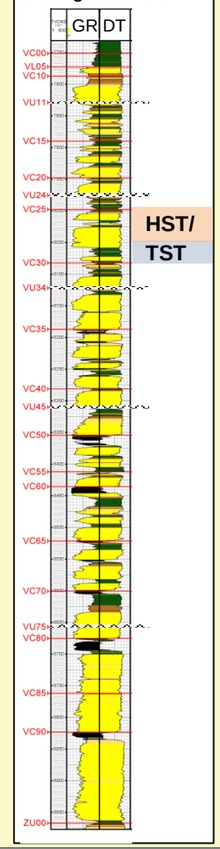

Appendix A6

VC25-VC30 Palaeogeographic Reconstruction

Date : October 28, 2014	Author : S. Kobelt	ENCL
Contour Interval :	File No. :	
Elevation Datum :	Santos Ltd ABN 80 007 550 923	

0 5 10
KM

Legend

Well Signature log

Well Log Signature — KINTA 1 — 25 ft

Palaeo-Environments of Deposition (See Chapter 6)

- Channel Belt
- Minor Channel/Crevass Splay Complex
- Lacustrine Uplands/Floodplains
- Peat Mire
- Amalgameted Sheet Sand Complex

Other

- Schematic: Non Depositional Feeder Channel
- Schematic: Incised Stream Through Peat Mire
- Interpreted Paleaflow Direction
- Schematic: Crevasse Splay

Absent Sections

- Interpreted Post Depositional Erosion
- Interpreted Non-Depositon
- Absent, Indeterminate

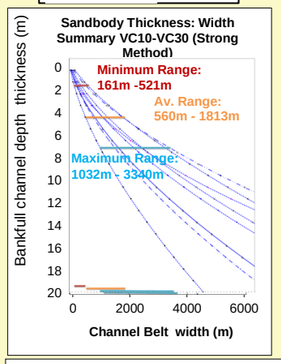

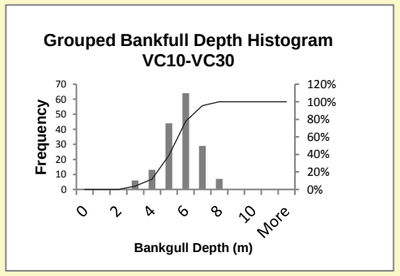

Summary: This interval is dominated by lacustrine environments again, with a possible coarse grained sediment source from the southwest, feeding the Della and Dullingari areas.

Notes: Log Depth Scale of 1:15000 map units (km) used for this interval. 1mm = 12ft vertical section.

460000M E 470000M E 480000M E 490000M E 500000M E 510000M E 520000M E

6900000M N 6890000M N 6880000M N 6870000M N 6860000M N 6850000M N

N W E S

Frequent coal stringers suggest a proximal/subordinate peat mire environment

KINTA 1 STRATHMOUNT 1 THREE QUEENS 1 NAPPACOONGEE 3 NAPPACOONGEE EAST 1 POORAKA 1 WILPINNIE 2 WILPINNIE 1 DELLA 3 DELLA 4 DELLA 14 DELLA 8 DELLA 10 DELLA 13 DELLA 7 DELLA 20 DELLA 16 DELLA 9 DELLA 6 CROWSNEST 2 CROWSNEST 1 BOW 1 BOW 2 DULLINGARI NORTH 15 BECKLER 4 BECKLER 3 KAPPA 1 GUDNUKI 1 DULLINGARI NORTH 16 DULLINGARI NORTH 9 DULLINGARI NORTH 14 DULLINGARI NORTH 11 BECKLER 5 GUDNUKI 2 GUDNUKI 3 DULLINGARI NORTH 17 DULLINGARI NORTH 12 DULLINGARI NORTH 6 DULLINGARI 51 DULLINGARI 39 DULLINGARI 16 DULLINGARI 24 BURKE 5 DULLINGARI 26 DULLINGARI 25 DULLINGARI 53 BURKE 7 BURKE EAST 1 DULLINGARI 38 DULLINGARI 30 DULLINGARI 1 BURKE 6 DULLINGARI 18 DULLINGARI 2 DULLINGARI 17

EPSILON 9 EPSILON 2 EPSILON 1 EPSILON 3 EPSILON 8 EPSILON 11 EPSILON 4 EPSILON 6 ROSENEATH 2

MUDERA 2 MUDERA 4 MOONA 1 MARABOOKA 3 MUDERA 9 MARABOOKA 2 MARABOOKA EAST 1 LEPENA 1 LEPENA 2 STRZELECKI 1 STRZELECKI 17 STRZELECKI 24 STRZELECKI 29 STRZELECKI 5 STRZELECKI 18 STRZELECKI 25 MARANA 1 AROONA 1 BAGUNDI 3 BAGUNDI 4 KIDMAN NORTH 2 KIDMAN NORTH 1 KIDMAN NORTH 4 KIDMAN 10 KIDMAN 1 KIDMAN 7 KIDMAN 3 COOLOON SOUTH 1 DIERI 1 CARARA 1 WANARA 1 NANIMA 1 STRZELECKI 2 BARATTA WEST 1 BARATTA 1 BARATTA 2 BARATTA SOUTH 1 TARWONGA 3 CHILDIE 1 CHILCARRIE 1 TARWONGA 1 TARWONGA 5 TARWONGA 2 MUNDI 5 MURTEREE 1 GRYSTES 1 MUNDI 7 KAPINKA 1 BARCOOLOO 1 PELKETA 1 KEETO 2 KEETO 1 TILPAREE A1 LANCER 1 PLOTOSUS 1

PIRA 2 PIRA 1 COOCHILARA 1 COOCHILARA 2 BOONGALA 1 DILCHEE 1 KERNA NORTH 1 GAHNIA 1 KERNA 7 KERNA 1 ALISMA 1 KERNA 4 MOON 2 MOONA 1 PLANTAGO 1 ALLAMBI 1 HORNET 1 WITCHETTY 1 TOOLACHEE NORTH 1 TOOLACHEE 2 KELBROOK 1 TOOLACHEE 43 TOOLACHEE 41 TOOLACHEE 40 VERBENA 1 TOOLACHEE 5 TOOLACHEE 52 TOOLACHEE EAST 1 TOOLACHEE 9 TOOLACHEE 4 TOOLACHEE 23 TOOLACHEE 46 TOOLACHEE 22 TOOLACHEE 24 TOOLACHEE 14 TOOLACHEE 35 TOOLACHEE 34 TOOLACHEE 38 TOOLACHEE 42 TOOLACHEE 27 TOOLACHEE 31 TOOLACHEE 32 TOOLACHEE 39 TOOLACHEE 10 TOOLACHEE 30 TOOLACHEE 28 TOOLACHEE 3 TOOLACHEE 7 MATARANKA 1 TOOLACHEE 45 TOOLACHEE 20 MUNKARIE 3 MUNKARIE 1 MUNKARIE 5 CHIRON 2 CHIRON 1 CURRUMBIN 1 GIDGEE 1 EGLINT 1

STOKES NORTH 1 STOKES 3 STOKES CENTRAL 1 METTIKA 3 METTIKA 1 STOKES 8 STOKES 4 STOKES 7 STOKES 1 STOKES 2 STOKES SOUTH 1 MARSILEA 1 AMYEMA 1 BRUMBY 2 BRUMBY 9 BRUMBY 5 BRUMBY 1 QUASAR SOUTH 1 KULTARR 1 RANGER SOUTH 1 TEEGAL 1 MIRANDA 1 WILLS 1 PYTHON 1

Type Section: Dullingari North 8

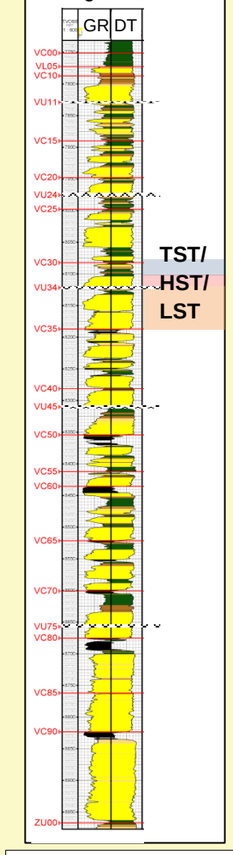

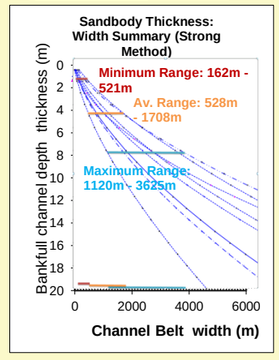

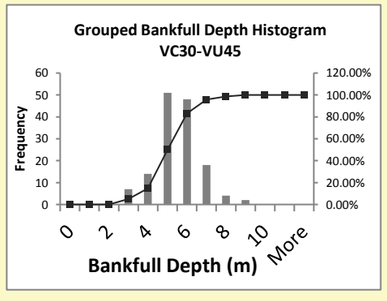

Appendix A7

VC30-VC35 Palaeogeographic Reconstruction

Date : October 28, 2014	Author : S. Kobelt	ENCL
Contour Interval :	File No. :	
Elevation Datum :	Santos Ltd ABN 80 007 550 923	

0 5 10 KM

Legend

Well Signature log

Well Log Signature — KINTA 1 — 25 ft

Palaeo-Environments of Deposition (See Chapter 6)

- Channel Belt
- Minor Channel/Crevass Splay Complex
- Lacustrine Uplands/Floodplains
- Peat Mire
- Amalgameted Sheet Sand Complex

Other

- Schematic: Non Depositional Feeder Channel
- Schematic: Incised Stream Through Peat Mire
- Interpreted Paleaflow Direction
- Schematic: Crevasse Splay

Absent Sections

- Interpreted Post Depositional Erosion
- Interpreted Non-Depositon
- Absent, Indeterminate

Summary: The sequence boundary (VU34) and following TST, within this interval result in widespread amalgamated sheet sand deposits across the majority of the study area.

Notes: Log Depth Scale of 1:20000 map units (km) used for this interval. 1mm = 16ft vertical section.

460000M E 470000M E 480000M E 490000M E 500000M E 510000M E 520000M E

6900000M N 6890000M N 6880000M N 6870000M N 6860000M N 6850000M N

N W E S

Increasing floodplain facies and decreasing individual sand thicknesses

Type Section: Dullingari North 8

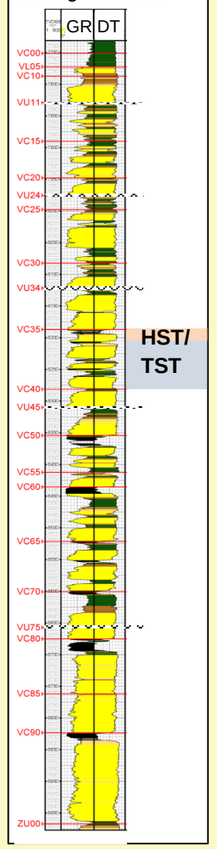

HST/ TST

Appendix A8

VC35-VC40 Palaeogeographic Reconstruction

Date : October 28, 2014	Author : S. Kobelt	ENCL
Contour Interval :	File No. :	
Elevation Datum :	Santos Ltd ABN 80 007 550 923	

0 5 10 KM

Legend

Well Signature log

Well Log Signature — KINTA 1, 25 ft

Palaeo-Environments of Deposition (See Chapter 6)

- Channel Belt
- Minor Channel/Crevass Splay Complex
- Lacustrine Uplands/Floodplains
- Peat Mire
- Amalgameted Sheet Sand Complex

Other

- Schematic: Non Depositional Feeder Channel
- Schematic: Incised Stream Through Peat Mire
- Interpreted Paleaflow Direction
- Schematic: Crevasse Splay

Absent Sections

- Interpreted Post Depositional Erosion
- Interpreted Non-Depositon
- Absent, Indeterminate

Sandbody Thickness: Width Summary (Strong Method)

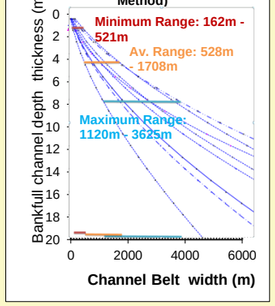

Grouped Bankfull Depth Histogram VC30-VU45

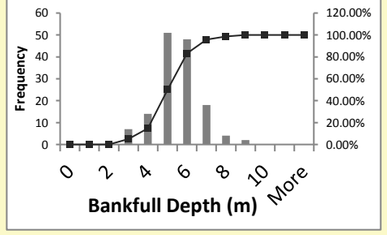

Summary. Thick Sands in the northwest and increasing crevasse splays in the northeast suggest a major depositional trend towards the northwest. Large section results in difficulty to reconstruct interval with more resolution. This interval could be further divided by the local VL37 horizon for higher resolution intervals.

Notes: Log Depth Scale of 1:30000 map units (km) used for this interval. 1mm = 24ft vertical section.

460000M E 470000M E 480000M E 490000M E 500000M E 510000M E 520000M E

6900000M N 6890000M N 6880000M N 6870000M N 6860000M N 6850000M N

N W E S

Appendix A9

VC40-VU45 Palaeogeographic Reconstruction

Date : October 28, 2014	Author : S. Kobelt	ENCL
Contour Interval :	File No. :	
Elevation Datum :	Santos Ltd ABN 80 007 550 923	

0 5 10
KM

Type Section: Dullingari North 8

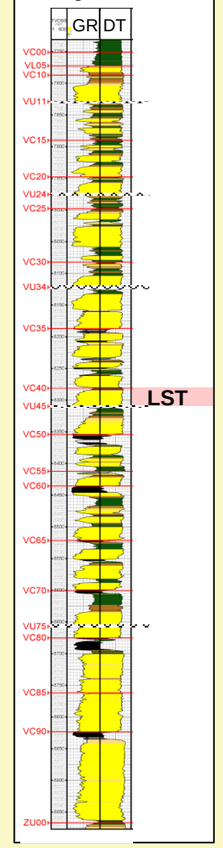

Legend

Well Signature log

Well Log Signature — KINTA 1 — 25 ft

Palaeo-Environments of Deposition (See Chapter 6)

- Channel Belt
- Minor Channel/Crevass Splay Complex
- Lacustrine Uplands/Floodplains
- Peat Mire
- Amalgameted Sheet Sand Complex

Other

- Schematic: Non Depositional Feeder Channel
- Schematic: Incised Stream Through Peat Mire
- Interpreted Paleaflow Direction
- Schematic: Crevasse Splay

Absent Sections

- Interpreted Post Depositional Erosion
- Interpreted Non-Depositon
- Absent, Indeterminate

Sandbody Thickness: Width Summary VC30-VU45 (Strong Method)

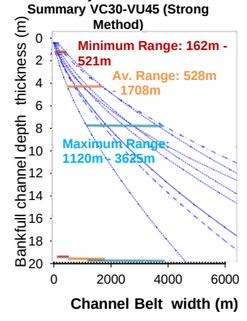

Grouped Bankfull Depth Histogram VC30-VU45

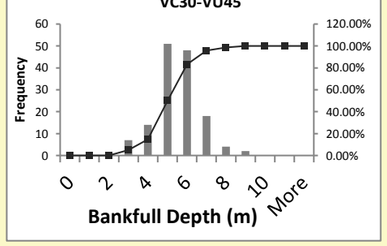

<u>Summary:</u> The Toolachee Trend starts to fill and onlap, hosting two channel axes feeding into the Allunga Trough. The Mettika and Western channel axis became active again during this period.

<u>Notes:</u> Log Depth Scale of 1:15000 map units (km) used for this interval. 1mm = 12ft vertical section.

460000M E 470000M E 480000M E 490000M E 500000M E 510000M E 520000M E

6900000M N 6890000M N 6880000M N 6870000M N 6860000M N 6850000M N

N W E S

THREE QUEENS 1 NAPPACOONGEE EAST 1 NAPPACOONGEE 3 POORAKA 1 WILPINNIE 2 WILPINNIE 1 DELLA 3 DELLA 4 DELLA 14 DELLA 8 DELLA 10 DELLA 13 DELLA 7 DELLA 20 DELLA 2 DELLA 16 DELLA 9 DELLA 6 GUDNUKI 2 MUDERA 2 MUDERA 4 MOONA 1 MARABOOKA 1 MARABOOKA 3 MUDERA 6 MARABOOKA 2 MARABOOKA 4 MARABOOKA EAST 1 LEPENA 1 LEPENA 2 STRZELECKI 1 STRZELECKI 17 STRZELECKI 24 STRZELECKI 29 STRZELECKI 5 STRZELECKI 25 MARANA 1 STRZELECKI 15 COOLOON SOUTH 1 KATINGAWA 1 KIDMAN NORTH 2 KIDMAN NORTH 1 ARCONA 1 BAGUNDI 3 BAGUNDI 4 KIDMAN NORTH 4 KIDMAN 10 KIDMAN 7 KIDMAN 3 DIERI 1 WANARA 1 NANIMA 1 CARAKA 1 BARATTA WEST 1 BARATTA 1 BARATTA 2 BARATTA SOUTH 1 TOOLACHEE NORTH 1 TOOLACHEE 1 TARWONGA 3 CHILDIE 1 CHILCARRIE 1 TARWONGA 1 TARWONGA 5 TARWONGA 2 MUNDI 5 MURTEREE 1 GRYSTES 1 MUNDI 7 KAPINKA 1 BARCOOLOO 1 PELKETA 1 KEETO 2 KEETO 1 MATARANKA 1 CANBERRA 1A TILPAREE A1 LANCER 1 PLOTOSUS 1

KINTA 1 STRATHMOUNT 1 CROWSNEST 2 CROWSNEST 1 DULLINGARI NORTH 18 BOW 2 BECKLER 4 BECKLER 3 GUDNUKI 1 DULLINGARI NORTH 3 BECKLER 5 DULLINGARI NORTH 17 GUDNUKI 3 DULLINGARI NORTH 8 DULLINGARI 51 DULLINGARI 4 DULLINGARI 26 DULLINGARI 25 DULLINGARI 45 DULLINGARI 23 BURKE 5 BURKE 2 BURKE 9 BURKE 8 BURKE 6 BURKE EAST 1 PIRA 2 PIRA 1 DILCHEE 1 DILCHEE 2 DILCHEE 4 COOCHILANDA 1 COOCHILANDA 2 GONGALA 1 GAHNIA 1 ALISMA 2 ALISMA 1 KERNA NORTH 1 KERNA 7 KERNA KERNA 2A KERNA 3 KERNA 5 KERNA 4 MOON 2 MOON 1 KAPPA 1 MONTEGUE 1 EPSILON 9 EPSILON 2 EPSILON 1 EPSILON 3 EPSILON 8 EPSILON 11 EPSILON 4 EPSILON 6 ROSENEATH 2 METTIKA 3 METTIKA 1 METTIKA 5 METTIKA 2 MARSILEA 1 AMYEMA 1 BRUMBY 9 BRUMBY 5 BRUMBY 12 BRUMBY 1 STOKES NORTH 1 STOKES 3 STOKES CENTRAL 1 STOKES 8 STOKES 4 STOKES 7 STOKES 1 STOKES 2 STOKES SOUTH 1 TOOLACHEE 37 TOOLACHEE 43 TOOLACHEE 41 TOOLACHEE 40 VERBENA 1 TOOLACHEE 5 TOOLACHEE 44 TOOLACHEE 52 TOOLACHEE EAST 1 TOOLACHEE 6 TOOLACHEE 4 TOOLACHEE 23 TOOLACHEE 46 TOOLACHEE 24 TOOLACHEE 35 TOOLACHEE 14 TOOLACHEE 38 TOOLACHEE 42 TOOLACHEE 27 TOOLACHEE 12 TOOLACHEE 39 TOOLACHEE 22 TOOLACHEE 31 TOOLACHEE 10 TOOLACHEE 18 TOOLACHEE 30 TOOLACHEE 25 TOOLACHEE 7 TOOLACHEE 3 TOOLACHEE 45 TOOLACHEE 20 KELBROOK 1 MUNKARIE 3 MUNKARIE 1 MUNKARIE 8 MUNKARIE 4 MUNKARIE 6 CHIRON 2 CHIRON 1 MARAKU 1 CURRUMBIN 1 GIDGEE 1 EGLINT 1 PYTHON 1 QUASAR SOUTH 1 RANGER SOUTH 1 MIRANDA 1 WILLS 1 TEEGAL 1 ALLAMBI 1 HORNET 1 WITCHETTY 1

Type Section: Dullingari North 8

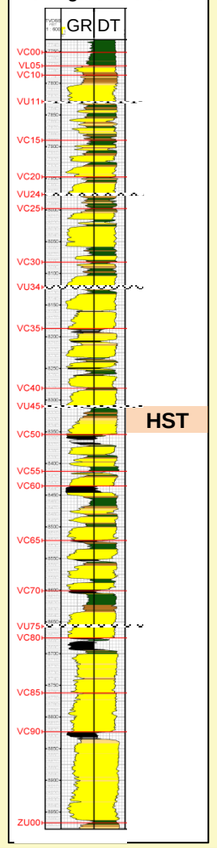

Sandbody Thickness: Width Summary VU45-VC55 (Strong Method)

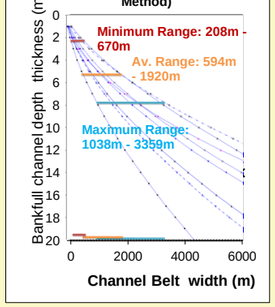

Appendix A10

VU45-VC50 Palaeogeographic Reconstruction

Date : October 28, 2014	Author : S. Kobelt	ENCL
Contour Interval :	File No. :	
Elevation Datum :	Santos Ltd ASN 80 007 550 923	

0 5 10 KM

Legend

Well Signature log

Well Log Signature — KINTA 1 — 25 ft

Palaeo-Environments of Deposition (See Chapter 6)

- Channel Belt
- Minor Channel/Crevass Splay Complex
- Lacustrine Uplands/Floodplains
- Peat Mire
- Amalgameted Sheet Sand Complex

Other

- Schematic: Non Depositional Feeder Channel
- Schematic: : Incised Stream Through Peat Mire
- Interpreted Paleaflow Direction
- Schematic: Crevasse Splay

Absent Sections

- Interpreted Post Depositional Erosion
- Interpreted Non-Depositon
- Absent, Indeterminate

Grouped Bankfull Depth Histogram VU45-VC55

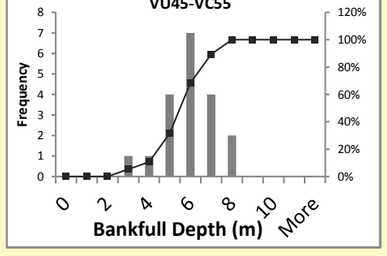

Summary: It is hard to assess the full extent of deposition of this interval due to erosion by the VU45 interval. The Allunga and Nappamerri Troughs are interpreted to still be active, whereas the Mettika Trough has switched back to the Tooolachee East Trough, feeding into the Allunga Trough.

Notes: Log Depth Scale of 1:15000 map units (km) used for this interval. 1mm = 12ft vertical section.

460000M E 470000M E 480000M E 490000M E 500000M E 510000M E 520000M E

6900000M N 6890000M N 6880000M N 6870000M N 6860000M N 6850000M N

N W E S

Appendix A11

VC50-VC55 Palaeogeographic Reconstruction

Date : October 28, 2014	Author : S. Kobelt	ENCL
Contour Interval :	File No.	
Elevation Datum :	Santos Ltd ABN 80 007 550 923	

0 5 10
KM

Legend

Well Signature log

Well Log Signature — KINTA 1 — 25 ft

Palaeo-Environments of Deposition (See Chapter 6)

- Channel Belt
- Minor Channel/Crevass Splay Complex
- Lacustrine Uplands/Floodplains
- Peat Mire
- Amalgameted Sheet Sand Complex

Other

- Schematic: Non Depositional Feeder Channel
- Schematic: Incised Stream Through Peat Mire
- Interpreted Paleaflow Direction
- Schematic: Crevasse Splay

Absent Sections

- Interpreted Post Depositional Erosion
- Interpreted Non-Depositon
- Absent, Indeterminate

Type Section: Dullingari North 8

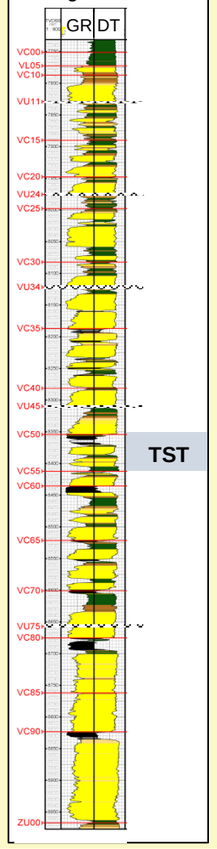

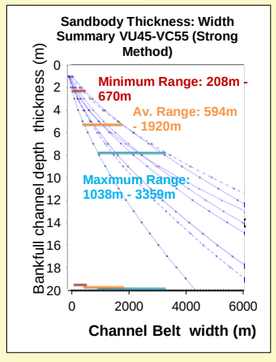

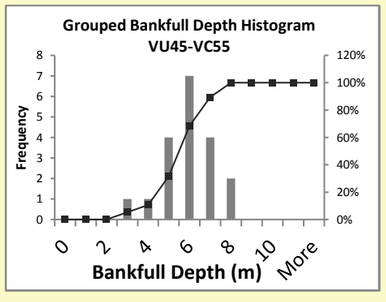

Summary: VC50 coal is a regional that covered the entire study area, this map focusses on the interval before widespread coal development. Coals are still extensive and dominate the area.

Notes: Log Depth Scale of 1:15000 map units (km) used for this interval. 1mm = 12ft vertical section.

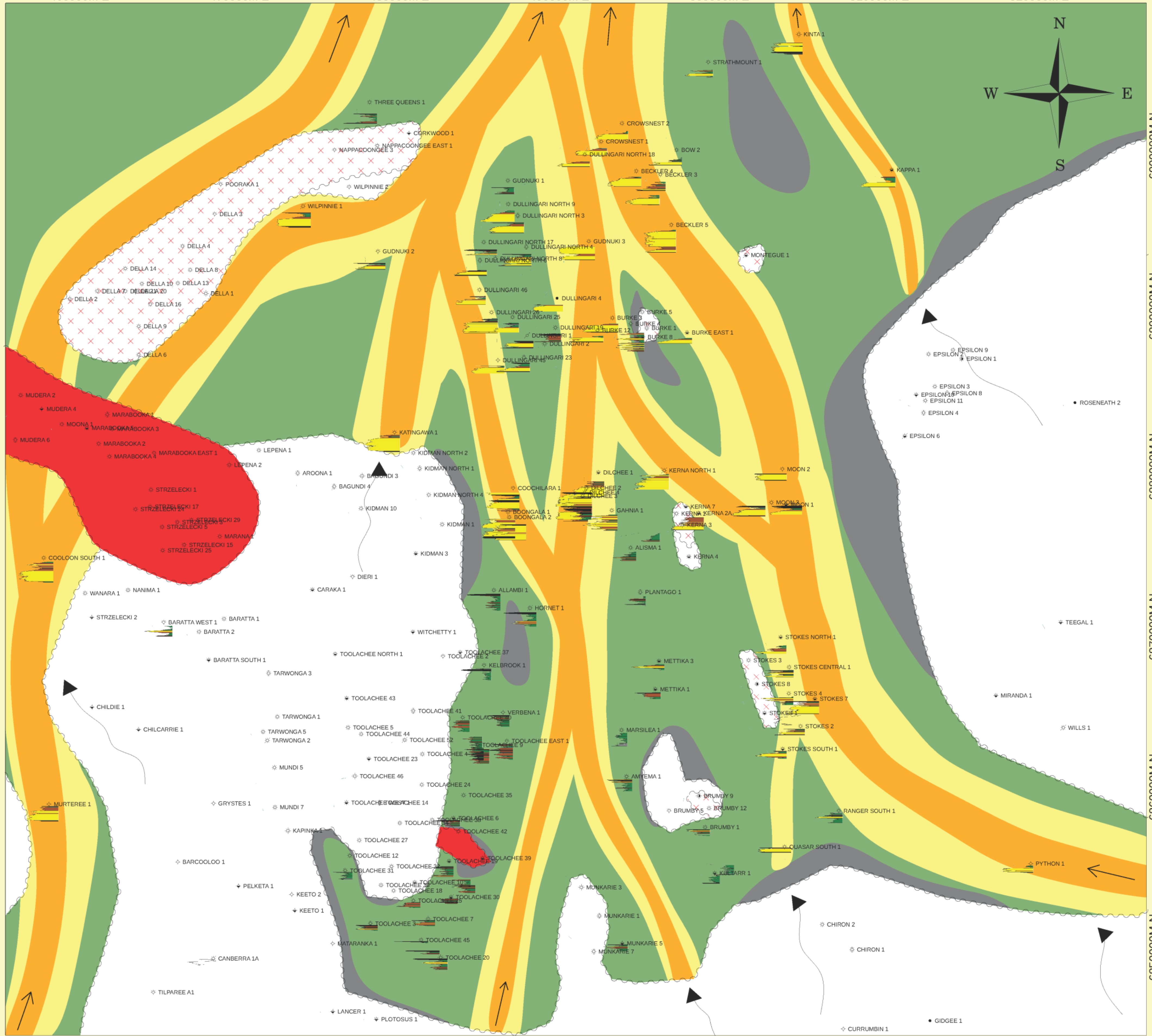

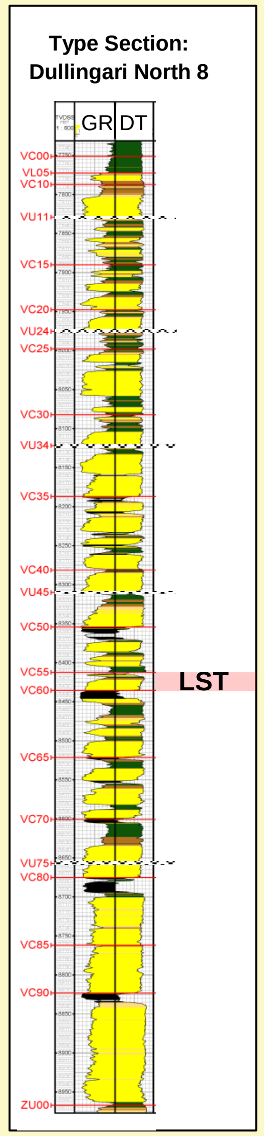

Appendix A12

VC55-VC60 Palaeogeographic Reconstruction

Legend

Well Signature log

Well Log Signature — KINTA 1, 25 ft

Palaeo-Environments of Deposition (See Chapter 6)

- Channel Belt
- Minor Channel/Crevasse Splay Complex
- Lacustrine Uplands/Floodplains
- Peat Mire
- Amalgameted Sheet Sand Complex

Other

- Schematic: Non Depositional Feeder Channel
- Schematic: Incised Stream Through Peat Mire
- Interpreted Paleaflow Direction
- Schematic: Crevasse Splay

Absent Sections

- Interpreted Post Depositional Erosion
- Interpreted Non-Depositon
- Absent, Indeterminate

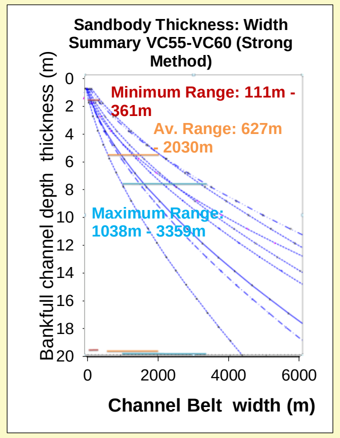

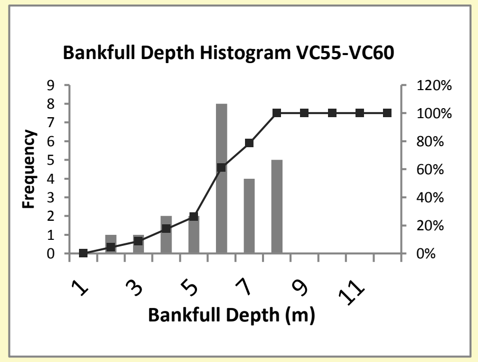

Summary: The Chanel axis along the Western edge of the area activates (intersected by Murturee 1), draining into the Allunga and Nappamerri systems, suggesting a sediment supply increase from the southwest.

Notes: Log Depth Scale of 1:15000 map units (km) used for this interval. 1mm = 12ft vertical section.

460000M E 470000M E 480000M E 490000M E 500000M E 510000M E 520000M E

6900000M N 6890000M N 6880000M N 6870000M N 6860000M N 6850000M N

N W E S

Appendix A13

VC60-VC65 Palaeogeographic Reconstruction

Date : October 28, 2014	Author : S. Kobelt	ENCL
Contour Interval :	File No. :	
Elevation Datum :	Santos Ltd ABN 80 007 550 923	

0 5 10 KM

Legend

Well Signature log

Well Log Signature — KINTA 1 — 25 ft

Palaeo-Environments of Deposition (See Chapter 6)

- Channel Belt
- Minor Channel/Crevass Splay Complex
- Lacustrine Uplands/Floodplains
- Peat Mire
- Amalgameted Sheet Sand Complex

Other

- Schematic: Non Depositional Feeder Channel
- Schematic: Incised Stream Through Peat Mire
- Interpreted Paleaflow Direction
- Schematic: Crevasse Splay

Absent Sections

- Interpreted Post Depositional Erosion
- Interpreted Non-Depositon
- Absent, Indeterminate

Type Section: Dullingari North 8

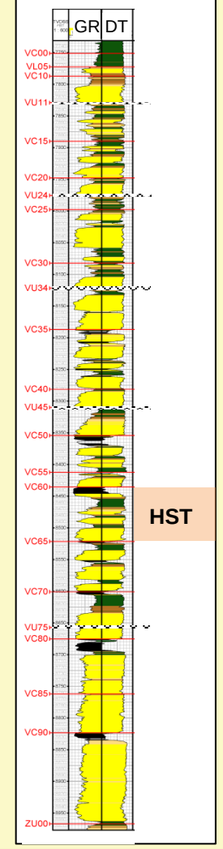

Sandbody Thickness: Width Summary VC60-VC65(Strong Method)

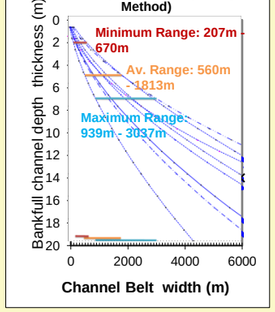

Bankfull Depth Histogram VC60-VC65

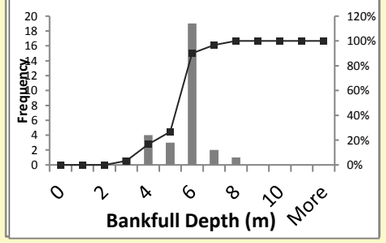

Summary: The Allunga Trough is the most active Trough, while the Toolachee East Trough has been shut off during this time, dominated by peat mire and lacustrine environments

Notes: Log Depth Scale of 1:20000 map units (km) used for this interval. 1mm = 16ft vertical section.

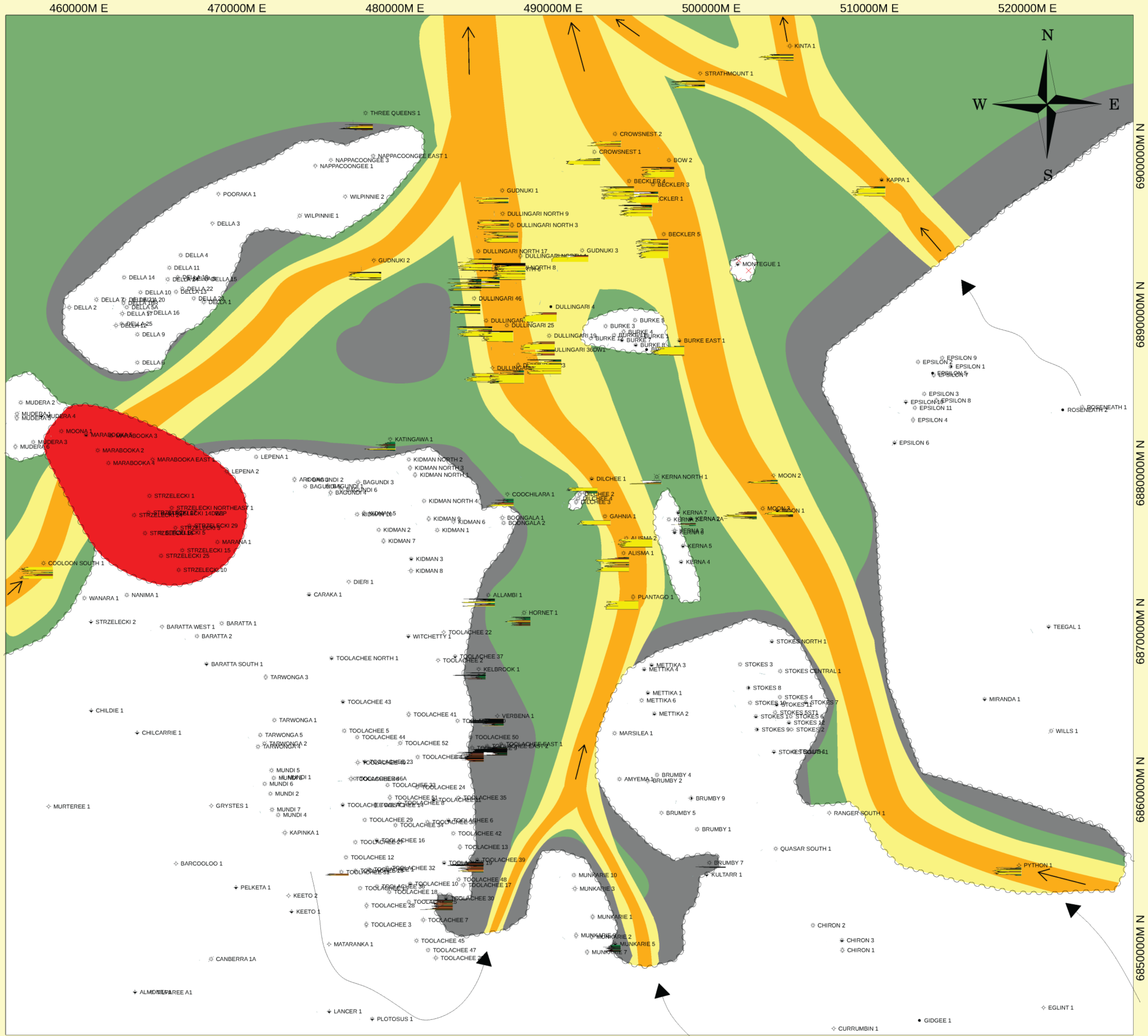

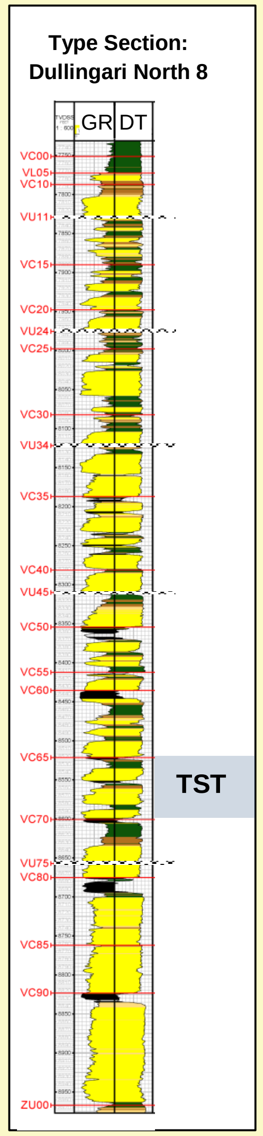

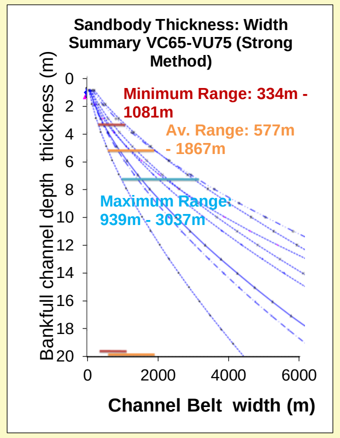

Appendix A14

VC65-VC70 Palaeogeographic Reconstruction

0 5 10
KM

Legend

Well Signature log

Well Log Signature

Palaeo-Environments of Deposition (See Chapter 6)

- Channel Belt
- Minor Channel/Crevasse Splay Complex
- Lacustrine Uplands/Floodplains
- Peat Mire
- Amalgameted Sheet Sand Complex

Other

- Schematic: Non Depositional Feeder Channel
- Schematic: Incised Stream Through Peat Mire
- Interpreted Paleaflow Direction
- Schematic: Crevasse Splay

Absent Sections

- Interpreted Post Depositional Erosion
- Interpreted Non-Depositon
- Absent, Indeterminate

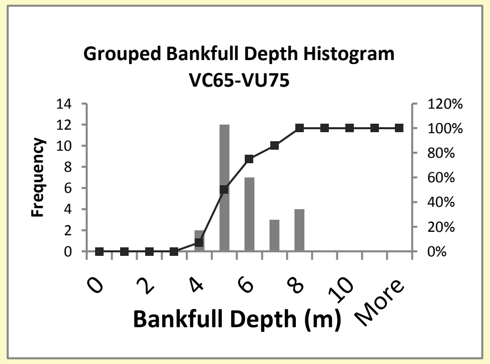

<u>Summary:</u> The Mettika, Toolachee East and Allunga Troughs are all active during this interval.

<u>Notes:</u> Log Depth Scale of 1:30,000 map units (km) used for this interval. 1mm = 24ft vertical section.

460000M E 470000M E 480000M E 490000M E 500000M E 510000M E 520000M E

6900000M N 6890000M N 6880000M N 6870000M N 6860000M N 6850000M N

N W E S

Type Section: Dullingari North 8

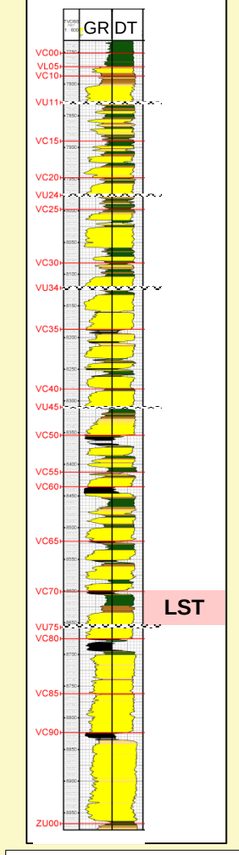

Appendix A15

VC70-VU75 Palaeogeographic Reconstruction

Date : October 28, 2014	Author : S. Kobelt	ENCL
Contour Interval :	File No. :	
Elevation Datum :	Santos Ltd ABN 80 007 550 923	

0 5 10 KM

Legend

Well Signature log

Well Log Signature — KINTA 1 — 25 ft

Palaeo-Environments of Deposition (See Chapter 6)

- Channel Belt
- Minor Channel/Crevass Splay Complex
- Lacustrine Uplands/Floodplains
- Peat Mire
- Amalgameted Sheet Sand Complex

Other

- Schematic: Non Depositional Feeder Channel
- Schematic: Incised Stream Through Peat Mire
- Interpreted Paleaflow Direction
- Schematic: Crevasse Splay

Absent Sections

- Interpreted Post Depositional Erosion
- Interpreted Non-Depositon
- Absent, Indeterminate

Sandbody Thickness: Width Summary VC65-VU75 (Strong Method)

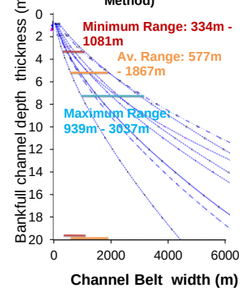

Grouped Bankfull Depth Histogram VC65-VU75

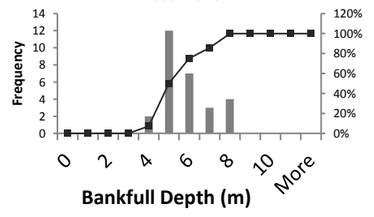

<u>Summary:</u> Large amounts of coarse grained sediment shedding off of the basement from the south feed all of the major troughs in the area during this interval.

<u>Notes:</u> Log Depth Scale of 1:20,000 map units (km) used for this interval. 1mm = 16ft vertical section.

Appendix A16

VU75-VC80 Palaeogeographic Reconstruction

Date : October 29, 2014	Author : S. Kobelt	ENCL
Contour Interval :	File No. :	
Elevation Datum :	Santos Ltd ABN 80 007 550 923	

460000M E 470000M E 480000M E 490000M E 500000M E 510000M E 520000M E

6900000M N 6890000M N 6880000M N 6870000M N 6860000M N 6850000M N

N W E S

0 5 10 KM

Gudnuki 2 Small Coal Preservation (not to scale)

Legend

Well Signature log

Well Log Signature — KINTA 1 — 25 ft

Palaeo-Environments of Deposition (See Chapter 6)

- Channel Belt
- Minor Channel/Crevass Splay Complex
- Lacustrine Uplands/Floodplains
- Peat Mire
- Amalgameted Sheet Sand Complex

Other

- Schematic: Non Depositional Feeder Channel
- Schematic: Incised Stream Through Peat Mire
- Interpreted Paleaflow Direction
- Schematic: Crevasse Splay

Absent Sections

- Interpreted Post Depositional Erosion
- Interpreted Non-Depositon
- Absent, Indeterminate

Type Section: Dullingari North 8

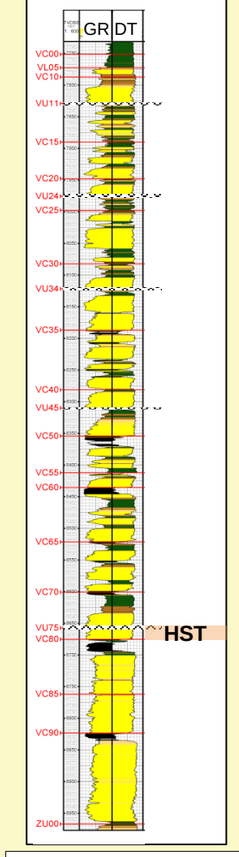

Sandbody Thickness: Width Summary VU75-VC80 (Strong Method)

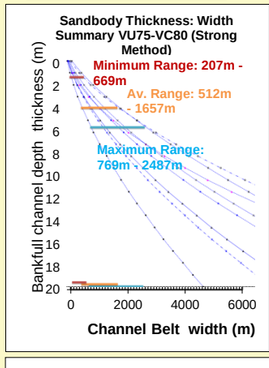

Grouped Bankfull Depth Histogram VU75-ZU00

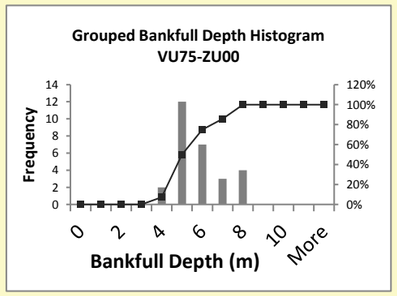

<u>Summary:</u> The NE-SW striking basement lineaments visible on the VC50-ZU00 isochron are interpreted to have influenced the drainage patterns into the Nappamerri Trough.The same depositional axes are active as in the lower VC80-VC100 interval.

<u>Notes:</u> Log Depth Scale of 1:20,000 map units (km) used for this interval. 1mm = 16ft vertical section.

460000M E 470000M E 480000M E 490000M E 500000M E 510000M E 520000M E

6900000M N 6890000M N 6880000M N 6870000M N 6860000M N 6850000M N

N W E S

Gudnuki 2 Small Coal Preservation (not to scale)

Appendix A17

VC80-ZU00 Palaeogeographic Reconstruction

Date : October 28, 2014	Author : S. Kobelt	ENCL
Contour Interval :	File No. :	
Elevation Datum :	Santos Ltd ABN 80 007 550 923	

0 5 10 KM

Type Section: Dullingari North 8

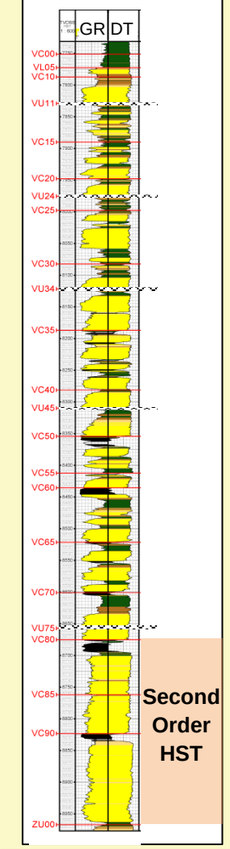

Legend

Well Signature log

Well Log Signature — KINTA 1 — 50 ft

Palaeo-Environments of Deposition (See Chapter 6)

- Channel Belt
- Minor Channel/Crevass Splay Complex
- Lacustrine Uplands/Floodplains
- Peat Mire
- Amalgameted Sheet Sand Complex

Other

- Schematic: Non Depositional Feeder Channel
- Schematic: Incised Stream Through Peat Mire
- Interpreted Paleaflow Direction
- Schematic: Crevasse Splay

Absent Sections

- Interpreted Post Depositional Erosion
- Interpreted Non-Depositon
- Absent, Indeterminate

Sandbody Thickness: Width Summary VU75-VC80 (Strong Method)

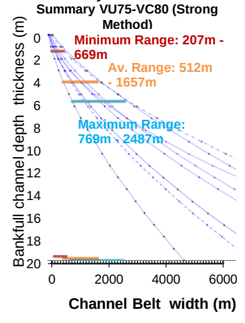

Grouped Bankfull Depth Histogram VU75-ZU00

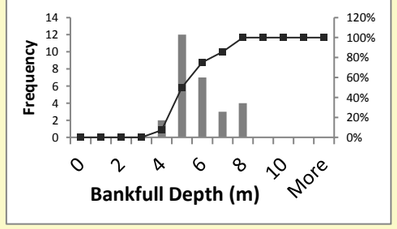

Summary: This map is a composite map of 5 Chronostratigraphic intervals and so channel thickness estimates were not considered applicable for this map. This interval is dominated by sandy load fill along basement lows with peat mires growing off of structural highs.

Notes: Log Depth Scale of 1:40,000 map units (km) used for this interval. 1mm = 32ft vertical section.

Appendix B: Bankfull Measurement Histograms

Appendix B1: Histogram of the entire data set of bankfull measurements measured from all Patchawarra intervals.

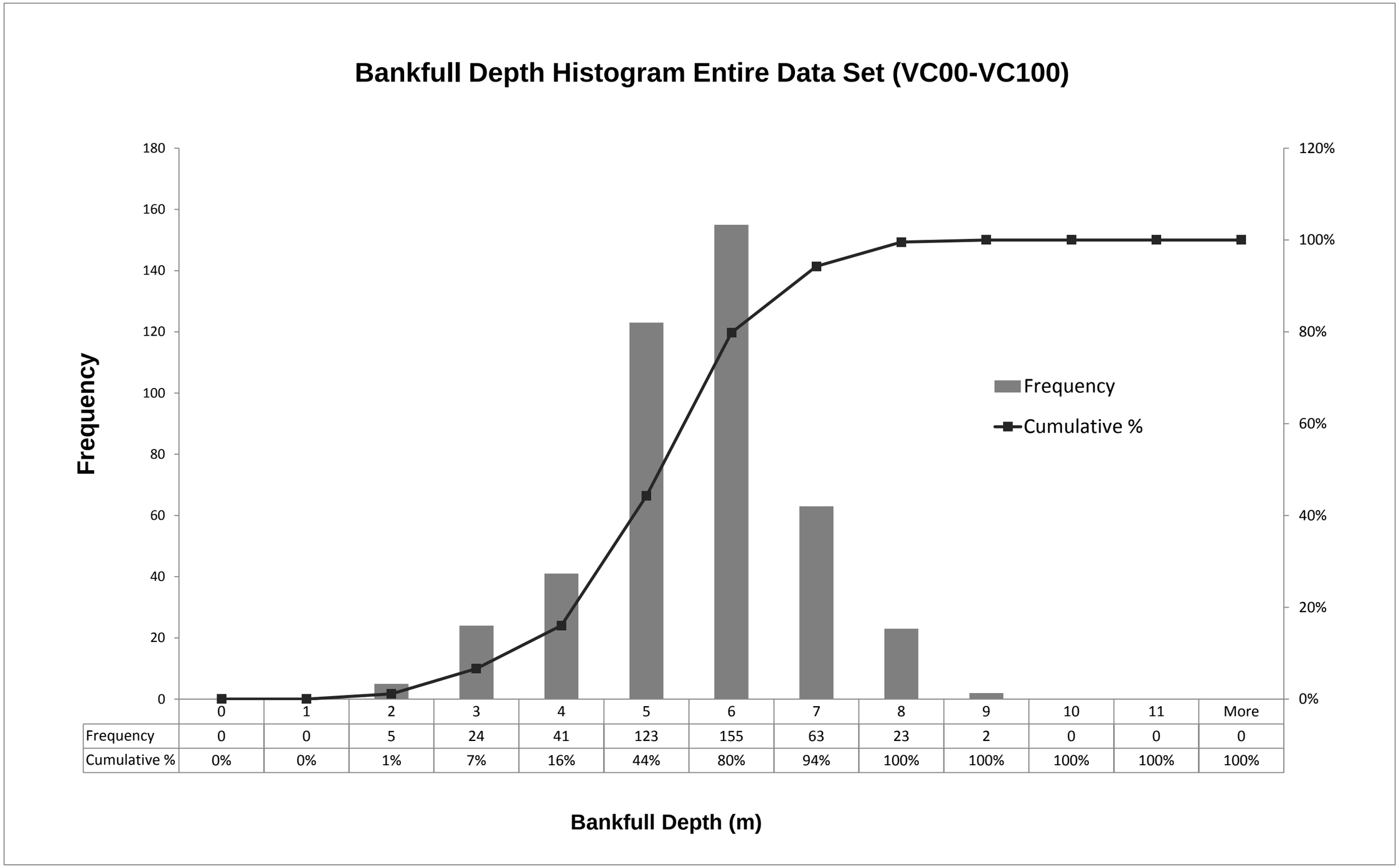

	0	1	2	3	4	5	6	7	8	9	10	11	More
Frequency	0	0	5	24	41	123	155	63	23	2	0	0	0
Cumulative %	0%	0%	1%	7%	16%	44%	80%	94%	100%	100%	100%	100%	100%

Appendix B2: Histogram of the VL05-VC10 interval bankfull measurements, this interval was not interpreted to be a part of a larger population set.

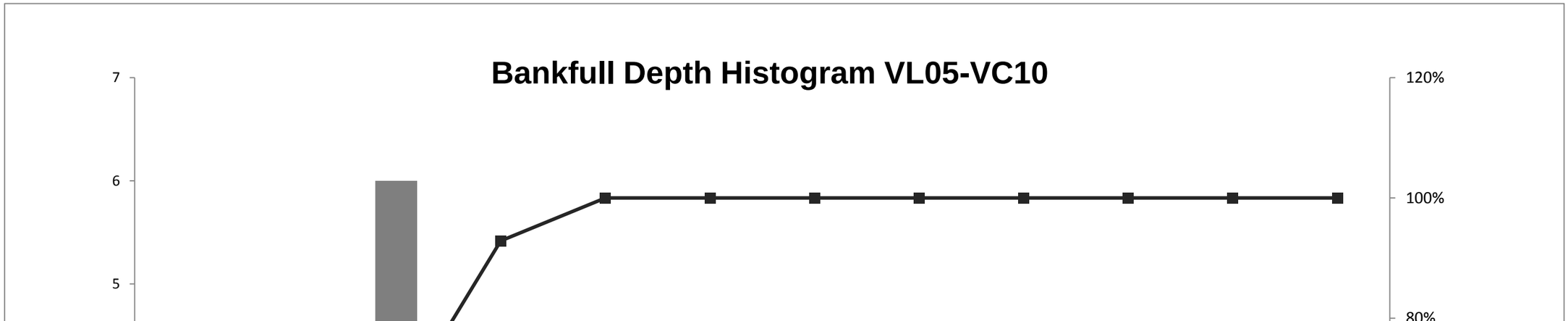

	1	2	3	4	5	6	7	8	9	10	11	More
Frequency	0	3	6	4	1	0	0	0	0	0	0	0
Cumulative %	0%	21%	64%	93%	100%	100%	100%	100%	100%	100%	100%	100%

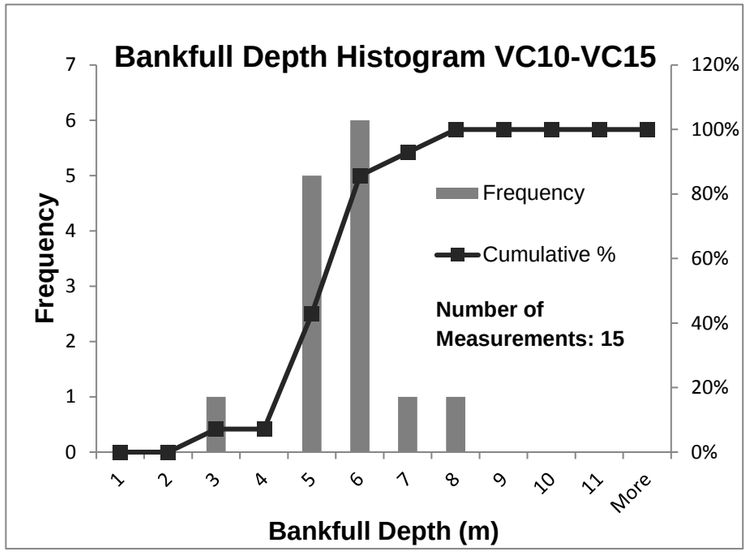

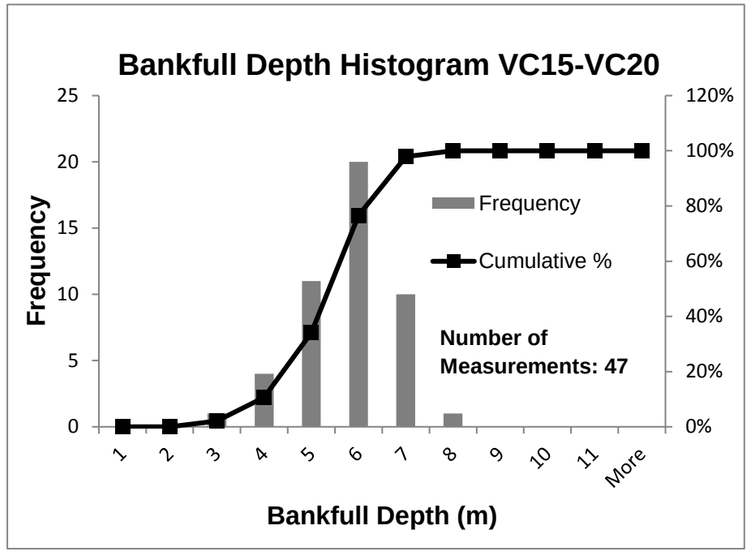

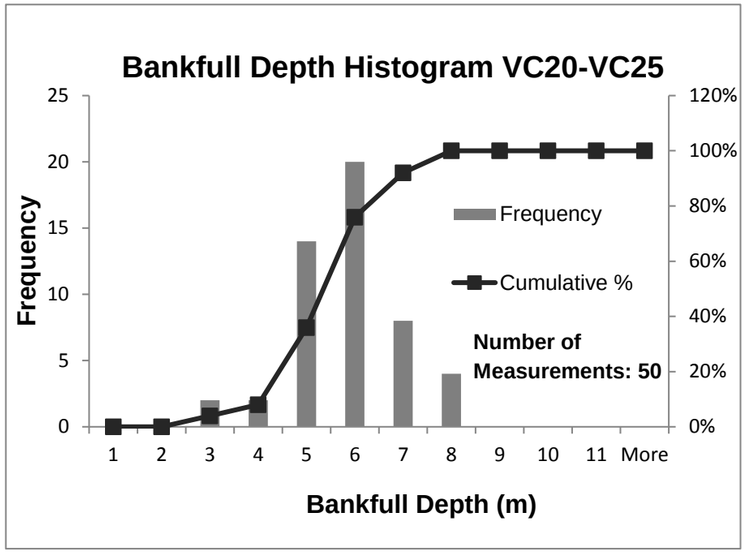

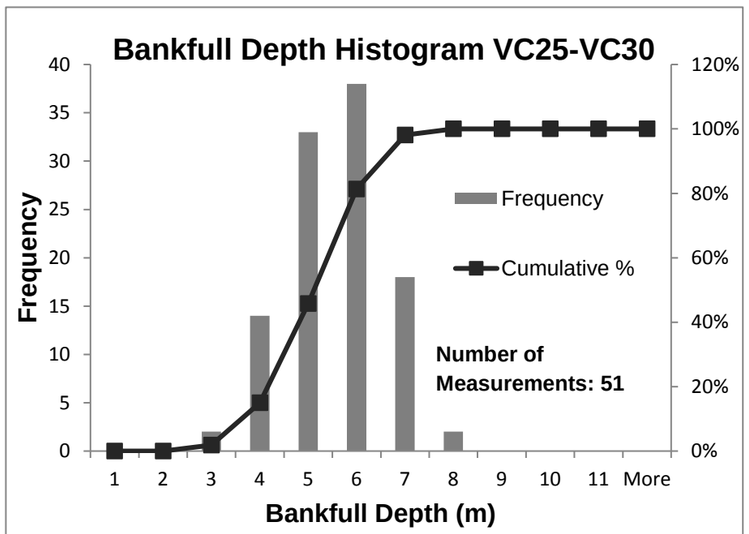

Appendix B3: Histograms of the VC10-VC30 individual interval bankfull measurement populations, as well as the grouped VC10-VC30 population.

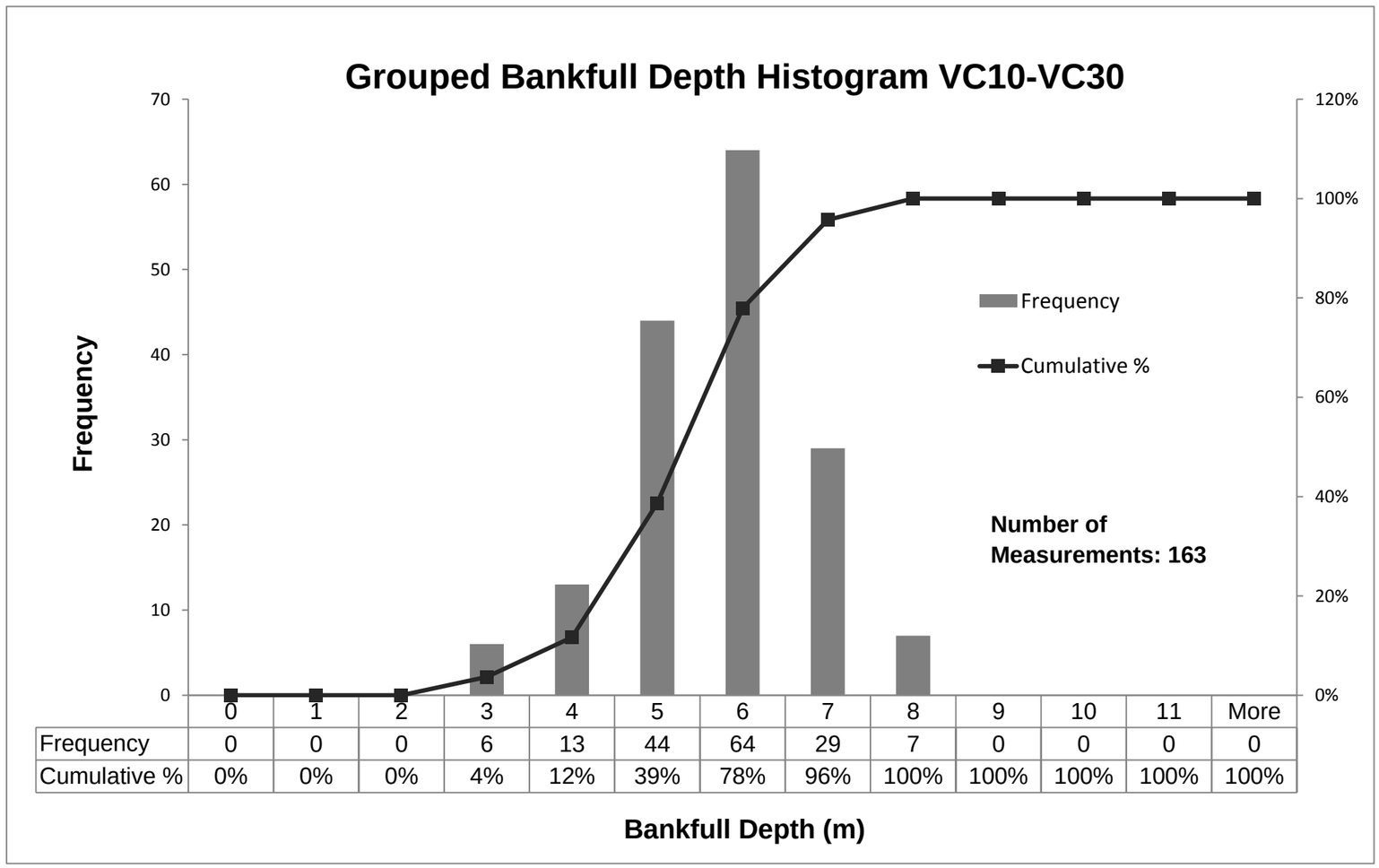

	0	1	2	3	4	5	6	7	8	9	10	11	More
Frequency	0	0	0	6	13	44	64	29	7	0	0	0	0
Cumulative %	0%	0%	0%	4%	12%	39%	78%	96%	100%	100%	100%	100%	100%

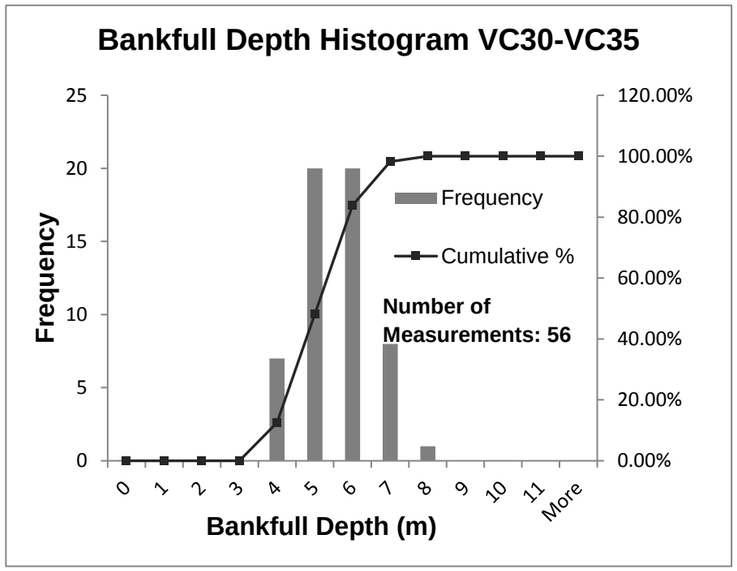

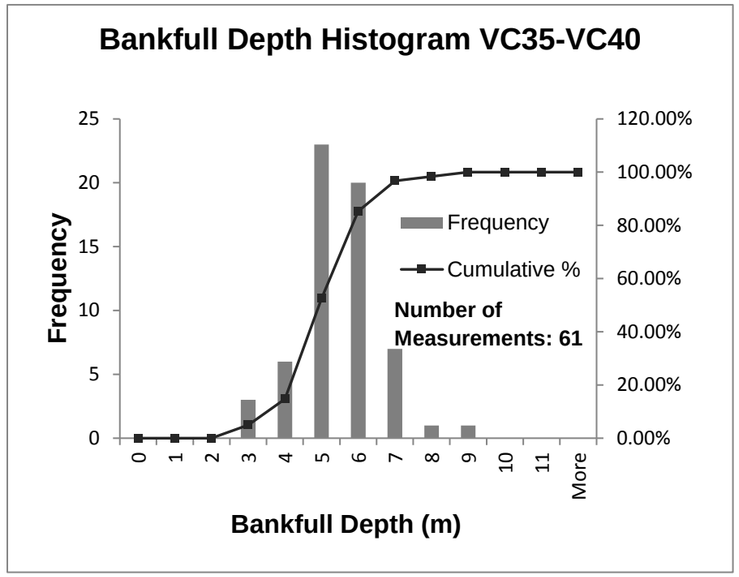

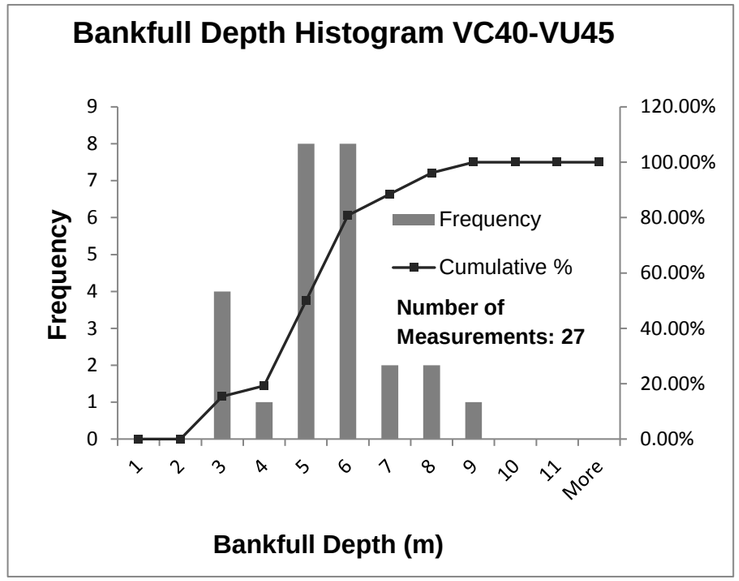

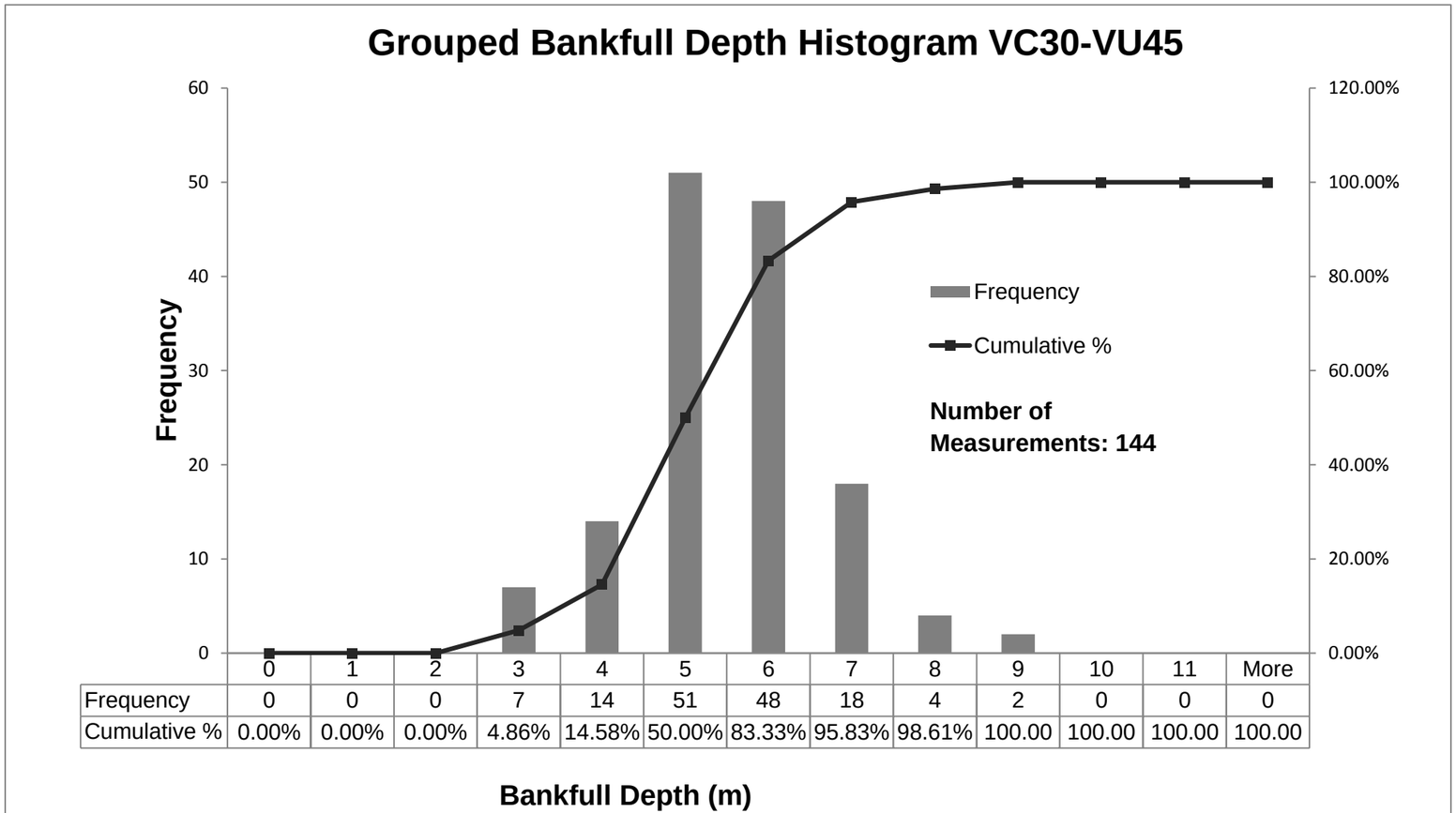

	0	1	2	3	4	5	6	7	8	9	10	11	More
Frequency	0	0	0	7	14	51	48	18	4	2	0	0	0
Cumulative %	0.00%	0.00%	0.00%	4.86%	14.58%	50.00%	83.33%	95.83%	98.61%	100.00	100.00	100.00	100.00

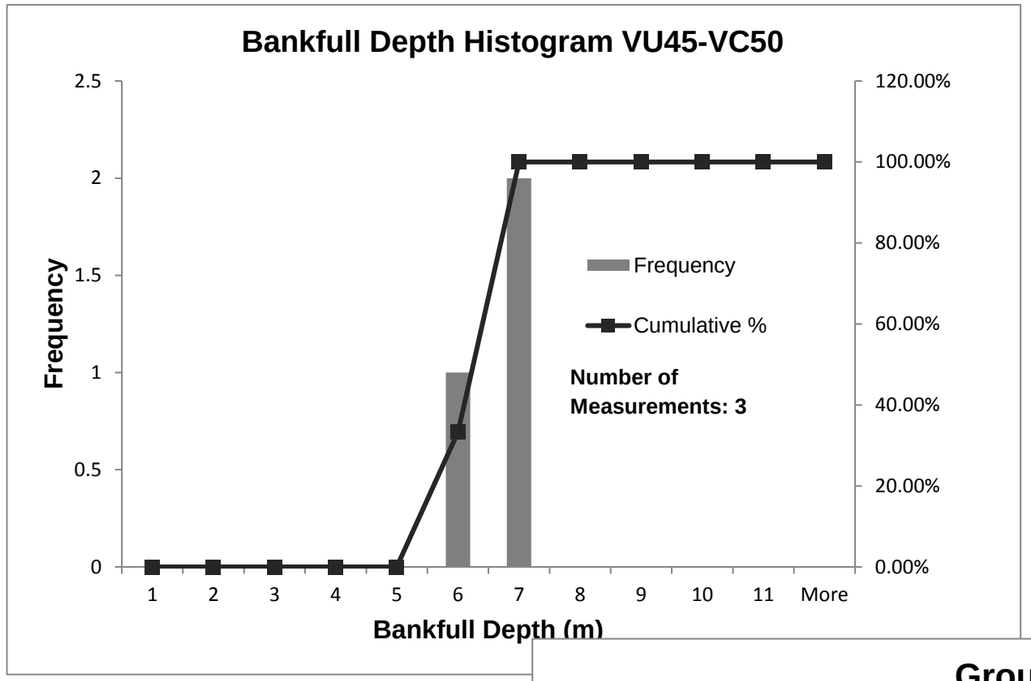

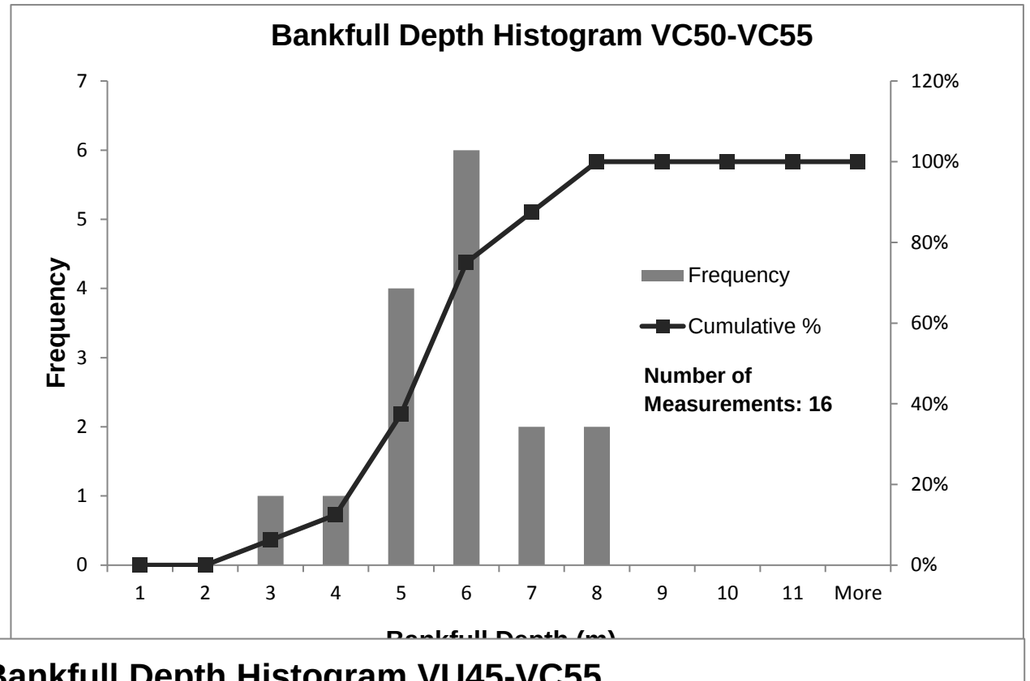

Appendix B5: Histograms of the VU45-VC55 individual interval bankfull measurement populations, as well as the grouped VU45-VC55 population.

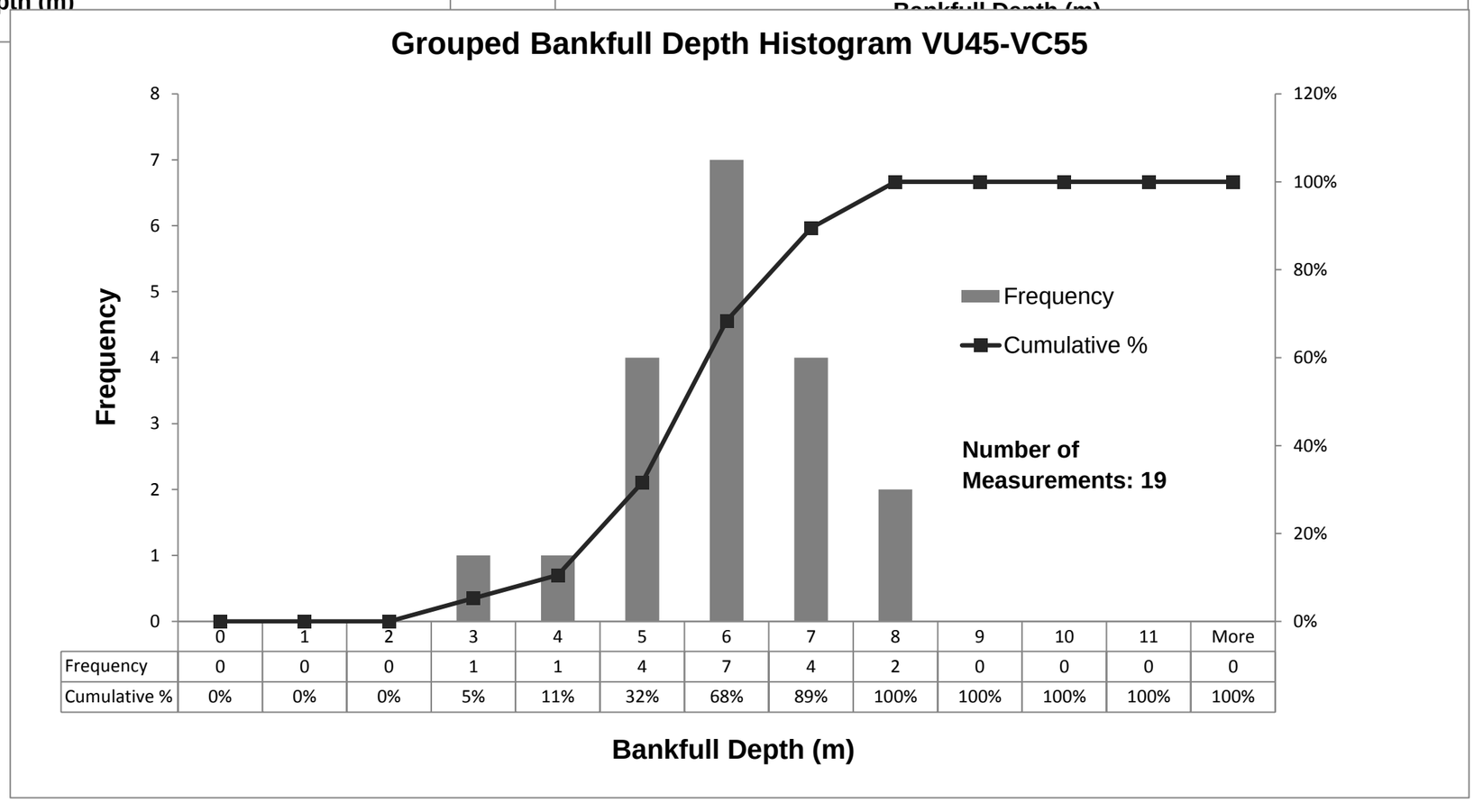

	0	1	2	3	4	5	6	7	8	9	10	11	More
Frequency	0	0	0	1	1	4	7	4	2	0	0	0	0
Cumulative %	0%	0%	0%	5%	11%	32%	68%	89%	100%	100%	100%	100%	100%

Appendix B6: Histogram of the VC55-VC60 interval bankfull measurements, this interval was not interpreted to be a part of a larger population set

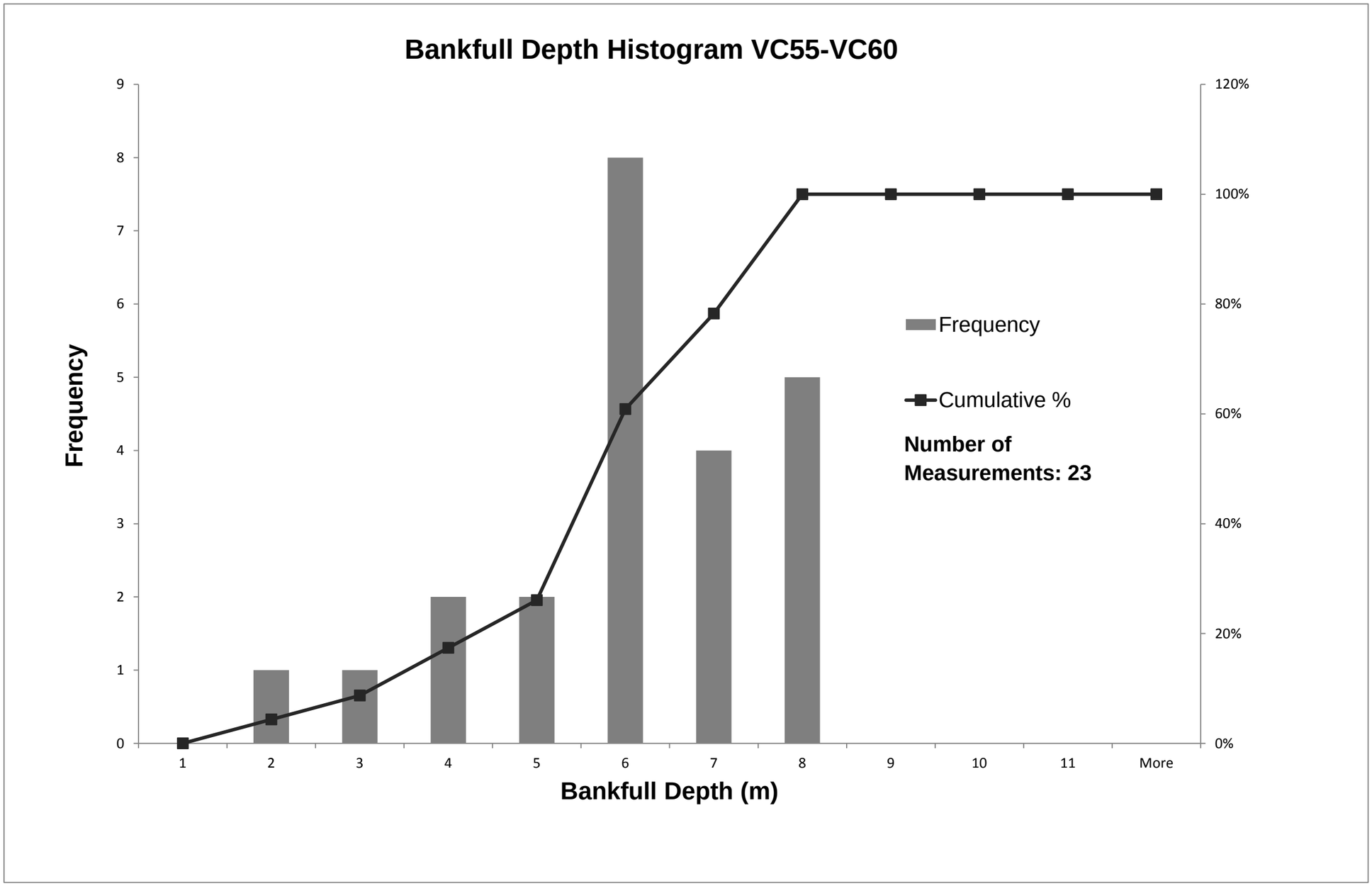

Appendix B7: Histogram of the VC60-VC65 interval bankfull measurements, this interval was not interpreted to be a part of a larger population set

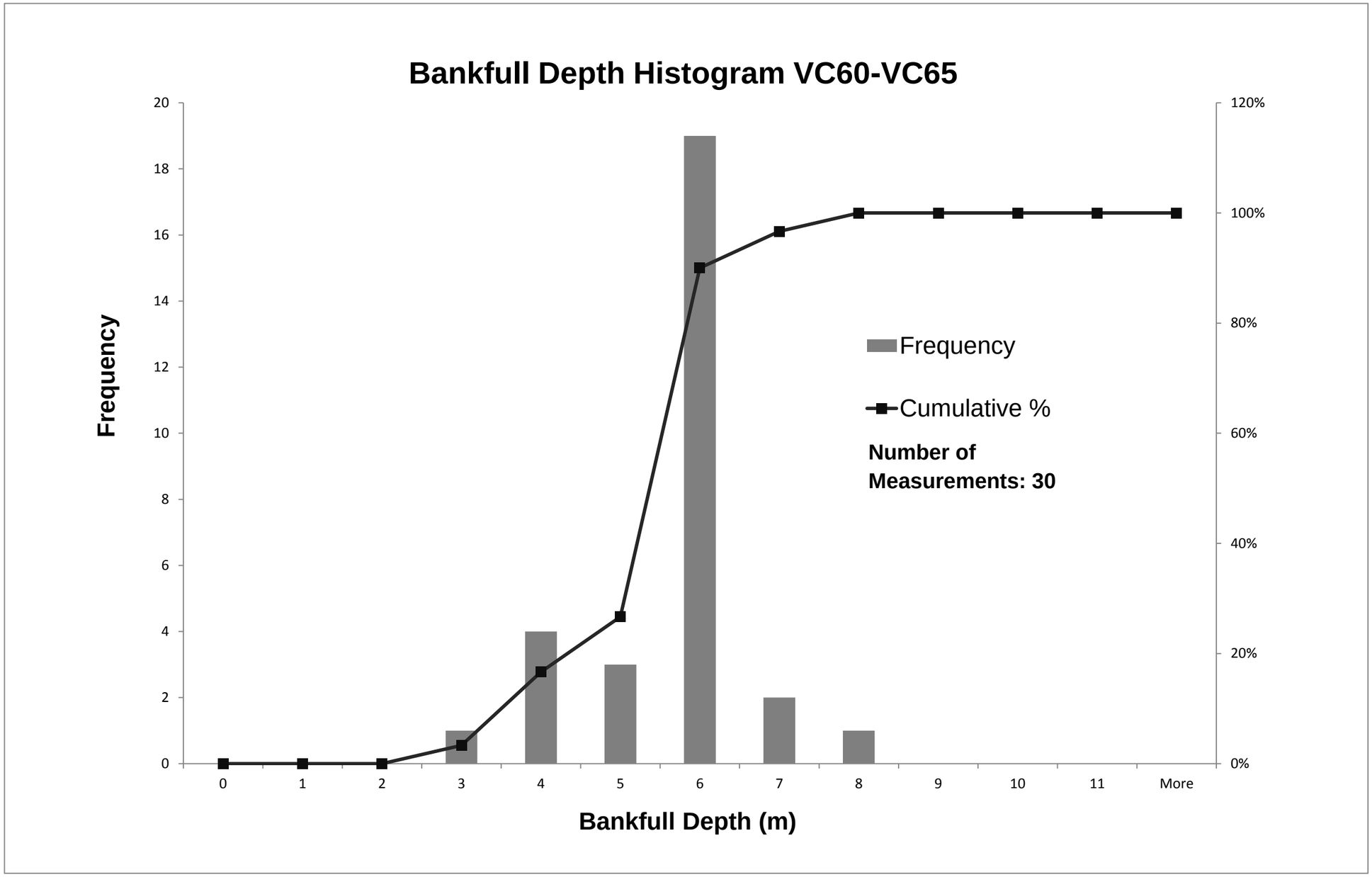

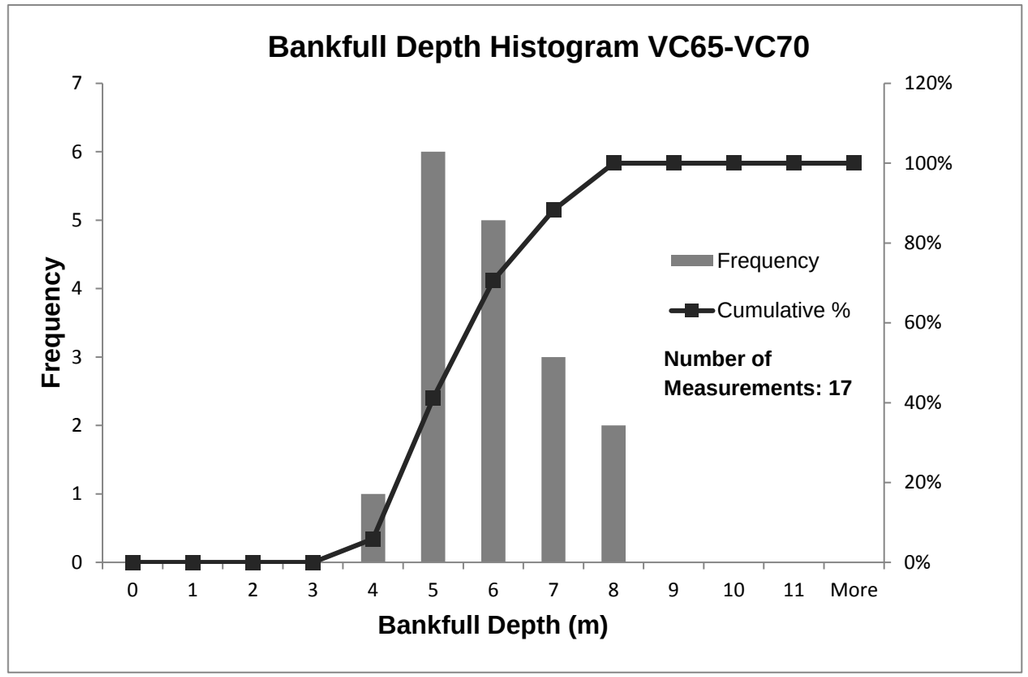

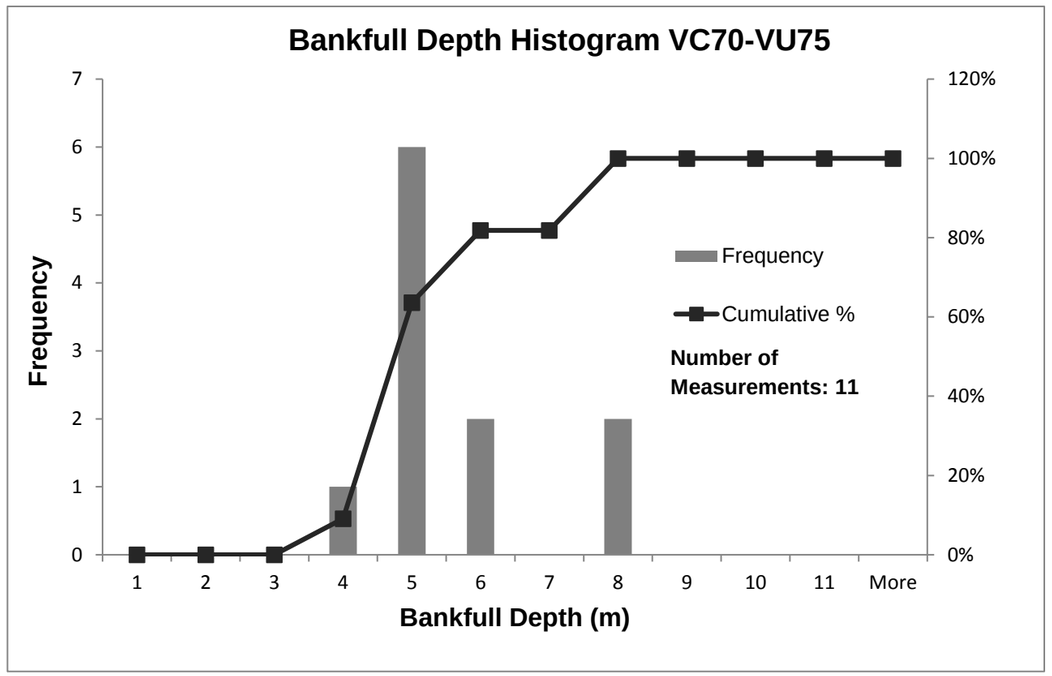

Appendix B8: Histograms of the VC65-VU75 individual interval bankfull measurement populations, as well as the grouped VC65-VU75 population.

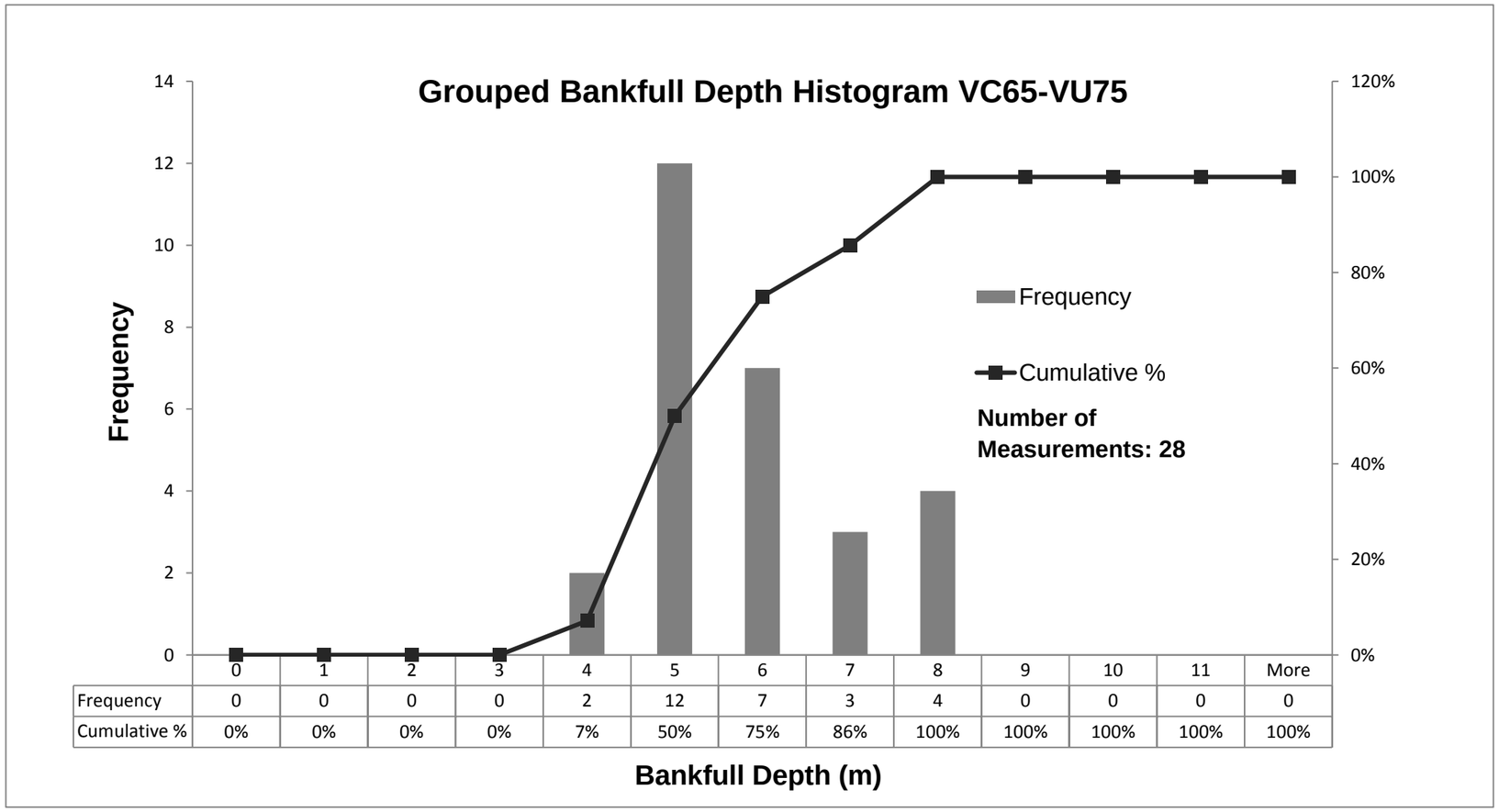

	0	1	2	3	4	5	6	7	8	9	10	11	More
Frequency	0	0	0	0	2	12	7	3	4	0	0	0	0
Cumulative %	0%	0%	0%	0%	7%	50%	75%	86%	100%	100%	100%	100%	100%

Appendix B9: Histogram of the VU75-VC100 combined interval bankfull measurements. Individual interval histograms are not displayed due to a lack of measurements able to be taken in the VC80-VC100 intervals.

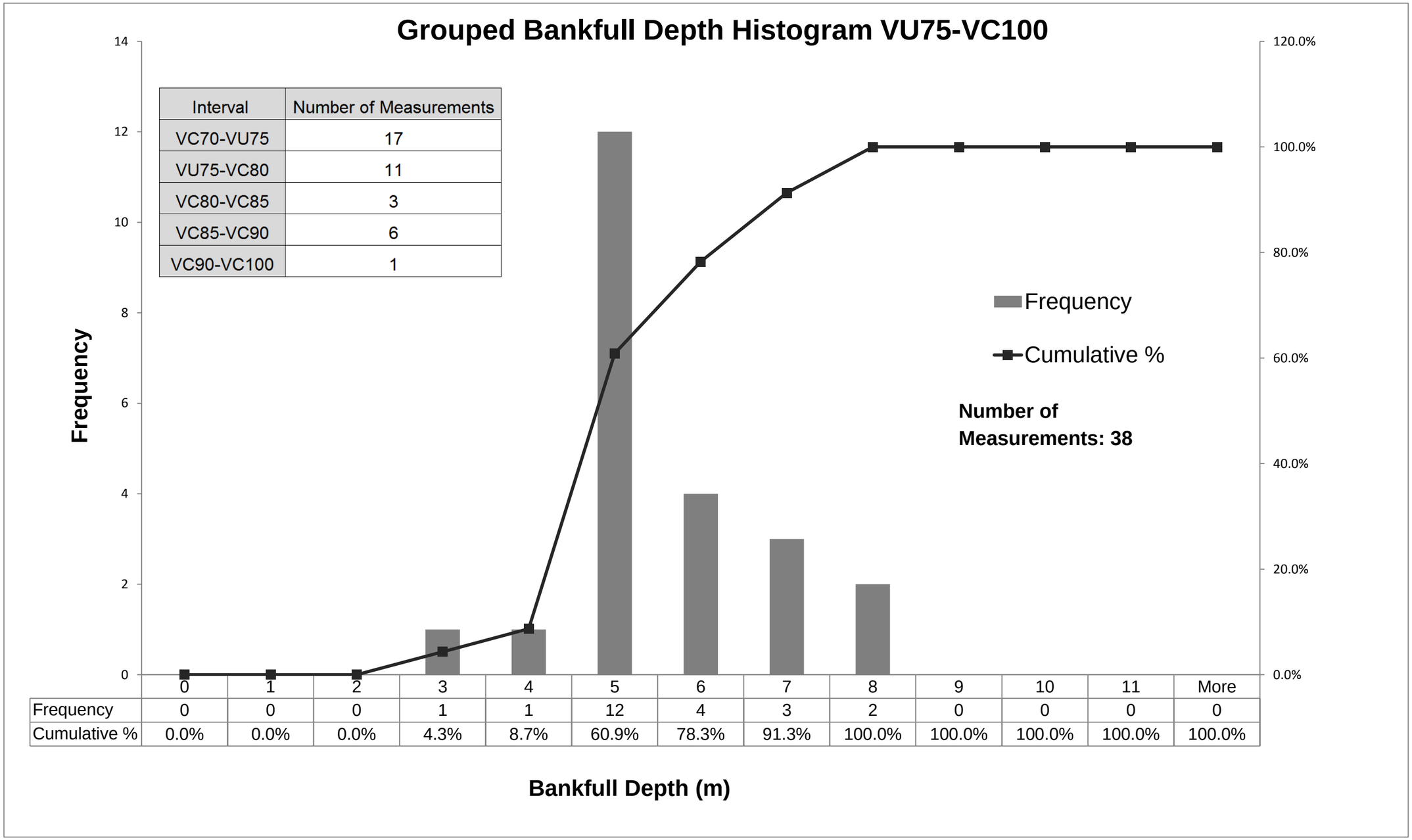

Interval	Number of Measurements
VC70-VU75	17
VU75-VC80	11
VC80-VC85	3
VC85-VC90	6
VC90-VC100	1

	0	1	2	3	4	5	6	7	8	9	10	11	More
Frequency	0	0	0	1	1	12	4	3	2	0	0	0	0
Cumulative %	0.0%	0.0%	0.0%	4.3%	8.7%	60.9%	78.3%	91.3%	100.0%	100.0%	100.0%	100.0%	100.0%

Appendix C: Channel Belt Width Plot Estimation

Appendix C1: Channel Belt Width plot for Grouped Bankfull VL05-VC10

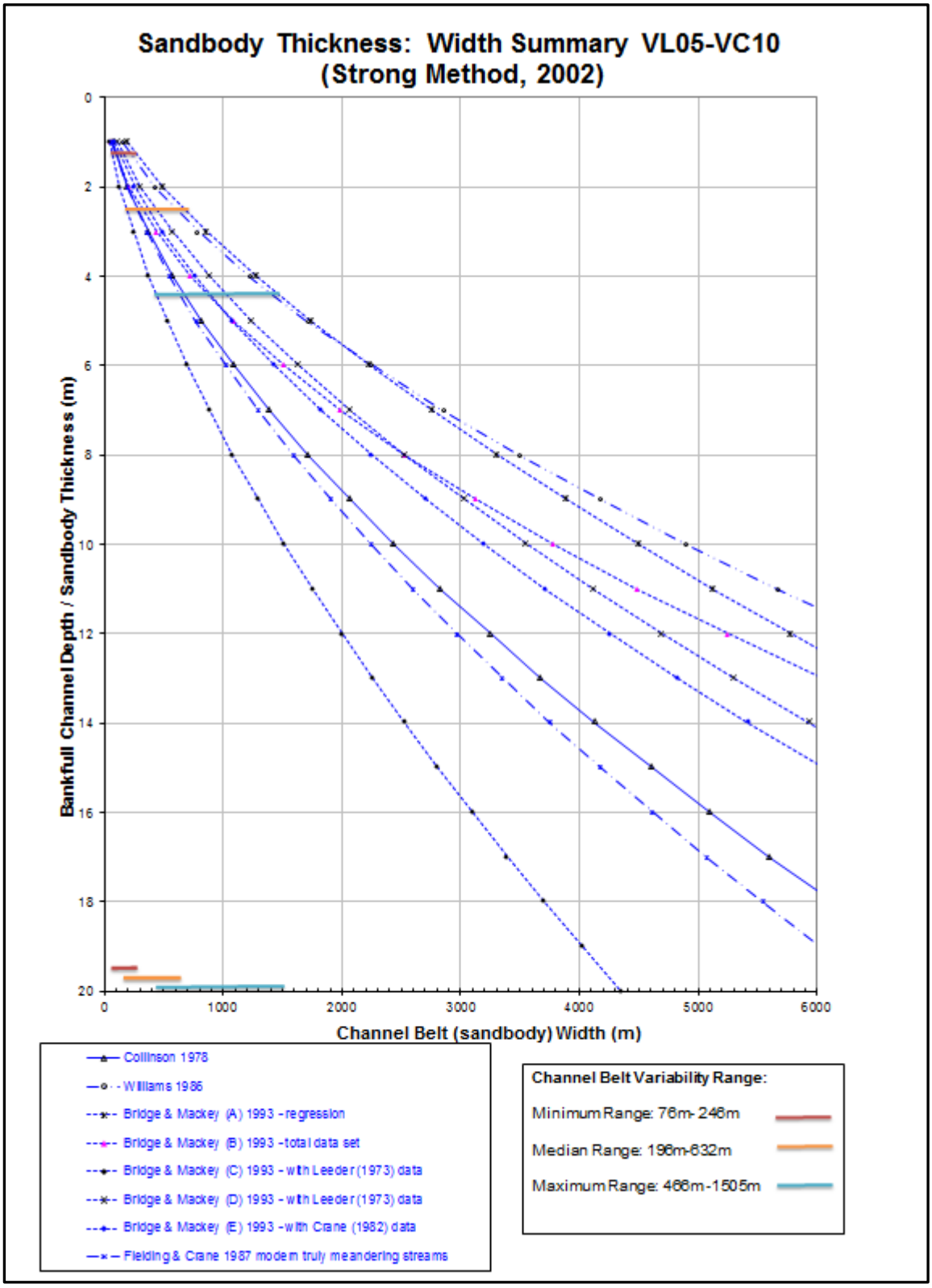

Appendix C2: Channel Belt Width plot for Grouped Bankfull VC10-VC30

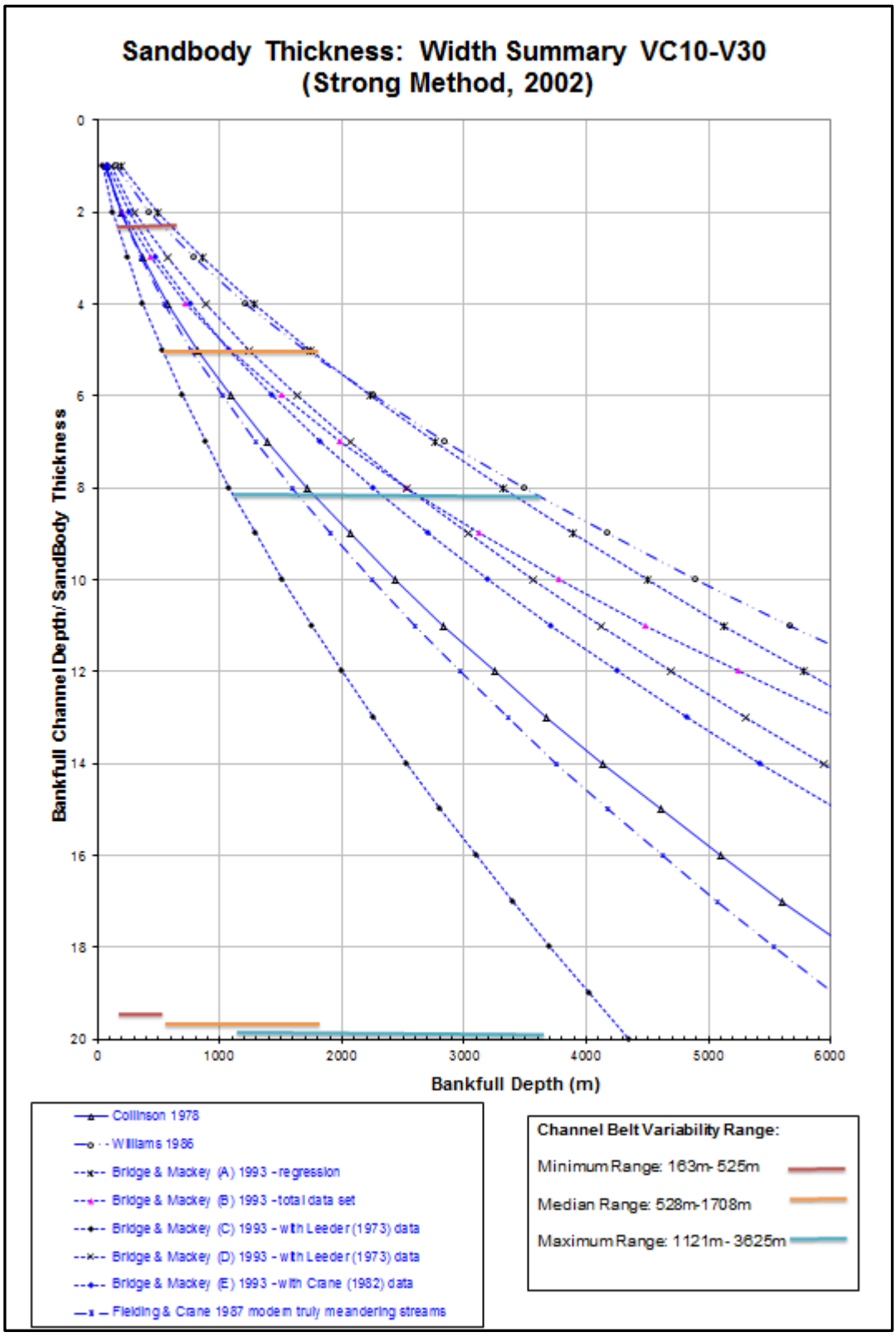

Appendix C3: Channel Belt Width plot for Grouped Bankfull VC30-VU45

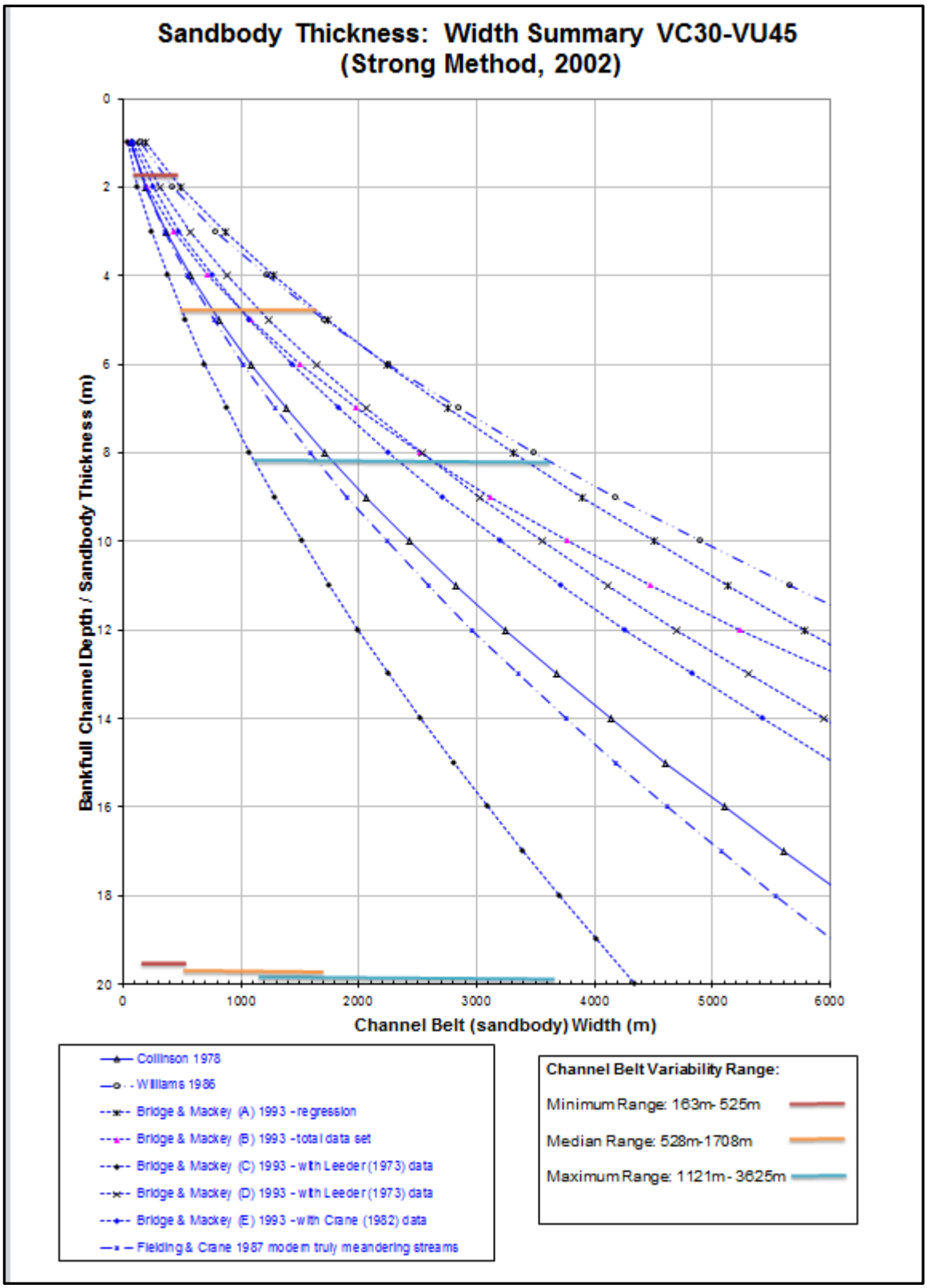

Appendix C4: Channel Belt Width plot for Grouped Bankfull VU45-VC55

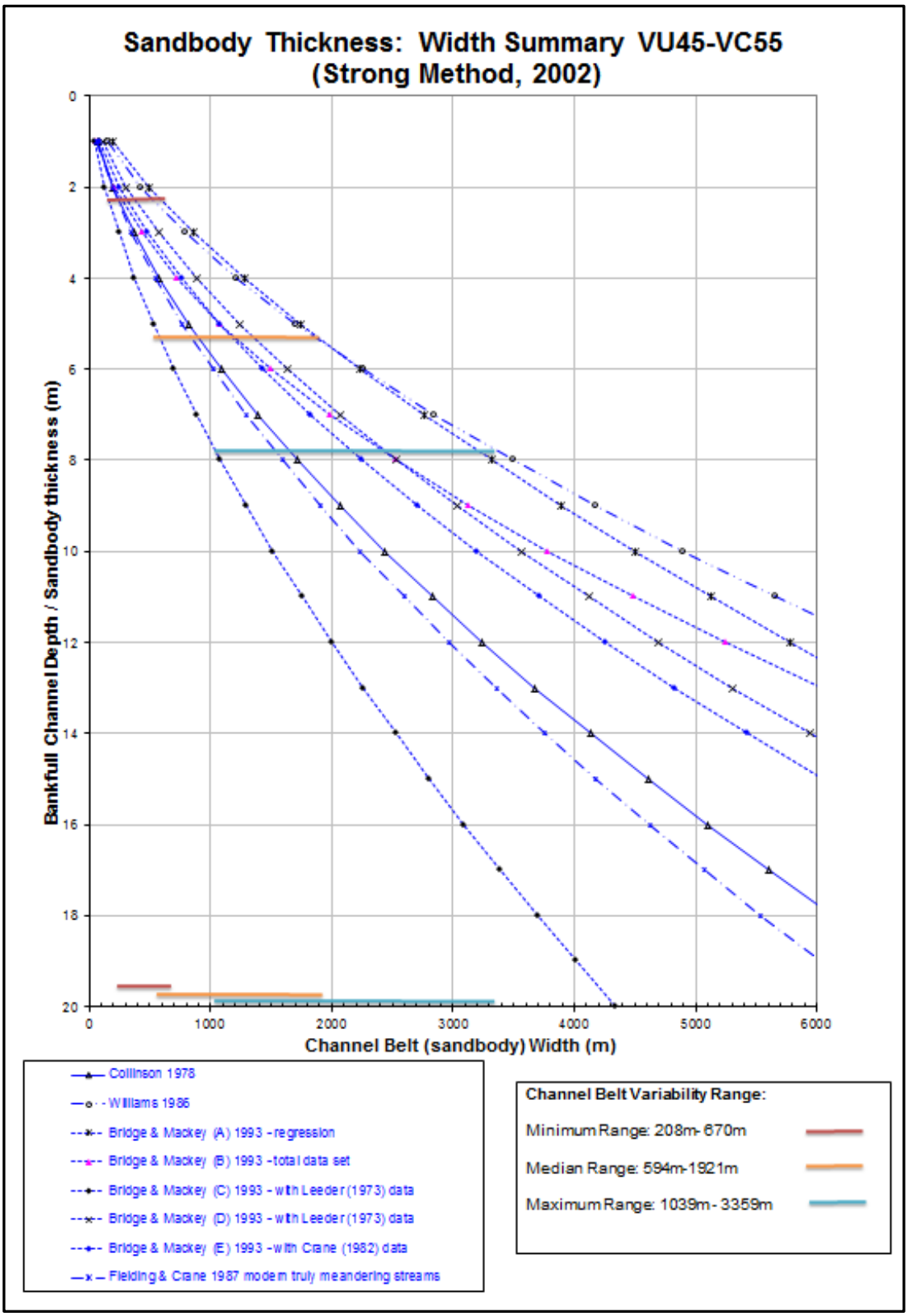

Appendix C5: Channel Belt Width plot for Grouped Bankfull VC55-VC60

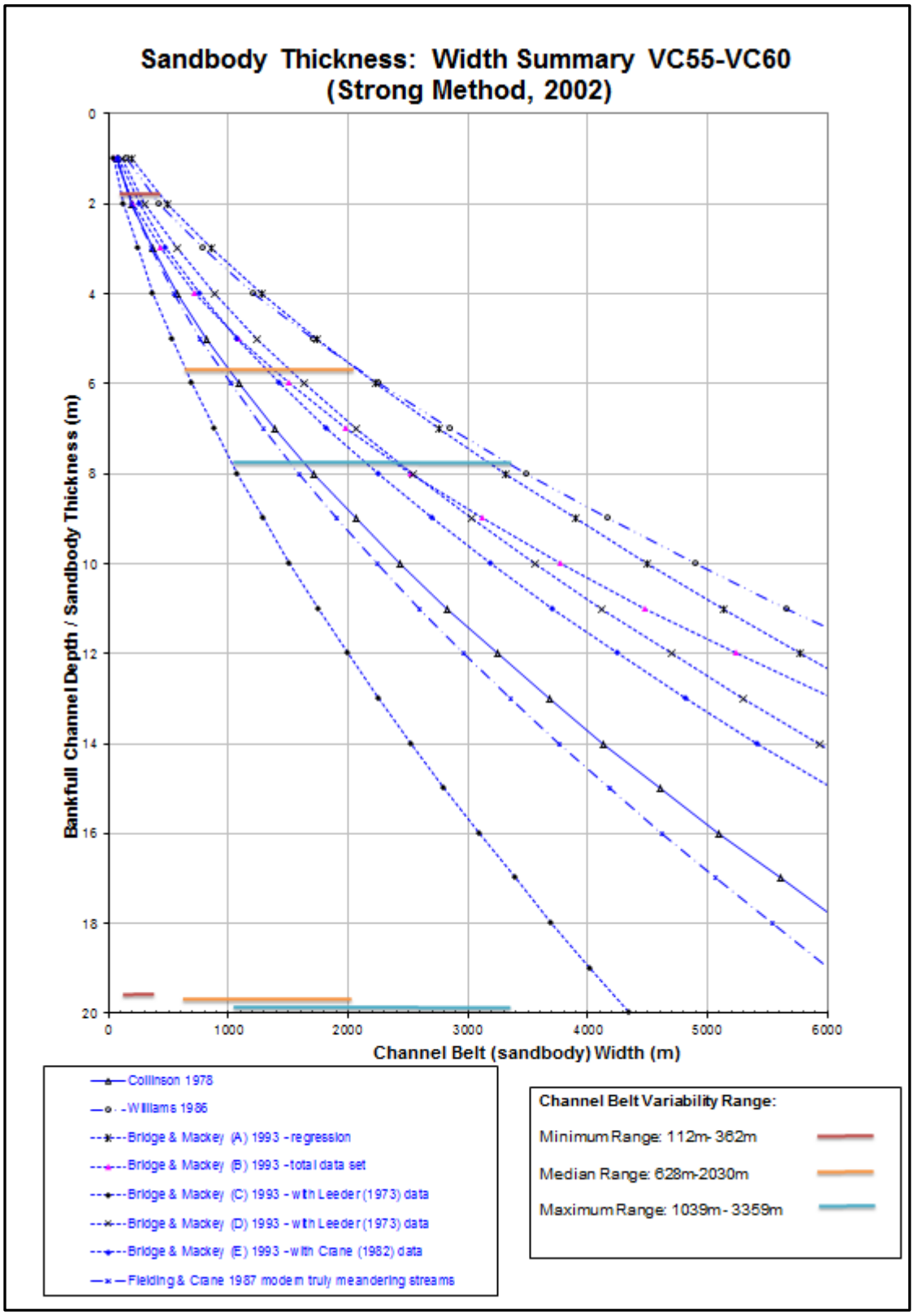

Appendix C6: Channel Belt Width plot for Grouped Bankfull VC60-VC65

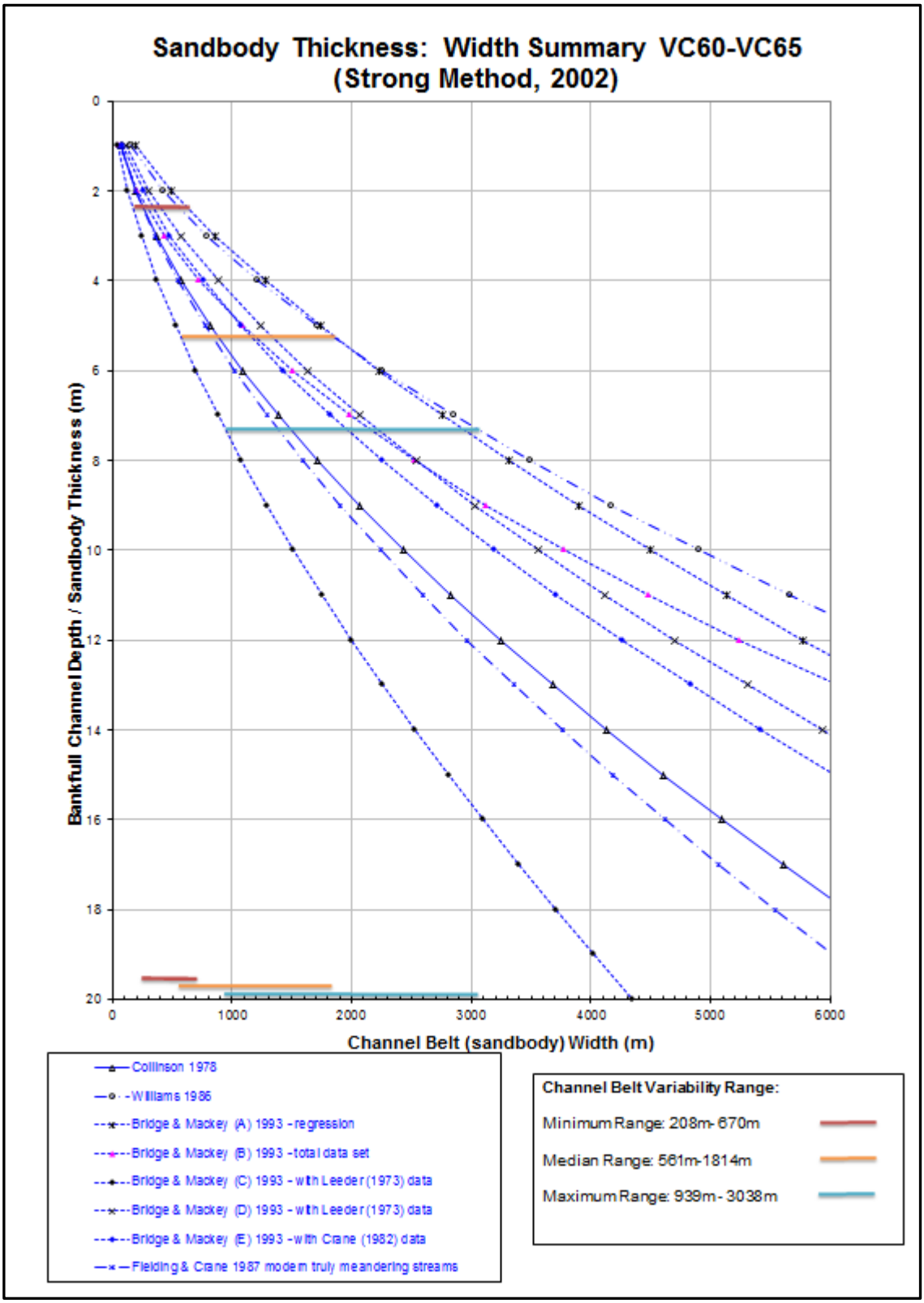

Appendix C7: Channel Belt Width plot for Grouped Bankfull VC65-VU75

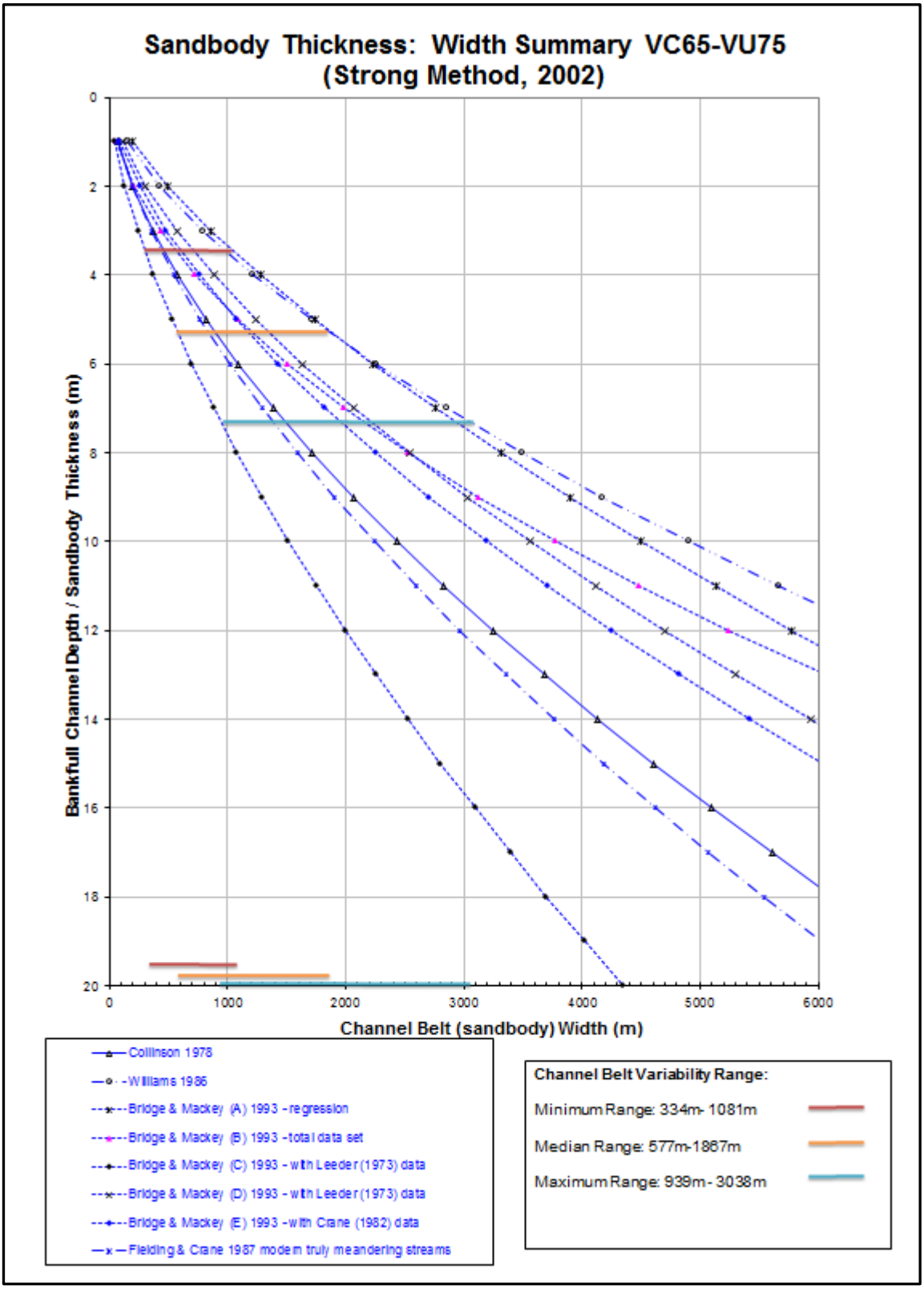

Appendix C8: Channel Belt Width plot for Grouped Bankfull VU75-VC100

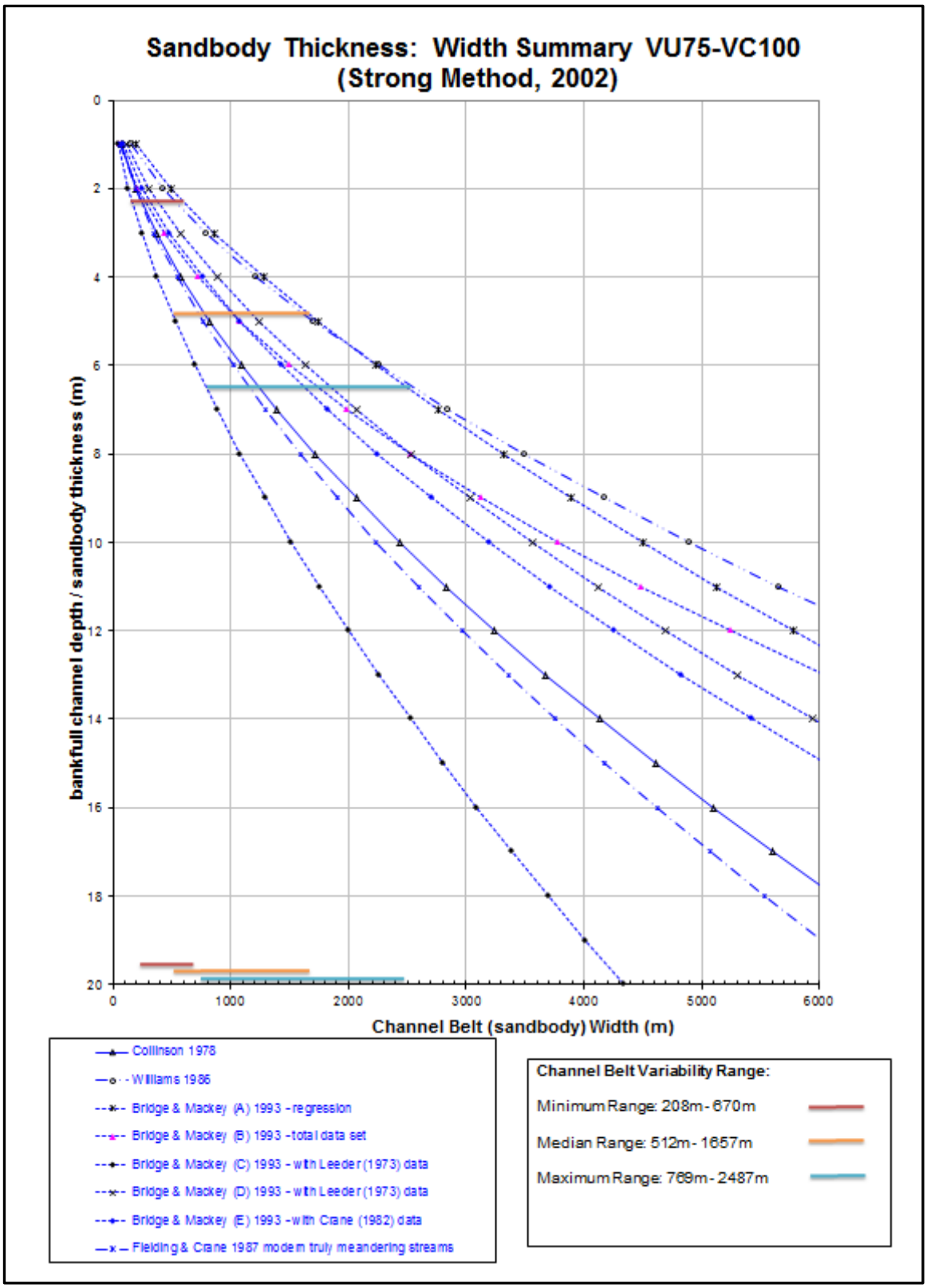

Appendix D: Bankfull Measurements Table

Appendix D: Bankfull measurements of all wells in the Tenapperra Study Area. Measurements were given a confidence rating of 1 (green),2 (orange) or three (omitted from this table). An arbitrary compaction factor of 10% has already been applied to the measurements in this table.

Well Name	Bankfull Thickness (m)																		
Interval	VC00 -VL05	VL05 - VC10	VC10 - VC15	VC15 - VC20	VC20 - VC25	VC25 - VC30	VC30 - VC35	VC35 - VC40	VC40 - VU45	VU45 - VC50	VC50 - VC55	VC55 - VC60	VC60 - VC65	VC65 - VC70	VC70 - VU75	VU75 - VC80	VC80 - VC85	VC85 - VC90	VC90-VC100
ALISMA 1		1.4	4.6			7.3	6.4		6.9				5.0	7.3					
ALISMA 2			7.3										5.5						
ALLAMBI 1					7.3									3.7					
ALMONTA 1					7.3														
AZOLLA 1							5.9												
BAGUNDI 1																			
BAGUNDI 2																			
BAGUNDI 3			4.6				3.7												
BAGUNDI 4																			
BAGUNDI 5		1.8	5.0		5.5														
BAGUNDI 6																			
BARATTA 1							6.4												
BARATTA 2							4.6												
BARATTA SOUTH 1						4.1													
BARATTA WEST 1				4.6	4.6														
BARCOOLOO 1			5.5																
BECKLER 1		3.2				5.5						5.9							
BECKLER 2																			
BECKLER 3					6.9	5.9							5.9						
BECKLER 4	2.3	2.3			6.9														
BECKLER 5						6.4	6.4												
BOONGALA 1												6.4	3.7						
BOONGALA 2							5.0					5.5	5.5						
BOW 1				5.5		6.4													
BOW 2								4.6	2.3										
BRUMBY 1								4.6											
BRUMBY 10																			
BRUMBY 11					5.0	4.6													

Well Name	Bankfull Thickness (m)																		
Interval	VC00 -VL05	VL05 - VC10	VC10 - VC15	VC15 - VC20	VC20 - VC25	VC25 - VC30	VC30 - VC35	VC35 - VC40	VC40 - VU45	VU45 - VC50	VC50 - VC55	VC55 - VC60	VC60 - VC65	VC65 - VC70	VC70 - VU75	VU75 - VC80	VC80 - VC85	VC85 - VC90	VC90-VC100
BRUMBY 12																			
BRUMBY 13																			
BRUMBY 2						4.1		4.1											
BRUMBY 3																			
BRUMBY 4																			
BRUMBY 5																			
BRUMBY 6		1.6			7.8	4.6													
BRUMBY 7						2.7													
BRUMBY 8		2.3				3.7	3.7	4.6											
BRUMBY 9		1.8																	
BURKE 1						4.6		4.6											
BURKE 11	3.2					5.5													
BURKE 12						4.6							4.1						
BURKE 3												3.7	5.0						
BURKE 4						5.0						1.8							
BURKE 5							4.6												
BURKE 6																			
BURKE 7						5.5	3.7												
BURKE 8								5.5											
BOW 1																			
BOW 2																			
BURKE EAST 1													5.0						
CANBERRA 1A		4.6																	
CARAKA 1					2.7	6.9		7.3	2.7										
CHILCARRIE 1				2.7	5.5														
CHILDIE 1								4.6											
CHIRON 1																			
CHIRON 2																			
CHIRON 3					5.5														
COOCHILARA 1							5.5					5.5							
COOCHILARA 2											5.5								
COOLOON SOUTH 1				6.9															
CROWSNEST 1							5.9						4.6						

Well Name	Bankfull Thickness (m)																		
Interval	VC00 -VL05	VL05 - VC10	VC10 - VC15	VC15 - VC20	VC20 - VC25	VC25 - VC30	VC30 - VC35	VC35 - VC40	VC40 - VU45	VU45 - VC50	VC50 - VC55	VC55 - VC60	VC60 - VC65	VC65 - VC70	VC70 - VU75	VU75 - VC80	VC80 - VC85	VC85 - VC90	VC90-VC100
CROWSNEST 2																			
CROWSNEST 3																			
CURRUMBIN 1																			
DELLA 1																			
DELLA 10																			
DELLA 11																			
DELLA 12																			
DELLA 13																			
DELLA 14																			
DELLA 15							5.5												
DELLA 16							4.1												
DELLA 17																			
DELLA 18R																			
DELLA 19			4.6			4.1													
DELLA 2																			
DELLA 20																			
DELLA 21																			
DELLA 22							4.1												
DELLA 23																			
DELLA 24																			
DELLA 25						5.9													
DELLA 3																			
DELLA 4																			
DELLA 5A																			
DELLA 6																			
DELLA 7																			
DELLA 8		3.2		4.6	4.6														
DELLA 9																			
DIERI 1				6.9															
DILCHEE 1						4.6					4.1		5.0						
DILCHEE 2									4.6										
DILCHEE 3							3.7												
DILCHEE 4				5.5															
DULLINGARI 1																			

Well Name	Bankfull Thickness (m)																		
Interval	VC00 -VL05	VL05 - VC10	VC10 - VC15	VC15 - VC20	VC20 - VC25	VC25 - VC30	VC30 - VC35	VC35 - VC40	VC40 - VU45	VU45 - VC50	VC50 - VC55	VC55 - VC60	VC60 - VC65	VC65 - VC70	VC70 - VU75	VU75 - VC80	VC80 - VC85	VC85 - VC90	VC90-VC100
DULLINGARI 17				5.5				3.7											
DULLINGARI 18				3.7							3.2	6.9	5.5	4.6					
DULLINGARI 19								5.0					5.9						
DULLINGARI 2											4.6			6.4	4.6				
DULLINGARI 22								5.5			5.5								
DULLINGARI 23								5.5					7.3	6.4					
DULLINGARI 24													5.5		4.1				
DULLINGARI 25					5.5			3.2				4.6	5.0		7.3				
DULLINGARI 26											5.9		5.5	4.6				5.5	4.6
DULLINGARI 3								5.5	5.5					5.0					
DULLINGARI 36DW1				5.5					6.9										
DULLINGARI 39								5.5											
DULLINGARI 4																			
DULLINGARI 40DW1									4.6										
DULLINGARI 44																			
DULLINGARI 45			5.5	5.0				6.9	6.9	6.9			4.6		7.3				
DULLINGARI 46		2.7						4.6			5.5	5.9	6.4	5.5	5.9		6.4		4.6
DULLINGARI 49								6.4											
DULLINGARI 51																			
DULLINGARI 52																			
DULLINGARI 53																			
DULLINGARI 54				5.9															
DULLINGARI 55																			
DULLINGARI 57																			
DULLINGARI 61																			
DULLINGARI NORTH 1								4.1	7.3	6.9	6.4	6.9		6.4					
DULLINGARI NORTH 10																			
DULLINGARI NORTH 11			4.1	5.0	5.0	5.0													
DULLINGARI NORTH 12			5.5	6.9															
DULLINGARI NORTH 13ST1								4.1											
DULLINGARI																			

Well Name	Bankfull Thickness (m)																		
Interval	VC00 -VL05	VL05 - VC10	VC10 - VC15	VC15 - VC20	VC20 - VC25	VC25 - VC30	VC30 - VC35	VC35 - VC40	VC40 - VU45	VU45 - VC50	VC50 - VC55	VC55 - VC60	VC60 - VC65	VC65 - VC70	VC70 - VU75	VU75 - VC80	VC80 - VC85	VC85 - VC90	VC90-VC100
NORTH 14																			
DULLINGARI NORTH 15																			
DULLINGARI NORTH 16					5.5			6.4	8.2								4.6		
DULLINGARI NORTH 17																			
DULLINGARI NORTH 18											7.8	7.8							
DULLINGARI NORTH 19																			
DULLINGARI NORTH 20																			
DULLINGARI NORTH 3									5.5		5.0								
DULLINGARI NORTH 4								5.5			7.3		6.9						
DULLINGARI NORTH 5				5.0															
DULLINGARI NORTH 6						5.0					2.7								
DULLINGARI NORTH 8				6.9			6.9							7.3			5.0		
DULLINGARI NORTH 9											4.1	5.0	3.7	4.6					
EGLINT 1																			
EPSILON 1						5.9		6.4											
EPSILON 10																			
EPSILON 11		2.3																	
EPSILON 2																			
EPSILON 3																			
EPSILON 4		3.7																	
EPSILON 6		2.7																	
EPSILON 7																			
EPSILON 8																			
EPSILON 9																			
GAHNIA 1					4.1	5.5													
GIDGEE 1																			
GIDGEE 2																			
GRYSTES 1																			

Well Name	Bankfull Thickness (m)																		
Interval	VC00 -VL05	VL05 - VC10	VC10 - VC15	VC15 - VC20	VC20 - VC25	VC25 - VC30	VC30 - VC35	VC35 - VC40	VC40 - VU45	VU45 - VC50	VC50 - VC55	VC55 - VC60	VC60 - VC65	VC65 - VC70	VC70 - VU75	VU75 - VC80	VC80 - VC85	VC85 - VC90	VC90-VC100
GUDNUKI 1				6.9		5.0						7.3			5.5				
GUDNUKI 2											5.0	5.0		4.6					
GUDNUKI 3								5.0											
HORNET 1																			
KAPINKA 1				7.8			6.9												
KAPPA 1							4.1					6.4	3.7	5.0					
KATINGAWA 1																			
KEETO 1																			
KEETO 2																			
KELBROOK 1				6.4	5.0			3.7											
KERNA 1							4.1	8.2											
KERNA 2A						5.9	4.6	5.0											
KERNA 3				4.1	4.1	6.4													
KERNA 4						5.0													
KERNA 5							6.9		7.3										
KERNA 6					6.9														
KERNA 7								4.1											
KERNA NORTH 1			2.7	3.7			5.5	4.1			6.4		5.9	5.5	3.7				
KEWARRA 1				5.5		5.5													
KIDMAN 1																			
KIDMAN 10																			
KIDMAN 2																			
KIDMAN 3					5.5														
KIDMAN 4																			
KIDMAN 5																			
KIDMAN 7				6.4															
KIDMAN 8			5.0				4.6												
KIDMAN 9				5.9															
KIDMAN NORTH 1					4.1		4.6												
KIDMAN NORTH 2					4.6														
KIDMAN NORTH 3							4.6												
KIDMAN NORTH 4				5.5															

Well Name	Bankfull Thickness (m)																		
Interval	VC00 -VL05	VL05 - VC10	VC10 - VC15	VC15 - VC20	VC20 - VC25	VC25 - VC30	VC30 - VC35	VC35 - VC40	VC40 - VU45	VU45 - VC50	VC50 - VC55	VC55 - VC60	VC60 - VC65	VC65 - VC70	VC70 - VU75	VU75 - VC80	VC80 - VC85	VC85 - VC90	VC90-VC100
KINGSTON RULE 1																			
KINTA 1				5.0		3.7	4.6	4.6					5.9						
KULTARR 1								5.0											
LANCER 1																			
LEPENA 1																			
LEPENA 2									3.2										
MARABOOKA 1																			
MARABOOKA 2																			
MARABOOKA 3			4.6					5.0											
MARABOOKA 4																			
MARABOOKA 5																			
MARABOOKA 6																			
MARABOOKA 7																			
MARABOOKA EAST 1						6.4			5.0										
MARAKU 1						6.9													
MARANA 1																			
MARSILEA 1								2.7											
MATARANKA 1																			
METTIKA 1																			
METTIKA 2				5.0	5.0			3.7	5.0										
METTIKA 3						3.2			5.0			4.6							
METTIKA 4				3.7	2.3	2.3			4.6										
METTIKA 5								3.7	4.6										
METTIKA 6						3.7	3.7	4.1											
MONTEGUE 1				6.9		4.6	7.3												
MOON 1							5.5												
MOON 2			4.1		5.0	5.5			4.6				2.7	4.6		4.6	4.1		
MOON 3															4.6				
MOONA 1						4.1	4.6	4.1	4.6			2.7					4.1		
MUDERA_1						6.9		4.6					5.0						
MUDERA_6								6.4				5.5							
MUDERA_2								5.0											
MUDERA_3								2.7	4.6				5.0						

Well Name	Bankfull Thickness (m)																		
Interval	VC00 -VL05	VL05 - VC10	VC10 - VC15	VC15 - VC20	VC20 - VC25	VC25 - VC30	VC30 - VC35	VC35 - VC40	VC40 - VU45	VU45 - VC50	VC50 - VC55	VC55 - VC60	VC60 - VC65	VC65 - VC70	VC70 - VU75	VU75 - VC80	VC80 - VC85	VC85 - VC90	VC90-VC100
MUDERA_4								4.6											
MUDERA_6								5.9											
MUDERA_5								3.7	2.7										
MUNDI 1				5.5															
MUNDI 2																			
MUNDI 3																			
MUNDI 4							4.6												
MUNDI 5																			
MUNDI 6																			
MUNDI 7							4.6												
MUNKARIE 1																			
MUNKARIE 10							5.5												
MUNKARIE 2																			
MUNKARIE 3																			
MUNKARIE 4							5.0												
MUNKARIE 5																			
MUNKARIE 6																			
MUNKARIE 7																			
MUNKARIE 8							3.7												
MUNKARIE 9																			
MURTEREE 1					5.9														
NANIMA 1																			
NAPPACOONGE E 1																			
NAPPACOONGE E 2																			
NAPPACOONGE E 3																			
NAPPACOONGE E EAST 1																			
PELKETA 1																			
PIRA 1				5.5		4.6		2.7		5.0									
PIRA 2				4.1	6.4			4.1											
PIRA 3			5.0					5.5											
PLANTAGO 1				5.5		3.7		4.6	2.7				3.7						
PLOTOSUS 1																			

Well Name	Bankfull Thickness (m)																		
Interval	VC00 -VL05	VL05 - VC10	VC10 - VC15	VC15 - VC20	VC20 - VC25	VC25 - VC30	VC30 - VC35	VC35 - VC40	VC40 - VU45	VU45 - VC50	VC50 - VC55	VC55 - VC60	VC60 - VC65	VC65 - VC70	VC70 - VU75	VU75 - VC80	VC80 - VC85	VC85 - VC90	VC90-VC100
POORAKA 1																			
PYTHON 1				4.1							4.6								
QUASAR 1				4.1															
QUASAR SOUTH 1							4.6												
QUASAR SOUTHEAST 1												7.8							
RANGER SOUTH 1				4.6			5.5						5.9						
ROSENEATH 2				4.6															
SARAH 1																			
SKIPTON 1																			
STOKES 1																			
STOKES 10																			
STOKES 11																			
STOKES 12						3.2													
STOKES 2					3.7		5.9												
STOKES 3																			
STOKES 4						4.1						3.7							
STOKES 5ST1									5.0										
STOKES 6							4.1		5.0										
STOKES 7								5.0											
STOKES 8					4.6		4.1	4.6											
STOKES 9						3.7													
STOKES CENTRAL 1																			
STOKES NORTH 1							4.1												
STOKES SOUTH 1					3.2	5.0		4.6											
STRATHMOUNT 1								4.6				5.5	5.9	5.5	4.6	6.4			
STRZELECKI 1																			
STRZELECKI 10																			
STRZELECKI 14DEEP																			
STRZELECKI 14DW1																			
STRZELECKI 15																			

Well Name	Bankfull Thickness (m)																		
Interval	VC00 -VL05	VL05 - VC10	VC10 - VC15	VC15 - VC20	VC20 - VC25	VC25 - VC30	VC30 - VC35	VC35 - VC40	VC40 - VU45	VU45 - VC50	VC50 - VC55	VC55 - VC60	VC60 - VC65	VC65 - VC70	VC70 - VU75	VU75 - VC80	VC80 - VC85	VC85 - VC90	VC90-VC100
STRZELECKI 16																			
STRZELECKI 17																			
STRZELECKI 2																			
STRZELECKI 24																			
STRZELECKI 25					6.4														
STRZELECKI 29																			
STRZELECKI 3																			
STRZELECKI 5																			
STRZELECKI NORTHEAST 1																			
TALAQ 1																			
TARWONGA 1					5.0	5.5													
TARWONGA 2																			
TARWONGA 3																			
TARWONGA 4				4.6															
TARWONGA 5				5.5	4.6														
TEEGAL 1																			
TELLUS 1				5.9		6.9		4.1				7.3	5.9						
TELLUS SOUTH 1						6.9		6.9						4.1					
THREE QUEENS 1																			
TILPAREE A1																			
TOOLACHEE 1																			
TOOLACHEE 10								6.9											
TOOLACHEE 11					6.9														
TOOLACHEE 12																			
TOOLACHEE 13					5.5			5.5											
TOOLACHEE 14					4.6														
TOOLACHEE 15				3.7	5.0														
TOOLACHEE 16																			
TOOLACHEE 17							5.5												
TOOLACHEE 18									4.6										
TOOLACHEE 19																			
TOOLACHEE 2																			

Well Name	Bankfull Thickness (m)																		
Interval	VC00 -VL05	VL05 - VC10	VC10 - VC15	VC15 - VC20	VC20 - VC25	VC25 - VC30	VC30 - VC35	VC35 - VC40	VC40 - VU45	VU45 - VC50	VC50 - VC55	VC55 - VC60	VC60 - VC65	VC65 - VC70	VC70 - VU75	VU75 - VC80	VC80 - VC85	VC85 - VC90	VC90-VC100
TOOLACHEE 20			6.9					5.0											
TOOLACHEE 23																			
TOOLACHEE 24																			
TOOLACHEE 25																			
TOOLACHEE 26							6.9												
TOOLACHEE 27		3.2		5.0	5.0		5.0												
TOOLACHEE 28				4.6	4.6	4.6	5.0	5.9											
TOOLACHEE 29					4.1														
TOOLACHEE 3				6.9	4.6														
TOOLACHEE 30					4.6		5.0	5.5											
TOOLACHEE 31																			
TOOLACHEE 32																			
TOOLACHEE 33																			
TOOLACHEE 34					4.1														
TOOLACHEE 35																			
TOOLACHEE 36																			
TOOLACHEE 37																			
TOOLACHEE 38																			
TOOLACHEE 39							5.0								4.1				
TOOLACHEE 4																			
TOOLACHEE 40					5.9		5.5												
TOOLACHEE 41																			
TOOLACHEE 42																			
TOOLACHEE 43																			
TOOLACHEE 44																			
TOOLACHEE 45				6.4	7.3														
TOOLACHEE 46																			
TOOLACHEE 46A				4.1															
TOOLACHEE 47																			
TOOLACHEE 48																			
TOOLACHEE 49																			
TOOLACHEE 5																			
TOOLACHEE 50				5.9	6.4		5.0												
TOOLACHEE 51																			

Well Name	Bankfull Thickness (m)																		
Interval	VC00 -VL05	VL05 - VC10	VC10 - VC15	VC15 - VC20	VC20 - VC25	VC25 - VC30	VC30 - VC35	VC35 - VC40	VC40 - VU45	VU45 - VC50	VC50 - VC55	VC55 - VC60	VC60 - VC65	VC65 - VC70	VC70 - VU75	VU75 - VC80	VC80 - VC85	VC85 - VC90	VC90-VC100
TOOLACHEE 52																			
TOOLACHEE 6					6.9		5.5	5.5											
TOOLACHEE 7																			
TOOLACHEE 8					5.9		6.4												
TOOLACHEE 9							4.6												
TOOLACHEE EAST 1					5.5	5.9	4.1		5.0							6.4	2.7		
TOOLACHEE EAST 2		2.7					3.7	4.6							4.6				
TOOLACHEE NORTH 1																			
TOOLACHEE WEST 1																			
VERBENA 1																			
WANARA 1					5.5		5.9												
WILLS 1						6.4													
WILPINNIE 1												7.8							
WILPINNIE 2																			
WITCHETTY 1																			